MOLECULAR INVESTIGATIONS IN ANIMAL MODELS OF HUNTINGTON'S DISEASE

MICHAEL FREDERICK JAMES GILDER

A Thesis Presented for the Degree of Doctor of Philosophy, Ph.D

Department of Anatomy and Developmental Biology
University College London
1998

ABSTRACT

NF-κB is a transcription factor family, which includes the proteins p65, p50 and p52. Inducible in most cell types, NF-κB (p65) has been demonstrated to be present in the nuclei of cortical neurones. This work demonstrates that p65, p50 and p52 are also present in striatal neurones, and that p52 localises to neuronal nuclear bodies. Administration of the excitotoxin quinolinic acid (QA) or the glial activator ciliary neurotrophic factor (CNTF) leads to an increase of protein binding to NF-κB DNA oligonucleotides in a biphasic temporal manner. PAGE revealed no significant change in expression of known NF-κB proteins after either treatment, but a 35 kD protein of unknown identity is recognised by anti-p50, being transiently expressed following both QA and CNTF administration. Furthermore, p52 and p65 can be localised within glial cells following QA treatment. Endogenous levels of striatal CNTF are also seen to increase significantly at 168 hours post-lesion. These results implicate NF-κB in the regulation of the glial response to striatal lesion.

Polyglutamine repeats can bind via hydrogen bonding *in vitro,* and may lead to aggregation of proteins if mutation leads to increased trinucleotide repeat length. A preliminary study of the DNA binding, expression and localisation of the polyglutamine repeat transcription factors Brain-2 (BRN-2), glucocorticoid receptor and TATA binding protein (TBP) were investigated in the CNS of R6/2 transgenic mice expressing abnormal huntingtin protein (htt) possessing expanded polyglutamine repeats. These mice develop neuronal nuclear inclusions of aggregated htt and demonstrate symptoms similar to juvenile onset Huntington's disease. Increased protein binding to OCT consensus site DNA was found in the cortex of transgenes corresponding to BRN-2. This work provides no evidence that abnormal htt induces symptoms via transcriptional dysregulation, as has been proposed. However, decreased expression of BRN-2 is seen in the hypothalamic paraventricular nucleus in transgenic animals.

Keywords: Striatum, NF-κB proteins, quinolinic acid, ciliary neurotrophic factor, Huntington's disease, gliosis, polyglutamine repeat, transcription factor.

ACKNOWLEDGEMENTS

This thesis is dedicated to Sheila and Frederick, my mother and father, with thanks and love.

This page is a great pleasure to write. I owe a great many people thanks for their help during my time as a graduate student. **Dr. Stephen W. Davies** has been an extraordinary supervisor and friend. It has been a privilege to work for such a gifted scientist. I only hope I can live up to his faith in me. Much of the work in this thesis may not have been accomplished, had it not been for the kindness and expertise of **Dr. Kristen M. Hollen** who taught me how to run 'Westerns' and 'EMSAs' (and fix mountain bikes). My multi-talented friend **Suhel Miah** helped me to see things from a different perspective whenever life got a little tough. I thank him for his kindness and comradeship. I would probably never have completed this thesis without his optimistic support. Sincere thanks also go to **Mark Turmaine**, 'possibly the best electron microscopist in the world', for his help and friendship. Further thanks go to **Aysha Raza** for making the lab a brighter place to work in. I wish her luck with her own Ph.D research.

Thanks go to many other people who have assisted my research or provided friendly faces. These include **Harvinder Bains, Dr. Katherine Beardsall MRCP, Dr. Richard Purkiss, Bin Wang, Dr. Christopher Yeo** (for use of the AIS imaging system) and my contemporary Anatomy and Developmental Biology graduate students and the many IBSc medical students who are too numerous to mention. Sincere thanks go to **Dr. Barbara Fulton** for helping me to decide to pursue neuroscience while a Human Sciences undergraduate and for being my secondary supervisor. I gratefully acknowledge the **UCL Graduate School** for awarding my Research Scholarship and **Professor Geoffery Burnstock** for providing financial assistance during my second year. My gratitude goes also to **Dr. Gillian Bates,** and her group, especially **Dr. Laura Mangiarini** for their patience in harvesting tissue for my preparations. I am bound to have forgotten many other people who have helped me along the way and hope they accept my apologies.

Love and thanks go to all of my family for their support. To my parents **Sheila** and **Fred** for their love and for supporting me totally throughout my education. To my brothers and sisters: **Yvonne** and her artistic temperament, **Mark** for his advice and concern, **Chris,** for letting Mark out to play, **Julie** and **David** for being there if I needed them. Thanks also to **Steve Parkins**, old school friend and karaoke fiend.

TABLE OF CONTENTS

4.DISCUSSION

5.REFERENCES 282

LIST OF FIGURES

LIST OF TABLES

LIST OF ABBREVIATIONS

BRN-2	brain 2 transcription factor
CCB	cerebellum
CDV	canine distemper virus
ChAT	choline acetyltransferase
CNS	central nervous system
CNTF	ciliary neurotrophic factor
CTX	cortex
DRPLA	dentatorubropallido-Luysian atrophy
EMSA	electrophoretic mobility shift assay
GABA	gamma-amino butyric acid
GAD	glutamic acid decarboxylase
GFAP	glial fibrillary acidic protein
GR	glucocorticoid receptor
HD	Huntington's disease
HPRT	hypoxanthine phosphoribosyltransferase
htt	huntingtin protein (with expanded polyglutamine repeats)
IL-1	interleukin 1
KA	kainic acid
LMC	litter-mate control
MJD	Machado Joseph disease
NADPH-d	nicotinamide adenine dinucleotide phosphate diaphorase
NF-κB	nuclear factor kappa-B
NII	neuronal intra-nuclear inclusion
NGF	nerve growth factor
NLS	nuclear localisation signal
NMDA	N-methyl-D-aspartate
NPY	neuropeptide Y
OCT	octomer
OTF	octomer transcription factor
PAGE	polyacrylamide gel electrophoresis
PKC	protein kinase C
PVN	paraventricular nucleus of the hypothalamus (L/RPVN =left/right PVN)
QA	quinolinic acid
SCA	spinocerebellar ataxia
ST	striatum
TBP	tata binding protein
TF	transcription factor

INTRODUCTION

Structure and function of the striatum: a component of the basal ganglia

'The Corpus Striatum (superior ganglion of the cerebrum), has received its name from the striated appearance which its section presents, from white fibres diverging through its substance. The intra-ventricular portion is a large pear shaped mass, of a grey colour externally; its broad extremity is directed forwards into the fore-part of the body, and anterior cornu of the lateral ventricle; its narrow end is directed outwards and backwards, being seperated from its fellow by the thalami optici; it is covered by the serous lining of the cavity, and crossed by some veins of considerable size. The extra-ventricular portion is embedded in the white substance of the hemisphere.'

[Henry Gray, 1858]

The corpus striatum is a prominent subcortical nucleus. It is present in the central nervous system (CNS) of most higher vertebrates, being observed in mammals, birds, reptiles and a similar striatal structure is found within the phylogenetically older vertebrate species such as amphibians, cartilaginous fishes and lungfishes (Medina and Reiner, 1995). For the sake of this thesis, the striatum of three species in particular will be considered, that of the rat, the mouse and the human. As for a gross anatomical description of the striatum in humans, little can be added to that above written by Henry Gray in the 1800s (Gray, 1858). The striatum lies inferior to the cortex, embraced in its superior aspect by the white matter of the corpus callosum and bordered medially by the lateral ventricle. In rats and mice the striatum comprises one structure, penetrated by myelinated fibre fascicles. In humans, the striatum can be divided into the caudate nucleus and putamen, which although identical on a cellular and neurochemical basis, are divided by the white fibres of the internal capsule as it forms the corona radiata, thus appearing as two distinct anatomical structures in the primate brain. The ventral aspect of the striatum is described in both humans and rodents as the nucleus accumbens (Wilson, 1990).

The specific function of the striatum is still not well understood, most clues to its role arise from pathological studies of the basal ganglia network of the CNS, of which the striatum is a part. These disorders most notably include Huntington's[1] (HD), Parkinson's[2] (PD) diseases and hemiballismus, which will be studied in more detail later. However, to reduce the role of the striatum to control of movement alone would be to overlook its potential importance in controlling emotion and behaviour since it receives

[1] George Huntington, 19th century New England physician.
[2] James Parkinson, 19th century London physician, scientist and social reformer named the disorder 'paralysis agitans', renamed upon the insistence of Jean Martin Charcot, French neurologist.

input from all cortical regions including the limbic system as well. The basal ganglia consists of several other subcortical and subhalamic structures, including the globus pallidus internal and external segments (GPi/GPe)[3], subthalamic nucleus (STN), substantia nigra pars compacta and pars reticulata (SNpc/SNpr), ventral tegmental area (VTA) and the striatum (caudate, putamen and nucleus accumbens) itself. The SNr and GPi are structurally and neurochemically similar. This system plays a crucial role in the generation, accurate execution and maintenance of movement.

The main afferent input to the basal ganglia is received by the striatum (often considered the 'input' nucleus of the basal ganglia) and is from glutamate secreting cortical and hippocampal neurones and glutamatergic fibres from the intralaminar nucleus of the thalamus (Divac 1977, Fonnum 1981, Groenewegen and Berndse, 1994). The most extensive cortical input to the striatum appears to originate from the sensorimotor cortex. However the potential importance of the striatum in controlling emotion and behaviour is revealed by glutamatergic input from the limbic and para-limbic cortical areas and amygdala. These structures synapse primarily within the nucleus accumbens and ventral caudate and putamen. All information flow through the basal ganglia exhibits a somatotopic organisation (Divac et al.1977; Alexander and Crutcher, 1990; Parent and Hazrati, 1995). These excitatory glutamate fibres synapse upon the striatal projection neurones, the medium sized spiny neurones, which comprise 90 to 96 % of the striatum in the rat and cat respectively and approximately 70% in the human. They possess a cell body diameter of 12 to 14 μm and 'little granular endoplasmic reticulum' when compared to striatal interneurones (Kemp and Powell, 1971). Medium sized spiny cells possess smooth nuclear membranes, a feature which allows them to be distinguished from the medium sized interneurones of the striatum when using electron microscopy. These cells obtain their name from the small protuberances or 'spines', which cover the distal two-thirds of their dendrites. These spines; 'consist of a dilated head on a narrow stalk of varying length, though some are sessile, some have branched stalks with two heads and others branched heads' (Kemp and Powell, 1971). It is upon the heads of these spines that the afferent glutamatergic fibres terminate and form excitatory synapses (Kemp and

[3] Globus pallidus internal and external segments are descriptive for human anatomy. In rodents the internal segment is referred to as the entopeduncular nucleus.

Powell, 1971; Bouyer et al.1984 and Smith and Bolam, 1990). Kemp and Powell, who conducted the superb classic structural study of the striatal neurones using Golgi and Nissl staining in combination with electron microscopy, could not trace the axons of the medium sized spiny cells and were not aware of their projection status. The spines of the striatal projection neurones may be essential for allowing facilitation or attenuation of the excitatory input from the cortex, for it is here that the second major afferent input to the striatum (and therefore the basal ganglia) is also received. Dopaminergic fibres from the substantia nigra pars compacta terminate and form synapses upon the neck of the spines of the projection neurones, (Freund et al, 1984 and Smith and Bolam, 1990) as demonstrated by tyrosine hydroxylase immunoreactivity of these synaptic boutons. Dopaminergic input from the SNpc may have an excitatory or inhibitory action upon the striatal projection neurones, depending upon whether or not they express the excitatory D1 or inhibitory D2 dopamine receptor (Gerfen, 1992). The striatum also receives serotonergic input from the dorsal raphe nucleus and noradrenergic fibres from the locus coeruleus (Wilson, 1990). Several other cell types exist in the striatum and demonstrate consistency in morphology, like the projection neurones, from rodent to man. All other neuronal cell types within the striatum are interneurones, forming local circuitry, each population making up between 1 to 5% of the total cell population of the striatum. The most prominent striatal interneurones are those described by Kemp and Powell as 'very large, generally fusiform....long axon cells'[4] possessing a somatic diameter of 20 to 30 μm, now commonly referred to as giant striatal interneurones. Like all striatal interneurones, these giant cells possess indented nuclear profiles and very few, if any, spines. These cells are undoubtedly cholinergic since they are immunoreactive for choline acetyl transferase

[4] The size and prominent axons of these cells (1mm) led to the mistaken conclusion by Ramon y Cajal (1911) that they may have been the striatal projection cells. Retrograde tracing analysis of medium-sized neurones demonstrated otherwise. This original belief provided support for the integrative 'funneling' hypothesis of information processing through the basal ganglia, i.e that the greater amount of cortical information entering the striatum was reduced to the output from the giant cholinergic cells alone. It is now widely accepted, however that the basal ganglia allow parallel processing of information through the spiny projection neurones along a number of anatomically distinct 'loops' or basal ganglia-thalamocortical circuits, notably the limbic, association, oculomotor and motor loops. The latter is considered in this introduction and the diagram below (Alexander and Crutcher, 1990).

(McGeer et al. 1974, Bolam et al. 1984[1] and Phelps et al. 1985) and endogenous histochemisty localises acetylcholinesterase to them (see Methods; Karnovsky and Roots, 1964, Satoh et al. 1983 and Bolam et al. 1984[2]). This further demonstrates that these cells cannot be projection neurones, for striatal projections do not contain acetylcholine (Fonnum, 1974). Giant cholinergic cells represent less than 2% of all striatal cell types observed (Kemp and Powell, 1971).

The other prominent interneurone type is that of the medium sized aspiny striatal cell, which appears to exist in two or three distinct chemical profiles. The first is a population of GABAergic neurons that are immunoreactive for the GAD-67 isoform of glutamic acid decarboxylase and the calcium binding protein parvalbumin (Cowan et al. 1990 and Kita et al. 1990). There also appears to be a group of GAD-67 reactive interneurones (projection neurones are positive for the GAD-65) that contain the calcium binding protein calretinin (Kubota et al.1993). Yet another population stains with nicotinamide adenine dinucleotide phosphate diaphorase (Scherer-Singler et al. 1983, Kowall et al. 1987; NADPH diaphorase: see Methods) and is immunoreactive for nitric oxide synthetase (NOS) and the neuropeptides somatostatin (Difiglia and Aronin 1982) and neuropeptide Y (NPY) (Kawaguchi et al. 1995). Finally, a small population of interneurons have been identified in the cat, which make up less than 1% of the total population of striatal neurones, which are immunoreactive for vasoactive intestinal polypeptide (VIP) (Vincent and Reiner, 1988). Striatal interneurones appear to synapse upon the cell body or proximal shaft of the spiny projection neurones, unlike dopaminergic and glutamatergic fibres (Smith and Bolam 1990). The function of striatal interneurones is far from clear. However both parvalbumin positive (GAD-67) and somatostatin positive (NOS/NADPH-diaphorase) receive input from the cortex as well as contacting projection neurones and may be responsible for feedforward inhibition of certain striatal regions. Giant cholinergic interneurones receive input from the parafasicular nucleus of the thalamus, the cortex and the projection cells themselves as well as some dopaminergic fibres from the substantia nigra pars compacta. This high number of inputs combined with the large dendritic trees of these cells indicates that they may play a role in 'integrating synaptic inputs over relatively large regions' (Kawaguchi et al.1995).

From this complex network of striatal cells, the projection neurones connect to other components of the basal ganglia. It is here that we must examine the medium sized spiny neurones in a little more detail to fully understand the manner in which the striatum may control movement. The projection neurones of the striatum are GABAergic (Fonnum, 1978 and Ribak et al. 1979) and therefore all output from the striatum is inhibitory. However, the projection neurones can be divided into two groups, the action of one group, the so-called type I projection neurones facilitating movement and the type II inhibiting movement. Type I neurones project predominantly to the substantia nigra pars reticulata (SNr) and globus pallidus internal segment (GPi)/entopeduncular nucleus (EP) (Burns et al. 1983), which are considered the primary output nuclei of the basal ganglia. Type I projection neurones produce the neuropeptides substance P (SP) (Bolam et al. 1983 and Izzo et al, 1987) and dynorphin (DYN) (Vincent et al. 1982), as well as GABA (Penny et al. 1986) and express the D1 dopamine receptor (Gerfen et al 1988, Gerfen et al 1990). These neurones project straight to the output nuclei and are referred to as the 'direct' striatonigral pathway of the basal ganglia. Output from the SNr and GPi/EP is GABAergic and therefore inhibitory to its target; the neurones of the ventral thalamus, in particular the centromedian nucleus (CM), nucleus ventralis anterior pars magnocellularis (VAmc) nucleus ventralis anterior pars parvocellularis (VApc) and nucleus ventralis lateralis pars oralis (VLo). These thalamic nuclei in turn project to pre-motor and primary motor cortex (Alexander and Crutcher, 1990). The output of the ventral thalamus is glutamatergic and therefore excitatory to the motor cortex. Understanding these anatomical connections allows us to hypothesize that the type I neurones inhibit the SNr and GPi/EP, thus disinhibiting the thalamic output to the motor cortex allowing movement to occur. Type II projection neurones secrete the neuropeptide enkephalin (ENK) (Pickel et al. 1980) as well as GABA and express the D2 dopamine receptor (Gerfen et al 1988, Le Moine et al.1990 and Gerfen et al 1990). These neurones project to the SNr and GPi/EP via the globus pallidus internal segment (GPe) and the sub-thalamic nucleus (STN) respectively and are therefore described as the 'indirect' pathway of the basal ganglia. This indirect pathway is inhibitory to movement, for its inhibitory input to the GPe allows the STN, which is normally under the inhibitory GABAergic influence of the GPe, to excite the SNr/GPi with its glutamatergic input. This permits

inhibition of the thalamus by the GABAergic output of the SNr/GPi and therefore ultimately inhibition of the motor cortex (Gerfen, 1992). This model simplifies the anatomical connections of the STN somewhat as it also receives input from the cortex. Furthermore, although the presentation of the basal ganglia model proposed here is still viable, it has been proposed that this view is somewhat 'striato-centric' and that inhibition of the GPe leading to disinhibition of the STN is oversimplified. This is due to the GPe possessing a more complex projection pattern, sending afferents to the entopeduncular nucleus and reticular thalamic nuclei as well as the STN (Cheeselet and Delfs, 1996). Hemiballismus/ballismus is a hyperkinetic disorder typified by a wild, uncontrollable flailing of the upper limb(s). The reason for this is usually a lesion of the sub-thalamic nucleus, which is no longer able to inhibit the activity of the output nuclei when it is itself disinhibited from control the GPe, allowing overexcitation of the motor cortex and ultimately the hyperkinetic limb itself. It can also now be understood how dopaminergic input from the substantia nigra pars compacta (SNpc), by synapsing on projection neurone spines, can also facilitate movement. The neurones of the direct pathway possess excitatory D1 receptors, while those of the indirect inhibitory D2. Although perhaps oversimplified, this goes some way to explaining why degeneration of the dopaminergic neurones of the SNpc in Parkinson's disease leads to the classical symptoms of that disorder, rigidity, bradykinesia and akinesia: a poverty of movement (DeLong, 1990). Experimental physiological evidence supports this anatomical description. Electrophysiological recording of nigral (SNpr) GABAergic neurones revealed that these neurones became silent when eye movements were executed, correlating with hypothesised direct pathway inhibition of the output nuclei (Hikosaka and Wurtz, 1983).

So far we have considered two levels of organisation within the basal ganglia, that of somatopic input from the cortex to the striatum, and two divergent output pathways from the striatum. Another level of organisation exists however. Regions of neurochemical heterogeneity exist within the striatum and these areas may be essential in understanding the clinical picture of Huntington's disease. These heterogenous regions are described 'patch and matrix' or 'striosome and matrix'. Patches appear to be regions of striatal neurones which are u-opiate receptor rich (Pert et al. 1976), receive input from the amygdala, pre-frontal and limbic cortex and deep cortical layer V and layer VI

(Gerfen, 1984). Projection neurones from these regions synapse upon the dopaminergic neurones of the substantia nigra pars compacta (SNpc) and also receive input from GABAergic interneurons. Matrix regions are rich in acetylcholinesterase (Graybiel and Ragsdale, 1978), somatostatin and calbindin (Gerfen, 1985), projection neurones synapsing upon the output nuclei (GPi/SNpr, as determined by calbindin immunoreactivity), and receiving input from the thalamus and superficial layer V of sensorimotor, frontal, parietal and occipital cortex (Gerfen, 1984). The matrix also receives input from the cholinergic, GABAergic and NADPH-d interneurones (Gerfen, 1992). Huntington's disease will not be discussed in detail here, but it appears that it is the patch or striosome region of the striatum which contains the first groups of cells to degenerate in HD, the pathology then progressing to the matrix (Hedreen and Folstein, 1995). This is of course the component of the striatal projection neurones, which synapses upon and inhibits the dopaminergic cells of the SNpc, which in turn project to the striatum, facilitating movement. Loss of patch cells may cause disinhibition of this dopaminergic projection, causing increased excitation of the direct pathway and perhaps partially explaining the hyperkinesis observed in HD.

Now that a brief description of the structure, cellular components, connections and function of the striatum has been presented, we may turn to a discussion of the symptoms and pathology of Huntington's disease. Understanding the anatomy of the striatum allows us to more fully appreciate how degeneration of this nucleus contributes to HD.

Figure 1.1 Simplified Circuit Diagram of the Basal Ganglia

(Refer to text for full explanation. Adapted from Alexander and Crutcher, 1990)
Blue arrows represent GABA pathways, Red Glutamate and Green Dopamine.
For clarity, other transmitters (including the neuropeptides enkephalin,
substance P and dynorphin) have been omitted, as have certain pathways (for example, the SNr output to the superior colliculus). Letters in brackets refer to disorders associated with degeneration of those areas of the basal ganglia HD; Huntington's disease, PD; Parkinson's disease and HB; hemiballismus. Note that the separation of Patch and Matrix from type I and II neurone boxes is purely schematic, as is the separation of Patch from Matrix.

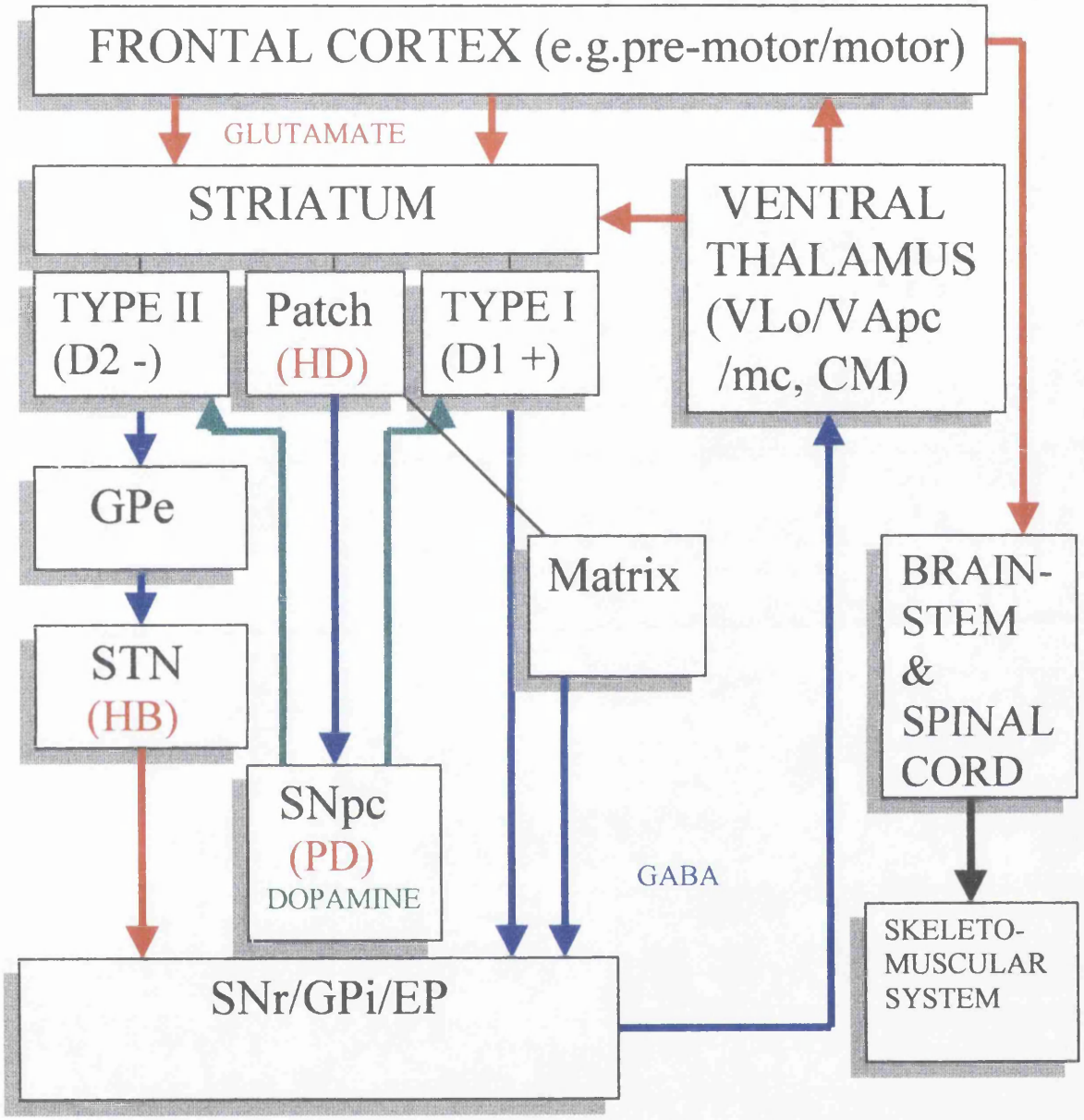
FRONTAL CORTEX (e.g.pre-motor/motor)
GLUTAMATE
STRIATUM
VENTRAL THALAMUS (VLo/VApc /mc, CM)
TYPE II (D2 -)
Patch (HD)
TYPE I (D1 +)
GPe
STN (HB)
Matrix
BRAIN-STEM & SPINAL CORD
SNpc (PD) DOPAMINE
GABA
SKELETO-MUSCULAR SYSTEM
SNr/GPi/EP

Figure 1.2 Striatal Projection Neurones and Interneurones

1.(Upper Left). Light photomicrograph of medium-sized spiny projection neurone of the rat, stained using the Golgi (Silver staining) technique. Notice the proliferation of spiny protuberances upon the cellular dendrites (Smith and Bolam, 1990).

2.(Upper right). Camera lucida drawings of (A) medium-sized spiny projection neurone (which were initially believed to be merely interneurones) and (B) medium sized aspiny cell from the caudate nucleus of the cat (Kemp and Powell, 1971).

3.(Lower left) Two cholineacetyltransferase (ChAT) immunoreactive striatal cholinergic interneurones demonstrating a characteristic morphology (large striatal cells) in a 40μm thick section of rat striatum (Phelps et al. 1985)

4.(Lower right) Electron micrograph of the nucleus of a medium-sized aspiny interneurone in the cat striatum, clearly demonstrating the characteristic indented nuclear profile which distinguishes this cell type from the smooth nuclear profile of the spiny projection cell when observed at high magnification (Kemp and Powell, 1971).

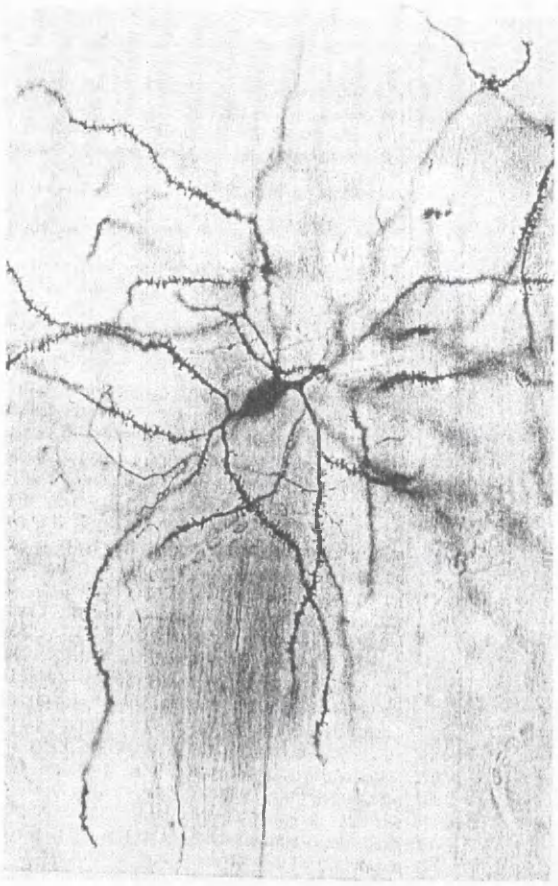

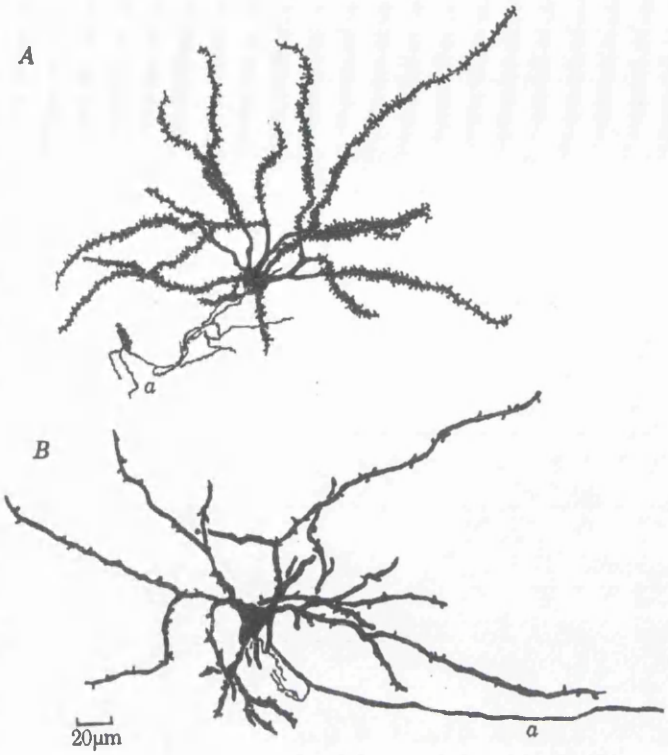
A
a
B
20μm
a

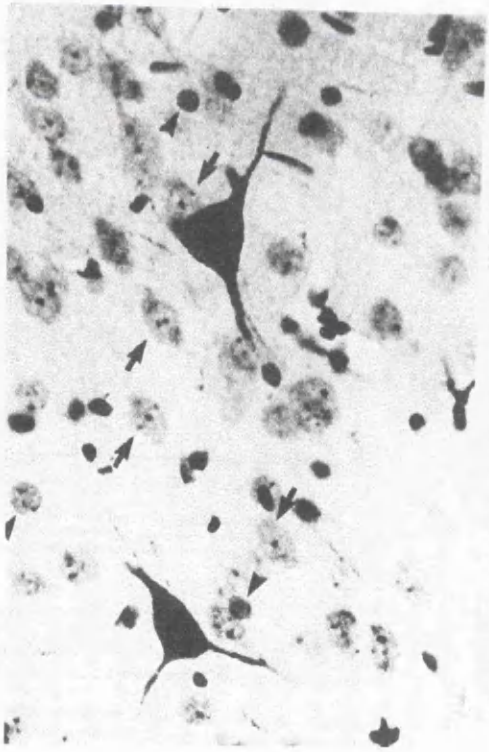

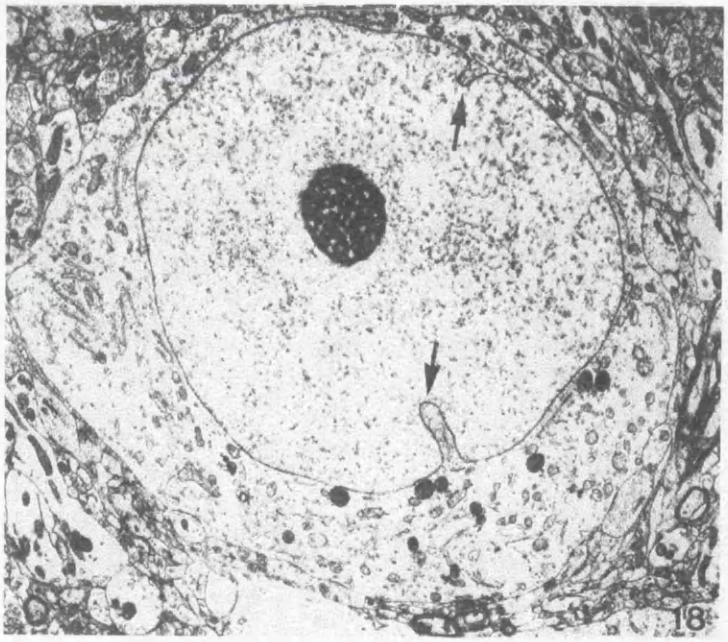
18

Huntington's disease and the quinolininc acid model of neurodegeneration

'I recall it as vividly as though it had occurred but yesterday....Driving with my father through a wooded road leading from East Hampton to Amagansett we suddenly came upon two women, mother and daughter, both tall and thin, almost cadaverous, both bowing, twisting, grimacing. I stared in wonderment, almost in fear. What could it mean?'

[George Huntington, 1909] [5]

As Henry Gray was describing the topographical anatomy of the corpus striatum, George Huntington was making his first childhood observation of choreiform patients. George Sumner Huntington was the third generation of a family of New England physicians who became aware of a strange, inherited movement disorder within the local population. Huntington's first and only contribution to medical literature was his paper describing these twisting, writhing patients (Huntington, 1872) whose disorder was to bear his name.

HD is typically characterised by hyperkinetic involuntary movements. The onset of the disease typically occurs between the fourth and fifth decade, although as we shall see later, it may be much earlier, symptoms appearing even in infants. Initial symptoms are usually of a neuropsychiatric nature typified by hypersexuality, anti-social behaviour and depression[6]. The patient later demonstrates purposeless, jerky choreiform ('dance-like') motions, slow writhing of the limbs or (athetosis) and saccadic eye movements. Additional symptoms may include dysarthia, dystonia and dysphagia. These movements may initially be accommodated into daily living to some extent, but as the disease progresses they become more and more uncontrollable. Interestingly, these movements disappear in sleep, just as Parkinson's disease patients lose their rigidity and tremor. Cognitive impairment occurs and patients often end their lives demented and, in contrast to the earlier hyperkinesis, rigid and akinetic approximately fifteen years after symptomatic onset (Harper, 1991). The juvenile form of the disease[7] typically presents

---

[5] George Huntington, address, 1909 New York Medical Society, recalling incident in 1858 (Harper,1991).
[6] Huntington's transgenic mice display early pathology in the cingulate cortex, a region anatomically associated with the limbic system. If this is also the case in humans, it could implicate cingulate cortex degeneration as a possible cause of early psychiatric symptoms in HD (S.W.Davies, personal communication).
[7] Juvenile HD is sometimes referred to as Westphal variant HD after the physician who first described juvenile rigidity (Bird, 1980).

with a different clinical picture, typified by rigidity, tremor, epileptic seizures and myoclonus usually following a brief period of choreiform hyperkinesis (Bird, 1980). A feature, which may be of relevance to later work in this thesis, is the neuroendocrinologic symptoms seen in HD patients. Individuals often demonstrate an increase in appetite despite increasing weight loss and cachexia. Furthermore, the fertiltity rate of women with HD appears to be increased when compared to normal sister controls, and altered production of gonadotrophic releasing hormone (GnRH) was implicated. These symptoms strongly indicate hypothalamic abnormalities (Bird, 1980), however, further work indicated no difference between control subjects and HD patients when GnRH function was examined, although the results were described as 'difficult to analyse' (Lavin et al. 1981). There is no treatment available for HD at time of writing.

Pathology is dramatic, with massive enlargement of the lateral ventricle visible upon post-mortem, mainly due to atrophy of the caudate and putamen of the striatum[8] and thinning of the cerebral cortex. HD patients typically demonstrate a 30% reduction in weight of the cortex, hippocampus and thalamus before gross pathology is visible, indicating dramatic shrinkage of the CNS early in the disease. In contrast, reduction in size and weight of the striatum is progressive as the disease advances (de la Monte et al.1988). Pathological grading is presented as five stages (Vonsattel et al. 1985) illustrating disease progression at post-mortem. Grade 0 patients show no sign of gross brain pathology, but demonstrate psychiatric symptoms of the type described above. However, reactive astrocytosis is found when immunocytochemistry is carried out upon striatal sections using antibodies raised to the astrocyte marker glial fibrilary acidic protein (GFAP). The astrocytes appear in distinctive zones, which match the patches of the striatum, indicating that striatal degeneration appears here first (Hedreen and Folstein, 1995; see previous chapter)[9]. Eventually reactive astrocytosis fills the matrix as well, indicating degeneration of the whole striatum. Grade I patients also demonstrate no sign of gross brain pathology (except shrinkage), but histological analysis reveals up to 50% of striatal projection neurones may have been lost. Grades II to IV describe increasing

[8] Loss of neurons in the caudate and putamen was first described by Alzheimer in 1911.
[9]Hedreen and Folstein surveyed 163 clinically diagnosed cases of HD. Reactive astrocytosis of the patch compartment is not the only indicator of initial degeneration, a reduction in the patch marker AChE is also observed (Ferrante et al.1987)

atrophy of the caudate, putamen and cortex. As well as astroglial proliferation, a distinctive pattern of cell loss is seen in the striatum. The projection neurones die most markedly. The reduced levels of glutamic acid decarboxylase (Bird and Iversen, 1974) and GABA (50%) in homogenised HD striatum evidence this. Other projection neurone markers are also reduced throughout the dorsal striatum, notably substance P and enkephalin. *in situ* hybridsation studies of preproenkephalin mRNA in HD brain demonstrated a significant reduction, when compared to normal controls and pre-symptomatic individuals (Albin et al. 1991) as did immuocytochemistry for enkephalin (Sapp et al. 1995). However, levels of SP and ENK do not appear to be altered in the nucleus accumbens (Kowall et al. 1987). Striatal levels of dopamine, serotonin and noradrenaline were not reduced, indicating that the neurones of the substantia nigra, raphe nuclei and locus coerleus do not die in HD. Somatostatin is of course also present in the NADPH-d population of interneurones. Studies have demonstrated that somatostatin levels may be fivefold greater in HD striatum than controls (Aronin et al. 1983). This increase is apparently due to the survival of NADPH-d neurones in HD and therefore an overall increase in the proportion of these cells (and their somatostatin). A dramatic sparing of NADPH-d/SS/NPY interneurones occurs in HD. NADPH-d positive neurones usually account for less than 2% of the striatal neurone population. However in late stage HD, they may account for a 10 to 30% proportion of neurones present (Ferrante et al. 1985, Ferrante et al.1987) and NADPH-d activity does not appear to decrease in HD tissue (Ferrante et al. 1987). However, NADPH-d levels do apparently decrease overall as HD progresses, as demonstrated in post-mortem tissue (Morton et al. 1993).

Diaphorase neurones are not the only population of interneurones that are spared. The giant cholinergic cells are also resistant to loss, although not as strikingly as the diaphorase neurones (Ferrante et al. 1986). As already mentioned, both AChE and ChAT are localised to giant cholinergic cells, but although AChE levels in these cells are preserved in HD, ChAT levels are not, showing a significant decrease. This may be due to loss of giant cell synapses with projection cells (Ferrante et al.1987).

The reasons for sparing of these neuronal types are still not clear. It is known that NADPH-d neurones are extremely resistant to various toxic substances including CO, sulfanilamide, tertrachlormethane and thalidomide (Thomas and Pearse, 1964). It has

long been thought likely that projection neurones are more vulnerable to stress due to the metabolic demands of maintaining long axonal processes. However, this hypothesis does not explain why the striatum in particular is predominantly destroyed in HD, when, as we shall see soon, the product of the HD gene is ubiquitously expressed.

HD presents with a prevalence of 7-10 per 100 000 globally. There appear to be foci of the disease globally, with a higher than normal incidence in the Moray Firth and East Anglia in the UK and Boston in the US. There is a particularly large HD population at Lake Maracaibo in Venezuela[10] (Jenkins and Conneally, 1989). As these foci suggest, HD is a genetic disease presenting in a classical autosomal dominant form (i.e. 50% of progeny of effected individuals will present with the disease). HD in the Lake Maracaibo families has been traced back to a German sailor who settled there in the 1860s and the Boston kindred to three English pilgrims who sailed to Salem from Yarmouth, Norfolk in 1630 (Bird, 1980). In 1982 researchers linked the disease to band 16.3 on the p arm of chromosome 4 (Gusella, 1983) but obviously at this stage nothing was known about biochemical abnormality that was present. This revealed yet another interesting fact. HD must be caused by a 'gain of function' mutation to the HD gene product, for in the condition known as Wolf-Hirschorn syndrome, the top of chromosome 4 is totally deleted, yet sufferers show no related symptoms to HD patients. A 210 kb region of this chromosome labelled IT15 (interesting transcript 15) was isolated by the Huntington's Disease Collaborative Research Group (HDCRG, 1993). The gene demonstrated expansion of CAG repeats in HD sufferers at the 5' end, which coded for polyglutamines in the actual protein, which was eventually named huntingtin. Huntingtin is a large protein of ~350kD, making it difficult to visualise on PAGE. No protein homologous to huntingtin has yet been found. Normal individuals in Boston demonstrate from 6 to 34 CAG repeats, HD sufferers from 37 to 100. In a sample from Cardiff, the normal range was 9-34 the HD range 30 to 70. These figures demonstrate that the threshold of repeats varies from individual to individual, some individuals with 34 repeats being asymptomatic, some with 30 progressing to develop HD. Huntingtin is ubiquitously expressed in both normal individuals and HD patients, although at higher levels in brain, testes, spleen and lungs. Many groups investigated localisation of huntingtin in normal

(Hoogeveen et al. 1993, Strong et al. 1993) and normal and HD brain (Sharp et al, 1995, Landwehrmeyer et al. 1995) demonstrating its widespread expression throughout the brain. It was shown that huntingtin is normally a cytoplasmic protein associated with cellular vesicles in cortical synaptosomes (DiFiglia et al. 1995). The function of huntingtin is still not known.

The gain of function hypothesis was further supported by the production of transgenic mice. In these animals the mouse homologue of huntingtin, Hdh, was disabled. Heterozygotes displayed no adverse symptoms (most HD sufferers are heterozygotic, with the exception of some of the population at Lake Maracaibo), indicating again that human HD is caused by a gain of function of the protein. However, homozygote mice with two inactivated copies of the gene failed to develop and died before birth (Duyao et al, 1995).

Expanded trinucleotide repeats are found in several other neurological diseases, including spinobulbar muscular atrophy (SBMA), dentatorubral-pallidoluysian atrophy (DRPLA) and spinocerebellar ataxia (SCA). HD (at least where neuropsychiatric symptoms are concerned) as do all the above disorders, demonstrates 'anticipation', an earlier onset of disease in subsequent generations if inherited from the father[11] (HDCRG, 1993, Ross et al. 1993 and La Spada et al. 1994).

For the moment we will leave discussion of HD and discuss the use of quinolinic acid (QA) as a model of neurodegeneration with relevance to HD, for this paradigm has been used widely in this thesis. Since QA is an agonist of the N-methyl-D-aspartate (NMDA) glutamate receptor (Schwarcz et al. 1983 and Vezzani et al. 1986), a brief review of the glutamate receptors and excitotoxicity will be undertaken.

L-glutamate is the principal excitatory amino acid (EAA) neurotransmitter found within the vertebrate nervous system (Fagg and Foster, 1983), it being present in the mammalian brain at a higher concentration than any other amino acid. In the 1960s and early 1970s it was thought that the action of glutamate was mediated by one receptor type, but research has demonstrated a fascinating range of glutamate receptors which can broadly be divided into two groups. Those receptors which open an ion channel in response to glutamate binding, and those that transduce glutamate binding into an

[10] Of 10,766 individuals studied, 371 presented with HD, 84 had possible HD, those with a 50% risk=1,266, those who had grandparents with HD=2395 and those normal=6651.
[11] In myotonic dystrophy (DM) anticipation occurs via maternal inheritence.

intracellular signalling cascade, the ionotropic (iGLU) and the metabotropic (mGLU) receptors respectively. The ionotropic receptors can again be classified according to compounds which stimulate their activation. These include the NMDA and non-NMDA iGLU receptors, the non-NMDA receptors being subdivided yet again into the AMPA (amino-3-hydroxy-5-methyl-4-isoazoleproprionic acid) and KA (kainic acid) classes. Despite this relatively straightforward classification of iGLU receptors, a wide range of compounds capable of stimulating them have been identified. Glutamate of course stimulates the activation of all three. NMDA selectively stimulates the NMDA receptors, as do the compounds ibotenic acid (IA), acromelic acid (ACRO) and quinolinic acid (QA). AMPA receptors are selectively stimulated by AMPA and quisqualic acid (QQA) and the KA receptors by kainic acid and domoic acid (DMA). There is some overlap between the activity of the AMPA and KA receptor function as both of these non-NMDA types permit the influx of Na^+ ions while stimulation of the NMDA receptor permits the influx of Na^+ and Ca^{++} ions (in 'exchange' for K^+). It is this extra capability of the NMDA receptor, which appears to enhance its excitotoxic potential (Lodge and Johnson, 1990 and Young and Fagg, 1990).

Ionotropic glutamate receptors are comprised of distinct subunits. Each subunit possess a stretch of amino acids which is partially embedded within the cell membrane, which form a channel pore, the site of calcium permeability. Each subunit possesses three full transmembrane domains in addition to the stretch of amino acids which partially embeds within the membrane (Hollman et al, 1989 and Moriyoshi et al. 1991). Characterisation of the receptor subunits has demonstrated that the NMDA receptor may be constructed from any of the five subunits NR1, NR2A, NR2B, NR2C and NR2D. The AMPA receptor subunits are designated GluR1 to GluR4 and KA receptor components GluR5 to GluR7 and KA1 and 2. The ion channel of NMDA receptors is partially blocked when the neurone is at resting potential by Mg^{++} ions. It is only by depolarisation of the post-synaptic membrane via the non-NMDA AMPA and KA receptors initially that this Mg^{++} block may be pushed from the channel allowing the NMDA receptor to carry more current (Evans et al. 1978; Mayer and Westbrook, 1987). This blockage of the NMDA receptor channel explains the mode of operation of the non-competitive NMDA receptor antagonists such as Zn^{++}, Mn^{++} and indeed Mg^{++} itself as well as the compound

MK801 (Turski et al. 1991). Further to this, the NMDA receptor also appears to require the binding of glycine as a coactivator, to a separate site from that of glutamate, to permit the influx of calcium (Monaghan et al, 1989). To function physiologically, the NMDA receptor must comprise one NR1 subunit and is usually found as a heteromeric assembly of NR1 plus several of the other receptor subunits (Monyer et al. 1992; Monyer et al. 1994). After secretion from the synapse, glutamate is reabsorbed by the neurone via a sodium dependant uptake system, the cell requiring two sodium ions for every molecule of glutamate taken up (Fonnum, 1984).

Most, if not all, neuronal types present in the striatum express the NMDA receptor. However the NADPH-d/SS/NPY neurones appear to possess NMDA receptors composed of different subtypes than the other neurones of the striatum. About 80% of NADPH-d/SS/NPY neurones are immunoreactive for the NMDA NR1 subunit, about 17% of them strongly positive (Kumar et al. 1997), demonstrating the presence of NMDA receptors on these cells. However, using immunocytochemical double-labelling, it has been demonstrated that whereas 95% of striatonigral neurones, 96% of enkephalin containing neurones and 100% of giant cholinergic interneurones are immunoreactive for the NR2A and NR2B NMDA subunits, no somatostatin (NADPH-d/SS/NPY) containing neurones were reactive for NR2A/2B (Chen and Reiner, 1996). It has been proposed that this differential distribution of NMDA receptor subunits may partially explain the resistance of NADPH-d interneurones to quinolinic acid neurotoxicity (Chen and Reiner, 1996).

The excitotoxic hypothesis (and indeed the term excitotoxicity) was proposed by Olney some 28 years ago, although the ability of glutamate to induce degeneration of retinal neurones was observed prior to this (Lucas and Newhouse, 1957). This excitotoxic

hypothesis of neuronal death proposed that neurones expressing glutamate receptors and exposed to high levels of the excitatory amino acid (EAA) glutamate or glutamate analogues can be overstimulated to the point of death. The cells become depolarised to such a state that internal calcium increases to a level at which internal homeostasis is lost and the neurone dies (Olney, 1969, Olney, 1971). Experimental evidence demonstrates that neurones exposed to high levels of glutamate initially undergo dendritic (dendrosomatic) swelling, before the cell body also swells and ruptures, leading to necrotic and apoptotic death. The mechanism by which glutamate and its analogues induce toxicity appears to be mediated by an excessive movement of extracellular calcium [Ca^{++}] and sodium [Na^{+}] into the cell. The physiologic impact of this is to disrupt cellular homeostasis, one of the consequences of which is the increased uptake of water which results in the dendrosomatic swelling outlined above. Further to this, Ca^{++} also disrupts normal mitochondrial function and also results in the activation of enzymes capable of producing toxic free radicals, both mechanisms are implicated in ultimately leading to the death of the neurone (Whetsell, 1996). This is a rather general view of the manner by which excessive exposure to glutamate may induce cell death, but what are the calcium dependant pathways that may activate neuronal death mechanisms? One potentially lethal pathway may lead to the activation of nitric oxide synthase (NOS/NADPH diaphorase), which exists in constitutive and inducible forms and generates nitric oxide (NO). Both forms require activation via calcium binding to the calcium binding protein calmodulin (Choi, 1993; Dugan and Choi, 1994). NO is a free radical gas, which appears to have an important role in long-term potentiation (LTP). Like all free radicals NO possesses a unpaired electron, making it a highly reactive entity as it may 'extract' electrons from other cellular molecules, and in doing so can damage membrane lipids, proteins and DNA (Olanow, 1993). Free radicals are formed in all cells as a by-product of oxidative phosphorylation via the reduction of molecular oxygen, but excessive amounts may be enough to lead to cell death. It has been demonstrated that inhibitors of NOS (monomethyl-L-arginine and N^{G}-nitro-L-argininine) are capable of reducing the impact of NMDA mediated neuronal death in cortical neurone cultures (Dawson and Dawson, 1991). NOS is also capable of creating the superoxide radical (O_2^{-}) and

hydrogen peroxide (H_2O_2) which, besides being toxic itself, is capable of generating further free radicals, including the hydroxyl radical ($OH^{\bullet}$) and the highly reactive (and damaging) peroxynitrite ($ONOO^-$) (Olanow, 1993). It has been shown that neurones produce both superoxide and hydroxyl radicals after exposure to NMDA, and that free radicals inhibit the uptake of glutamate by glia and increase its release by hippocampal cells (Dugan and Choi, 1994).

Another deleterious action of excessive calcium influx can be damage to the cell membrane. NMDA receptor stimulation activates the enzyme phospholipase A2 in striatal neurones (Dumuis et al. 1988). Phospholipase converts membrane lipids to lysophospholipids and free fatty acids by hydrolysis, and direct damage to the cell membranes is not the only factor involved here. Arachadonic acid is released by the activity of this enzyme and can itself be metabolised into prostaglandins, leukotrienes and hydroxyeicosateraenoic acid, the production of all of which can result in the formation of further free radicals (Dugan and Choi, 1994). Arachadonic acid and other free fatty acids released by the action of phospholipase A_2 may interfere with membrane integrity and alter the function of membrane associated proteins, including the NMDA receptor itself. Arachadonic acid application increases the probability of NMDA ion channels being open, leading to even greater calcium influx and further phospholipase A2 activation (Miller et al. 1992), and in addition to this, arachadonic acid inhibits the uptake of glutamate by glial cells (Barbour et al. 1989).

The activation of NOS, phospholipase A_2 and potentially other protein kinases and lipases is not the only means by which calcium influx may alter the neurones integrity. Calcium acts as a powerful intracellular messenger, which may propagate signals to the nucleus of neurones. Calcium influx from NMDA receptors leads to the activation of serum response factor (SRF) and ELK-1, which are transcription factors capable of binding to the serum response element (SRE) site. The SRE is found in the immediate early gene (IEG) c-fos promoter. This is just one example of how NMDA receptor activation can lead to long-term changes in neuronal function (Ghosh and Greenberg, 1995, Gallin and Greenberg, 1995).

Is there any evidence that excitotoxicity may play a causitive role in neurodegenerative disorders? It was long believed that many such diseases and

conditions could be caused by environmental toxins. Evidence for excitotoxic environmental toxins playing a central role in neurodegeneration was present in many forms. Lathyrism is a neurological condition presenting with a tingling sensation at nerve endings, fasiculation and flaccid paralysis linked with degeneration of lower motor neurones. Historically the condition is ancient and is still recorded in regions of Ethiopia and Bangladesh. It is caused by ingestion of the chickling pea of the plant *Lathyrus sativas,* which contains an amino acid analogue, BOAA, which is an agonist at the AMPA glutamate receptor (Ludolph and Spencer 1996). This provided strong evidence that an environmental glutamate receptor analogue could induce neurodegeneration. Another example, demonstrating exact correlation between ingestion of an excitotoxin and neurodegeneration occurred in 1987 in Newfoundland. Individuals presented with headache and seizures before entering coma and dying. These individuals had ingested domoic acid from algae contaminated blue mussels. Domoic acid is a homologue of kainic acid (KA) (Teitelbaum et al. 1990). More tenuously ingestion of the false sago palm *Cycas circinalis* by islanders of Guam and Rota correlated with a high incidence of a neurodegenerative disorder, the ALS-parkinsonian dementia complex of Guam. Indigenous peoples knew that *Cycas* was toxic and implemented a thorough washing procedure before ingesting flour made from the plant, but the toxin, BMAA can not be totally removed. BMAA undergoes a reaction with bicarbonate and then binds to glutamate receptors. There is still no evidence to demonstrate that BMAA from *Cycas* was responsible for this disease complex and experimental evidence which is present (Spencer et al. 1987), is relatively inconclusive. It is interesting to note, however, that as islanders diets have become more westernised, the incidence of the disorder has decreased. At post-mortem degeneration of the hippocampus and sensorimotor cortex could be observed. This is all very well for what may be particularly rare cases of ingestion of toxins, but what of more common neurological disorders? Excitotoxic death caused by over stimulation of NMDA receptors has been hypothesised in eplileptic seizures (Clark, 1994) and brain ischaemia (Simon, 1984) in which extracellular glutamate levels can rise markedly.

Since the striatum receives such enormous glutamatergic input from the cortex and thalamus, and the excitotoxic hypothesis appeared to have some experimental and clinical

evidence supporting it, injection of glutamate agonist excitotoxins was undertaken by various groups. The goal in these situations was to see if a similar pattern of cellular degeneration to that of HD, notably loss of projection cells and sparing of cholinergic and diaphorase interneurones could be induced experimentally in the rat striatum. Initially the glutamate analogue excitotoxin and AMPA receptor agonist kainic acid (KA), extracted from seaweed, was injected intrastriatally (Coyle and Schwartz, 1976). KA produced a relatively similar pathology to HD, giving rise to an axon and glial sparing lesion while striatal neurones underwent degeneration. However, a dramatic loss of NADPH diaphorase neurones appeared to make it unsuitable as a chemical model of the disorder, but another glutamate analogue and NMDA receptor agonist, quinolinic acid (QA) which produced a similar pathology to KA , without the loss of giant cholinergic cells seemed to offer several advantages (Kohler and Schwartz, 1983). QA as a toxin, it was thought initially, could play a real role in the aetiology of HD for it is endogenously present in the mammalian CNS in micromolar amounts as a tryptophan metabolite. It was subsequently discovered that QA, when injected in various millimolar amounts at different rates, caused varying states of neurodegeneration by excitotoxicity (Vezzani et al. 1991, Forloni et al. 1992, Perez-Navarro, 1994). Various groups have reported different claims concerning the nature of survival of interneurones and extent of cell death when using QA microinjection as a model of neurodegeneration. However, the claim by Beal and colleagues (Beal et al, 1986, Beal et al 1991) that NADPH-d/SS/NPY interneurones are selectively spared in the QA model and that levels of somatostatin and NPY increase six months after lesion (as in HD) appears not to be correct. When cell counts to determine survival of different neuronal populations are restricted to the lesion core, and not conducted throughout the entire striatum, it can be seen that cholinergic neurones demonstrate a high degree of survival (74% survival). However, only 18% of NADPH-d neurones survive (Davies and Roberts, 1987, Davies and Roberts, 1988). The increase in somatostatin reported by Beal et al. appears to be due to compensatory increase in this neuropeptide by surviving NADPH-d/SS/NPY interneurones surrounding the lesion core (Boegman, 1987, Boegman and Parent, 1988). Furthermore the discrepancy in numbers of surviving cholinergic neurones between these groups can also be explained. The higher death rate reported by Beal et al. when compared to other groups (Boegman, 1987,

Boegman and Parent 1988, Davies and Roberts 1988) is probably due to the extremely high level of QA microinjected by Beal et al. (240nmol).This contrasts with the 60 nmol used by Davies and Boegman.

The above work demonstrates that microinjection of QA into the rat striatum does not correspond fully to the pattern of cell death found in HD. However the role of excitotoxicity in the pathology of HD may still be of importance and it is generally believed that injection of 60nmol QA into the striatum provides a defined zone of neurodegeneration, and a useful model of Huntington's disease.

The creation and careful study of Huntington's transgenic mice have recently provided major insight into Huntington's disease. This mouse model has revealed a striking aspect of the pathology of HD that had been overlooked in human post-mortem tissue: intra-nuclear inclusions. Furthermore, this discovery has triggered a satisfying unity in the understanding of many neurodegenerative diseases, particularly those which involve trinucleotide repeat proteins. Discussion of this mouse model continues in chapter five along with that of polylglutamine repeat transcription factors.

Figure 1.3 Huntington's Disease

1.(Upper Left)George Huntington as a young man. Huntington was credited with excellent clinical observation by his contemporary, Sir William Osler, eventually Professor of Medicine at Johns Hopkins Hospital. Osler said of his 1872 paper "there are few instances in the history of medicine in which a disease has been more accurately, more graphically or more briefly described".[15] Osler was greatly interested in HD and undertook studies of diseased brains. He was frustrated that he could not discern any specific pathology (Harper, 1991).

2.(Upper right) Comparison of gross change in size of HD brain from a 39 year old female patient (bottom) with the brain of a normal 39 year old female (top). The dramatic shrinkage of the cortex can be seen easily (Harper, 1991).

3.(Lower left) Gliosis (demonstrated by Kluver-Barrera stain for astrocytes) in the caudate nucleus of a HD brain (bottom) compared with a section from a normal caudate nucleus (top) (x320). An increase in the number of astrocytes can be discerned.

4.The Guthrie Family (Lower right).This interesting photograph illustrates the autosomal dominant nature of Huntington's disease and hints at some of the clinical symptoms. The photograph shows the famous US folksinger Woody Guthrie as a child (left) and his family. Woody would die aged 55 of HD while his brother, George (to the front of the picture), would not develop the disease. Their mother, Nora, in shadow to the rear, can be seen standing rigidly with her arms behind her back to hide their choreiform movement. Her face is out of focus, possibly due to an inability to remain still and her thin figure hints at cachexia. She had suffered from HD for several years when this photograph was taken. Neuropsychiatric symptoms were present. Nora was confined to an asylum at 39 after attacking her husband, Charley (to the right of Woody) with a kerosene lamp. (Stephen N.Austad-Woody Guthrie Archives).

[15] Osler, W (1894) Case of heredity chorea. Johns Hopkins Hospital Bulletin 5:119-129 (Harper 1991).

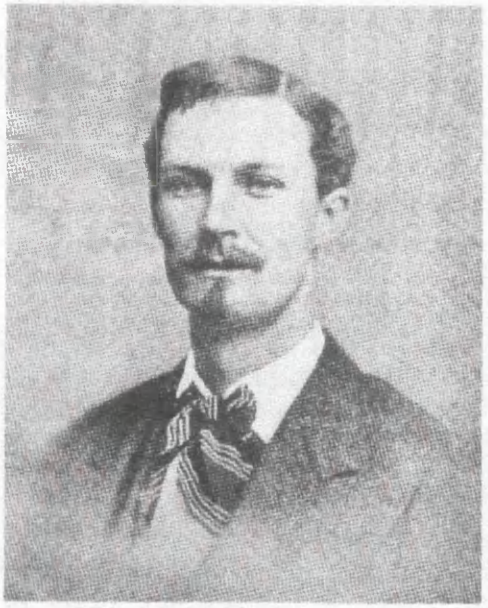

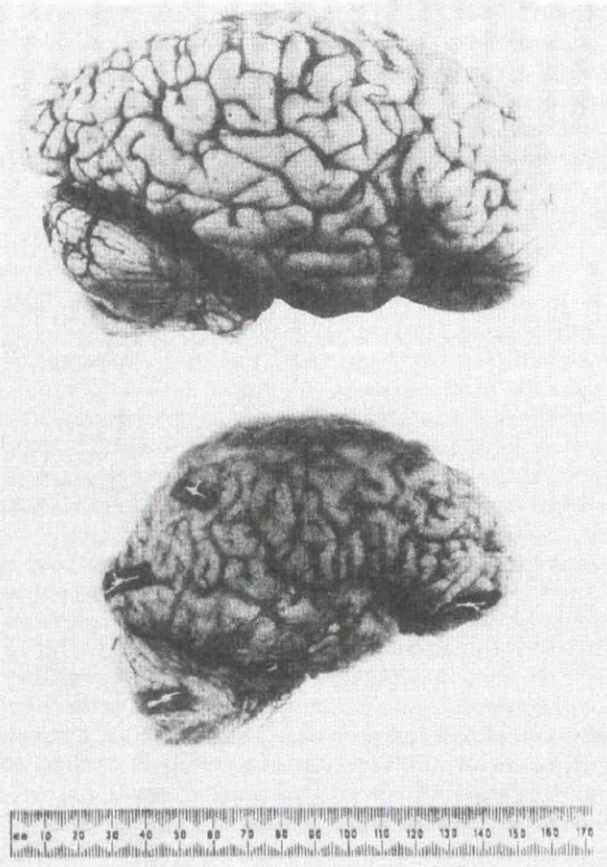

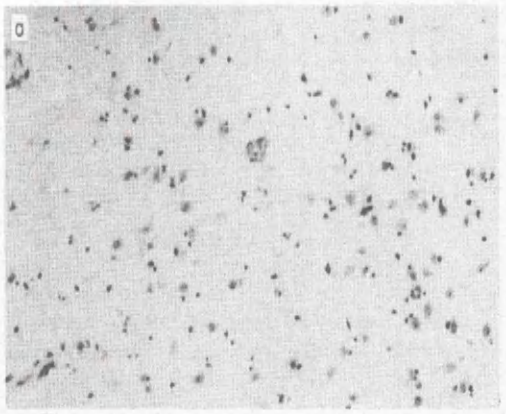
a

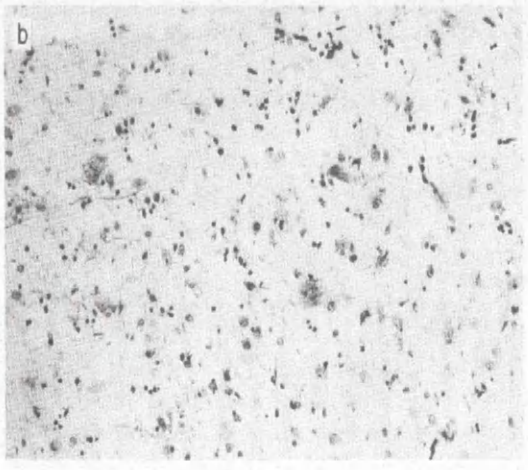
b

Figure 1.4 Huntington's Disease (continued)

1.(Upper left) CT scan demonstrating enlargement of the lateral ventricles due to atrophy of the caudate nucleus in a HD 45 year old male patient (right), when compared with a normal control of the same age which demonstrates a normal concave contour (left) (Harper, 1991).

2.(Upper right) Coronal sections through a HD brain (bottom) and a normal control (top). The caudate nucleus is labelled c, the putamen p. Enormous enlargement of the lateral ventricles can again be seen due to atrophy of the striatum (caudate and putamen). Cortical thinning can also be observed in the HD patient.

3.(Lower half) HD patient attempting to hold arms outstretched straight before her. Hyperkinesis (choreiform movement) is demonstrated by the inability to hold the limbs level and still (Harper, 1991)

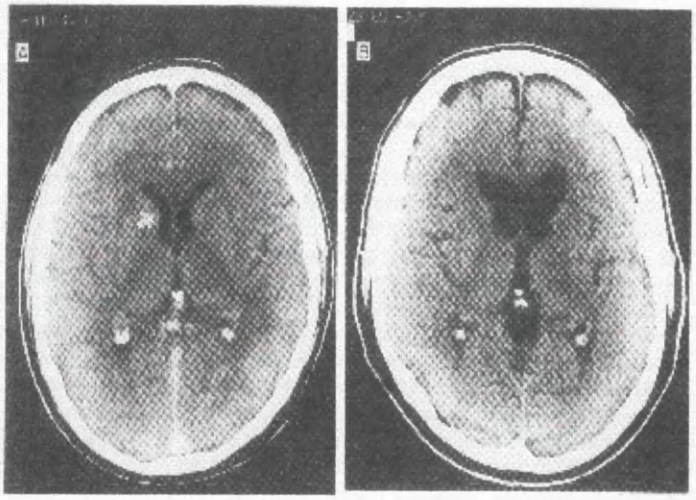
A
B

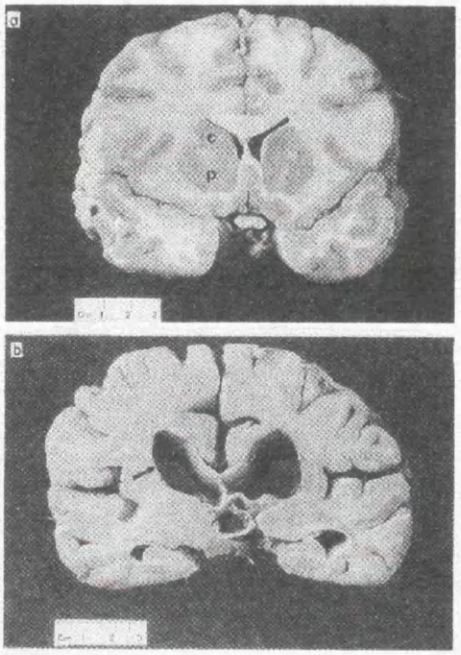
C
P
D

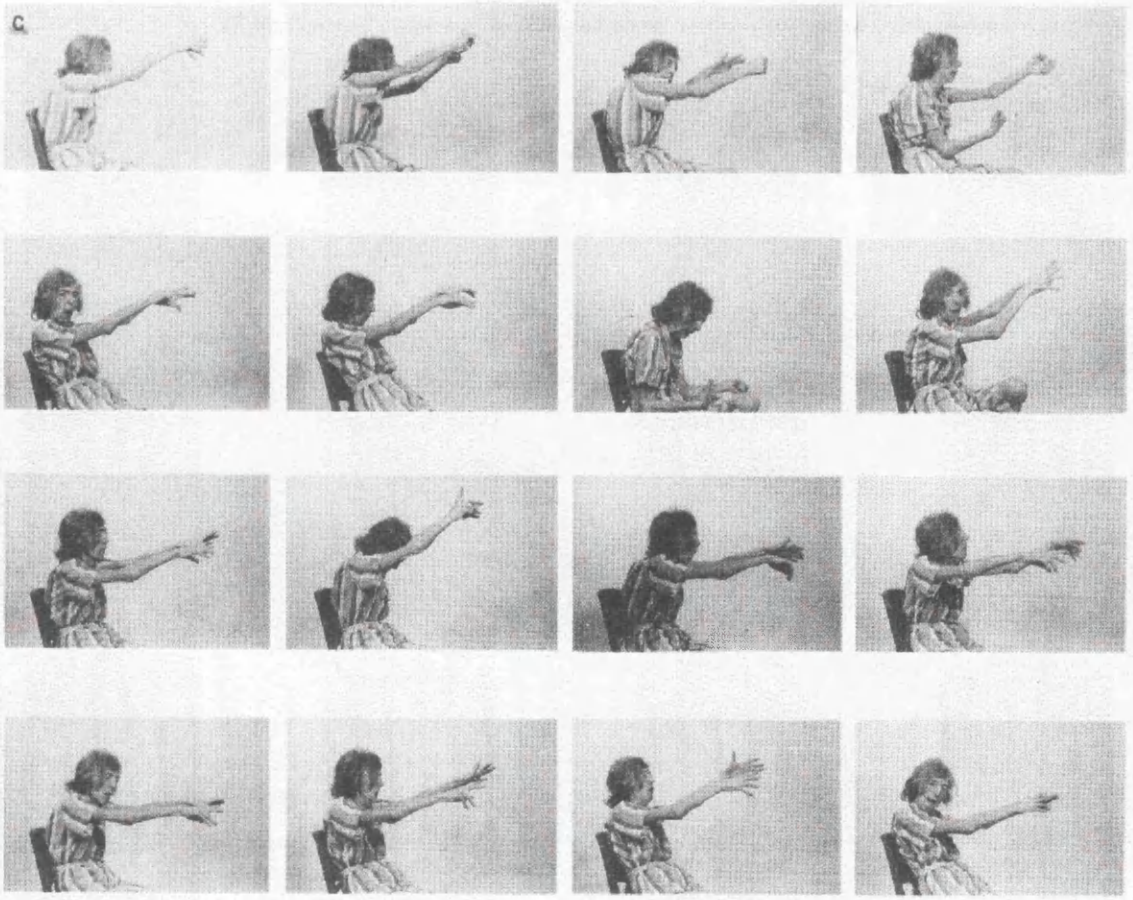
C

Ciliary neurotrophic factor

"Although reactive astroglia, reactive microglia, and invading blood-bourne macrophages appear acutely following an insult to the CNS, it remains uncertain how these cells influence neuron survival, axonal regeneration or recovery of neurologic function."

[Giulian et al. 1993]

Ciliary neurotrophic factor is a molecule central to this work, as its endogenous and exogenous activity is examined in the QA model of neurodegeneration. A brief outline of its role as a neuroprotective agent and inducer of reactive gliosis will follow. Discovery and understanding of this fascinating protein began with the culturing of ciliary ganglion neurones from chick embryos, which provided a useful bioassay to search for survival molecules in these cells (Helfland et al, 1976 and Adler, 1979). In 1984 the purification of a protein molecule from eight day chick embryo ciliary ganglion neurones and associated muscle cells with a molecular weight (Mr) of 20 400 D and an isoelectric point of five was described (Barbin et al, 1984). Cultures of these neurones could not survive for 24 hours without the addition of this protein, which was initially named ciliary neuronotrophic factor, now renamed ciliary neurotrophic factor (CNTF). Furthermore it was demonstrated that CNTF could support longer than 24 hours survival of certain cultures of chick and rodent sensory and sympathetic ganglia. CNTF was later identified from extracts of adult rat sciatic nerve by using chick embryo ciliary neurones to localise CNTF which had been transferred to nitrocellulose filters after gel electrophoresis (Carnow et al. 1985). Earlier experiments had demonstrated that chick CNTF could support neuronal survival when as little as 2 ng was loaded per lane. Two rat peptides were identified at 24 and 19 kD. This helped to accelerate and widen research into the biological properties of CNTF. Transgenic mice that expressed CNTF in neurones from the beginning of neuronal differentiation, had increased survival of dorsal root ganglion cells for a period during developmental apoptosis (Tolosano et al. 1996) although this neuronal survival did not extend into adulthood. Although CNTF does not appear to be expressed early in development (mRNA being undetectable in the sciatic nerve of newborns and first being detected on the fourth day after birth; Stockli et al. 1989), it does have potent influence on embryonic cell phenotype. E14/E17 cultures of cortical precursor cells can be stimulated to differentiate into astrocytes, rather than developing along a

neuronal lineage, after CNTF treatment (Bonni et al.1997). This indicates that CNTF (or any as yet unknown CNTF-like molecule with a developmental role) is important in gliogenesis. CNTF was demonstrated to promote 02A progenitor cells to differentiate to type 2 astrocytes in culture (Hughes et al. 1988). The molecule also had the ability to change neuronal phenotype, by altering the differentiation of E7 chick sympathetic neurones by stopping proliferation and inducing the expression of vasoactive intestinal peptide (VIP) (Ernsberger et al. 1989). In sympathetic cultures from newborn rats, CNTF increases choline acetyltransferase (ChAT) levels and reduces the activity of tyrosine hydroxylase (Saadat et al 1989). More recent work has also demonstrated that CNTF is able to induce a cholinergic phenotype in E14 serotonergic precursors; the 5-HT producing neurones were reduced by up to 90% but after removal of CNTF a change of phenotype back to 5-HT expression was observed (Rudge et al. 1996). CNTF also has the ability to be protective to motorneurones. 1.5ng/ml was able to maintain 64% of chick embryonic motorneurones in culture at three days and 53% at 5 days (Arakawa et al 1990). CNTF has also been found to prevent the death of motorneurones in the facial nerve of newborn rats after axotomy (Sendtner et al. 1990). Furthermore, transfected D3 cells secreting CNTF, when injected IP into the mouse mutant progressive motor neuronopathy (pmn), appeared to increase survival time and improve motor function (Sendtner et al. 1992). Further work has shown high levels of CNTF in myelin related Schwann cells in rat sciatic nerve which fell after axotomy, leading investigators to conclude that there is a direct interaction between the axon and Schwann cell. This interaction appears to determine the levels of CNTF expressed by the Schwann cells (Friedmann et al. 1992). Motorneurone-CNTF interaction suggested that CNTF may be therapeutic in some degenerative diseases (Sendtner et al. 1994) and led to clinical trials in which recombinant human CNTF (rhCNTF) was administered subcutaneously to patients suffering from amyotrophic lateral sclerosis (ALS). No improvement of isometric muscle strength was seen in those patients given rhCNTF compared to the control group and unpleasant side effects meant that only limited doses could be given to many patients (ALS Study Group, 1996). Despite this wide range of activities CNTF does not appear to be a target derived molecule with an important, if indeed any, role to play in neural development. There are two principal reasons for this, the first being that CNTF does not

appear to be secreted by cells that produce it. HPLC analysis of cloned and purified rat CNTF from sciatic nerve demonstrated no signal peptide sequence labelling the protein for export or consensus sequences for glycosylation (Stockli et al. 1989). Furthermore, expression of a cDNA clone in HeLa cells led to production but not secretion of CNTF. This does not rule out the active secretion of CNTF *in vivo* totally, however, since IL-1 also possesses no signal peptide but is released by activated macrophages after cleavage by the enzyme convertase (Kostura et al. 1989). Secondarily, CNTF is not expressed in rat sciatic nerve until after target regulated neuronal cell death is over, perhaps hinting further that CNTF is a lesion release molecule rather than one secreted by some unknown mechanism (Stockli et al. 1989).

Analysis of amino acids in CNTF from human, rat, rabbit and chicken demonstrates high sequence homology, with 80% of identical amino acid sequences occurring in four distinct clusters which appear to constitute alpha-helices. This provides CNTF with a 'four helix bundle' structure, very similar to that for growth hormone, IL-6, IL-11 and oncostatin M (Bazan, 1991). Site directed mutagenesis of CNTF indicates that that residue 63 (Arginine in rat, Glutamic acid in human) is essential for CNTF to maintain biological activity. Structural analysis of crystalline CNTF using multi-wave anomalous diffraction (MAD) reveals CNTF to be in a dimeric state, each unit adopting a 'double crossover four helix bundle fold', two helices of each monomer binding to create the dimer. The remaining helices show pronounced 'kinks' which are proposed to contact the CNTF receptor alpha component, but due to the low concentrations of CNTF detected in the extracellular environment, it is still proposed that monomeric CNTF is the biologically active form (McDonald et al. 1995).

The CNTF receptor complex comprises three separate components: two, glycoprotein 130 (gp 130) and leukaemia inhibitory factor receptor-beta (LIFRB) also act as receptors for other cytokines including IL-6 and leukaemia inhibitory factor (LIF) and are described as beta components. The CNTFRα is a member of the class I cytokine receptor family. These receptors (e.g. the gp 130 component of CNTFRα) possess an extracellular type I cytokine receptor family domain, a conserved length of 200 amino acids comprising two fibronectin type III modules of β pleated sheet structure. The region between two opposing Type I domains (eg. that between LIF and gp 130) is thought to act

as a 'pocket' into which the CNTFRα/CNTF complex can bind (Bazan, 1990; Patthy et al. 1990). However the actions of CNTF are largely restricted to neural tissue due to the distribution of the alpha component of the receptor (CNTFR-alpha/α). CNTFRα can be detected in the superior cervical ganglion, dorsal root ganglion, ciliary ganglion, ventral spinal cord, cortex, striatum, substantia nigra pars reticulata and trigeminal nucleus of the adult rat by *in situ* hybridisation (Ip et al, 1993). Immunocytochemistry localises CNTFRα to neurones of the monkey striatum (Kordower et al. 1997). Although CNTF appears not to be expressed at detectable levels in the newborn, CNTFRα and the other receptor components are expressed early in development, northern analysis indicating high levels as early as E11 in the rat embryo. This may indicate that there is a related molecule to CNTF that is capable of binding to the CNTFRα receptor, but has a function in regulating development. Further evidence for this is provided by transgenic 'knockout' studies (see below). CNTFRα has no signal transduction role, it being linked to the cell membrane by a glycosyl phosphatidylinositol (GPI) linkage and having no transmembrane domain, its sole purpose appearing to be the capture of CNTF (Davis et al.1991). IL-6 is also dependant upon such a component, IL-6α, but LIF binds directly to gp130. The initial event in receptor formation/activation appears to be the binding of CNTF to CNTFRα, which then binds to gp 130 which is anchored to the cell membrane by its transmembrane domain, followed by recruitment of the second signalling component, LIFRβ (Stahl and Yancopoulos, 1994). After dimerisation of the beta components, tyrosine phosphorylation of gp 130 and LIFR is reported and this appears to be due to the interaction of beta components with the JAK/TYK family of cytoplasmic protein kinases, Jak1, Jak2 and Tyk2 (Stahl et al. 1994), thereby initiating a downstream signalling cascade.

Mice lacking the CNTF gene displayed no behavioural or anatomical abnormality except for a slight reduction in the number of facial nerve motor neurones and possibly a reduction of spinal motor neurones (Masu et al. 1993). In contrast to this study, mice lacking the gene for the CNTFRα die soon after birth and have gross abnormalities of their motor systems with reduced numbers of motor neurones in brainstem nuclei and spinal cord, indicating that another ligand may activate CNTFRα during development (DeChiara et al. 1995).

There is currently some evidence that CNTF may have therapeutic potential in HD due to its apparent protection of striatal neurones from QA lesion. CNTF (0.78mg/ml, 9.84 micrograms/day) or the CNTF receptor agonist 'Ax 1' was administered by an osmotic pump into the striatum of rats via a cannula three or four days before injection of 50 nmol of QA. This protocol was demonstrated to provide significant 'marked protection' of striatal medium sized spiny neurones, as determined from Nissl stained nuclei counts, from excitotoxicity (Anderson et al. 1996). Implantation of modified human CNTF secreting fibroblasts (BHK cell line) into the rat lateral ventricle twelve days before injection of 225 nmol of QA demonstrated significant survival of projection neurones and cholinergic interneurones, but not NADPH-diaphorase neurones (Emerich et al. 1995). These studies are currently providing a basis to administer CNTF to HD patients, in much the same way that the protection of motorneurones by CNTF initiated clinical trials in ALS patients.

Evidence is growing that CNTF release is central to activating brain glia. Before we discuss the experimental evidence for this, it is worth briefly considering the natural history of reactive gliosis. Gliosis is a morphological and molecular alteration of astrocytes and microglia, which is a ubiquitous response by the mammalian CNS to many forms of insult; traumatic, infectious, genetic or idiopathic (Norenberg 1994, Eddleston and Mucke, 1993). Gliosis may be induced experimentally by excitotoxins, such as quinolinic acid (Popoli et al. 1994) and kainic acid (Jorgensen et al, 1993) and ibotenic acid (Hantraye, 1990), as well as cytokines, including interleukin-1 (Giulian et al. 1988). Gliosis is identified by an increase of the cytoskeletal protein glial fibrillary acidic protein (GFAP) in astrocytes (Hatton et al. 1993) whereas microglia demonstrate an increase of various receptors and surface antigens such as OX-42 (Shaw et al. 1990). Gliosis is seen in the brain of Huntington's disease patients at post-mortem examination in the striatum and cortex (Selkoe et al. 1982 and page 52) and globus pallidus (Wakai et al. 1993). The molecular mechanisms responsible for induction of gliosis are not well understood, but there are strong indications that a wide variety of cytokines play an important role. The interleukins IL-1, IL-2, IL-6 and TNF-alpha appear to be involved in glial activation (Balasingham et al, 1994) by directly binding to astrocyte borne receptors and altering

patterns of gene expression. Work in this thesis includes the study of CNTF for, unlike the molecules listed above, little work had been undertaken concerning gliosis up to 1995, and it seemed doubly interesting because of its restriction to the nervous system and 'lesion-release' nature. CNTF has been demonstrated to induce astrogliosis and activation of microglia, as determined by increased GFAP and microglial markers ED1 and OX6. In the neonatal (PD5) rat 48 hours after intracerebral injection of 0.5ug of CNTF, leading to hypertrophied astrocytes reaching from the pial surface to the corpus callosum (Kahn et al. 1995). No contralateral spreading of microglia was noted, but interestingly when CNTF was co-injected with TNF-alpha (.25ug) a synergistic activity was noted, astrogliosis being more dramatic and intruding into the contralateral hemisphere. It has been proposed that this contralateral spreading is mediated by gap junction communication. Reduced staining of non-hypertrophied astrocytes was seen in control animals. Intracerebral injection of CNTF into adult mice (.36ug) also produces an increase in GFAP and as little as 50ng was capable of 'widespread induction' of GFAP. Mice injected with inactivated CNTF showed no GFAP increase, except immediately around the injection site. Furthermore, the creation of a transgenic mouse that overexpressed CNTF caused an increase in the number of GFAP positive cells in the olfactory bulb and spinal cord, but intriguingly, nowhere else in the CNS (Winter et al, 1995). CNTF administered to the thalamus of adult rats after cingulotomy via minipump delivering 84ug of CNTF over two weeks also induced astogliosis. Hypertrophied GFAP positive astrocytes were seen compared to weaker GFAP staining of non-hypertrophied cells in control animals infused with vehicle solution (Clatterbuck et al.1996). PCR of rat optic nerve, which contains no neuronal cell bodies, using 250ng of total RNA and oligonucleotide primers for both CNTF and the CNTFRα, yielded amplification products at expected size for both CNTF and CNTFRα. This further supports earlier work indicating that CNTF is both produced by and active upon certain types of glial cells. Part of this thesis work concentrates upon the action of exogenous CNTF upon reactive glial cells in the rat striatum. As this work was completed, similar work was published by Lisovoski et al. demonstrating that adenovirus mediated transfer of CNTF into the rat striatum causes hypertrophy of astrocytes. This, along with the work in this thesis, provides further evidence for CNTF being an endogenous glial activator (Lisovski et al.

1997). That astrocytes may be both synthesisers and recipients of CNTF, is indicated by the immunocytochemical localisation of CNTF in cultured rat brain cells exhibiting the morphology of type I astrocytes (Stockli et al. 1991). in *situ* hybridisation localises the CNTFRα in neurones in layer V of the cerebral cortex, hippocampal formation and subependymal layer of the third ventricle in rats. However, after aspiration lesion to the cortex, CNTFRα localises in cells bordering the wound site, suggesting astrocytic, fibroblastic or macrophagic localisation (Rudge et al. 1994). Similar observations were made (Ip et al, 1993) following aspiration lesion of the cortex and underlying dorsal hippocampus also using *in situ* hybridisation. Northern analysis of cultured hippocampal astrocytes detected a 2.2Kb transcript corresponding to CNTFRα as also detected in adult rat brain and cultured hippocampal neurones (Rudge et al. 1994). Aspiration lesion of rat striatum induced maximal gliosis, as determined by GFAP immunocytochemistry, seven days after lesion, astrocytes stained being 30 times greater than in normal striatum. Northern blot analysis demonstrated that CNTF mRNA was most highly expressed at this seven-day peak of astrogliosis, again providing some evidence for astrocytic CNTF production (Asada et al. 1995).

Clues to the intracellular pathways that may be activated by CNTF and perhaps lead to reactive gliosis have begun to appear. CNTF induces tyrosine phosphorylation of the transcription factor p91 (also known as STAT [signal transducer and activator of transcription]1α) in SK-N-MC cell cultures as well as phosphorylation of the related proteins p89 and p88, as determined by western blots. It is not yet known if phosphorylation of p91 is carried out by the Jak1/2 or Tyk-2 kinases associated with the CNTF receptor complex. Protein binding to the p91 consensus sequence by SK-N-MC cell preparations after treatment with CNTF on EMSA was visible, but no shift was seen in control preparations (Bonni et al. 1993). This sequence was named CNTF-RE (**TTC**CCCG**AA**) and sequences resembling it are present in human c-fos, mouse c-fos, mouse tis-11, rat jun B, rat SOD 1. Related sequences are present in both mouse and human GFAP genes, the latter indicating that phosphorylated p91 may play a role in partially activating astrocytes. Work by Perez-Otano et al. Hinted at the possible involvement of the NF-κB transcription factors. Rats injected IP with kainic acid demonstrated reactive gliosis in the hippocampus and entorhinal cortex and the p65

subunit of the NF-κB family of transcription factors was expressed in both non-neuronal and neuronal cells in the damaged regions two days after injection. Double immunocytochemistry (GFAP and p65) confirmed localisation of NF-κB in astrocytes. EMSA demonstrated binding to the NF-κB consensus DNA in kainate treated hippocampal extract but not in controls (Perez-Otano et al. 1996). Interestingly, genes such as those coding for the interleukins and tumour necrosis factor (TNF), possess a NF-κB binding site (Miyamoto and Verma, 1995) and TNF and many interleukins are secreted by both astrocytes and microglia/macrophages (McGeer and McGeer, 1995).

Figure 1.5. Structure of CNTF and CNTF Receptor Formation.

1. (Upper left) A line diagram of the three dimensional structure of CNTF illustrating the 'double crossover four helix bundle fold'. The position of residue 63 is marked, which is crucial to the function of CNTF. Mutation of this amino acid leads to the loss of CNTF activity (McDonald, et al. 1995).

2. (Upper right). A computer generated image of the CNTF molecule again demonstrating the four alpha helix bundle structure of CNTF. The three dimensional structure of CNTF is related to that of IL-6, IL-11 and oncostatin M (Promega).

3. The upper part of the diagram below schematically illustrates the shared Class I cytokine receptor components which comprise the receptors for LIF, IL-6, OSM and IL-11, as well as CNTF. Note the specific alpha component of the CNTFR complex which converts the LIF receptor to a CNTF receptor. The lower part of the diagram illustrates recruitment of the components of the CNTF receptor complex, the process beginning with the capture of CNTF by the CNTFR alpha component which is then able to bind to a beta (Class I cytokine receptor) component (gp 130 or LIFR). Formation of the receptor complex activates phosphorylation of downstream signalling proteins such as p91 (STAT1 alpha) via the receptor associated JAK (or TYK) cytoplasmic kinases.(Stahl and Yancopoulos, 1994).

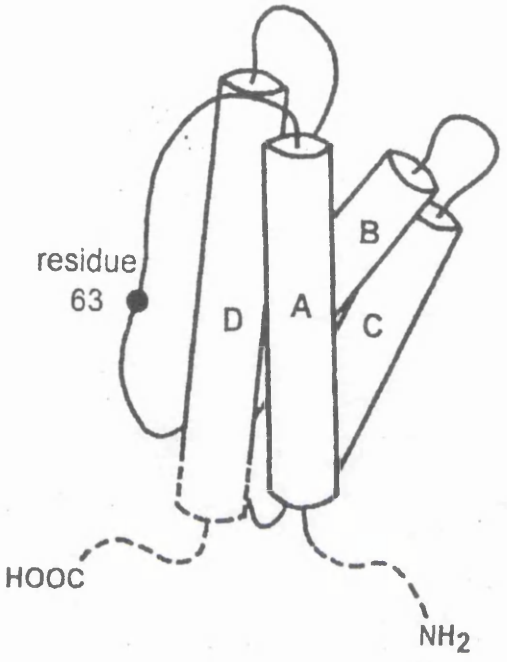
residue
63
D
A
B
C
HOOC
NH2

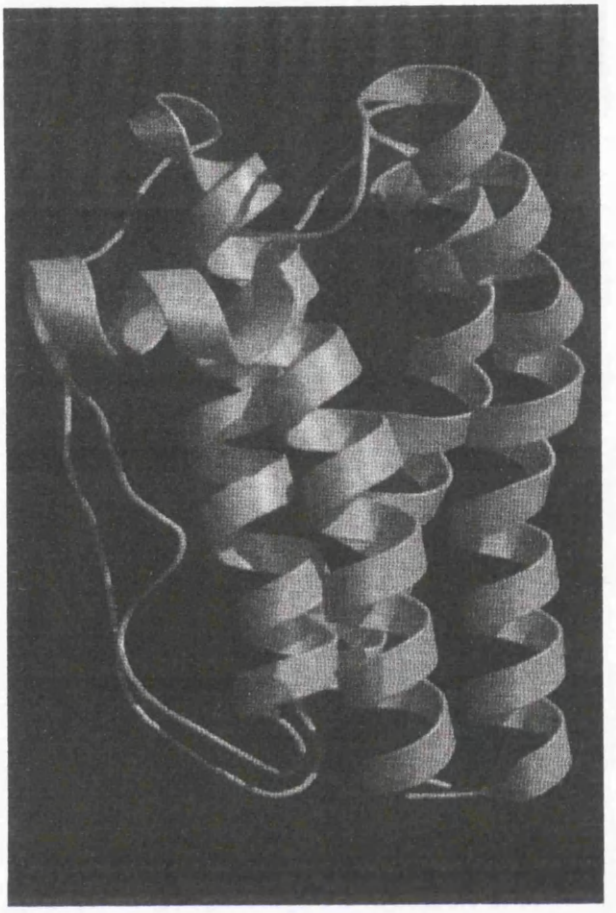

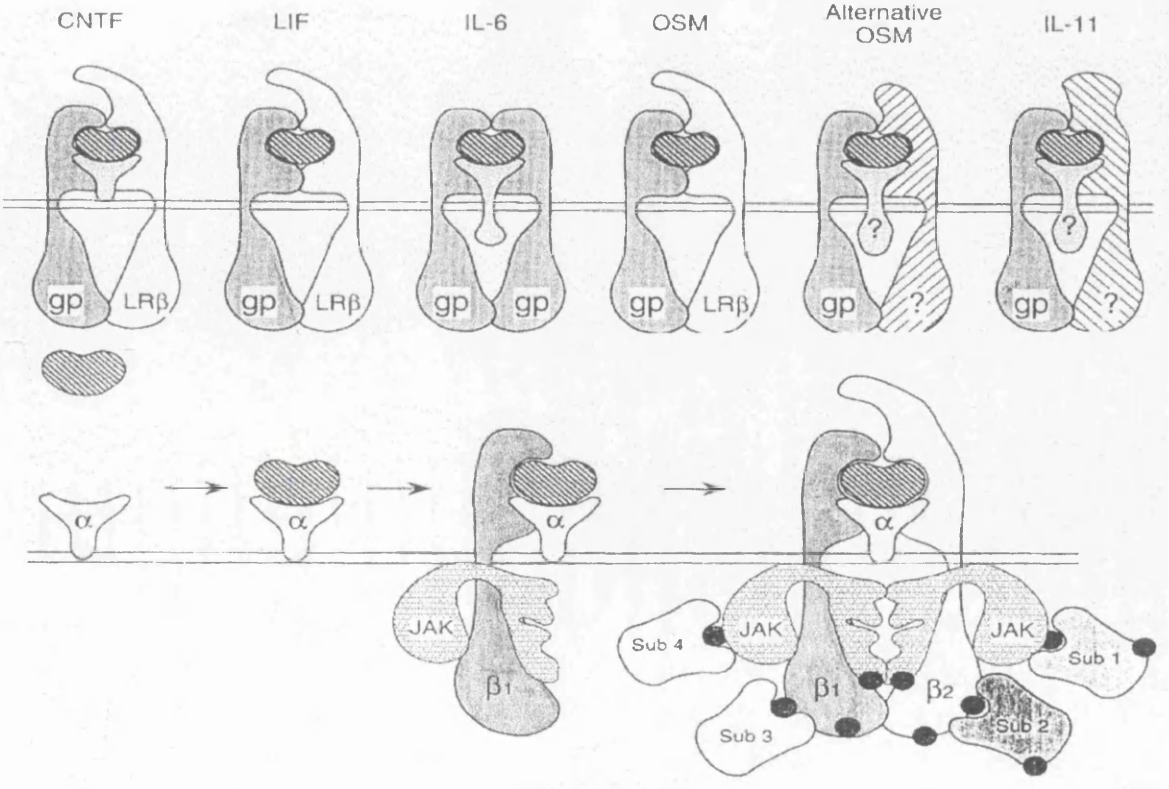
CNTF
LIF
IL-6
OSM
Alternative OSM
IL-11
gp
LRβ
?
α
JAK
β1
β2
Sub 1
Sub 2
Sub 3
Sub 4

Figure 1.6 CNTF and the Response to CNS Injury

1.(Upper left) Two forms of CNTF are visible upon western blots (PAGE). In this case 12 micrograms of human recombinant CNTF was loaded in lane A (without heating in SDS sample buffer) and B (after heating in SDS sample buffer). In B, ~40 kD and ~20 kD protein bands are visible (McDonald et al. 1991).

2. (Upper right) Detection of CNTF mRNA by *in situ* hybridisation following cortical aspiration lesion in rat. The CNTF mRNA is localised to the edge of the wound site, the region where reactive astrocytes are also seen to proliferate (Ip et al. 1993).

3. (Middle left) Immunocytochemical localisation of CNTF in cultured rat hippocampal astrocytes (Rudge et al. 1994).

4. (Middle right) Detection of CNTF receptor mRNA by *in situ* hybridisation following aspiration lesion. As well as widespread receptor mRNA being visible throughout the CNS (particularly in the hippocampus and cortex), as is seen in control brain, increased receptor mRNA can be seen along the wound border (Rudge et al. 1994).

5. (Lower diagram) GFAP immunoreactivity in thalamus of control rat brain (left) and following CNTF treatment via intraventricular infusion (right). Prominent immunoreactivty of reactive astrocytes can be observed in the CNTF treated thalamus (Clatterbuck et al. 1996).

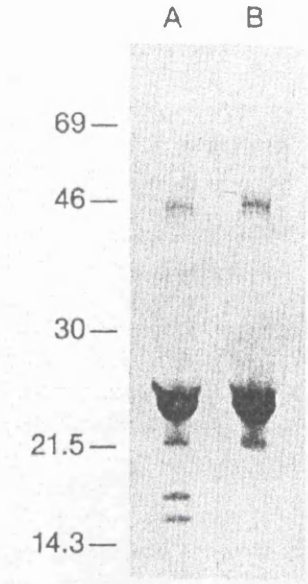
A
B
69
46
30
21.5
14.3

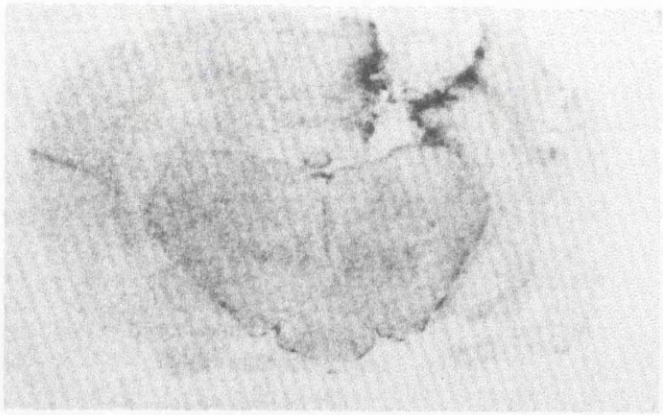

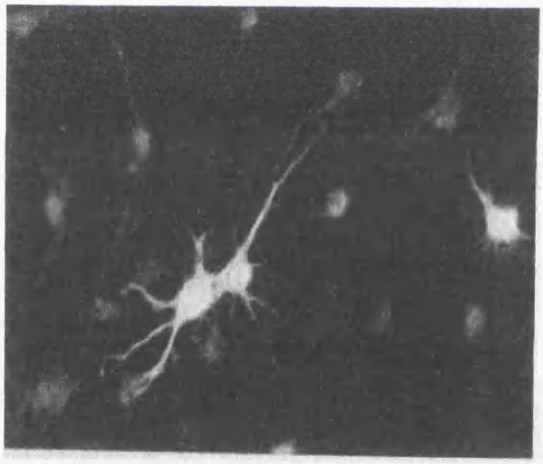

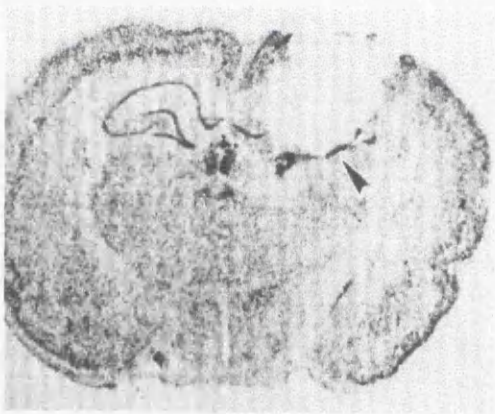

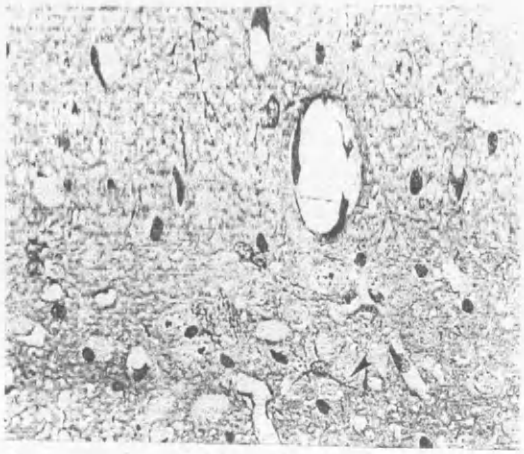

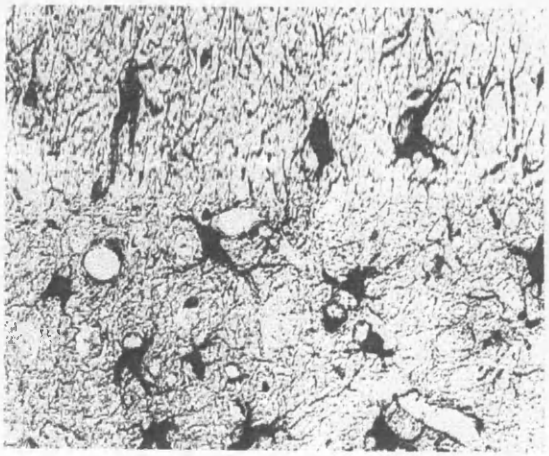

The NF-κB family of transcription factors: expression and function in the CNS

"..evidence has begun to accumulate that NF-κB is involved in brain function, particularly following injury and in neurodegenerative conditions.."

[O'Neill and Kaltschmidt, 1997]

The nuclear factor kappa B (NF-κB)[16] family of transcription factors were discovered as DNA binding proteins which could complex with the κB site on the light chain immunoglobulin enhancer (Sen and Baltimore, 1986). The NF-κB transcription factors differ from the immediate early genes such as Fos and Jun. The action of IEGs is controlled by gene induction via such proteins as serum response factor (SRF) or CRE binding protein (CREB) and protein synthesis. NF-κB proteins are already present in the cell bound to cytoplasmic inhibitors. Therefore they are not dependent upon a signalling pathway leading to the nucleus. Upon activation, they can immediately translocate to the nucleus, providing the cell with fast reaction to stimuli and not necessarily requiring an increase in cellular NF-κB protein load (Latchman, 1995, and Gilmore, 1996). This capacity for rapid response is combined with a high degree of sensitivity to activating stimuli. In B cell precursors activation of ten IL-1 receptors is sufficient to lead to a NF-κB response within minutes of ligand binding (Stylianou et al. 1992). When this sensitivity and speed is combined with the large number of genes which are strongly induced by NF-κB, many of which are intra and extracellular messengers (including cytokines, neuropeptides and interferons), the capacity for this family of proteins to rapidly amplify signals between cells, and throughout a tissue, is enormous (O'Neill and Kaltschmidt, 1997).

The NF-κB family appears to exist as two distinct groups: those that require proteolysis to become mature, functional proteins (Class1) and those that are not derived from precursors (Class 2). The first group includes p50/NF-κB 1 (Kieran et al. 1990, Ghosh et al. 1990 and Meyer et al. 1991) which is derived from the precursor p105 and p52/NF-κB 2 (Schmid et al. 1991) which is cleaved from p100. In mammals, the second

[16] The term NF-kB is usually used to describe the p50/p65 heterodimeric complex, but within this thesis the term refers to all Rel proteins concerned, namely p65,p50 and p52.

group consists of p65/Rel A (Nolan et al. 1991), Rel/c-Rel (Wilhelmsen and Temin, 1984) and Rel B (Ryseck et al. 1992). These proteins obtain their name from the three hundred amino acid long so-called Rel homology domain (a highly conserved N-terminal sequence) they possess which contains the DNA binding region, dimerization domain and nuclear localisation signal (NLS). The nuclear localisation signal of the NF-κB proteins may be masked preventing nuclear translocation of the proteins from the cytoplasm thereby preventing their role in transcriptional activation. Those derived from precursor molecules (p105/p100) possess seven ankyrin repeat domains (ANK) within their C-terminus which, through folding of the molecule via a glycine rich 'hinge' region can mask the NLS (Henkel et al. 1992). ANK domains are a commonly found mechanism involved in protein interaction (for review; Michaely and Bennett, 1992). Cleaved precursor molecules (ie.p50/p52) and the Rel members of the NF-κB family may be retained in the cytoplasm by binding of the NLS to the five to seven ankyrin repeat domains found within the IκB (Inhibitor κB) family of proteins. Mutation of these IκB ankyrin domains prevent these molecules from inhibiting NF-κB DNA binding (Inoue et al. 1992). The IκB family includes IκB-alpha (Baeuerle and Baltimore, 1988[1]), IκBβ (Davis et al.1991) and IκB-gamma (Inoue et al. 1992[2]). IκB-gamma is an interesting molecule, for it corresponds exactly to the C-terminal ankyrin repeat domain of the p50 precursor p105. It is indeed translated from a 2.6kb p105 mRNA variant, producing the 70 kD IκB-gamma, rather than the protein p50, which derives from a 4.0kb mRNA variant (Inoue et al 1992). However, the 2.6 kb mRNA fragment could not be detected in brain. Of interest is that Inoue et al. also discovered a 37 kD protein which was originally thought to be a cleavage product of the 70kD IκB-gamma protein when derived from the p105 precursor, which was reactive to antisera specific to p105 or IκB-gamma. Further structural analysis revealed, however, that the 37 kD protein was unrelated to the 70 kD IκBβ and not derived from the 2.6kb mRNA fragment (Inoue et al 1992). IκB may not be merely a family of cytoplasmic inhibitors, however. *in vitro* experiments have shown that IκB can remove bound NF-κB from DNA by diffusion, and IκB is small enough to move through nuclear pores, although it is not clear if this system operates *in vivo* (Zabel et al.

1990, Gilmore, 1996). One of the genes induced by NF-κB is in fact IκB-alpha, which indicates a self-regulating ability, particularly if IκB-alpha can enter the nucleus and remove NF-κB (de Martin et al., 1993, Gilmore, 1996). It must be remembered that NF-κB is constitutively active in some cells, but may also have to respond to external stimuli placing demands upon the cell.

Therefore, there are two types of complexes of NF-κB proteins found retained in the cytoplasm. Homo/heterodimers (eg. p65:p50) bound to one of the IκB family of molecules, that can enter the nucleus following phosphorylation triggered release of the IκB protein, which may be subsequently degraded via the ubiquitin-proteasome pathway. The second type of complex being that of a mature NF-κB protein bound to an unprocessed NF-κB precursor which can, for example, undergo phosphorylation via a protein kinase (Ghosh and Baltimore 1990) to be processed to a mature configuration before translocation to the nucleus can occur. It has been estimated that the vast majority of cellular p65 is retained by being bound in the precursor state, or bound to another precursor (80%), while the remainder is bound to IκBα or other IκB molecules (Rice et al. 1992). IκBα phosphorylation occurs upon serines 32 and 36 and that of IκBβ on serines 19 and 23. Phosphorylation *in vitro* can be mediated by protein kinase C, cAMP dependent protein kinase and casein kinase II (Baeuerle and Henkel, 1994). The kinase responsible for *in vivo* phosphorylation eluded discovery for some time, although it was believed to be part of a large 700 kD complex which required ubiquitination for activation, which and was indeed found to phosphorylate IκBα on serines 32 and 36 (Chen et al. 1996). However, recently these kinases have been identified. These proteins were indeed serine kinases which were discovered in HeLa cells by biochemical purification of the S32/S36 phosphorylation activity of IκBα after administration of tumour necrosis factor alpha (TNFα) by Michael Karin's group. The kinase proteins indeed comprised part of a large 500-900 kD protein complex and were isolated by purifying the fraction which retained IκBα phosphorylation activity, as 85 and 87 kD molecules. These proteins were labelled IKKα (I-κB kinase-alpha) (DiDonato et al. 1997) and IKKβ (Zandi et al.1997, Stancovski and Baltimore, 1997), respectively. The 85 kD IKKα had been previously sequenced and identified as a serine-threonine kinase labelled CHUK (Connelly and

Marcu, 1995). The IκB proteins appear not to vary in their affinity for c-Rel and p65, but in their response to different stimuli that activate NF-κB, IκB-alpha phosphorylation providing a rapid and transient phase of NF-κB actvity, IκB-beta a more persistent phase of NF-κB activity (Thompson et al. 1995). Despite the conversion of the p100 and p105 precursors to p50 and p52, "full length p100 and p105 when synthesised in vivo can bind DNA as well as their processed counterparts, p52 and p50" (personal communication to T.Gilmore from D. Baltimore in Goodbourn, 1996). The binding affinity of these proteins is reduced, however.

Little is known about the proteases involved in NF-κB precursor cleavage. However cleavage of p105 and p100, which occurs within the glycine rich hinge region, is known to involve an ATP dependant protease in COS cells (Fan and Maniatis, 1991). It has also been demonstrated that the protease of the HIV1 virus can process p105/p50 in vivo (Riviere et al. 1991).

Although IKK phosphorylation of the IκB proteins or proteolytic cleavage of NF-κB precursors may produce proteins capable of entering the nucleus, NF-κB factors are phosphoproteins and require phosphorylation to become active. NF-κB proteins possess a protein kinase A (PKA) recognition and phosphorylation site in the Rel domain (Arg-Arg-X-Ser) close to the amino acids required for nuclear localisation and protein (NF-κB) binding, phosphorylation occurring upon the serine residue (Gilmore, 1996). When cells are stimulated with phorbol ester, hyperphosphorylation of the Rel domain of p50 results. This increased phosphorylation of p50 correlates with increased protein-DNA binding (Li et al. 1994).

NF-κB proteins bind to DNA with high affinity, the p50 homodimer wrapping tightly around the consensus site producing a form described by Baltimore as a 'butterfly' (Baltimore and Beg, 1995). The main form of the consensus binding site is GGGACTTTCC[17]. When complexing to DNA, NF-κB proteins may require interaction with high mobility group-like proteins (HMG) to carry out gene induction. An example is the κB site in the IFN beta promoter which requires the binding of NF-κB and HMG I(Y). HMG I(Y) apparently binds to the minor groove of DNA while NF-κB contacts the major

groove and as such the HMG protein is a promoter specific coactivator of NF-κB, to allow transcriptional activation of IFN beta. Furthermore, NF-κB proteins can directly interact with other transcription factors, including the AP-1 proteins c-Jun and c-Fos, which bind to the Rel domain of p65 via the AP-1 bZIP leucine zipper domain (Stein et al. 1993). The activity between p65 and AP-1 appears to be synergistic, the combination of p65 plus Fos or Jun demonstrating increased protein-DNA binding to the 5' long terminal repeat of the HIV1 promoter. NF-κB has also been demonstrated to interact with the general factors TBP and TFIIB and this is probably a prerequisite for initiating transcriptional activation (Kerr et al. 1993, Xu et al, 1993), and the zinc finger proteins glucocorticoid receptor (GR) (Ray and Prefontaine, 1994) and Sp1 (Perkins et al. 1993), as well as the activating transcription factor family (ATF) and NF-IL-6 (for reviews see Miyamoto and Verma 1995, Thanos and Maniatis 1995 and Baeuerle and Baltimore 1996). This dynamic interaction with other factors presents an important fact, namely that activated NF-κB can have an impact upon transcriptional activation without binding to DNA itself, possibly acting as activator or repressor, depending on the circumstances (Gilmore, 1996). An active example of NF-κB interactivity is demonstrated by the activation of the c-jun N terminal protein kinase (JNK) by inducers of NF-κB, namely UV radiation and the inflammatory cytokine IL-1 alpha. JNK phosphorylates c-jun and ATF-2, both of which can then interact with NF-κB (Gupta et al. 1995). The interaction of NF-κB (p65/p50) with these molecules may be dependant upon co-operative binding of the HMG I (Y) proteins and possibly other transcription factors.

A great diversity of stimuli are capable of activating NF-κB. These include the interleukins, including IL-1 and IL-6, tumour necrosis factor-alpha, activators of protein kinase C, oxidative stress, phorbol ester, HIV, the neurotrophin nerve growth factor (NGF) (Tong and Perez-Polo, 1996) (via the p75 neurotrophin receptor), cellular depolarisation/synaptic activity/LTP, the amyloid B peptide and developmental changes. In response to the variety of stimuli which activate it, NF-κB has in turn an enormous range of genes it is able to induce. These include IL-1, IL-6 (Sparacio et al. 1992), IL-2 receptor alpha chain HIV viral proteins, tumour necrosis factor-alpha, cellular adhesion

[17]This may be generally determined as GGGRN/NYYCC, R= purine, N=purine or pyrimidine, Y=pyrimidine (Gilmore, 1996).

molecules, enzymes such as COX-2 and iNOS, interferons, immunoreceptors of MHC class I, and the neuropeptides dynorphin and proenkephalin (see reviews Baeuerle and Henkel, 1994, Miyamoto and Verma, 1995, Thanos and Maniatis, 1995, Barnes and Karin, 1997 and O'Neill and Kaltscmidt, 1997).

NF-κB has been implicated in the inflammatory process due to the cytokine genes, which induce inflammation, possessing NF-κB binding sites in their promoter regions. These genes include the interleukins IL-1, IL-2, IL-6, IL-8 and IL-2 receptor alpha chain (see above). It appears that glucocorticoids, widely used clinically as anti-inflammatory agents, prevent NF-κB from inducing interleukin gene expression, as well as directly down regulating IL-6 gene expression. Two main modes of operation appear to occur, the first being a direct interaction the activated glucocorticoid receptor and p65 in the nucleus, making it physically unable for p65 to bind the κB site (Ray and Prefontaine, 1994; Mukaida et al. 1994 and Caldenhoven et al. 1995). Secondly, the glucocorticoid dexamethasone can increase expression of IκB alpha, thereby inhibiting NF-κB and preventing it from activating interleukins and perhaps other inflammation mediating genes (Scheinman et al. 1995 and Auphan et al. 1995). Furthermore, the salicylate compounds, including aspirin and sodium salicylate also appear to be able to reduce NF-κB activity binding activity (Grilli et al. 1996).

Interest in the role of NF-kB in the CNS was initiated when it was demonstrated that the HIV virus that causes AIDS demetia complex (ADC) possesses an NF-κB site. In neuronal cultures transfected with the HIV-promoter-B-galactosidase constructs NF-κB was demonstrated to activate the HIV promoter (Rattner et al. 1993). Since this observation has been made, a greater insight into NF-κB function in the CNS has been obtained. During mouse and rat brain development three main NF-κB factors can be detected in rat brain homogenates, albeit relatively late in embryo development, in the 17 day old embryo and five day old pup, and identified by antibody neutralisation experiments. These factors were two heterodimers consisting of c-Rel/p65 and p65/p50 and a p50 homodimer, all being generally expressed. In the adult rat p65/p50 was still generally expressed and the major detectable factor in adult brain (Bakalkin et al. 1993). Further evidence that NF-κB is not essential in early development is provided by NF-κB transgenic 'knockout mice'. Mice in which the p65 gene had been ablated did not die

until embryonic day 16 (Beg et al.1995), roughly corresponding with the time of activation of the p65 heterodimers reported by Bakalkin et al. 'Knockouts' of p50 (Sha et al.1995), c-rel (Kontgen et al. 1995) and rel B (Weih et al.1995) all survived beyond birth. This relative unimportance of NF-κB in mammalian development contrasts with the function of similar proteins in *Drosophila*, in which the NF-κB related protein DORSAL appears to be essential for normal embryogenesis, being responsible for the ventralisation effect. DORSAL is retained in the cytoplasm in a similar manner to p50, p65 etc. by the IκB homologue CACTUS (St. Johnston and Nusselin-Volhard, 1992)[18]. Work by Schmidt-Ullrich et al. undertook to elucidate the anatomical localisation of NF-κB during development has revealed the expression of p105 throughout development of the mouse CNS by inserting a construct containing the B-galactosidase (lacZ) reporter gene under a NF-κB (p105) promoter. At embryonic day 12.5 lacZ expression could be detected in the spinal medulla and the cerebellar, olivary and pontine nuclei. This was the earliest localisation of NF-κB in the mice, the next system to express lacZ was the immune, with localisation in the thymus being observed at embryonic day 13.5. At day 18.5 lacZ expression could also be detected in the limbic system (epithalamus) and remained in the regions observed at day 12.5. Use of anti-B gal and anti-GFAP antibodies demonstrated that B-gal could not be co-localised with GFAP immunoreactivity, indicating that only neurones were expressing NF-κB. However, lacZ expression after birth began to spread throughout the CNS, appearing in the cerebral cortex on post-natal day 6 and the cerebellar cortex on day 8. In the adult, lacZ expression was observed in the cortical layers (except layer one), the dentate gyrus and areas CA1 and CA3 of the hippocampus, as well as the granule cells of the cerebellum. This indicates a role for NF-κB in the late development of the CNS in general, but not during early embryogenesis (Schmidt-Ullrich et al. 1996). The hypothesis of Schmidt-Ullrich et al. that NF-κB is predominantly involved in maintenance of tissues after maturation, appears to be further confirmed by another transgenic mouse created using a HIV-LTR-lacZ construct, also under an NF-κB promoter, which demonstrates expression of lacZ at similar time points (Buzy et al. 1995).

[18] In *Drosophila*, several genes have been identified that appear to define a 'prototypic' NF-κB system similar to that observed in mammals. As well as DORSAL and CACTUS, a gene named pelle encodes a serine kinase that is likely to

In many cell types, NF-κB is an inducible transcription factor, but it appears that both immune cells and and many types of neural cells possess constitutively active NF-κB. Work by Kaltschmidt et al. demonstrated the following: 1. Neuronal cultures of hippocampal and cortical cells from rat demonstrate constitutive expression of a luciferase reporter gene under HIV-1 promoter dependant upon NF-κB binding, which can be abolished when IkB-alpha was co-expressed in culture 2. EMSA of rat cortical tissue also demonstrates constitutive NF-κB activity 3. Immunocytochemistry for p65 of mouse cortex and hippocampus demonstrated staining of a subset of neurones (Kaltschmidt et al. 1994).

Various stimuli have been observed to activate NF-κB in the CNS. Probably of greatest interest is that activation of ionotropic glutamate receptors (NMDA/AMPA) via the agonist kainate (or by increasing extracellular potassium levels) in a primary cerebellar granule cell culture produces NF-κB (p65) activation. A 5 minute pulse of kainate (a duration which did not produce neurotoxicity) exposure in cultures from 5 to 8 day old rat cerebellum produced strong p65 immunoreactivity 45 minutes later (Kaltschmidt et al. 1995). It was further reported that this activation of p65 could be blocked by administering an antioxidant, pyrrolidine dithiocarbamate (PDTC) for 10 minutes prior to kainate exposure. This strongly indicates that in this paradigm at least, the activation of NF-κB via NMDA/AMPA receptors is mediated by products of oxidation, reactive oxygen intermediates (ROIs). It has been shown that other activators of NF-κB such as IL-1, TNF and Beta amyloid peptide also produce ROIs (Behl et al. 1994) and it is possible that this may be a general mechanism involved in NF-κB activation. The ROI in particular may be hydrogen peroxide, as catalase overexpression may reduce NF-κB activation also (Kaltschmidt et al. 1995). This work also appears to explain how kainate exposure leads to MHC (major histocompatibility) class I molecule expression upon granule cells, since NF-κB regulates MHC class I expression. Direct application of glutamate to mouse cerebellar granule cell cultures also results in activation of NF-κB (p65). This appears to be especially important in development, for this activation occurs in cultures from 3 to 7 day old mice (mice of eight days and beyond demonstrate constitutive

---

be the *Drosophila* version of the IKK, responsible for phosphorylating CACTUS.

NF-κB activity) (Guerrini et al. 1995). This work is doubly interesting for it demonstrates that glutamate cannot directly activate NF-κB in astrocyte cell culture (as determined by EMSA) although IL-1 and TNF alpha can do so. Work by Guerrini et al. also possibly demonstrates localisation of p65 in synapses as punctate immunoreactivity (possibly synaptic boutons) could be observed around pyramidal cells in cortex and Purkinje cells in the cerebellum *in vivo*. The p50 subunit of NF-κB had previously been identified in synaptosomal fractions using PAGE (Kaltschmidt et al. 1993). Increased binding of NF-κB to oligonucleotides on EMSA by densitometric analysis has been demonstrated after pentylene tetrazole induced clonic-tonic seizures in rats, peaking at 24h (2 times increase) after administration, decreasing, then increasing again at 96h (Prasad et al.1993). This biphasic response observed after clonic-tonic seizure is interesting in relation to results obtained in this thesis. Seizures induced in adult rats by subcutaneous kainic acid administration also demonstrate increased NF-κB-DNA binding on EMSA between 4 hours and 5 days (Rong and Baudry, 1996). Increase in NF-κB mRNA is also reported after high frequency stimulation (HFS) induction of long term potentiation (LTP) by *in situ* hybridisation and EMSA in rat (Meberg et al. 1996). Furthermore, NF-kB DNA binding could be increased in primary neuronal culture on EMSA after administration of mu-receptor opioid agonist DAMGO as determined by image densitometry, reaching a maximum of 8-fold after 72h (Hou et al. 1996). NF-κB p65 and p50 subunits also appear to be upregulated in microglia as determined by immunocytochemistry in the condition experimental autoimmune encephalomyelitus (EAE) in rats (Kaltschmidt et al. 1994).

NF-κB may play a neuroprotective role in neurodegenerative disease, particularly Alzheimer's disease (AD). The B amyloid protein which is the major constitiuent of the pathological amyloid plaques found in AD brain and also late stage Down's syndrome (trisomy 21) activates NF-κB in cerebellar granule cells (Kaltschmidt, 1997). Furthermore, a glycated form of tau protein, the subunit of pathological neurofibrillary tangles also observed post-mortem in AD brain is also capable of activating NF-κB (Yan et al. 1996). B amyloid and possibly glycated tau appear to induce this NF-κB activation via the receptor for advanced glycation end products (RAGE) (Yan et al. 1996). It is still far from clear what the role of NF-κB after activation from B

amyloid and perhaps therefore in AD, may be. However, NF-κB may have a neuroprotective role in AD. Cultured neurones simultaneously exposed to B amyloid and the potent NF-κB activator tumour necrosis factor (TNF), demonstrate increased survival when compared to those exposed to B amyloid alone (Barger et al. 1995). It appears that direct or indirect NF-κB induction of the calcium binding protein calbindin 28K may play an important role in this neuroprotection as TNF treatment of neurones exposed to excitotoxic insult may lead to an eight fold increase in calbindin (Bruce et al. 1996). A neuroprotective role for NF-κB is further indicated by the creation of a Rel A (p65) 'knockout' transgenic mouse and mice overexpressing IkB protein in which cells demonstrate an increased sensitivity to TNF induced apoptosis (Beg and Baltimore, 1996 and Van Antwerp et al, 1996).

Figure 1.7 The NF-κB Family of Transcription Factors.

1. (Upper half) This schematic diagram demonstrates some of the major features of the two classes of the NF-κB proteins. Class I represents the precursor derived proteins p50 (p105) and p52 (p100) and Class II the non-precursor derived proteins c-Rel, p65 and RelB (the related *Drosophila* proteins Dorsal (see text) and Dif are also included in this list). RH indicates the Rel homology domain, site of DNA binding, NF-κB dimerisation and the nuclear localisation sequence (NLS) indicated by N. INS indicates a 25 amino acid insertion Class I NF-κB proteins possess. P indicates the protein kinase A phosphorylation site. 'Protease' indicates the cleavage site of the p100/p105 precursor molecules.TX ACT corresponds to the Class II transcriptional activation domain. (diagram from Gilmore, 1996).

2. (Lower half) This schematic diagram demonstrates the similarity between the ankyrin repeat domains of the precursor molecules and the individual IκB family members (including the related Bcl-3 protein and the *Drosophila* protein Cactus (see text). The shaded areas represent ankyrin repeat domains. PEST represents rapidly degraded regions rich in proline, serine and threonine (diagram from Gilmore, 1996).

	Gene	Protein
CLASS I	*nfkb1*	p50/p105
	nfkb2	p52/p100
CLASS II	c-*rel*	c-Rel
	relA	RelA (p65)
	relB	RelB
	dorsal	Dorsal
	dif	Dif

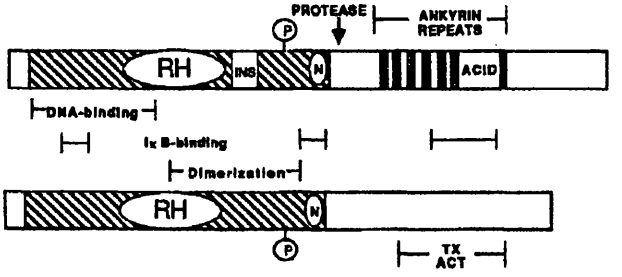

Protein	MW (kDa)
p105	105
IκB-γ	70
p100	100
IκB-α	37
IκB-β	41
Bcl-3	47
Cactus	52 (zygotic) 53 (maternal)

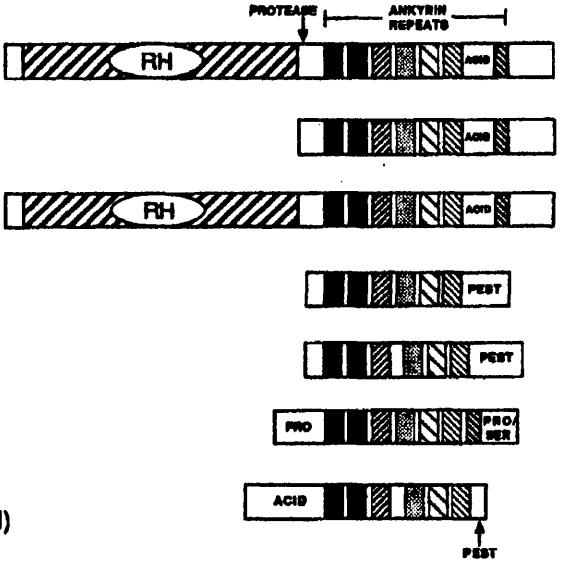

Figure 1.8 Tools for studying NF-κB in the CNS

1. (Upper right) A schematic diagram of some pathways to activation of NF-κB. The question mark indicates the uncertainty concerning the protein responsible for NF-κB precursor cleavage and indeed the entity responsible for phosphorylation of NF-κB. The IKK proteins responsible for I-κB phosphorylation leading to NF-κB release have recently been discovered (see text). Diagram from O'Neill and Kaltschmidt, 1997.

2. (Upper left) The specifity of an anti-p50 subunit antibody (in this case an antibody that recognises the proteins n-terminus) is demonstrated upon this western blot (PAGE). The upper protein band of ~100 kD indicates recognition of the precursor molecule p110 (since designated p105). The lower protein band of ~50 kD indicates the faster migrating cleaved p50 protein. Molecular weights are indicated along the left of the figure. The tissue loaded here was total cell homogenate from whole brain. From Kaltschmidt et al. 1993.

3. (Middle left) The antibody described above is here used on varying fractions of tissue from rat cerebral cortex . Of interest is the middle protein band(s) which are likely to be breakdown product(s) of the p110 (p105) precursor, indicating that cleavage of the ankyrin repeat domain may not be clean and instantaneous. Molecular weights are indicated along the left. Br=total brain, P=pellet, S=supernatant, Sy=synaptosome, Mi=mitochondria. From Kaltscmidt et al. 1993.

4.(Middle right) Electrophoretic mobility shift assay (EMSA) using an NF-κB p32 labelled oligonucleotide to study NF-κB DNA binding in PC12 cells. Of interest are the two complexes arrowed, the upper complex hypothesised to represent the p65/p50 heterodimer, the lower, faster migrating complex a p50 homodimer. From Tong and Perez-Polo, 1996)

5.(Lower left) EMSA using an NF-κB oligonucleotide to study NF-κB DNA binding in astrocytes. Lanes three and four demonstrate increased protein DNA binding following treatment with IL-1 and TNF respectively, while lanes one and two demonstrate no significant increase in DNA binding. Note the presence of one major complex, presumably the p65/p50 heterodimer identified by Bakalkin et al. (1993). From Guerrini et al. 1995.

6.(Lower right) EMSA using an NF-κB oligonucleotide to study NF-κB-DNA binding in rat cortex following traumatic brain injury. S=sham injured control, time scale following true injury follows above lanes. Note peak of binding between 3 and 7 days. Note again also, the one major complex of protein-DNA binding. From Yang et al, 1995.

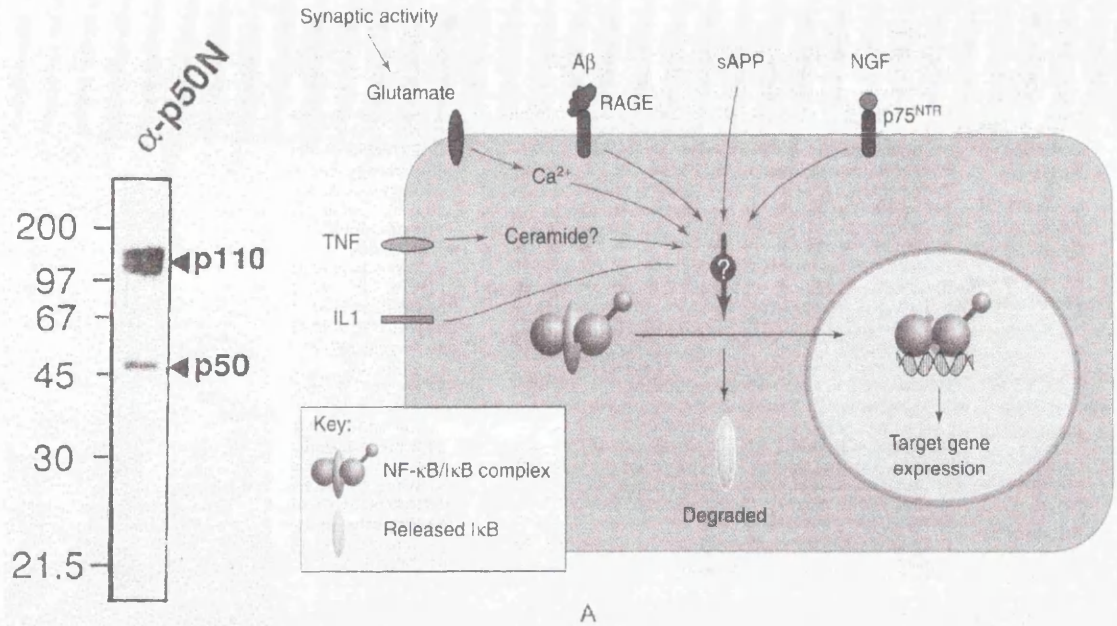
α-p50N
200
97
67
45
30
21.5
p110
p50
Synaptic activity
Glutamate
Aβ
RAGE
sAPP
NGF
p75NTR
Ca2+
TNF
Ceramide?
IL1
?
Key:
NF-κB/IκB complex
Released IκB
Degraded
Target gene expression

A

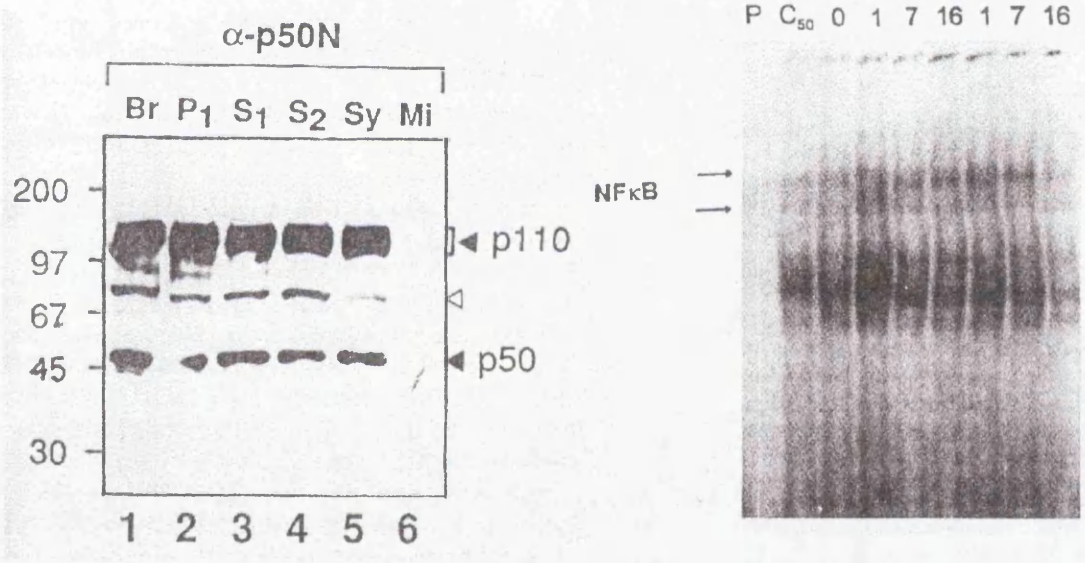
α-p50N
Br P1 S1 S2 Sy Mi
200
97
67
45
30
p110
p50
1 2 3 4 5 6
NGF
- - - - + + +
P C50 0 1 7 16 1 7 16
NFκB

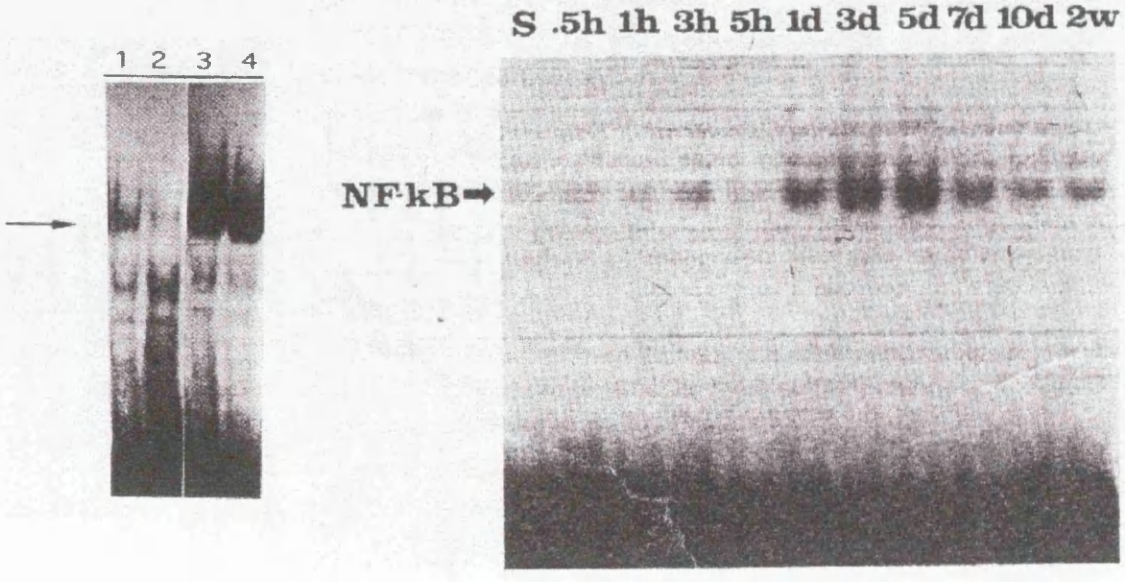
1 2 3 4
S .5h 1h 3h 5h 1d 3d 5d 7d 10d 2w
NF-kB

Huntington transgenes and the polyglutamine zipper hypothesis

"Pathological effects may arise when expanded glutamine repeats cause proteins to acquire excessively high affinities for each other or for other proteins with glutamine repeats"

[Stott, Blackburn, Butler and Perutz, 1995]

The HD transgenic mice were created by microinjection of a 1.9 kb ScaI-EcoRI fragment from the 5' end of the human HD gene from a juvenile patient which comprised exon 1 of the protein including section of the promoter sequence, exon 1 and 130 CAG repeat units. This fragment was propagated in E.coli, in which CAG repeats are unstable, leading to DNA which varied in repeat size after microinjection of the DNA preparation into single cell CBAxC57BL/6 embryos. This resulted in the production of various mouse lines with differing repeat lengths, all derived from one transgenic founder mouse (R6) in which different lengths of DNA fragments had integrated into five regions of this founders genome (Mangiarini et.al 1996). Backcrossing of R6 created four transgenic lines carrying expanded CAG repeats, named R6/0, R6/1, R6/2 and R6/5. The size of length of repeats in each line was determined by PCR amplification followed by sequence analysis (Mangiarini et al. 1996) and revealed that R6/0 possessed 142 repeats, R6/1:116, R6/2:144 and that R6/5 mice possessed repeat lengths between 128 to 156. R6/1 hemi and homozygotes, R6/2 hemizygotes and R6/5 homozygotes all develop a neurological phenotype, whereas R6/0 mice remain symptom free (see below, Mangiarini et al. 1996 and Davies et al. 1997).

All transgenic mice studied in this thesis were of the R6/2 line, as they possessed a high number of CAG repeats, without exceeding the highest number found in human patients with juvenile onset HD, as do those mice of the R6/5 line with 156 repeats. Typically at ten weeks, although it can be observed much earlier at four, R6/2 mice begin to demonstrate a progressive neurological phenotype, which is strongly indicative of a motor disorder. It is difficult to accurately describe neurological symptoms in mice using clinical criteria designed for humans, however the mice do seem to display a chorea like movement, along with resting tremor, mild ataxia, dyskinesia of the limbs (see Fig) and other, involuntary stereotyped movements. Tremor worsens as the mice age and increases markedly in stressful conditions. The mice suffer from epileptic seizures, particularly as a

result of being handled. This clinical picture is remarkably similar to that seen in human juvenile onset HD. As motor symptoms begin to exhibit themselves, the R6/2 mice also begin to demonstrate dramatic weight loss, end stage mice weighing as little as 60% of their normal littermate counterparts. The mice appear to eat frequently, if not more frequently than their normal siblings and food is being ingested, as revealed by examination of the gastro-intestinal tract at post-mortem (Mangiarini et al. 1996). R6/2 mice typically die[19] aged between 10 to 13 weeks of an unknown cause. Neuropathological studies of nine R6/2 mice after three weeks of demonstrating the above phenotype using thionin (Nissl) staining to perform cell counts and GFAP immunocytochemistry to observe astrocytic activity, revealed no significant difference between litter-mate controls (LMC) and transgenes. Transgenic brains were, however, smaller than those of their littermate controls ($19\%^{+}$- 1.6%).

These mice demonstrate that it is the CAG repeats present in the huntingtin protein that are capable of inducing a neurological phenotype leading to death. The mutation is not acting at the mRNA level in these mice as huntingtin protein can be detected upon western blot using the N-terminal antibodies AB78, HD1 and CAG53b, in the R6/1, R6/2 and R6/5 and also in HDex control lines comprising the same construct but with containing only18 repeats (Davies et al. 1997). Both mRNA and protein expression are absent in the R6/0 line, possibly because the integration event took place 'at a genomic region of unusual structure' (Mangiarini et al.1996). As has already been remarked in chapter two, HD is not the only polyglutamine repeat disorder. It represents a class of neurological diseases, all of which seem to be caused by the presence of an abnormal protein possessing polyglutamine trinucleotide repeats. There are at least seven other neurodegenerative conditions in which this seems to be the case and in which the gene has been cloned. These include spinocerebellar ataxia type I (SCA 1) (Orr et al. 1993) and Machado-Joseph disease or spinocerebellar ataxia type III (MJD/SCA3) (Kawaguchi et al. 1994), both of which are characterised by cerebellar pathology. This includes Purkinje cell loss and degeneration of the pontine and inferior olivary nuclei in SCA I (Zoghbi et al. 1993) and loss of the cerebellar molecular layer and pontine nuclei in SCA 3 (Durr et al. 1996). There are at least three other forms of SCA, labelled SCA2, SCA6 and SCA7

[19] Typically symptoms become so severe by 14 weeks that surviving mice are euthanased.

(David et al. 1997). Spino-bulbar muscular atrophy is an X-linked disorder which is a type of motor neurone disease featuring loss of both spinal and brain-stem motor neurones, as the name suggests (SBMA) (La Spada et al. 1991). Finally dentato-rubral-pallidoluysian atrophy (DRPLA), in which degeneration of the cerebellar dentate, red and subthalamic nuclei along with loss of Purkinje cells and the lateral cortical spinal tract occurs (Takahashi et al. 1988, Koide et al. 1994). With the exception of SBMA these disorders are all autosomal dominant and involve a normally ubiquitously expressed protein which possesses an abnormal polyglutamine repeat length in its structure with a pathogenic threshold at approximately 40 repeats[20], as does HD. In SBMA the extended repeat is found in the androgen receptor, but in the other disorders, as in HD, the normal function of the protein is not known. Transgenic mice have been used previously to create models of the SCA1 and SCA3 disorders, SCA 1 transgenes possessing 82 CAG repeats under the control of a Purkinje cell specific promotor became ataxic between 12 and 26 weeks of age (Burright et al 1995). SCA 3 transgenes possessing just a polyglutamine tract of 79 CAG repeats, also under a Purkinje cell promoter, demonstrated severe ataxia, although not when the whole SCA3 protein was mutated (Ikeda et al. 1996). This again indicates the toxicity of polyglutamine repeats alone.

Despite the striking phenotype of the HD mice, initially no apparent pathology or structural abnormality could be discerned. What could this mean? What was giving rise to these bizarre symptoms? What was the abnormal huntingtin protein doing in both the mice and humans to cause this disorder? Further neuropathological studies using a series of antibodies raised either to polyglutamine repeats or exon 1 of huntingtin protein for immunocytochemistry at light level revealed reactivity throughout the grey matter of the CNS of the control mice, as would be expected. In the control mice reactivity was localised to the cytoplasm, dendrites and axons of neurones and within the cytoplasm appeared to be associated with vesicular membranes. In control mice, huntingtin was never localised to the nucleus of neurones. Similar staining could be seen in transgenes. However, in the neuronal nucleus of transgenes, throughout the mouse CNS, 'densely stained circular inclusions' (Davies et al. 1997) could be seen. The inclusions presented a particularly striking sight. These inclusions were not visible in glial nuclei and

[20] SCA 6 appears to be the exception to this rule, it possessing a pathogenic threshold of 21 repeats (Ross,

counterstaining striatal and cortical neuronal nuclei with thionin (Nissl) stain revealed one immunoreactive inclusion for each neurone. It appears that the inclusions contain only abnormal huntingtin, since antibodies to other portions of the protein do not recognise the inclusion or localise in the nucleus. Electron microscopic studies of the nucleus of these cells revealed conclusively that these inclusions were neither the nucleoli of these cells, coiled bodies (accessory body of Cajal) or the sex chromatin (Barr bodies) of female mice (Davies et al. 1997). Furthermore, while no nuclear structure can be observed in control (LMC and HDex mice) when immunocytochemistry using an anti-ubiquitin antibody is conducted, the nuclear inclusions of transgenic mice are strongly immunoreactive for ubiquitinand this is confirmed by electron microscopic studies. The neuronal nuclear inclusions were not the only changes apparent after ultrasructural analysis. Extreme indentation of the nuclear membrane along with a possible increase in nuclear pore density could also be observed. Antibodies to tau protein, B-amyloid and phosphorylated epitopes of tau did not recognise the inclusions and immunocytochemistry for the transcription factors Fos B and NGFI-A which are constitutive in mouse neurones demonstrates exclusion of reactivity in the inclusion. Nuclear inclusions do not appear to be present in NADPH diaphorase or cholinergic interneurons and if inclusions were indeed the pathogenic element of HD this would go some way to explaining the survival of these neurones in HD, although not why they do not possess inclusions (Davies et al. 1997).

How does this presence of inclusions correlate with human HD pathology? Incredibly neuronal nuclear inclusions perhaps identical to those found in HD mice have previously been described at EM in biopsies from human HD tissue (Roizin et al. 1979). The indentation of nuclear membranes has also previously been described (Roos and Bots, 1983) as has the increase in nuclear pores (Tellez-Nagel et al. 1974). It is now becoming clear that nuclear inclusions and nuclear abnormalities are present in many CAG/polyglutamine repeat disorders, including SCA3/MJD (Paulson et al. 1997) and SCA1 (Skinner et al. 1997). Furthermore it is now apparent that CAG repeats when introduced into transgenes alone will form nuclear inclusions and produce a neurological phenotype which ultimately leads to death. This appears to be regardless of whether or not they are present in 'one of the classic repeat disorder genes' (Ordway et al.1997). The

---

1997).

latter work, in which a transgene containing 146 CAG repeats in the hypoxanthine-phosphoribosyltransferase (hprt) gene producing an expressed HPRT protein (not associated with any CAG disorder) with long polyglutamine repeats was created, led to a neurological phenotype. This strongly indicates that CAG/polyglutamine repeat disorders have a 'universal mechanism of pathology' in which the nature of the gene which possesses the repeats is largely irrelevant (Ordway et al. 1997). However, this does not explain the selective nature of cell death observed in most of these disorders. It is interesting to note that in this study, as in the HD mice, no evidence of neurodegeneration or gliosis was observed even though nuclear inclusions could be observed throughout the CNS and a neurological phenotype including seizure, was present (Ordway et al. 1997). The dominant questions which arise from the acquisition of this knowledge is just how do these polyglutamines form nuclear inclusions and how do nuclear inclusions induce a neurological phenotype?

It seems that the crucial threshold of repeat number has an important part to play in inclusion formation and hints that a relatively simple chemical process may be involved. Repeat thresholds are remarkably similar for all CAG/polyglutamine repeat disorders (HD/huntingtin=~37, DRPLA/Atrophin1=~49, SCA-1/Ataxin1=~40, SCA-2=~33, SCA-3=~55, SCA-7=~38, SBMA=~38) (Ross, 1997). In 1994, Max Perutz hypothesised that polyglutamine stretches of a certain length may be able to hydrogen bond to anti-parallel opposing lengths of polyglutamine forming a glutamine polar 'zipper'. This was based upon molecular modelling and X-ray diffraction experiments that indicated that synthetic poly(L-glutamine) formed hydrogen bonded β-pleated sheets (Perutz et al. 1994). Perutz also proposed that the normal function of polyglutamine repeats could be important in transcriptional regulation and pointed out *Drosophila* homeobox proteins as prime examples, such as the Abdominal B gene proteins, one of which comprises 32% glutamine repeats. When part of this protein sequence was deleted, DNA-binding was not altered, but transcriptional activity was reduced by half (Perutz et al. 1994). Glutamine rich regions in protein are a common transcriptional activation domain found in transcription factors. Glutamine and proline rich domains form one major class of activation domain, acidic domains, usually rich in serine or threonine form the other. Transcription factors in humans and rodents that possess the longest polyglutamine repeats are TATA binding

protein (TBP), containing all of its 38 glutamines in one stretch (Q17 in mouse), N-OCT 3 (also known as BRN-2 or OCT 3), containing 96% of its 25 polyglutamines in one stretch and the glucocorticoid receptor (GR), again containing 96 % of its 22 polyglutamines in one continuous region (Gerber, 1994 and Karlin and Burge, 1996). If polyglutamines could form polar zippers in vivo, could the abnormal repeat length of huntingtin or ataxin proteins, for example, disrupt transcriptional activation by perhaps binding out and disrupting neuronal transcriptional regulation? In 1995 an in vitro experiment demonstrated that modified chymotrypsin inhibitor 2 (CI2) from barley seeds incorporating ten glutamines in sequence would oligomerize, forming dimers and trimers. These bound proteins appeared to bind by hydrogen bonding, their glutamine stretches forming (3-pleated sheets, as determined by spectral analysis (Stott et al. 1995). Although this appears to confirm the theory of Perutz, it may not be directly applicable to transcription factor-huntingin or even huntingtin-huntingtin interaction in vivo, since the threshold for polyglutamine binding of CI2 seems to be low in comparison at 10 glutamines.

What will follow is a brief description of the transcription factors studied as examples of polyglutamine repeat proteins in this thesis. The following section of the introduction will not be a comprehensive discussion of these proteins, (BRN-2/N-OCT-3, TBP and glucocorticoid receptor) since this is beyond the scope of this introduction. In many respects the localisation, expression and DNA binding of TBP and GR transcription factors as studied later in this work is mainly an examination of the polyglutamine zipper hypothesis and not a detailed physiological study of these factors in the transgenic mice.

The OCT proteins, of which BRN-2 is a member, are a family of large (80-100 kD) transcription factors which contain an extensive conserved 150-160 amino acid domain labelled the Pit-Oct-Unc (POU) domain. These transcription factors bind to the octamer consensus sequence ATGCAAAT(NA), which can be found in the promoter sequences of various genes, including the B-cell immunoglobulins (Schaffner, 1989) and the histone H2B subunit gene (Fletcher et al. 1987). A related sequence to the octamer binding domain sequence was also found in the Pit-1 protein involved in regulating transcription in the pituitary gland and in the transcription factor unc-86 responsible for sensory neurone growth in nematode worms. The POU domain contains a sequence

related to the homeobox sequence and another characteristic sequence named the POU specific domain (Wegner et al. 1993). The homeobox domain contained by POU proteins differs from that in other homeobox transcription factors since its binding ability if of low affinity without the second POU specific domain present, functional activity of both domains being required for high affinity DNA binding. These two regions of the protein can be considered as dual components of the DNA binding element connected by a 'flexible linker sequence' (Latchman, 1995). A specific group of the OCT family transcription factors, the class III POU proteins, appear to be essential for development and function of the mammalian nervous system. These proteins appear to demonstrate a variety of extended amino acid repeats, BRN-1 containing alanine, glycine and proline repeats and BRN-2, containing alanine, glycine, proline and glutamine repeats (Sumiyama et al. 1996 and Yoshinobu et al, 1992). The glutamine repeats of BRN-2 lie at amino acids 130-151 in both human and mouse BRN-2 (N-OCT-3) genes. Many POU domain proteins of the OCT/BRN family are expressed in the developing mouse neural tube, including Pit-2, OCT-2, BRN-1, BRN-2, BRN-3 and Testes-1 (Tst-1), but BRN-2 is the most strongly expressed as determined by *in situ* hybridisation. With the exception of Pit-1, which is expressed biphasically in the pituitary during development, these proteins are also expressed throughout the adult mouse brain (Xi He et al. 1989). In the mouse brain, BRN-2 cDNA hybridizes particularly strongly to transcripts in the hypothalamus and hippocampus and the hybridisation signal for BRN-2 was significantly stronger than for BRN-1. BRN-1 was also expressed strongly in the hypothalamus and hippocampus, but could also be detected in the medullary zone of the kidney, where BRN-2 was absent. BRN-1 and BRN-2 are the most widely expressed class III POU domain proteins in the CNS. They were also localised to the cerebral cortex (layers II-V), the Purkinje cells of the cerebellum, the forebrain cholinergic system, midbrain dopaminergic system and the paraventricular nucleus of the hypothalamus (PVN) (Xi He et al. 1989).

In 1997 work by Hagino-Yamagishi confirmed the expression of BRN-2 in the mouse CNS by using immunocytochemistry upon cortical tissue. Co-localisation of the cell adhesion molecule NCAM-H to cells also expressing BRN-2 at similar stages of development in post-mitotic neurones led Yamagishi et al. to hypothesize that BRN-2 may be an important transcription factor controlling the migration and maturation of neurones

in the developing cortex (Hagino-Yamagishi et al. 1997) BRN-2 appears to be essential for the development of the hypothalamus and pituitary gland in the mouse, and possibly all mammals. This has been revealed by Schoenemann et al. and Nakai et al. by the use of transgenic mice. This work is of interest concerning some of the results of this thesis and will be covered in detail in the discussion.

Earlier work upon the P19 cell line provides evidence that BRN-2 may not only be essential for maturation of neuronal precursors, but may control the differentiation of neural precursors into glia or neurones (Fujii and Hamada, 1993). When BRN-2 activity was suppressed by antisense RNA, the P19 cells differentiated into skeletal and smooth muscle cells, BRN-2 presence being vital for formation of glial and neuronal cells.

OCT-1 appears to be a general octamer site transcription factor, which may control the expression of many 'housekeeping' genes (such as the histone H2B protein), and OCT-2A appears to be mainly a B-cell lymphocyte factor controlling immunoglobulin expression. However, work by Adriano Fontana's group has demonstrated up to six OCT binding complexes on EMSA using homogenate from cultured mouse astrocytes and human glioblastoma and neuroblastoma cell lines. What is more, these complexes are readily binding to the octamer DNA sequence, yet the proteins are known to be distinct from OCT-1 and OCT-2A since they are not recognised by antisera rasied to these two proteins (Schreiber et al. 1990). In cells of the nervous system and in melanoma cells, three distinctive binding complexes were particularly noticable. These complexes correspond to the binding activities of the OCT-1, OCT-2 (A&B) and N-OCT-3 proteins respectively (see plate). In newborn mouse brain or astrocyte culture, a fourth binding factor labelled N-OCT-4 could be discerned, as could two very low molecular weight proteins labelled N-OCT 5A and 5B. These factors could not be observed in adult mouse brain (Schreiber et al. 1990).

The protein labelled N-OCT-3 by Fontana's group was subsequently cloned from human tissue revealing a 443 amino acid protein containing 21 polyglutamine repeats (Schreiber et al. 1993). This protein structure was almost identical to the previously cloned mouse BRN-2 protein, the mouse protein possessing an extra two amino acid residues (Hara et al. 1992). Furthermore, Schreiber et al. proposed that the lighter proteins N-OCT 5A and 5B are produced by a different initiation of translation from the N-OCT –

3 mRNA, the mechanism of N-OCT-5 production is unlikely to be via alternative splicing since the mouse BRN-2 gene does not possess introns. Interestingly, the proteins N-OCT-5A and B seem unable to activate transcription (Schreiber et al. 1993).

In this thesis, the 'glucocorticoid receptor' is described as possessing 22 glutamine repeats in rodents, (Gerber, 1994), but in fact there are two types of receptor in the rat which will bind the hormone glucocorticoid (or corticosterone, the rat glucocorticoid) (DeKloet et al. 1975). Corticosteroid is secreted from the adrenal gland under conditions of physiological stress and appears to mediate the shutting down of non-essential metabolic activity such as growth, repair and the immune response (DeKloet and Reul, 1987, Sapolsky, 1992). The two receptors are described as the mineralocorticoid or type I corticosteroid receptor and the glucocorticoid receptor or type II corticosteroid receptor. The antibody used in this thesis recognises both forms of the glucocorticoid receptor (type I and II corticosteroid receptors) which are highly homologous, their DNA binding domains being identical, (Arriza et al. 1987) and possess a 22 glutamine repeat stretch. Immunocytochemistry indicates that the GR is expressed throughout the mammalian nervous system, in the striatum approximately 70% of neurones express the type I receptor (Ahima, 1991) and approximately 90% express the type II receptor (Ahima and Harlan, 1990). Both receptor types appear to be localised to medium sized neurones, and the numbers would suggest that most projection neurones express both types of GR. However, the type I receptor was also localised to large cells indicating a possible presence in the cholinergic neurones. Immunoreactivity for both receptors was strikingly nuclear. The type I corticosteroid receptor is capable of binding corticosterone and mineralocorticoids such as aldosterone with an extemely high affinity (Beaumont and Fanestil, 1983) while the type II corticosteroid receptor can bind corticosterone and the synthetic glucocorticoid dexamethasone with a relatively lower affinity than the type I receptor. From this point on they will be simply described as the 'glucocorticoid receptor'(GR). Since corticosterone is a liphophilic steroid molecule it is capable of diffusing directly through the membranes of neurones and glia where it may bind the GR. This ligand binding induces the receptor to change shape and disassociate from its chaperone heat shock proteins (Hsp 90, 70 and 56), which much like NF-κB and IκB, retain GR in the cytoplasm. Without its chaperones, GR is phosphorylated and

translocates to the nucleus, where it undertakes transcriptional regulation. Unlike many transcription factors like the IEGs or NF-κB (and indeed many other steroid receptors) GR binds DNA as a monomeric factor. Molecular analysis of the glucocorticoid receptor indicates that, like other molecules which act as transcription factors, the protein may be divided into hormone (corticosterone) binding, DNA binding and transcriptional activation domains (Green and Chambon, 1988). The DNA sequence to which the activated glucocorticoid receptor binds is described as the glucocorticoid response element (GRE) comprising the sequence (GGTACAnnnTGTTCT) (Strahle et al. 1987). It has also been demonstrated that a 'composite GRE' exists. A DNA site capable of being bound by both the GR and AP-1 transcription factors (Pearce and Yamamoto, 1993). The DNA binding domain of the glucocorticoid receptor, like that of all steroid receptors, forms a distinct domain for binding the GRE. This domain in the GR is rich in cysteines which, by binding to a centrally located zinc cation form a tetrahedral 'finger' (Evans and Hollenberg, 1988, Truss and Beato, 1993), the GR possesses two such domains.

So far in this introduction we have briefly considered several transcription factors, NF-κB, BRN-2 and GR. These proteins are of course regulatory transcription factors, enhancing or repressing the transcription of specific genes into mRNA by influencing the activity of the core basal transcription machinery which in turn binds to the core promoter elements, most notably the TATA box. Interactions between the regulatory and the basal factors are of course therefore essential for matching the rate of gene expression to the needs of the cell. For RNA polymerase II to begin transcription of any gene, the basal factors must bind to the core promoter (Buratowski, 1994), which comprises the TATA box and initiator elements. These basal elements can be divided into the TFIIA, B, D, E, F and H protein complexes, our polyglutamine containing TBP (38 kD, Roeder, 1996) comprises part of the TFIID complex and TBP itself is the first of this complex to bind, being specific for the TATA box (TATA,$^{T}/_{A}A^{T}/_{A}A$). TBP binds to the minor groove of DNA as a monomer (Lee et al. 1991) and appears to cause the DNA strand to bend dramatically bringing separate DNA sequences closer together in space. Assembly of the remaining basal machinery occurs upon the TBP protein, the complex of TBP plus its companion TBP associated factors (TAFs) being referred to as TFIID. DNA footprinting studies indicate that the DNA binding of TFIID complex is more extensive

than TBP alone (Roeder, 1996), the additional TFIID binding component appearing to be dTAF150 (Verrijzer et al. 1994). Some gene promoters do not possess TATA boxes, and it is therefore likely that the TFIID complex binds via the interaction of dTAF150 with the promoter initiator elements alone (Py Py A(+1) N $^{T}/_{A}$ Py Py)[21]. The presence of TBP is still essential for TFIID complex binding (Zenzie-Gregory et al. 1993). The sequence of basal factor assembly is illustrated in Fig. 1.13. The TBP is essential therefore for formation of the TFIID complex whether or not the core promoter possesses a TATA box. Little free TBP exists in human cells, TBP usually always being found bound to TAFs. TBP is likely to be a very ancient protein in evolutionary terms, the 180 amino acids of the carboxy terminal of TBP demonstrating 85% homology between TBP extracted from human and yeast. Examples of EMSAs using TBP DNA binding sequences can be seen in figure 1.12.

[21] N=any nucleotide, Py=pyramidine.

Figure 1.9 The Huntington's transgenic mouse I

1. (Upper figures). These photographs of R6/2 transgenic mice show several interesting features associated with this mouse model. The top photograph demonstrates the characteristic 'feet clasping' reflex posture of the R6/2 mouse when held by the tail, the control mouse on the left demonstrates the usual limb extension posture in response to this stimulus, as it attempts to steady itself. The lower photographs both illustrate the relatively smaller size of the R6/2 line and an R6/1-R6/2 cross when compared to control mice, as well as the slight morphological difference in skull shape. In the middle photograph, the R6/2 mouse and control are both 12 weeks of age, however the R6/2 transgene weighs 17.7g when compared to the control at 21.3g. In the lower photograph, both mice are 7 weeks of age, the R6/1-R6/2 cross weighing 10.1g, the control mouse 19.6g (Mangiarini et al. 1996)

2. (Lower figure) Photographs of Nissl (Thionin) staining through R6/2 (right) and littermate control (left) mouse forebrain transecting the striatum (cp). The reduced brain size of the R6/2 can be observed, as can the relatively larger ventricle (v) as compared to the control mouse (Mangiarini et al. 1996).

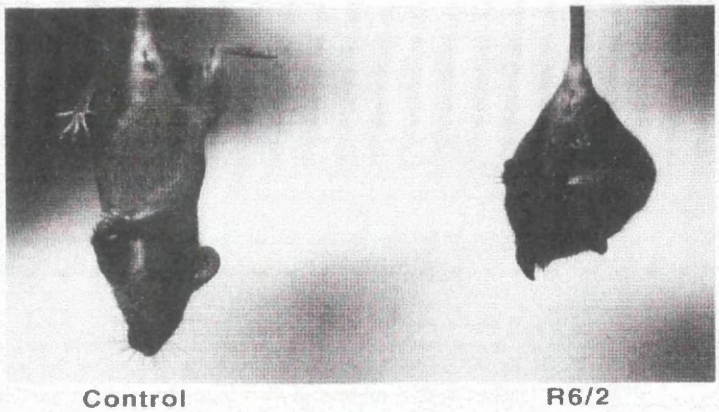

Control R6/2

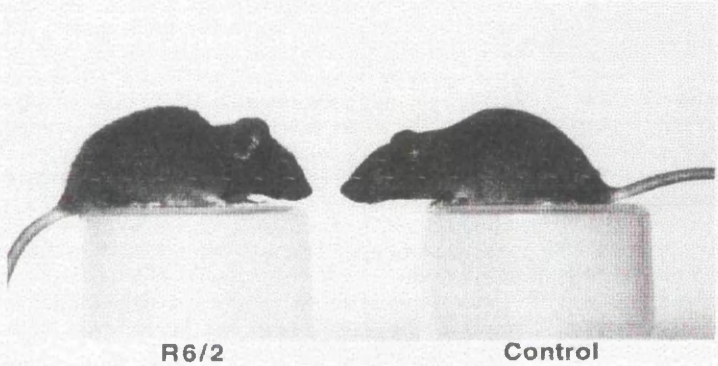

R6/2 Control

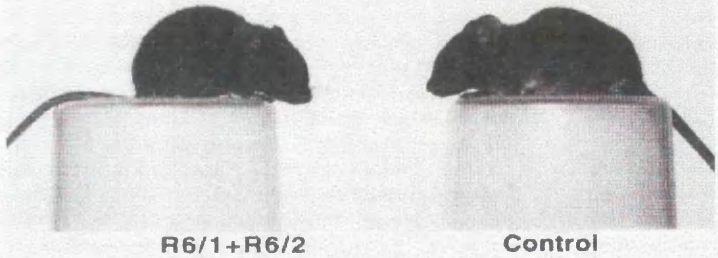

R6/1+R6/2 Control

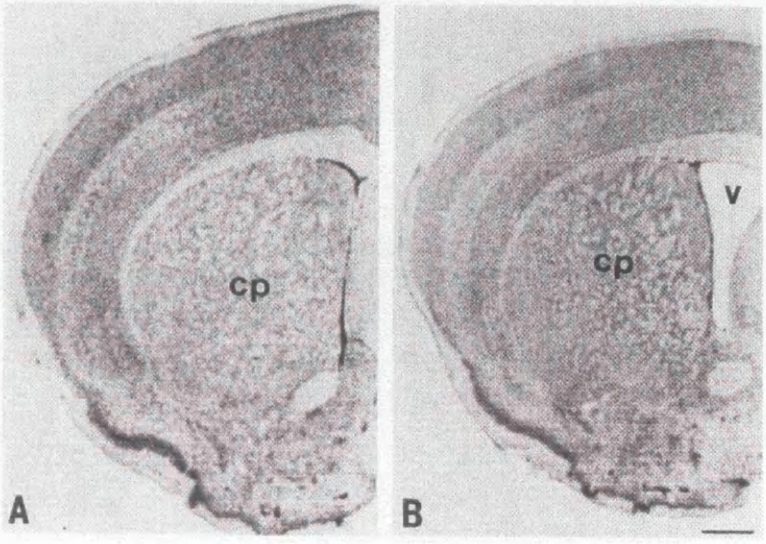

Figure 1.10 The Huntington's transgenic mouse II

1. (Upper left) Electron micrograph of the neuronal nucleus of a transgenic mouse demonstrating the lightly stained nuclear inclusion (NII) alongside the dark nucleolus (Nu) above (Davies et al. 1997).

2.(Upper right) Light photomicrograph of R6/2 transgenic striatum at low power. Nuclear inclusions can be seen throughout the striatum, labelled by an anti-huntingtin antibody. The number of immunoreactive inclusions is particularly striking. Regions of no immunoreactivity indicate the white fibres of the internal capsule (Davies et al. 1997).

3. (Middle) Electron microscopic localisation of huntingtin (left) and ubiquitin (right) in neuronal nuclear inclusions of transgenic mice via immunocytochemistry. Staining observed is the DAB reaction product. A single inclusion is observed in each nucleus. DAB immunocytochemistry is used throughout this thesis (Davies et al. 1997).

4. (Bottom) Graphical representation of loss of body weight (A) and brain weight (B) in R6/2 transgenic mice compared to litter mate controls. The table below (C) demonstrates the correlation between symptomatic onset and weight loss with the appearance of nuclear inclusions and nuclear indentation (Davies et al. 1997).

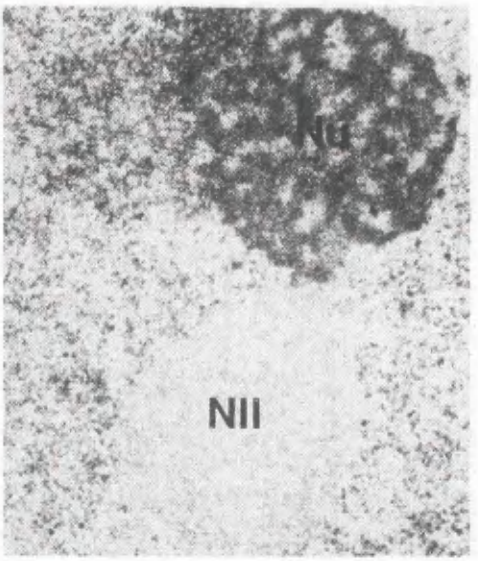

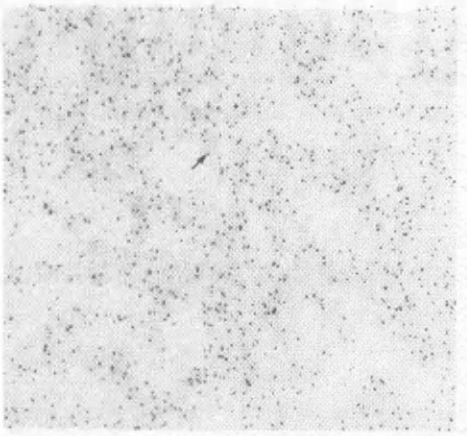

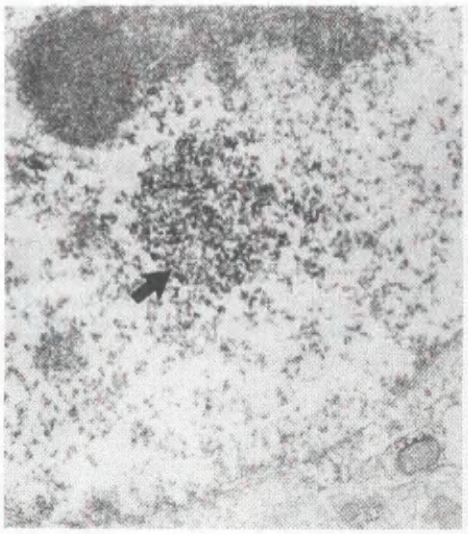

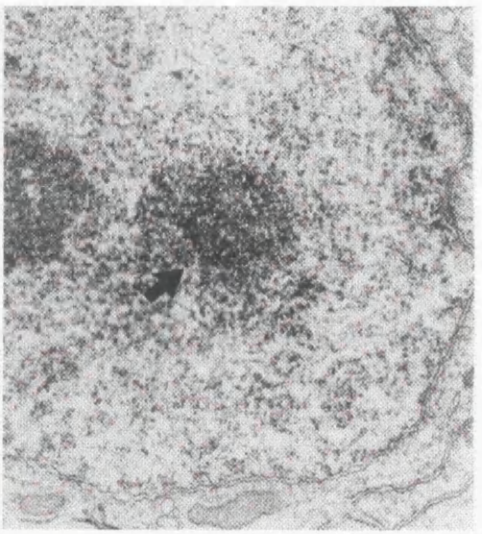

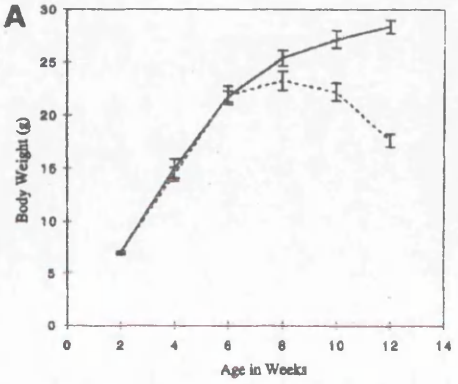

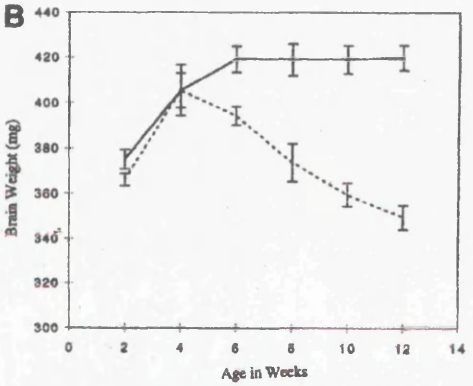

C

Disease Progression in 6/2 HT Mice

PHENOTYPE														
Brain Weight Loss	-	-	-	-	-	+	++	++	+++	+++	+++	+++	+++	+++
Body Weight Loss	-	-	-	-	-	-	-	+	+	+	++	+++	+++	+++
Symptoms	-	-	-	-	-	-	-	-	-	+	+	++	++	+++
NEUROPATHOLOGY														
htt in Nucleus	-	-	-	-	+	+	+	++	++	+++	+++	+++	+++	+++
Ubiquitin in Nucleus	-	-	-	-	-	-	+	+	+	+	++	+++	+++	+++
NII by EM	-	-	-	-	-	-	-	+/-	+	+	++	++	++	++
Nuclear Indentation	-	-	-	-	-	-	-	-	-	+	+	+	++	++
Age in Weeks	**2**	**3**	**3.5**	**4**	**4.5**	**5**	**6**	**7**	**8**	**9**	**10**	**11**	**12**	**13**

Figure 1.11 N-OCT-3/ BRN-2 and OCT complexes on EMSA

1. (Upper) The diagram opposite demonstrates the partial amino acid sequences of several POU domain proteins, including BRN-2 and OCT-1. The POU domain proteins are grouped into four classes according to overall sequence similarity; POU class I (PIT-1). POU class II (OCT-1, OCT-2), POU III (BRN-1, BRN-2 and Tst-1) and finally POU class IV (BRN-3, UNC-86). Regions of identical sequence are highlighted in black (commonly conserved amino acids are presented below the sequences) and the two DNA binding regions, the POU-specific domain and the POU-homeodomain, highly conserved sequences, are indicated (Xi He et al. 1989).

2. (Middle) EMSA demonstrating OCT binding complexes in various neural (LAN-1, SK-N-BE, SK-N-LE: all human neuroblastoma cells, LN-18, 308, 382, 215: all human glioblastoma cell lines) and non-neural cell lines (BJA human Burkitt lymphoma cells, Bowes human melanoma cells, COS-7 monkey kidney fibroblasts, L-cell mouse fibroblasts). Work by Schreiber et al. indicates that the three band binding complex in neural cells corresponds to OCT-1, N-OCT-2 (A&B) and N-OCT-3 (BRN-2) (see right of figure) (Schrieber et al. 1990).

3.(Lower) EMSA demonstrating OCT binding complexes in cells of the nervous system (adult and newborn mouse brain homogenate, mouse astrocyte culture and rat C6 glioma cells) and B lymphocytes (BJA-B). As well as the three band complex visible in adult brain, the additional protein-DNA complex of N-OCT-4 binding can be seen in newborn brain and astrocyte culture, as can the low molecular weight proteins N-OCT-5A and B (not seen here) (Schreiber et al, 1990).

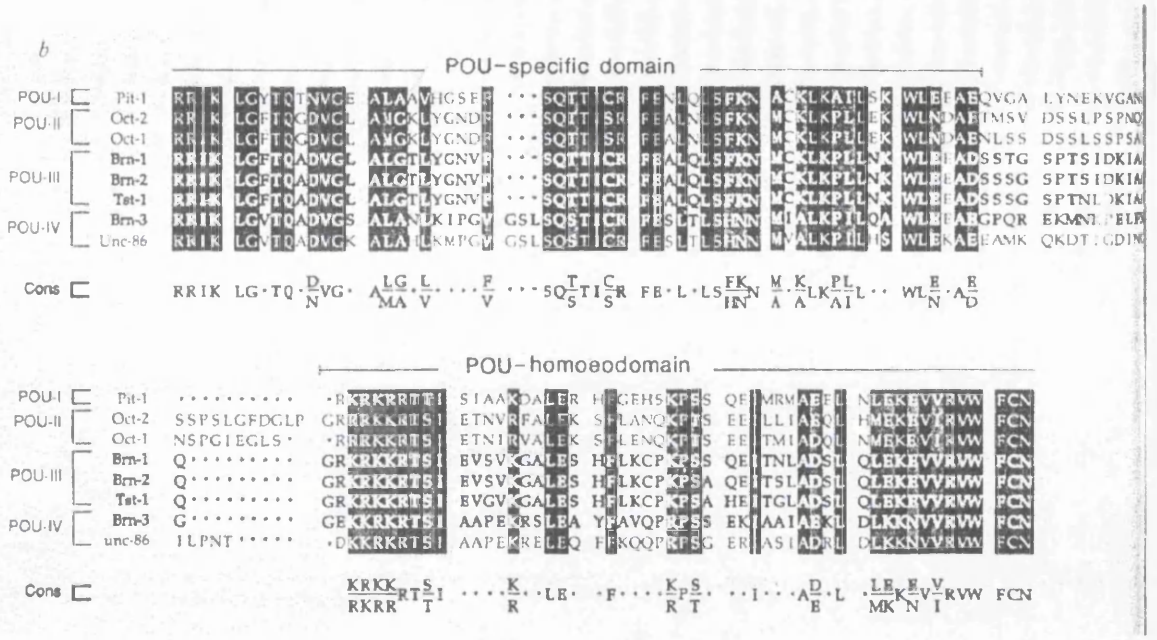
b
POU-specific domain
POU-I
POU-II
POU-III
POU-IV
Pit-1
Oct-2
Oct-1
Brn-1
Brn-2
Tst-1
Brn-3
Unc-86
Cons
POU-homoeodomain

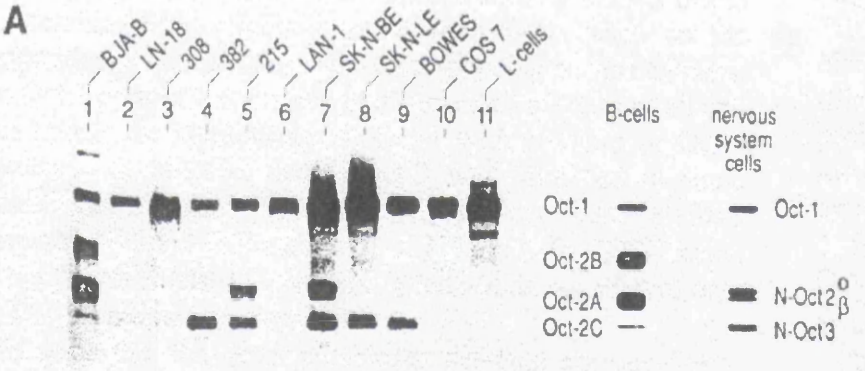
A
BJA-B
LN-18
308
382
215
LAN-1
SK-N-BE
SK-N-LE
BOWES
COS 7
L-cells
1 2 3 4 5 6 7 8 9 10 11
B-cells
nervous system cells
Oct-1
Oct-2B
Oct-2A
Oct-2C
N-Oct2
N-Oct3

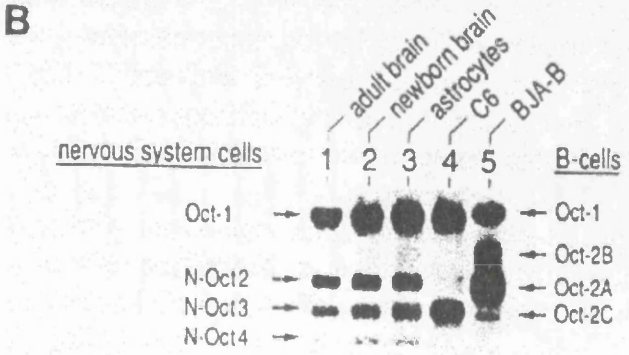
B
adult brain
newborn brain
astrocytes
C6
BJA-B
nervous system cells
1 2 3 4 5
B-cells
Oct-1
N-Oct2
N-Oct3
N-Oct4
Oct-1
Oct-2B
Oct-2A
Oct-2C

Figure 1.12 EMSAs using the TBP and GR consensus oligonucleotides

(A) Top left. EMSA using TATA box oligonucleotide and the addition of purified TBP and TFIIA complex. This work was conducted by Bellorini et al. to study the action of the antibiotic distamycin A (DIST) and the alkylating benzoyl mustard derivative tallimustine (TALL) upon TBP binding using an in *vitro* model. TBP and TFIID addition is indicated by arrows. It can be seen that the presence of both distamycin and tallmustine inhibit TBP/TFIIA binding. What is of great interest here is that two DNA binding complexes can be observed when both TBP and TFIIA are added (the DA complex). A smaller, high molecular weight band can be observed above the denser low molecular weight binding complex (which is not to be confused with the non-specific complex, NS), Although the authors do not comment upon this, two complexes can be seen, possibly TBP+TFIIA (heavy complex) and TBP alone (light complex)? (Bellorini et al. 1995)

(B) Top right. EMSA using TATA box oligonucleotide and the addition of purified TBP,TFIIB and TFIIA, again conducted by Bellorini et al. Of interest here are lanes one and two, lane one demonstrates a low molecular weight binding complex observed with the addition of purified TBP and TFIIA alone. Lane two shows a heavier molecular weight complex observed with the extra addition of TFIIB.

(C) Bottom left. Recogniton of TBP (TFIID) protein in human placental tissue using the TFIID (TBP) N-12 antibody (Santa Cruz). A molecular weight of 36 kD is given.

(D) Bottom right. EMSA using a GR binding site oligonucleotide and rat lung tissue. This EMSA demonstrates the action of addition of different unlabelled binding site oligonucleotides upon GR binding to its own p32 labelled DNA sequence. Control= tissue and GR oligonucleotide, other lanes = addition of AP-2, GRE (reduced binding), CRE and OCT (Peters et al. 1995).

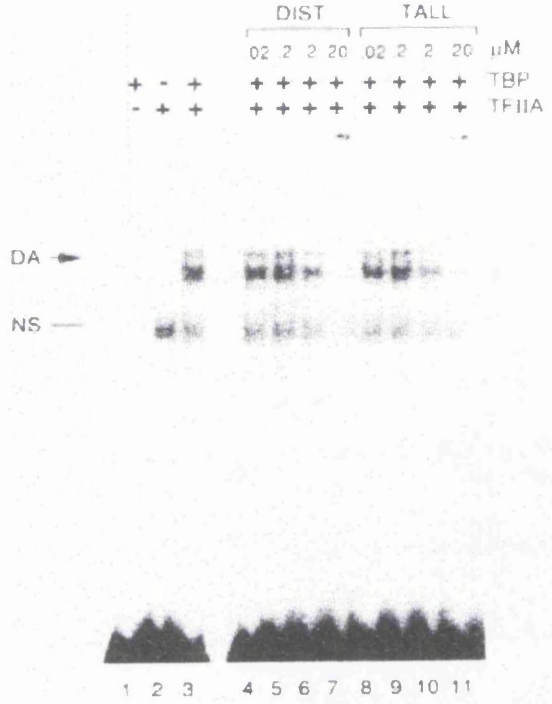
DIST
TALL
02 2 2 20 02 2 2 20 μM
TBP
TFIIA
DA
NS
1 2 3 4 5 6 7 8 9 10 11

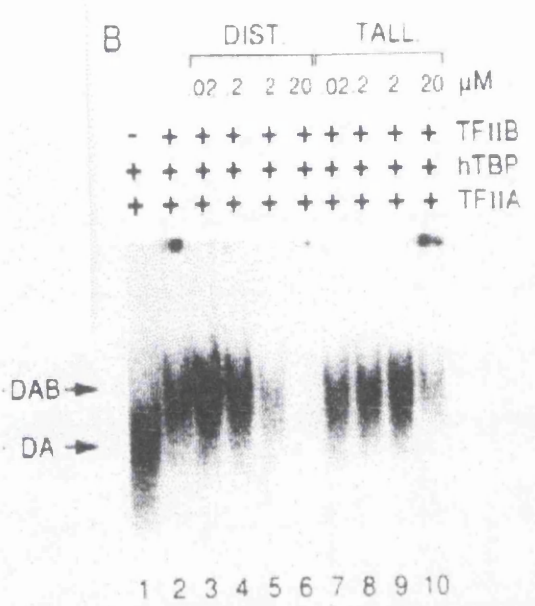
B
DIST
TALL
02 2 2 20 02 2 2 20 μM
TFIIB
hTBP
TFIIA
DAB
DA
1 2 3 4 5 6 7 8 9 10

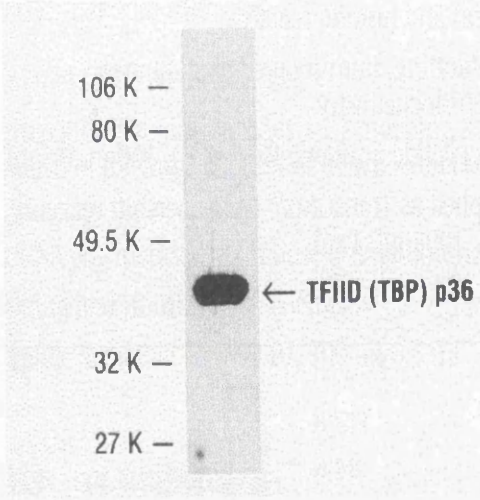
106 K
80 K
49.5 K
← TFIID (TBP) p36
32 K
27 K

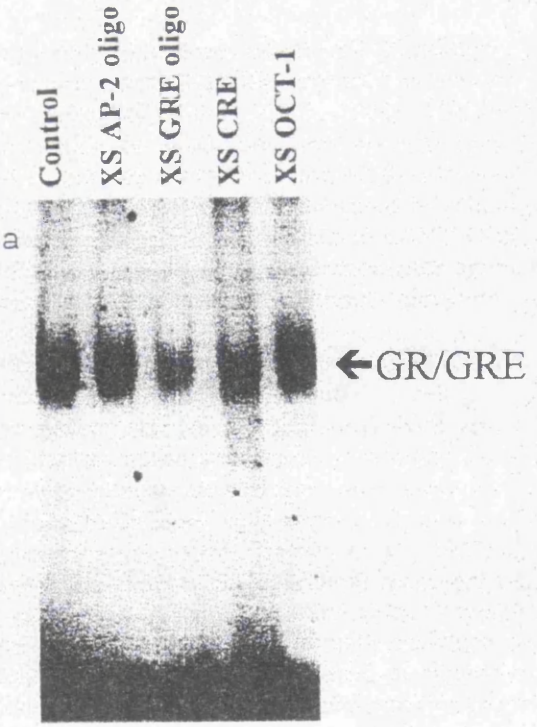
Control
XS AP-2 oligo
XS GRE oligo
XS CRE
XS OCT-1
a
←GR/GRE

Figure 1.13 Assembly of the core basal transcription proteins

The figure opposite illustrates the component proteins of the pre-initiation complex and their sequence of assembly upon the TATA box (-30 bases downstream) and initiator elements (+1 bases). The sequential assembly of the core proteins begins with the binding of the TFIID complex (TBP [one 38 kD protein] and TAFs [twelve protein subunits ranging from 15-250 kD]) to the TATA box (if present). This induces 'DNA bending'. The next step is the binding of the TFIIA complex (three subunits, 12, 19 and 35 kD), to TFIID. TFIIA appears to provide the TFIID complex with greater stability. Further subunits then combine in the order of TFIIB, TFIIF+RNA polymerase II, TFIIE and finally TFIIH. This forms the 'closed' or stable pre-initiation complex (PIC), the addition of all TF complexes extending the PIC to +30 position and embracing the initiator elements (IR, +1). In the presence of ATP the PIC is activated (DNA melting), hydrolysis of ATP being carried out by TFIIH. Phosphorylation of the carboxy-terminal domain of RNA polymerase II (CTD) by TFIIH leads to the dissociation of TFIIB, TFIIE and TFIIH itself. TFIID and TFIIA form a residual promoter complex (RPC), while TFIIF and RNA polymerase II form the elongation complex. Upon termination of transcription the elongation complex separates from DNA and the synthesised RNA and is free to be recruited to another PIC assembly sequence (Roeder, 1996).

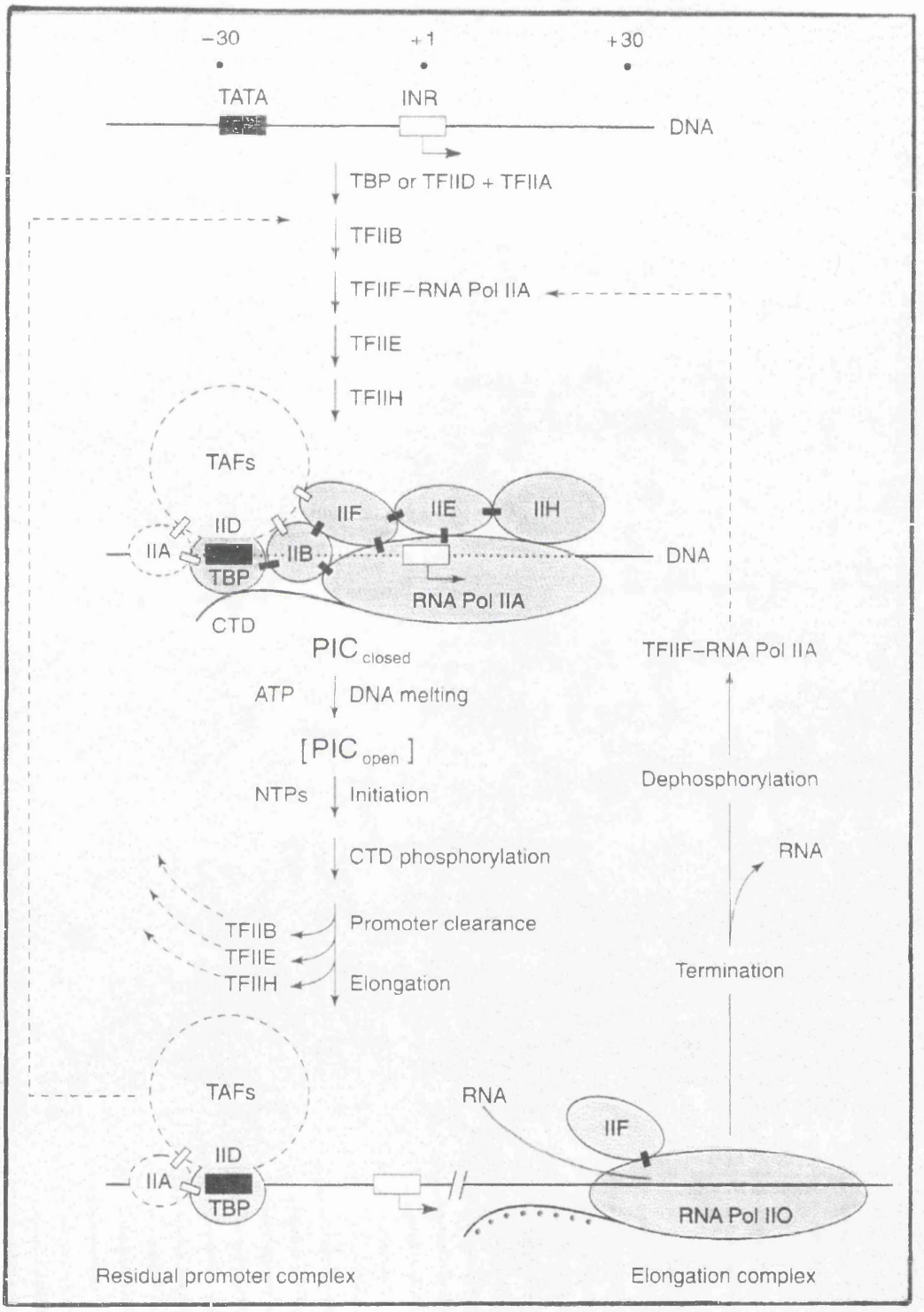
−30
+1
+30
TATA
INR
DNA
TBP or TFIID + TFIIA
TFIIB
TFIIF–RNA Pol IIA
TFIIE
TFIIH
TAFs
IID
IIA
TBP
IIB
IIF
IIE
IIH
DNA
RNA Pol IIA
CTD
PIC closed
ATP
DNA melting
[PIC open]
NTPs
Initiation
CTD phosphorylation
TFIIB
TFIIE
TFIIH
Promoter clearance
Elongation
TFIIF–RNA Pol IIA
Dephosphorylation
RNA
Termination
TAFs
IID
IIA
TBP
RNA
IIF
RNA Pol IIO
Residual promoter complex
Elongation complex

MATERIALS AND METHODS

STEREOTAXIC SURGERY[22] AND TISSUE FIXATION

Rat.

Male Sprague-Dawley rats (180-250g) were placed under neuroleptanalgesia using Hypnovel (midalozam) 0.5ml/kg i.p. and Hypnorm (fentanylfluanisone) 0.3ml/kg i.m.. The animals were then placed in a David-Kopf stereotaxic frame in the flat skull position to receive a 1 microlitre injection of either saline, 60nmol QA (2,3 pyridine dicarboxylic acid, Sigma) delivered in physiological (0.9%) saline, CNTF (1.5μg per ml, Regeneron) or a combination of QA and CNTF. Delivery was via a 30 gauge Hamilton syringe and solutions were injected gradually over 5 minutes at the following co-ordinates from bregma: AP+0.03, ML-0.25, DV-0.45 cm (Paxinos and Watson, 1986). Animals were then left for either 12h, 24h, 48h, 120h (5days) or 168h (7days) and those for immunocytochemistry or histochemistry were then anaesthetised with pentobarbitone (Sagatal, 100mg/kg i.p.) and then transcardially perfused. Perfusion was conducted first with 100ml of physiological saline, then followed by either 500ml periodate-lysine paraformaldehyde (2% paraformaldehyde, 0.1% L-lysine, 0.2% sodium-m-periodate buffered to pH 7.5 using 0.4M NaP) for immunocytochemistry or paraformaldehyde (4% paraformaldehyde buffered to pH 7.4 with 0.4M NaP) for acetylcholinesterase and NADPH diaphorase staining. All solutions were maintained at $4^{oc.}$ Brains were then removed from crania and post-fixed for 4h in perfusion fixative and finally cryoprotected by 80h in 30% sucrose before being cut on a freezing microtome into 40μm sections.

Mouse

HD R6/2 transgenic mice were terminally anaethetised with an IP injection of pentobarbitone (Sagatal, 100mg/kg i.p.) before either being perfused for immuno-cytochemistry (periodate-lysine-paraformaldehyde, above) or brains were removed for tissue preparation for PAGE or EMSA (below).

[22] Surgical proceedures described in this section were expertly performed by Dr.S.W.Davies.

ENDOGENOUS HISTOCHEMISTRY

Acetylcholinesterase staining

This was achieved by using a modified method of Karnovsky and Roots (1964). Animals for acetylcholinesterase (ACHE) staining were treated 270 minutes before perfusion with a depot injection of the irreversible acetylcholinesterase inhibitor, di-isopropyl-flurophosphate (DFP) dissolved in arachis oil at 2mg/kg i.m and aqueous atropine (atropine sulphate) at 10mg/kg i.p.. 40 μm sections for ACHE staining were incubated in a solution of the following composition at room temperature for 60 minutes (or until an appropriate degree of staining was achieved): 0.2M Tris maleate pH 5.7, 0.1M sodium citrate, 0.03M cupric sulphate and 0.005M potassium ferricyanide, and 0.05% acetylthiocholine iodide.

NADPH Diaphorase and Thionin (Nissl) staining

This was achieved by using the method of Vincent et al (1983). 40 μm sections were incubated in a solution of the following composition at 37°C for 30 to 60 minutes: 0.25mM nitroblue tetrazolium (NBT), 15mM sodium malate (disodium salt), 1.2mM NADPH, 0.1M Tris HCL (pH 8). After the histochemical procedures described above, all sections were washed in 0.1M Tris buffer (pH 7.4) and them mounted onto gelatinised slides. The mounted slides were left to air dry for 48 h before being passed through a series of graded alcohol concentrations (70% / 80% / 90% / 100% /100%) to dehydrate. The mounted sections were then taken through two changes of Histoclear for 10 minutes each and finally were coverslipped from Histoclear using DPX as a mountant. Sections for thionin staining (Nissl stain) were transferred to 0.1M Tris pH 7.4 after being cut and mounted directly upon gelatinised slides. These sections were then dehydrated (defatted) as described above before being rehydrated and placed in Nissl stain (1% thionin in 125 mM sodium acetate buffer (pH 6.0) for 20 seconds). Sections were destained in 95% alcohol before being finally dehydrated again and mounted from Histoclear.

IMMUNOCYTOCHEMISTRY

Primary antibodies were diluted in a buffer composed of 0.1M Tris-HCl, 0.3% Triton and 0.02% sodium azide. Sections were incubated in primary antibody for 3 days at 4°C, washed in 0.1M Tris-HCl pH 7.4 for 30 minutes before being incubated in the appropriate biotinylated secondary antibody for 90 minutes. Monoclonal antibodies were incubated with mouse (rat absorbed) biotinylated secondary, polyclonal with rabbit biotinylated secondary and chicken with anti-chicken biotinylated secondary) at a 1:200 dilution. Sections were again washed in 0.1M Tris-HCl pH 7.4 for 30 minutes before being incubated for 90 minutes with biotinylated horseradish peroxidase and avidin complex (ABC kit, Vector) at 1:100 dilution (10µl A + 10µl B + 0.98ml Tris). Sections were again washed in Tris for 30 minutes followed by 10 to 30 minutes in diaminobenzidine (DAB) solution (25mg/100ml Sigma DAB, 0.01% hydrogen peroxide in 0.1M Tris pH 7.4). Sections were again washed in 0.1M Tris-HCl pH 7.4 and mounted on gelatinised slides and allowed to air dry. Finally sections were dehydrated through graded alcohol solutions before being coverslipped from Histoclear with DPX as previously described.

CELL COUNTING METHODS

Cells were counted using an eyepiece sampling grid at 1.25 x 25 magnification. All interneurones (ACHE and diaphorase cells) were counted from a one in three series through the striatum, Nissil stained nuclei being counted as a sampled area from the central striatum (i.e. that covered by the eyepiece sampling grid) of both lesioned and unlesioned sides from two sections from each individual brain. Raw data from cell counts was corrected by the method of Abercrombie (1946), where

$P = A \times M/L + M$ where P = correct number of cells, A= raw cell count, L= average diameter of cells and M the section thickness. Cell body area (square micrometres) was calculated by random sampling of striata and drawing perikaryal profiles of either cholinergic or diaphorase neurones by camera lucida at 1.25 x 100 using an oil immersion objective lens. Each cell had to present a clear perikaryal outline characteristic of its type. The area of each profile was then calculated using TABLYT software and a graphics pad connected to a 486 PC.

PRIMARY ANTIBODIES

The following primary antibodies were used for immunocytochemistry and/or western blots:

Anti-NF-κB p65 subunit: Santa Cruz SC-109 rabbit polyclonal, immunogen of human origin, recognising amino acids 3-19 of amino terminal of mouse, rat and human. Used at 1:2000 for western blots and immunocytochemistry.

Anti-NF-κB p50 subunit: Santa Cruz SC-114 rabbit polyclonal, immunogen of human origin, recognising amino acids 350-363 (nuclear localisation sequence; NLS) of mouse, rat and human. Used at 1:2000 for western blots and immunocytochemistry.

Anti-NF-κB p52 subunit: Santa Cruz K-27 rabbit polyclonal, immunogen of mouse origin, recognising amino acids 298-324 of mouse, rat and human. Used at 1:1000 dilution for western blots and immunocytochemistry.

Anti-rat CNTF: Promega G1631 chicken polyclonal, immunogen rat recombinant CNTF. Used at 1:1000 dilution for western blots and immunocytochemistry.

Anti-GFAP (Western blots): Dakopatts Z334, rabbit polyclonal, used at 1:1000 dilution for western blots.

Anti-GFAP (Immunocytochemisty): Sigma clone G-A-5 monoclonal, immunogen of porcine origin. Used at 1:1000 for immunocytochemistry.

Anti-IkB-alpha/MAD-3 (C-21):Santa Cruz SC-371 rabbit polyclonal, immunogen of human origin, recognising amino acids 297-317 of carboxy terminus of mouse, rat and human. Used at 1:2000 for western blots and immunocytochemistry.

Anti-TFIID (TBP) Santa Cruz (N-12/SC-204): rabbit polyclonal IgG, immunogen of human origin, recognising amino acids 12-29 of the amino terminal domain of TFIID (TBP) p36 of mouse, rat and human. Used at 1:1000 for western blots and immunocytochemistry.

Anti-TBP (Laszlo Tora 3G3/2C1/4C2): mouse monoclonals, raised to TBP. Used at 1:2000 for western blots and immunocytochemistry.

Anti-Glucocorticoid receptor (M20/SC-1004): Santa Cruz rabbit polyclonal, immunogen of human origin corresponding to amino acids 5-20 of the amino terminus,

mouse, rat, and human reactive. Specific for GR-alpha and GR-beta, non-cross reactive with other steroid receptors. Used at 1:1000 for western blots and immunocytochemistry.

Anti-BRN-2 (C-20/6029): Santa Cruz goat polyclonal, raised against peptide corresponding to amino acids 424-443 mapping at the carboxy terminus of BRN-2 of human origin (identical to mouse sequence). Mouse, rat and human reactive. Used at 1:1000 for immunocytochemistry and western blotting.

Anti-Vasopressin (AB1565): Chemicon rabbit polyclonal, less than 1% reactive with oxytocin. Reactive to human, mouse, rat, sheep and rabbit. Used at 1:1000 for western blotting and 1:5000 for immuncytochemistry.

Anti-OX-42 (MAS 370C): Sera-lab mouse monoclonal anti-rat macrophage. Used at 1:1000 for immunocytochemistry.

NUCLEAR AND CYTOPLASMIC PROTEIN PREPARATION

For tissue to be used for western blots and EMSA experiments adult rats or mice were deeply anaesthetised with sodium pentobarbitone (Sagatal, 100mg/kg i.p.) at specified times or ages following lesion and sacrificed by cervical dislocation. The striatum from left and right sides of rats or the striatum, cortex or cerebellum from transgenic or control mice were dissected on ice. Tissue was immediately processed for protein purification (as follows). Nuclear binding proteins were purified according to the method of Andrews and Faller (1991). The entire procedure was performed at 4°C and all solutions contained a mixture of protease inhibitors with a final concentration of 100 μM leupeptin, 2μg/ml pepstatin, 1mM phenylmethanesulphonyl fluoride (PMSF), 9μg/ml aprotinin and 5mM dithiothreitol (DTT). Freshly harvested tissue was homogenised with a dounce homogeniser in a buffer containing 10mM HEPES-KOH pH 7.9, 1.5mM $MgCl_2$ and 10mM KCl and incubated for 10 minutes at 4°C. Samples were centrifuged at 7000g for 2 minutes (supernatant was removed, spun at 13 000 rpm for 30 minutes, supernatant was again taken and used as a cytoplasmic protein preparation). The pellet was then resuspended in 20 mM HEPES-KOH pH 7.9, 420 mM NaCl, 1.5 mM $MgCl_2$, 0.2 mM EDTA and 25% glycerol. Samples were incubated for 20 minutes at 4°C and centrifuged for 2 minutes at 7000g. The supernatant was denatured with Laemmli sample buffer (final concentration of 2% SDS, 10% 2-mercaptoethanol, 125mM Tris pH 6.8 and 0.1%

bromophenol blue) and stored at -20°C. The nuclear protein samples were shown to be free of contamination from the cytoplasmic compartment by western blots using an antibody against the cytoplasmic protein GFAP. Total protein concentration was measured using a modified Lowry assay (Bio-rad).

POLYACRYLAMIDE GEL ELECTROPHORESIS OF PROTEINS (WESTERN BLOTTING)

Protein totalling 20 to 60 μg was electrophoresed on a 10% SDS-polyacrylamide gel and transferred to Immobilon-P membranes (Millipore). Membranes were pre-incubated for 30 minutes in 1x TBS, 2% low fat milk (Marvel) and 0.5% Tween 20. This buffer was used at room temperature for all subsequent incubations. Filters were incubated in primary antibody for 2 hours (see above), washed three times, incubated in 1/2500 concentration of the appropriate horseradish peroxidase linked secondary antibody (anti-rabbit [Amersham] for polyclonal, anti-mouse for monoclonal [Promega] and anti-chicken for chicken antibodies [Promega]) for 2 hours. Washed three times and finally rinsed in 1x TBS. The western blot was detected by the electrochemiluminesence (ECL) technique (Amersham, see figure below from Amersham technical manual) and exposed to Kodak BioMax-MR autoradiograph film at varying exposures. When possible, control experiments to determine the specifity of the protein (protein bands) were performed by pre-incubation of the primary antibody with the immunogen to which it was raised (at concentrations recommended by the producer, usually 10x by weight) for 30 minutes. Mean optical density of the bands was determined by using a SeeScan or Image Station image analysis system (see below).

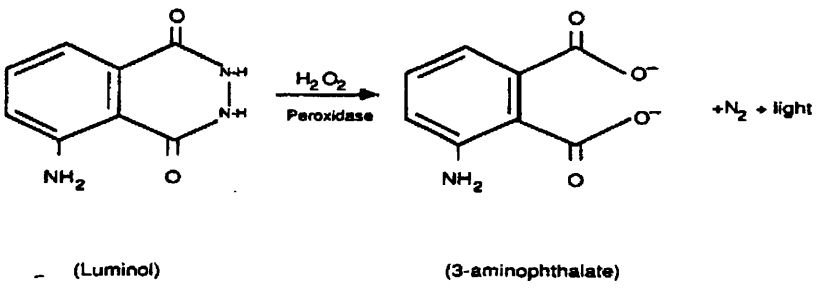

Figure 14. The oxidation of luminol by HRP in the presence of hydrogen peroxide.

ELECTROPHORETIC MOBILITY SHIFT ASSAY

Undenatured protein preparations described above were used for the EMSA assays. Consensus sequence oligonucleotides for the various EMSAs were as follows:

NF-κB 5'...AGT TGA GGG GAC TTT CCC AGG...3' (Promega)

SP-1 5'...ATT CGA TCG GGG CGG GGC GAG C...3' (Promega)

OCT 5'...TGT CGA ATG CAA ATC ACT AGA A ...3' (Promega)

TFIID 5'...GCA GAG CAT ATA AGG TGA GGT AGG A ...3' (Promega)

GR 5'...GAC CCT AGA GGA TCT GTA CAG GAT GTT CTA GAT ...3' (Santa Cruz).

Oligonucleotides were labelled with T4-polynucleotide kinase (Promega) using γ^{32}P ATP (Amersham) to 100 000 cpm /μl (amounting to approximately 0.8 pmol labelled oligonucleotide) and incubated for 30 minutes at room temperature with 2.5 μg of purified nuclear binding proteins in a buffer composed of 10 mM HEPES-KOH, 25 mM KCl, 0.5 mM EDTA, 0.125 mg/ml bovine serum albumin, 2 μM dithiothreitol, 40% glycerol and 10 μg/ml poly[d(I-C)] (Boehringer Mannheim). Bromophenol blue was added to a concentration of 0.01%. Samples were loaded on a pre-run non-denaturing 4% polyacrylamide gel and run at 4°C with a buffer of 6.7mM Tris, 3,3 mM sodium acetate, 1 mM EDTA pH 7.5. After electrophoresis, gels were dried under vacuum and exposed overnight to Kodak BioMax-MR film. For control experiments, unlabelled oligonucleotide was added to the above reaction in 10-20 fold excess to compete out binding and demonstate specifity of bands. For EMSA 'supershifts' the chosen antibody was incubated with the protein (in tissue homogenate) in binding buffer for two hours at 4 degrees C prior to the oligonucleotide binding reaction. Mean optical density of the protein-DNA binding complex 'bands' was determined by using a SeeScan or Image Station image analysis system (see below).

QUANTIFICATION OF PROTEIN/PROTEIN-DNA BINDING BY OPTICAL DENSITOMETRY

Traditionally, increase or decrease in protein levels upon western blots or DNA-protein binding on EMSA has been judged purely visually. However, with improving software

packages it is now possible to obtain a figure relating to the optical density of 'bands' visible on autoradiograph film derived from western blots or EMSA, among other assays, therefore indirectly and somewhat approximately quantifying the increase/decrease in protein expression or binding. This method has been applied in this thesis. Using initially SeeScan (which involved manual selection of each film band individually) and later the superior gel film scanning dedicated program on the Image Station system (Image Analysis) (where analysis of band density can be automatically performed by scanning the entire exposure), film images can be scanned into computer. Obviously, this method can only be applied to bands on the same film, as differences in film exposure time can cause variation in band optical density. However, to allow large population sizes, the value of many specific band densities have been recorded from many separate experiments and an average value taken (the Mean Arbritrary Densitometric Unit: ADU) thereby eliminating this potential for error. The relationship between protein load and densitometric reading is not a directly correlated increase, the densitometric reading lagging behind increasing protein levels. This is illustrated by the following figures and graphs, control experiments carried out on purified protein and tissue homogenates. These control experiments also indicate a reliable degree of sensitivity for the Immobilon-P membranes used for western blotting in this thesis, as a wide range of protein loads can be accurately detected.

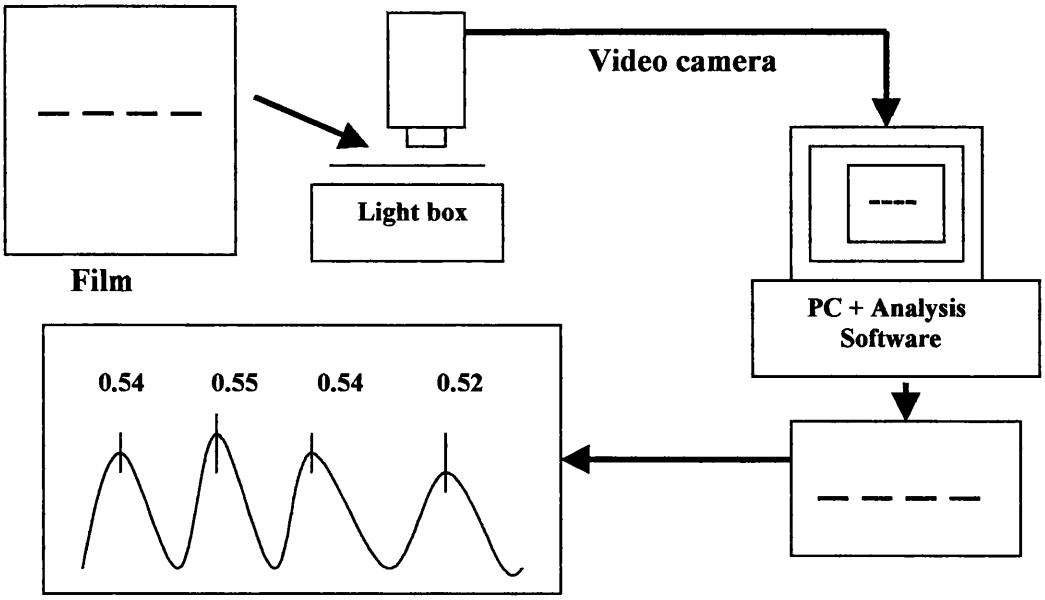

Figure 2.1 Control western blots of brain homogenate (nuclear) and purified protein

1.(Top) Purified recombinant human ciliary neurotrophic factor loaded upon a 10% SDS polyacrylamide gel as used throughout this work. The figures above the lanes indicate micrograms of rhCNTF protein loaded in Laemmli buffer into each lane. Filter was exposed to 1:1000 dilution anti-CNTF. Graph 2.1 gives the quantification of rhCNTF protein (40kD dimer) detectable upon the exposed film by optical densitometry using the Image Analysis system.

2.(Bottom) Striatal homogenate, nuclear fraction, from rat. Homogenate was loaded upon a 10% SDS polyacrylamide gel as used throughout this work. The figures above the lanes indicate the microlitres of total homogenate loaded into each lane. The filter was exposed to 1:1000 dilution of anti-p65. Graph 2.2 gives the quantification of p65 protein detectable upon the exposed film by optical densitometry using the Image Analysis system.

A

B

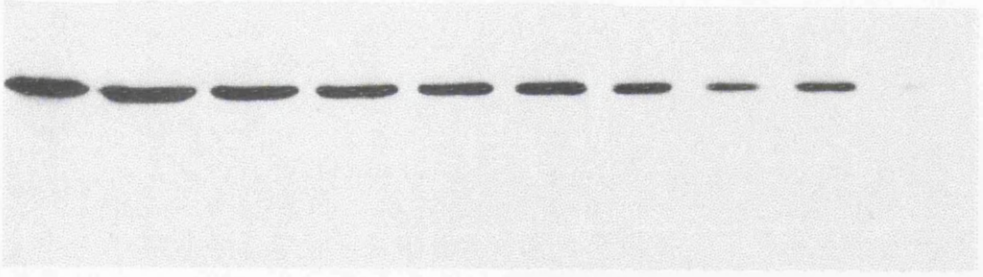

Figure 2.2 Optical densitometry of known amounts of purified rhCNTF protein.

The graph opposite shows optical densitometric readings from a computer scanned western blot exposure of four lanes containing known amounts of purified rhCNTF protein using Image Station. 1=0.06, 2=0.03, 3=0.015, 4=0.0075 micrograms on X-axis upon graph. Although the computer system is supposed to accurately determine protein increase/decrease, the system is not exact. A 100% increase in protein load does not produce a 100% increase in densitometric reading. A 50% reduction in protein load from 0.06 micrograms to 0.03 demonstrates a densitometric reading drop from ~0.33 ADU to ~0.24 ADU, a 27.28 % decrease (or increase if doubling of protein from 0.03 micrograms to 0.06 micrograms occurs). A 50% reduction in protein load from 0.03 micrograms to 0.015 micrograms demonstrates a densitometric reading drop from ~0.24 ADU to ~0.14 ADU, a 41.7% decrease. A 50% reduction in protein load from 0.015 micrograms to 0.0075 micrograms demonstrates a densitometric reading drop from ~0.14 ADU to ~0.1 ADU, a 28.572% decrease. This approximately equals a 32.51% (one third) increase/decrease with each doubling/halving of protein load. This relationship is perhaps more clearly illustrated by the correlation coefficient upon the following page.

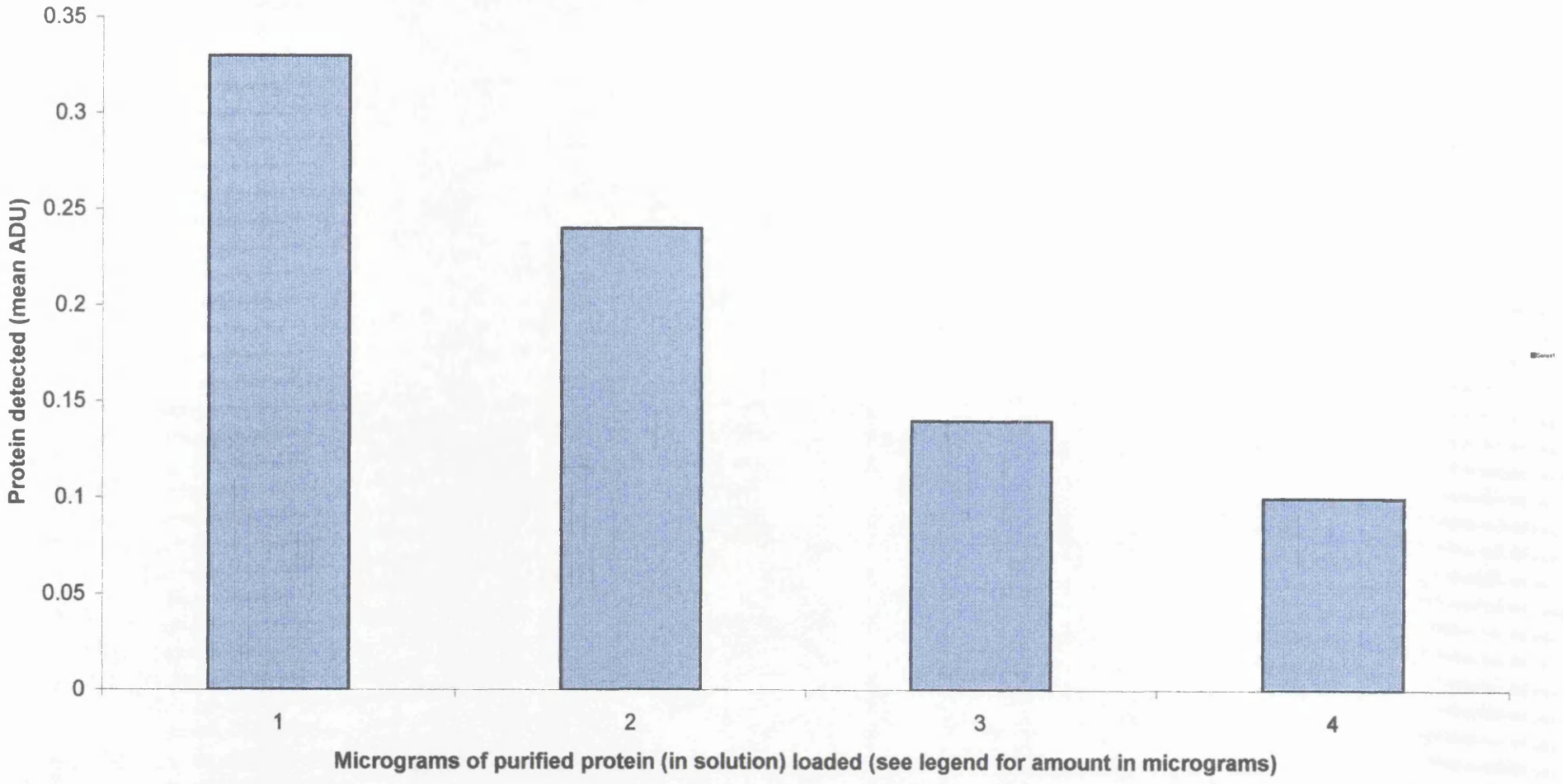
0.35
0.3
0.25
0.2
0.15
0.1
0.05
0
Protein detected (mean ADU)
1
2
3
4
Micrograms of purified protein (in solution) loaded (see legend for amount in micrograms)

Figure 2.3 Optical densitometry of p65 protein load from known volume of striatal homogenate protein (nuclear fraction).

The graph opposite shows optical densitometric readings from a computer scanned western blot exposure of nine lanes, containing known volume in microlitres of striatal tissue homogenate incubated with anti-p65 using Image Station. On X axis of graph, the figures represent the following volume of protein diluted 1:1 in loading buffer in microlitres: 1= 30, 2=22.5, 3=15, 4=11.25, 5=7.5, 6=5.6, 7=3.75, 8=2.8 and 9=1.87. Although the computer system is supposed to accurately determine protein increase/decrease, the system is not exact. A 100% increase in protein load does not produce a 100% increase in densitometric reading. A 50% reduction in protein load from 30 microlitres to 15 demonstrates a densitometric reading drop from ~0.34 ADU to ~0.26 ADU, a 23.52 % decrease (or increase if doubling of protein from 15 microlitres to 15 microlitres occurs). A 50% reduction in protein load from 22.5 microlitres to 11.25 microlitres demonstrates a densitometric reading drop from ~0.29 ADU to ~0.22 ADU, a 24.13 decrease. A 50% reduction in protein load from 15 microlitres to 7.5 microlitres demonstrates a densitometric reading drop from ~0.26 ADU to ~0.18 ADU, a 30.76% decrease. A 50 % reduction in protein load from 11.25 microlitres to 5.6 microlitres demonstrates a densitometric reading drop from ~0.22 ADU to ~0.17 ADU, a 22.7 % decrease. Sensitivity seems to be lost at very low loaded volumes (2.8 microlitres and 1.87 microlitres both provided an equal densitometric reading of ~0.12) but this level is well below amount loaded for PAGE (usually 15 to 30 microlitres). The 0.935 microlitre load could not be detected. Overall, however a 25.28 (one quarter) increase/decrease with each doubling/halving of protein load is observed. This is somewhat disappointing, but still provides a useful guide to protein increase/decrease, a one quarter/one third increase in ADU indicates a possible doubling of protein on PAGE.

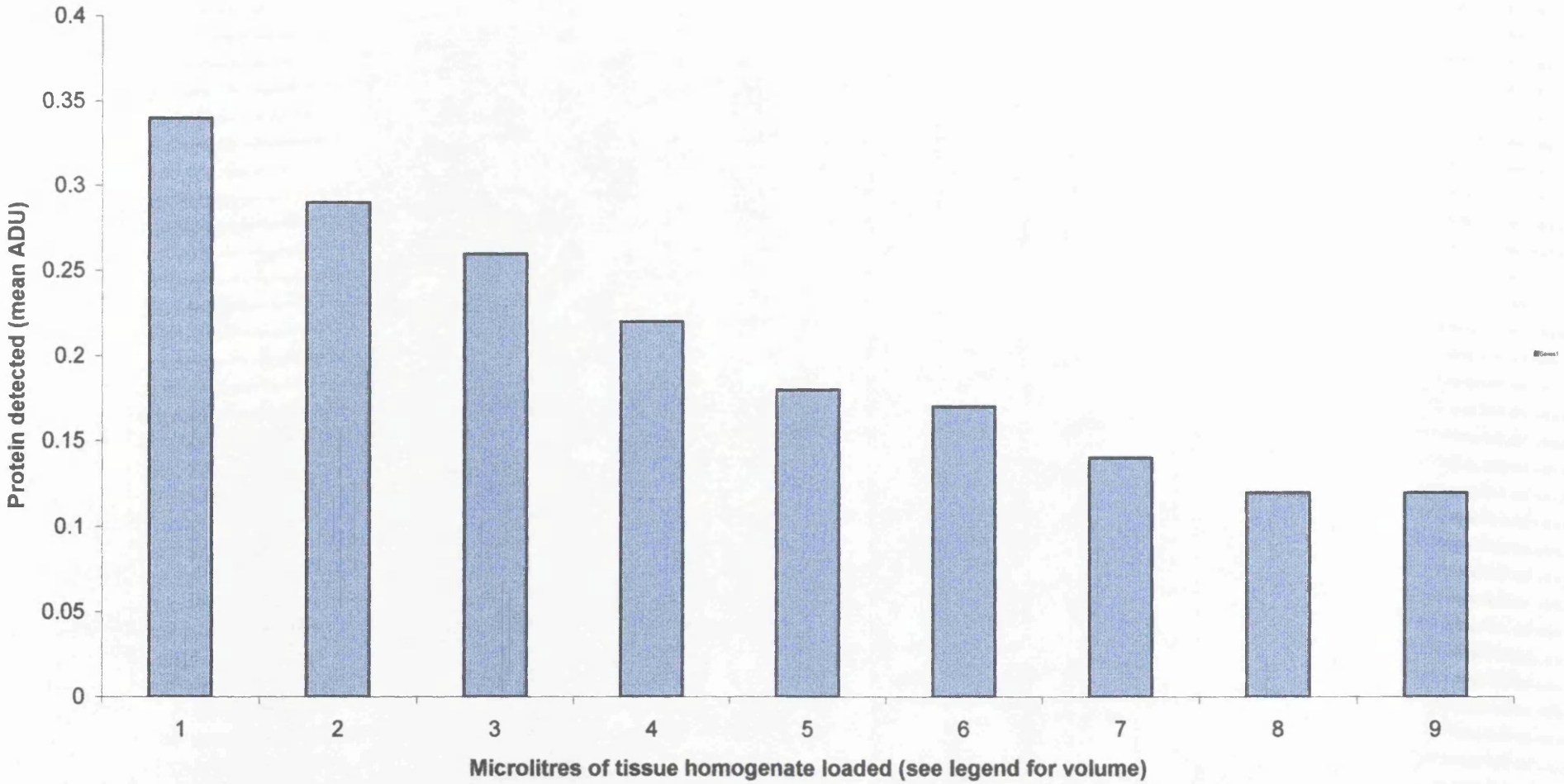
0.4
0.35
0.3
0.25
0.2
0.15
0.1
0.05
0
Protein detected (mean ADU)
1
2
3
4
5
6
7
8
9
Microlitres of tissue homogenate loaded (see legend for volume)

Figure 2.4 Correlation coefficients of protein load against protein detected in mean arbitrary densitometric units.

Graph 1. Demonstrates known amounts of purified rhCNTF protein (4=0.06, 3=0.03, 2=0.015, 1=0.0075 micrograms) on X-axis upon graph plotted against the mean ADU detected by the Image Analysis system. The coefficient for this relationship shows a positive correlation, although a weak one perhaps due to the small amount of data in each population. Correlation coefficient r=0.12

Graph 2. Demonstrates known amounts of striatal nuclear tissue homogenate incubated with anti-p65. On X axis of graph, the figures represent the following volume of protein diluted 1:1 in loading buffer in microlitres: 9= 30, 8=22.5, 7=15, 6=11.25, 5=7.5, 4=5.6, 3=3.75, 2=2.8 and 1=1.87. The coeffficient for this relationship shows a much stronger positive correlation at r=0.97.

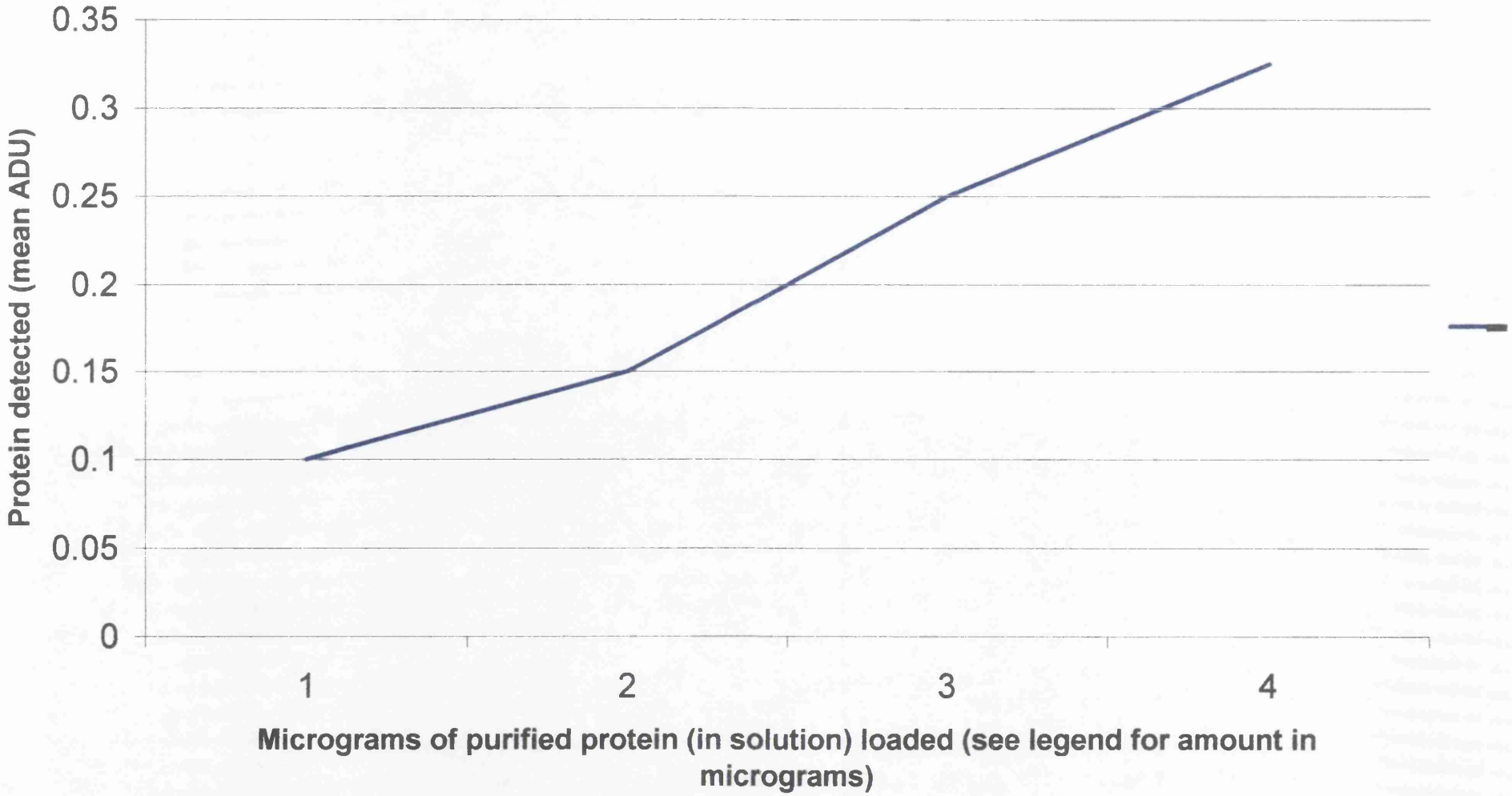
0.35
0.3
0.25
0.2
0.15
0.1
0.05
0
Protein detected (mean ADU)
1
2
3
4
Micrograms of purified protein (in solution) loaded (see legend for amount in micrograms)

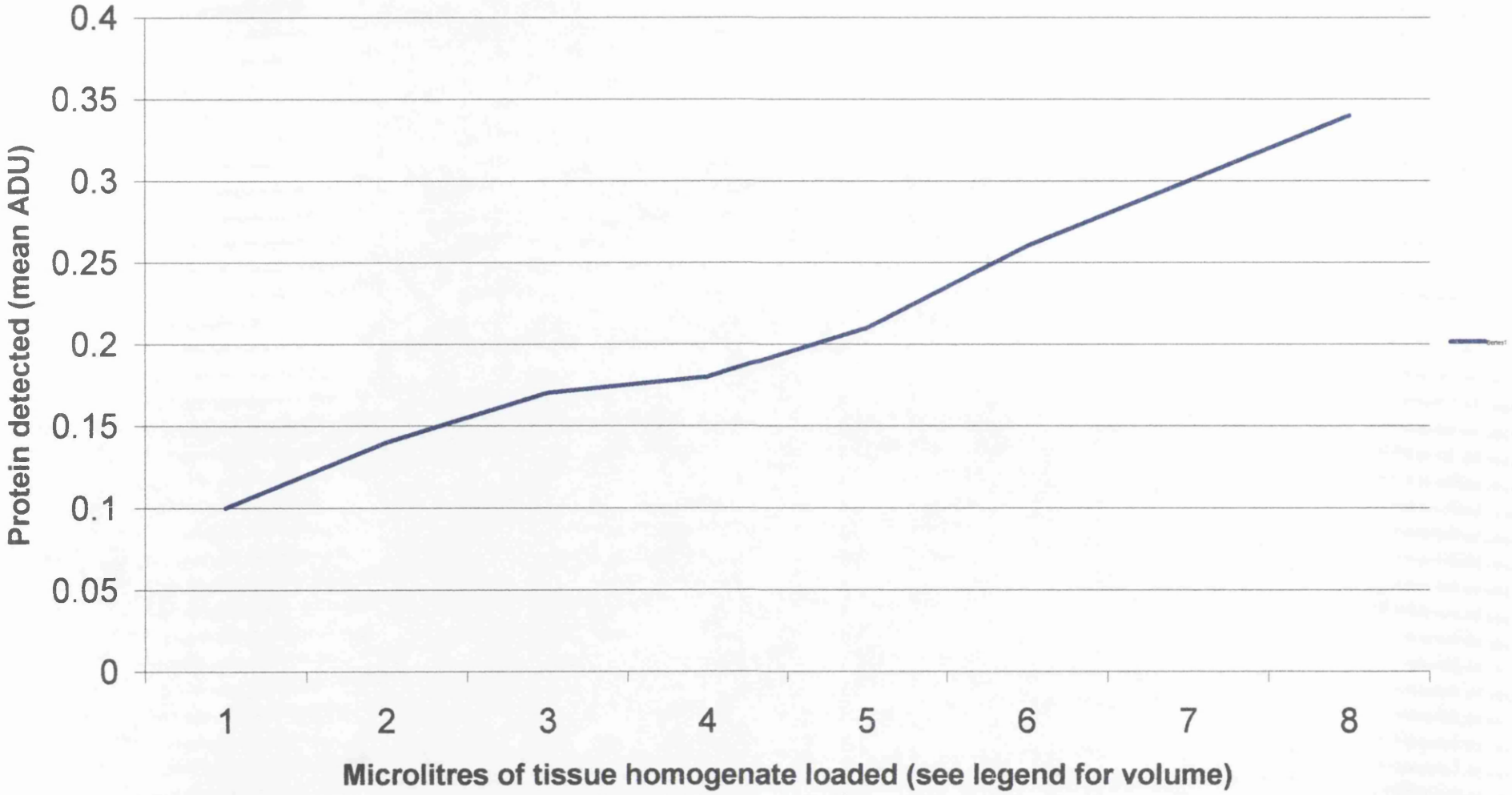
0.4
0.35
0.3
0.25
0.2
0.15
0.1
0.05
0
Protein detected (mean ADU)
1
2
3
4
5
6
7
8
Microlitres of tissue homogenate loaded (see legend for volume)

RESULTS

3.1 EXOGENOUS AND ENDOGENOUS ACTION OF CNTF IN NORMAL AND QA LESIONED RAT STRIATUM

Exogenous application of QA and CNTF+QA in the rat striatum.

Rat right striata were injected with 1µl QA (60nmol) alone or 1µl QA and CNTF (60nmol QA+ 1.5µg CNTF). Striatal interneurones were histochemically stained for acetylcholinesterase and NADPH diaphorase (Fig3.1/1 A,B,C & D), while analysis of projection neurones was undertaken by thionin (Nissl) staining of nuclei present at seven days post-lesion. Cell counts were conducted, all interneurones on each section, both left and right striata, being counted from a one in three series through the striatum using a sampling grid to prevent overlap of counts. The variation in number between lesioned and unlesioned sides of the striatum for all cell types was highly significant as would be expected in all QA treated animals. However no significant difference could be found in projection neurone cell number (Fig.3.1/G1), cholinergic interneurones or diaphorase interneurones (Fig.3.1/G2) between QA treated and QA and CNTF treated animals.

Furthermore, the somal area of cholinergic and diaphorase interneurones was measured at seven days post lesion, to observe any variation in QA versus QA+CNTF treated striatum. No difference in cell area between QA and QA+CNTF treated interneurones was observed (Fig.3.1/G3 and Fig.3.1/G4).

Exogenous application of CNTF very clearly produces a strong glial response, inducing the activation of both astrocytes, as determined by GFAP immunocytochemistry (Fig.3.1/6) and microglia as determined by OX-42 immunocytochemistry (Fig.3.1/7/8/9).

Endogenous CNTF and GFAP protein expression and localisation in the striatum after QA administration

Western blots of cytoplasmic striatal preparations from QA treated brains using the CNTF G1631 antibody demonstrated two major proteins migrating at 40 and 20 kD respectively (Fig 3.1/2). Both these two protein bands could be abolished by pre incubating the antibody with rhCNTF. When purified human recombinant CNTF was run upon western blots, two bands could also be identified at 40 and 20 kD. Densitometry of the 40kD band demonstrated a significant increase above control levels at 168 hours (seven days) after QA lesion (Fig 3.1/G5). Western blot for GFAP using the polyclonal

Z334 antibody demonstrated a visible, gradual increase in GFAP after QA lesion, with maximum levels demonstrated at seven days following treatment (Fig.3.1/3).

Immunocytochemistry using the G1631 antibody localised CNTF to cells exhibiting an astrocytic morphology at 120 hours (five days) and beyond in the rat striatum (Fig.3.1/4) resembling those found at the same time point in striatum immunoreactive for GFAP using monoclonal antibody G-A-5 (Fig.3.1/5). The peak of endogenous CNTF expression also coincides with the greatest point of ameboid microglial proliferation as determined by OX-42 immunoreactivity (Fig. 3.1/7/8/9). Weak CNTF reactivity in the control striatum could be observed in some neuronal perikarya, but immunoreactivity is more clearly observed in the overlying cortex.

Figure. 3.1/1

Cellular localisation (endogenous histochemistry) of acetylcholinesterase and NADPH diaphorase in normal rat striatum and following QA lesion at 24 hours post-treatment.

(A) Photomicrograph of endogenous histochemistry for striatal NADPH diaphorase interneurones in striatum following QA lesion. Scale bar = 30 μm.

(B) Photomicrograph of endogenous histochemistry for striatal NADPH diaphorase interneurones control (untreated) striatum. Scale bar = 30 μm.

(C) Photomicrograph of endogenous histochemistry (acetylcholinesterase) for striatal cholinergic interneurones in striatum following QA lesion. Scale bar = 60 μm.

(D) Photomicrograph of endogenous histochemistry (acetylcholinesterase) for striatal cholinergic interneurones in control (untreated) striatum. Scale bar = 60 μm.

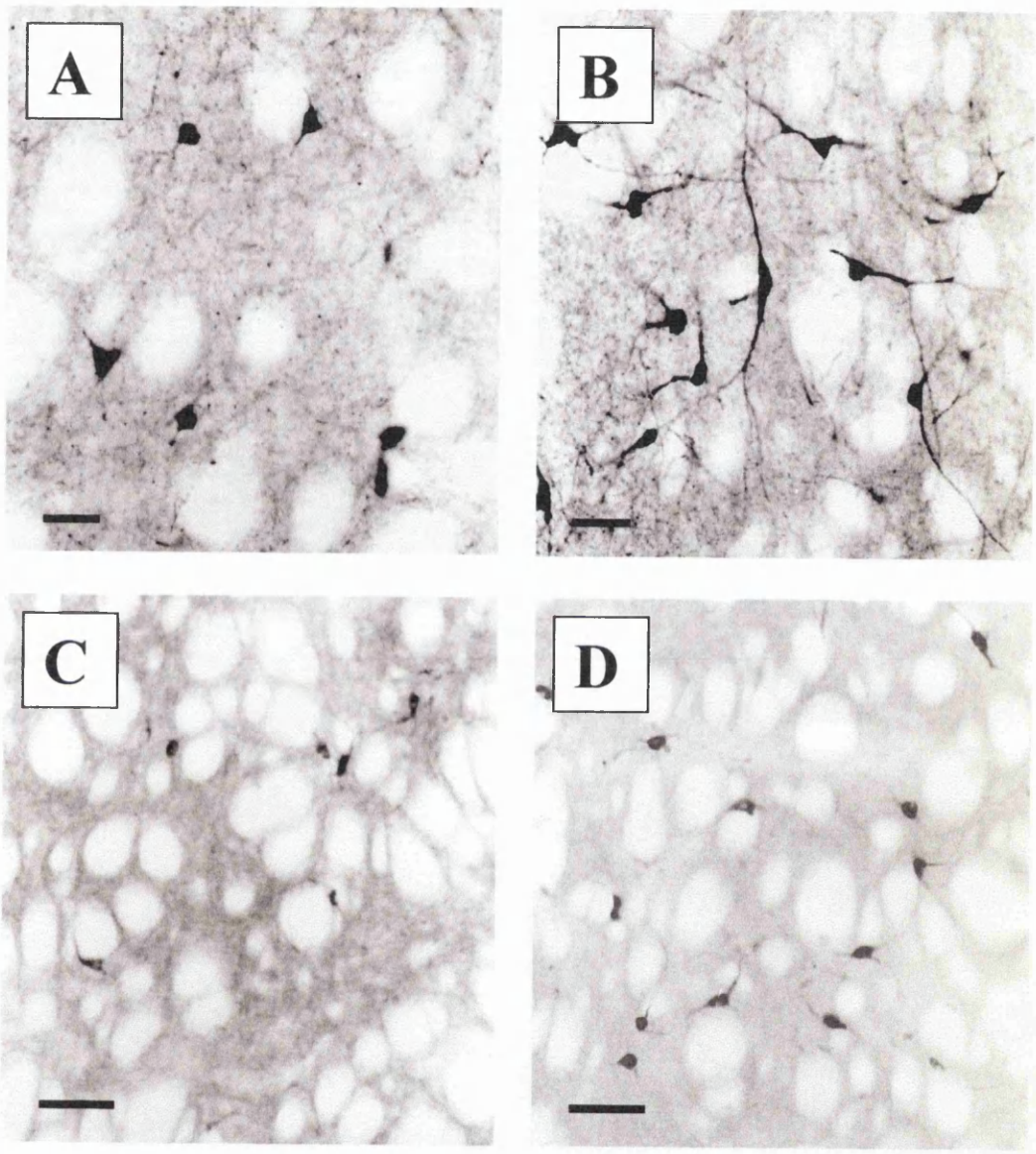
A
B
C
D

Figure. 3.1/G1

Mean cell number per sampled area thionin (Nissl) stained nuclei of striatal projection neurones after administration of QA or QA+CNTF

The graph opposite illustrates the survival of striatal projection neurones as determined by counting thionin (Nissl) stained nuclei following QA or QA+CNTF administration. Counts were conducted seven days following administration from a one in three series of 40 μm sections through the striatum. Bars demonstrate the standard error of each population from which the mean value was obtained. No significant difference between QA and QA+CNTF treated brains was observed (Student's t-test). Number of brains (N) = 5 per treatment (total N= 10).

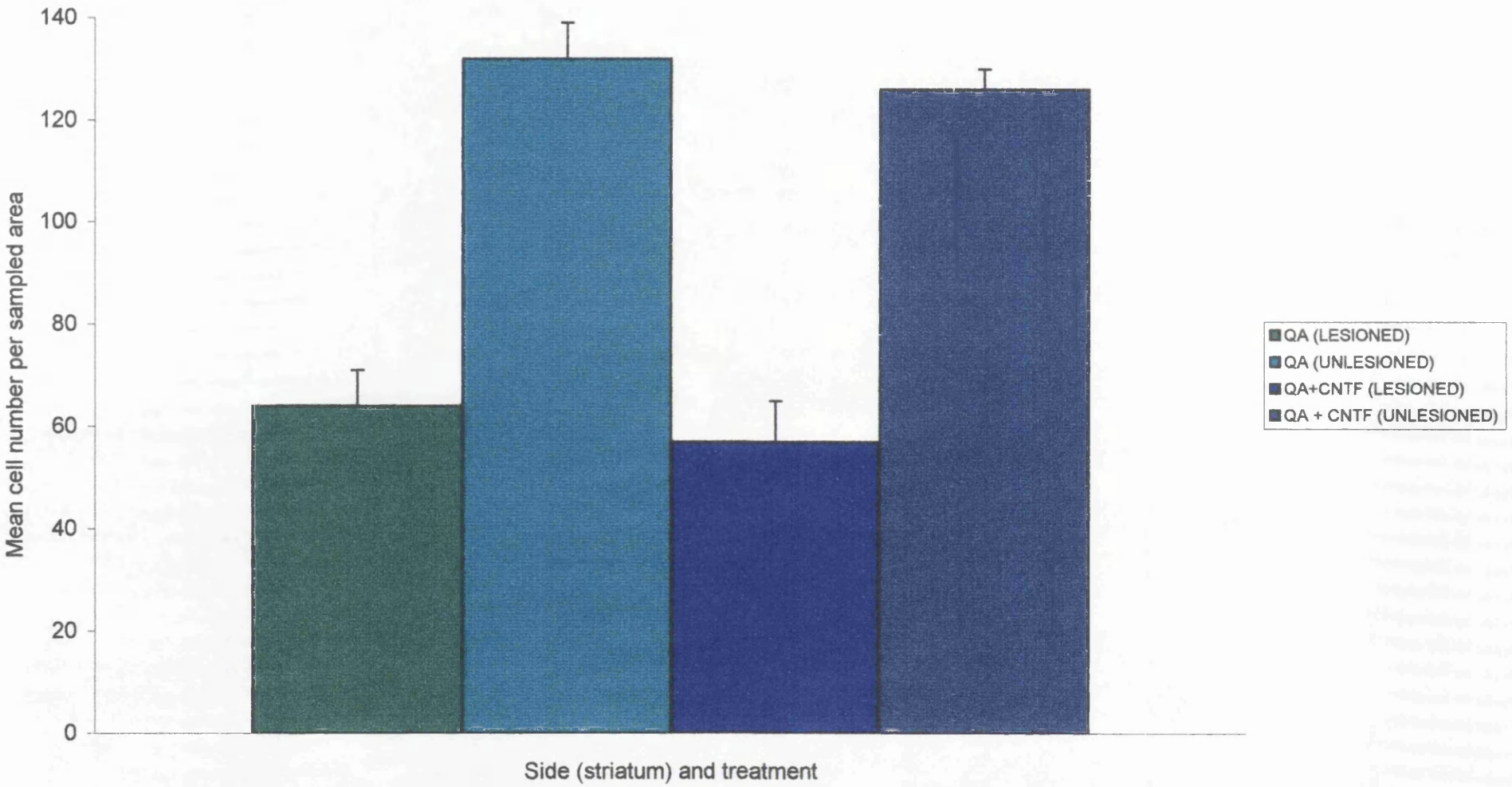
140
120
100
80
60
40
20
0
Mean cell number per sampled area
Side (striatum) and treatment
QA (LESIONED)
QA (UNLESIONED)
QA+CNTF (LESIONED)
QA + CNTF (UNLESIONED)

Figure. 3.1/G2

Mean percentage cell survival of striatal acetylcholinesterase or NADPH diaphorase interneurons seven days after administration of QA or QA+CNTF

The graph opposite illustrates the percentage survival of striatal interneurones as determined by counting all histochemically stained acetylcholinesterase and NADPH diaphorase neurones in a 1 in 3 series through the lesioned striatum following QA or QA+CNTF administration. Counts were conducted seven days following administration. Bars demonstrate the standard error of each population from which the mean value was obtained. No significant difference between QA and QA+CNTF treated brains was observed. Number of brains (N) = 5 per treatment (total N= 10).

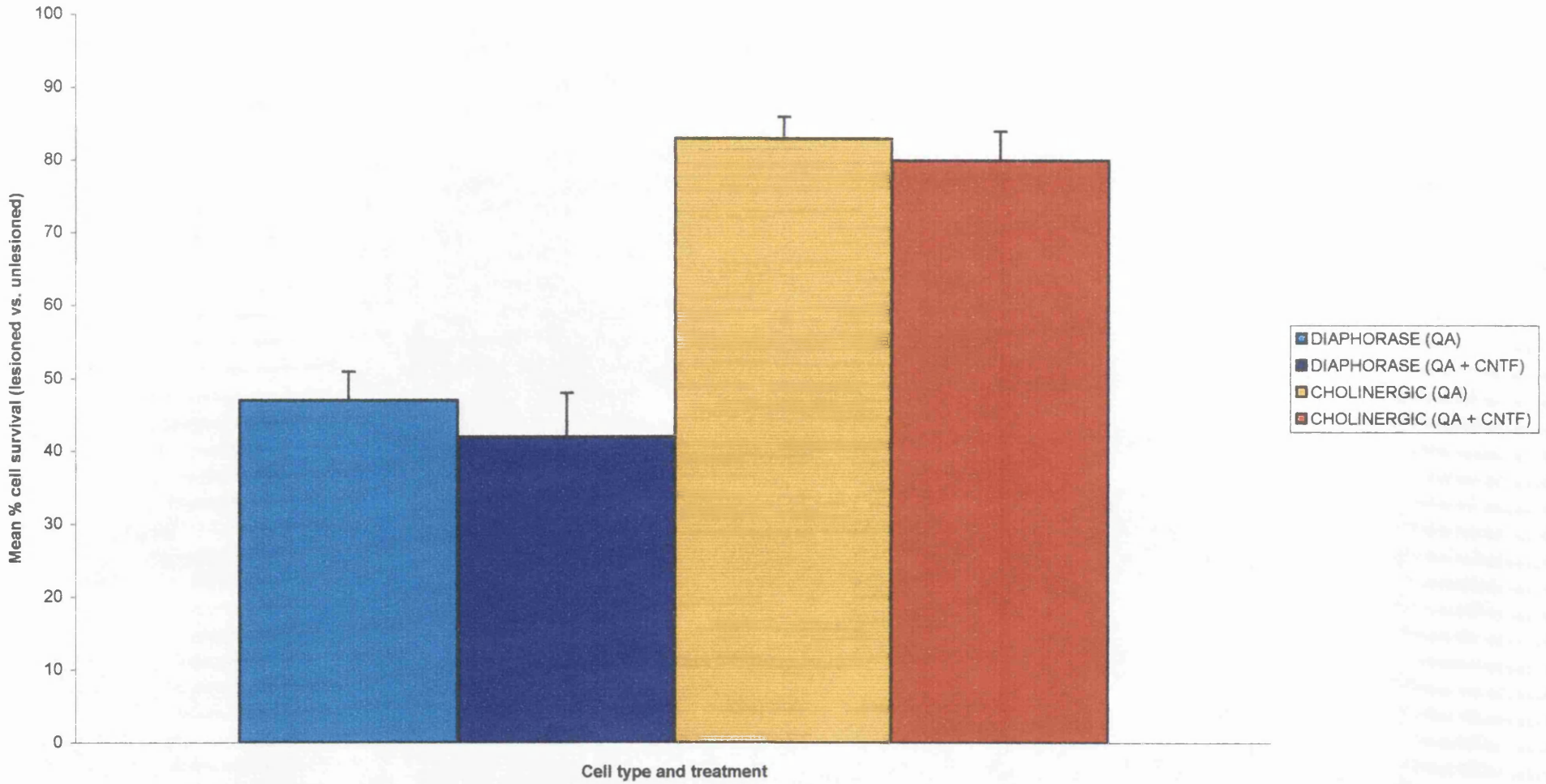
100
90
80
70
60
50
40
30
20
10
0
Mean % cell survival (lesioned vs. unlesioned)
Cell type and treatment
DIAPHORASE (QA)
DIAPHORASE (QA + CNTF)
CHOLINERGIC (QA)
CHOLINERGIC (QA + CNTF)

Figure. 3.1/G3

Mean somal cell area (square micrometers) of survival of striatal NADPH diaphorase interneurons seven days after administration of QA or QA+CNTF

The graph opposite illustrates the mean cell area of striatal diaphorase interneurones as determined by drawing somal profiles by camera lucida and measuring cell area using a computer system following QA or QA+CNTF administration. Study was conducted seven days following administration. Bars demonstrate the standard error of each population from which the mean value was obtained. No significant difference in cell area between QA and QA+CNTF treated brains was observed (Student's t-test). Number of brains (N) = 5 per treatment (total N= 10).

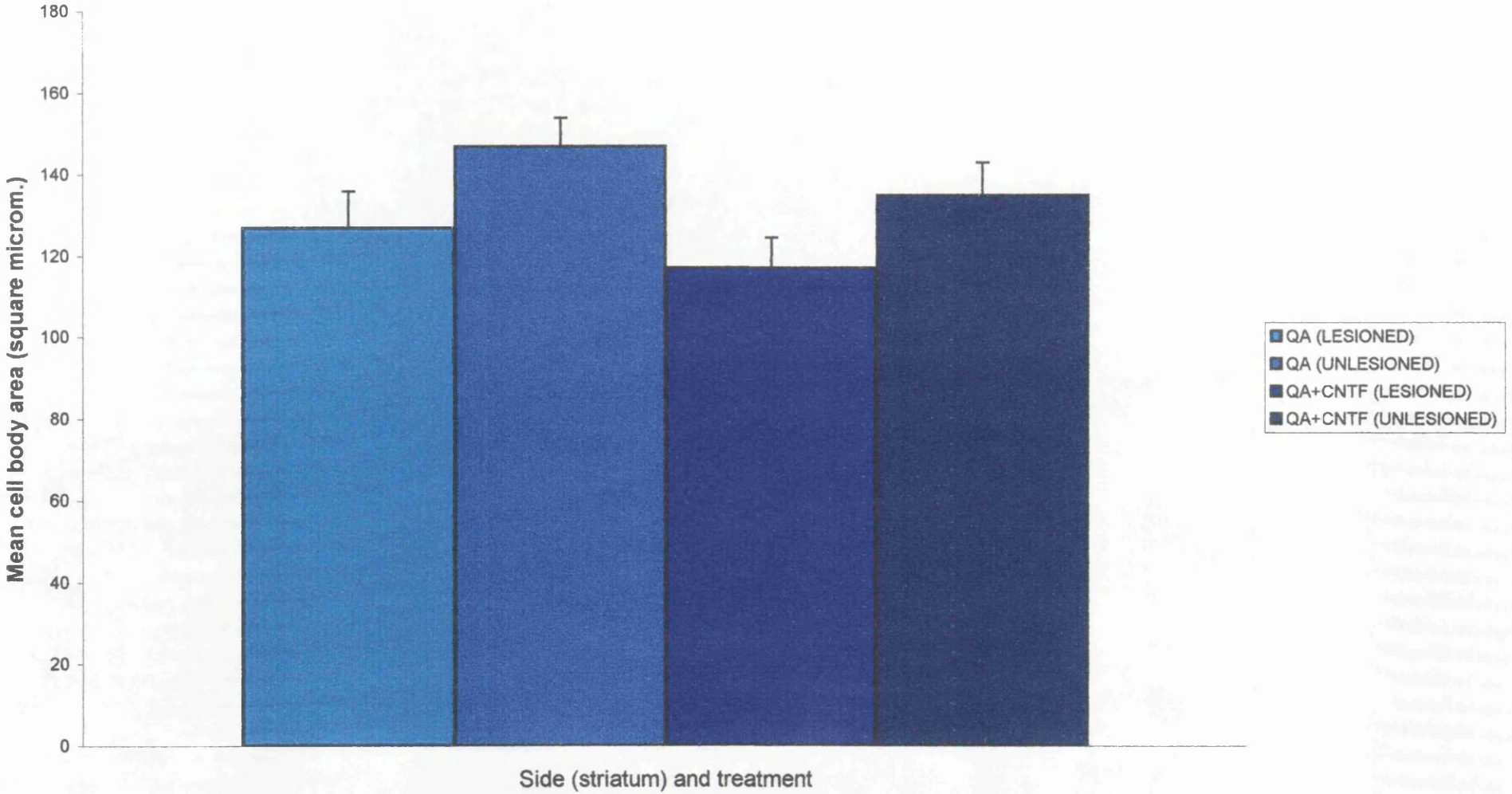
180
160
140
120
100
80
60
40
20
0
Mean cell body area (square microm.)
Side (striatum) and treatment
QA (LESIONED)
QA (UNLESIONED)
QA+CNTF (LESIONED)
QA+CNTF (UNLESIONED)

Figure. 3.1/G4

Mean somal cell area (square micrometers) of survival of striatal cholinergic interneurons seven days after administration of QA or QA+CNTF

The graph opposite illustrates the mean cell area of acetylcholinesterase positive interneurones as determined by drawing somal profiles by camera lucida and measuring cell area using a computer system following QA or QA+CNTF administration. Study was conducted seven days following administration. Bars demonstrate the standard error of each population from which the mean value was obtained. No significant difference in cell area between QA and QA+CNTF treated brains was observed (Student's t-test). Number of brains (N) = 5 per treatment (total N= 10).

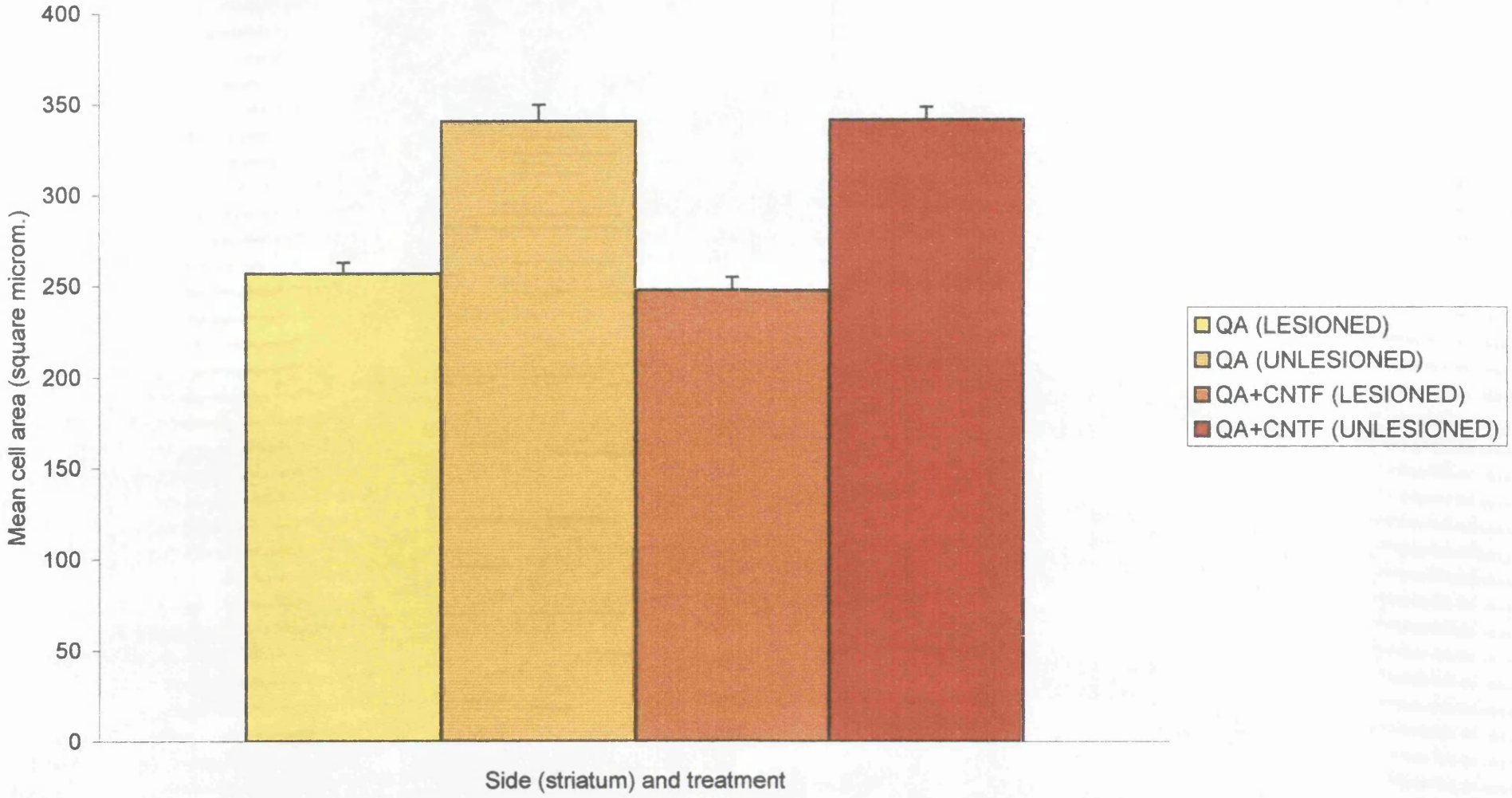
400
350
300
250
200
150
100
50
0
Mean cell area (square microm.)
Side (striatum) and treatment
QA (LESIONED)
QA (UNLESIONED)
QA+CNTF (LESIONED)
QA+CNTF (UNLESIONED)

Figure. 3.1/2

CNTF protein expression (PAGE) in controls and following Quinolinic acid lesion at 12, 24, 48, 120 and 168 hours post lesion.

(A) Western blot showing ciliary neurotrophic factor (CNTF) expression in control (untreated) rat striatum (ST), cortex (CTX) and cerebellum (CB) and quinolinic acid (QA) treated rats at 24 hours post-lesion (24). Two protein bands correlating to the purified protein (rhP sample recombinant human [rh] CNTF, courtesy Regeneron) are visible, one at 40 kD and another at 20 kD. Blocking experiment conducted with rhCNTF abolishes the 40 kD and 20 kD proteins in a control and 24 hour post lesion sample (BST C and 24) but not the higher molecular weight protein bands.

(B) Western blot showing ciliary neurotrophic factor (CNTF) expression in quinolinic acid (QA) treated rat striatum (both left unlesioned (LST) and right lesioned (RST) at 12, 24, 48, 120 and 168 hours post-lesion. An increase in CNTF (20 kD and 40 kD protein bands) expression in both lesioned and unlesioned sides can potentially be visualised at 168 hours (7 days) following lesion.

(C) Western blot showing ciliary neurotrophic factor (CNTF) expression in control (untreated) and quinolinic acid (QA) lesioned rat striatum at 12, 24, 48, 120 and 168 hours post-lesion. An increase in CNTF (40 kD/dimer protein band) can be visualised at 168 hours (7 days) following lesion and confirmed by optical densitometry. This western blot illustrates the usually weak appearance of the 20 kD CNTF protein band which makes detection by optical densitomery difficult or impossible. This low level of expression makes it difficult to obtain a large enough group of data to obtain definitive figures concerning the level of expression of this 20 kD/monomer. Densitometric analysis demonstrates a significant increase in endogenous CNTF (40 kD) levels in rat striatum following QA lesion at 168 hours (seven days) post-lesion (Fig.3.1/G5). Antibody used for all blots was Promega G1631 anti-chicken at 1:1000 dilution.

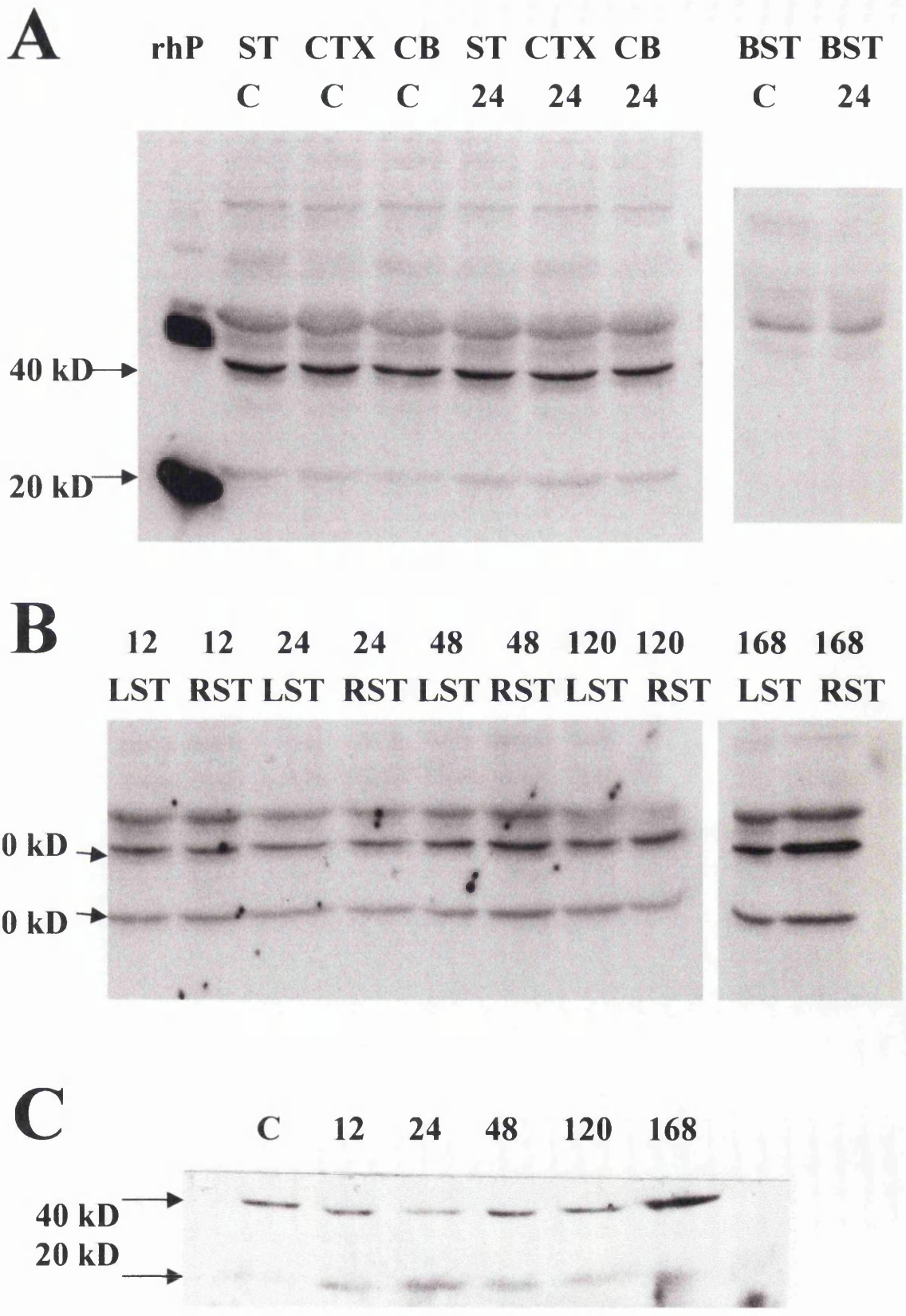
A
rhP
ST C
CTX C
CB C
ST 24
CTX 24
CB 24
BST C
BST 24
40 kD
20 kD
B
12 LST
12 RST
24 LST
24 RST
48 LST
48 RST
120 LST
120 RST
168 LST
168 RST
40 kD
20 kD
C
C
12
24
48
120
168
40 kD
20 kD

Figure. 3.1/G5

Densitometric analysis of dimeric CNTF protein expression (PAGE) in the striatum in controls and following QA lesion at 12, 24, 48. 120 and 168 hours post-lesion.

The graph opposite illustrates the protein expression (CNTF) in mean arbitrary densitometric units (ADU) following QA administration at various time points. Time after lesion is displayed in the key to the right. Bars demonstrate the standard error of each population from which the mean value was obtained. Protein expression in the 168 hours (seven days) population was demonstrated to be significantly different to that in the control population using Student's two-tailed t-test at $P=0.025$ ($P<0.05$=significant). Number of brains (N) = 6 per time period (i.e. 6 controls, 6 12h post lesion etc.) pooled as groups of two (i.e. experiment conducted three times per time period). Total N= 46.

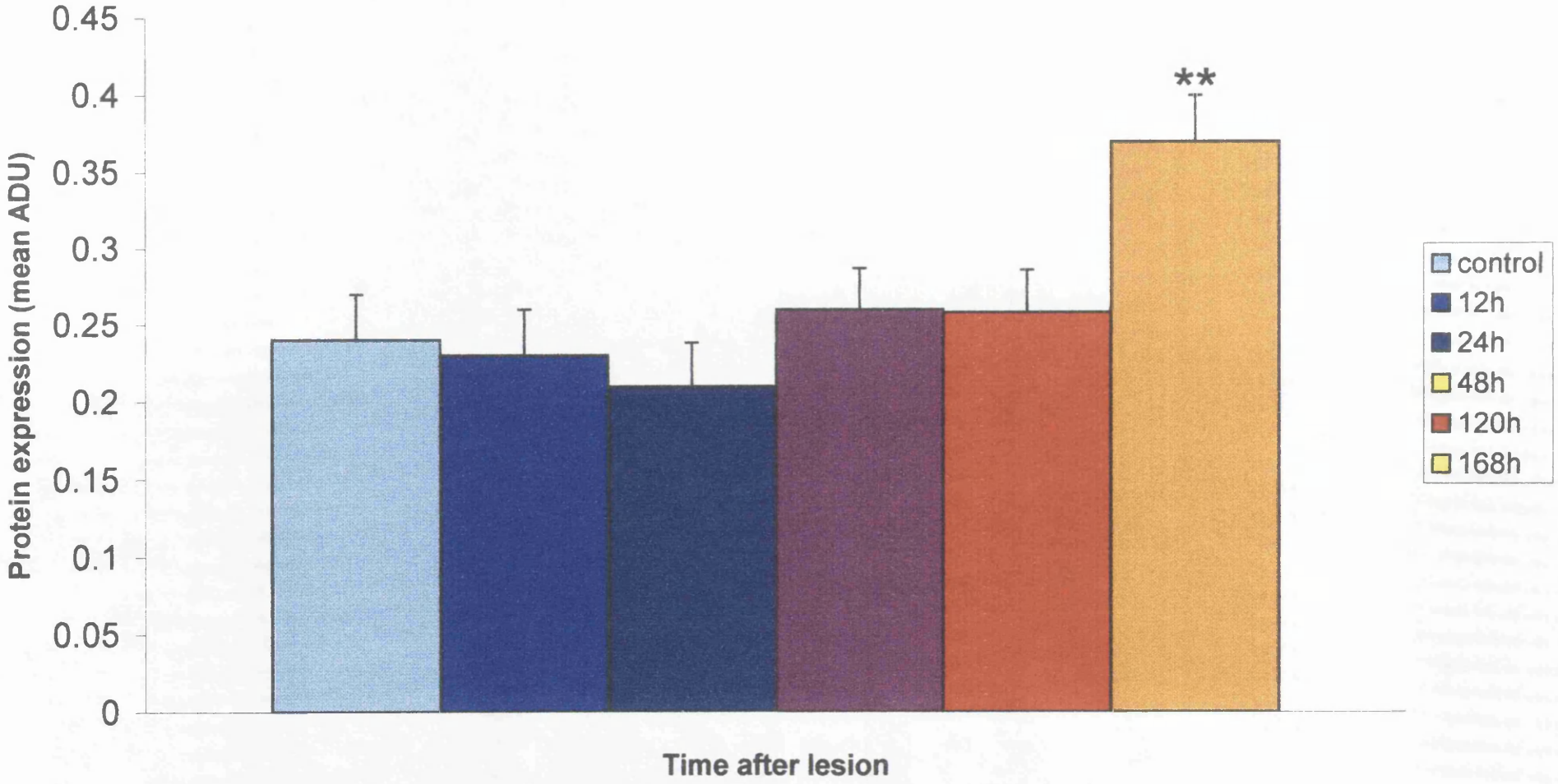
0.45
0.4
0.35
0.3
0.25
0.2
0.15
0.1
0.05
0
Protein expression (mean ADU)
**
control
12h
24h
48h
120h
168h
Time after lesion

Figure. 3.1/3

Glial fibrillary acidic protein (GFAP) expression (PAGE) in control striatum and following quinolininc acid (QA) lesion and CNTF treatment at 12, 24, 48, 120 and 168 hours post-lesion

(A)Western blot showing glial fibrillary acidic protein (GFAP) expression in control (untreated) and quinolinic acid (QA) treated rats at various time points post-lesion. The arrow indicates a protein species migrating at ~50 kD, the weight of a GFAP sub-unit. A gradual increase in expression can be seen as time after lesion progresses, reaching maximum expression at seven days post-lesion. This corresponds with GFAP expression in astrocytes observed using with immunocytochemistry (Fig.3.1/4). Antibody used was Dakopatts polyclonal Z334 used at 1:1000 dilution.

(B) Western blot showing glial fibrillary acidic protein (GFAP) expression in control (untreated) and CNTF treated rats at various time points post-lesion. The arrow indicates a protein species migrating at ~50 kD, the weight of a GFAP sub-unit. A gradual increase in expression can be seen at 12 hours following treatment and again at 168 hours (seven days). However, expression of GFAP following CNTF does not seem to be as great as that following QA. Antibody used was Dakopatts polyclonal Z334 used at 1:1000 dilution.

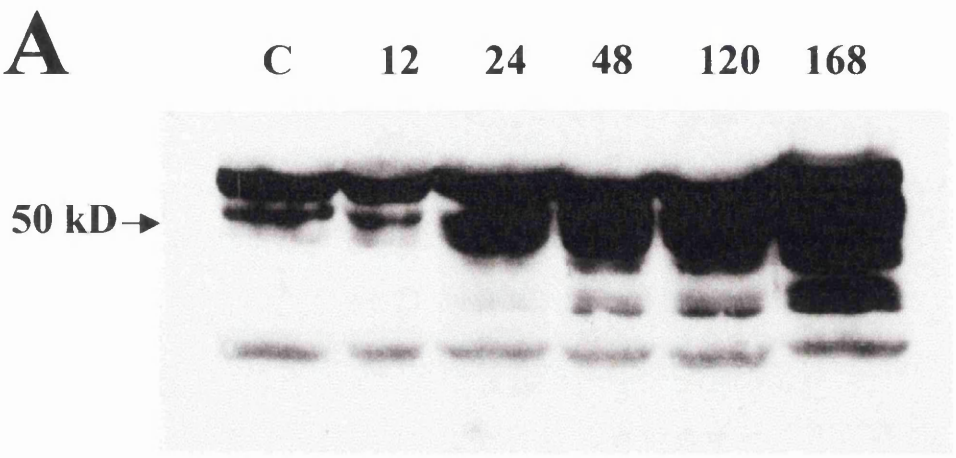
A
C
12
24
48
120
168
50 kD

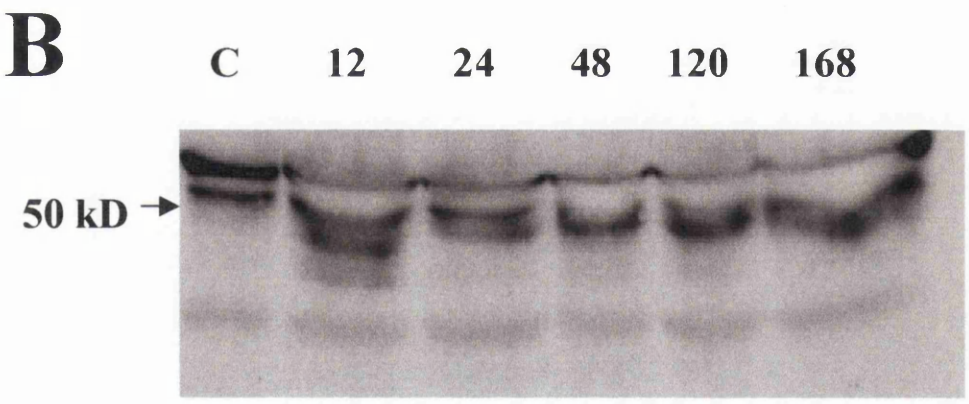
B
C
12
24
48
120
168
50 kD

Figure. 3.1/4

Cellular expression (immunocytochemistry) of CNTF in controls and following QA lesion.

(A) Photomicrograph of immunocytochemistry for ciliary neurotrophic factor (CNTF) in control striatum. The dark perikarya of some CNTF reactive neurones can be observed (arrowed). Scale bar = 40 μm. Antibody used was Promega G1631 anti-chicken at 1:1000 dilution.

(B) Photomicrograph of immunocytochemistry for ciliary neurotrophic factor (CNTF) in control cortex. The dark perikarya of CNTF reactive neurones can be observed. Some pyramidal neurones clearly demonstrating cytoplasmic localisation and nuclear exclusion of CNTF are arrowed. Scale bar = 40 μm.

(C) Photomicrograph of immunocytochemistry for ciliary neurotrophic factor (CNTF) in QA lesioned striatum at 168 hours (seven days) post-lesion. Scale bar = 40 μm. CNTF positive reactive astrocytes (arrowed) are visible showing a similar morphology to those immunoreactive for GFAP.

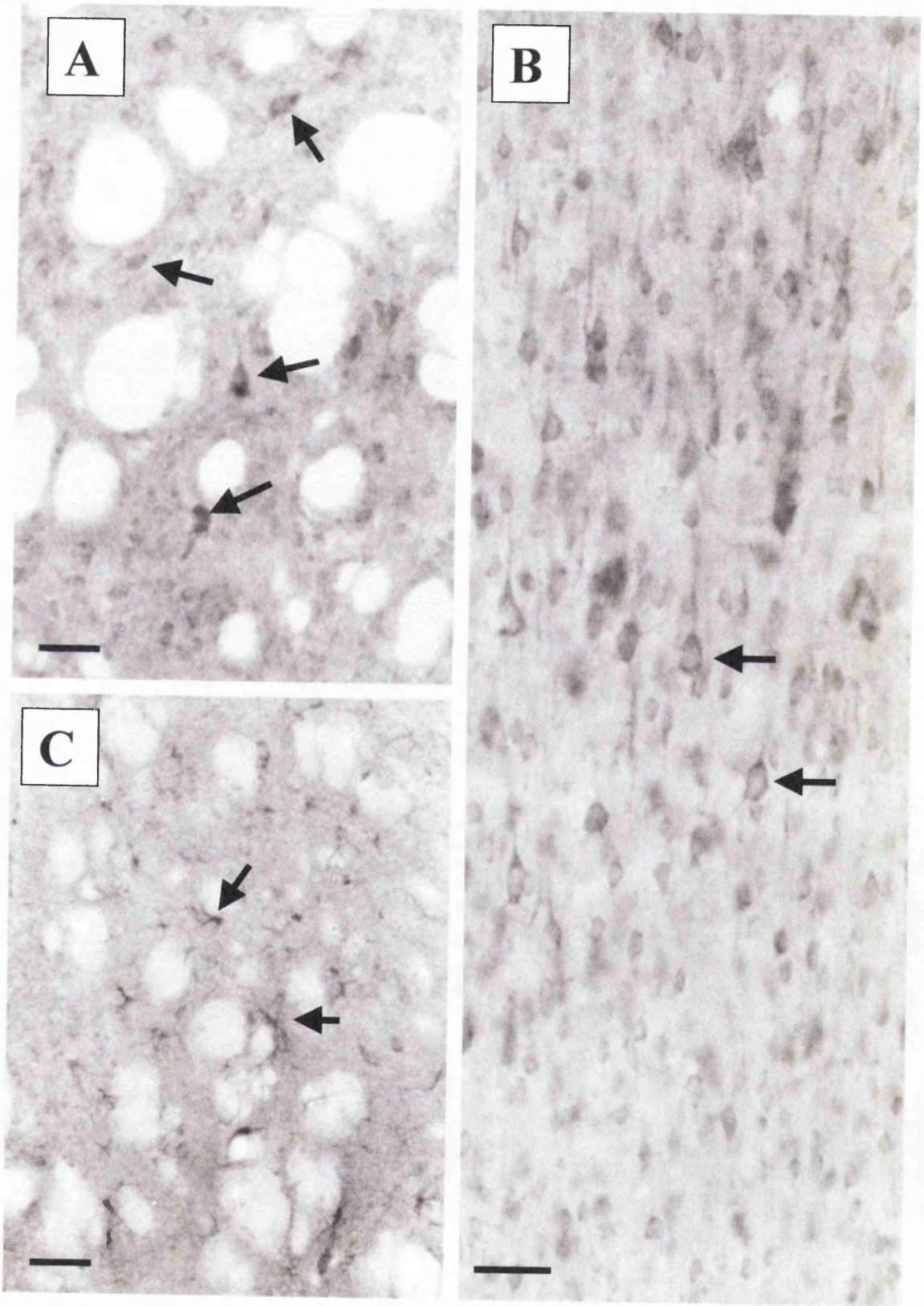
A
B
C

Figure. 3.1/5

Cellular expression (immunocytochemistry) of GFAP in rat striatum following CNTF treatment.

(A) Photomicrograph of immunoreactivity for glial fibrillary acidic protein (GFAP) 48 hours following CNTF treatment in striatum. Some reactive filamentous processes can be observed (blue arrow), as can some cell bodies (red arrow) but few cells exhibiting distinctive astrocyte morphology can be seen. Antibody used Sigma G-A-5 monoclonal at 1:1000.

(B) Photomicrograph of immunoreactivity for glial fibrillary acidic protein (GFAP) in striatum at 72 hours following CNTF treatment. GFAP reactive processes are again visible (blue arrow) as are reactive astrocytes (red arrow).

(C) Photomicrograph of immunoreactivity for glial fibrillary acidic protein (GFAP) in striatum at 120 hours (five days) following CNTF treatment. GFAP reactive astrocytes are clearly visible.

(D) Photomicrograph of immunoreactivity for glial fibrillary acidic protein (GFAP) in CNTF treated striatum at 168 hours (seven days) post lesion. Dark and large GFAP reactive astrocytes can clearly be seen in the striatum with radiating filamentous processes (red arrow). The cell bodies of these astrocytes are somewhat larger than those observed following QA lesion. Scale bars = 30 μm.

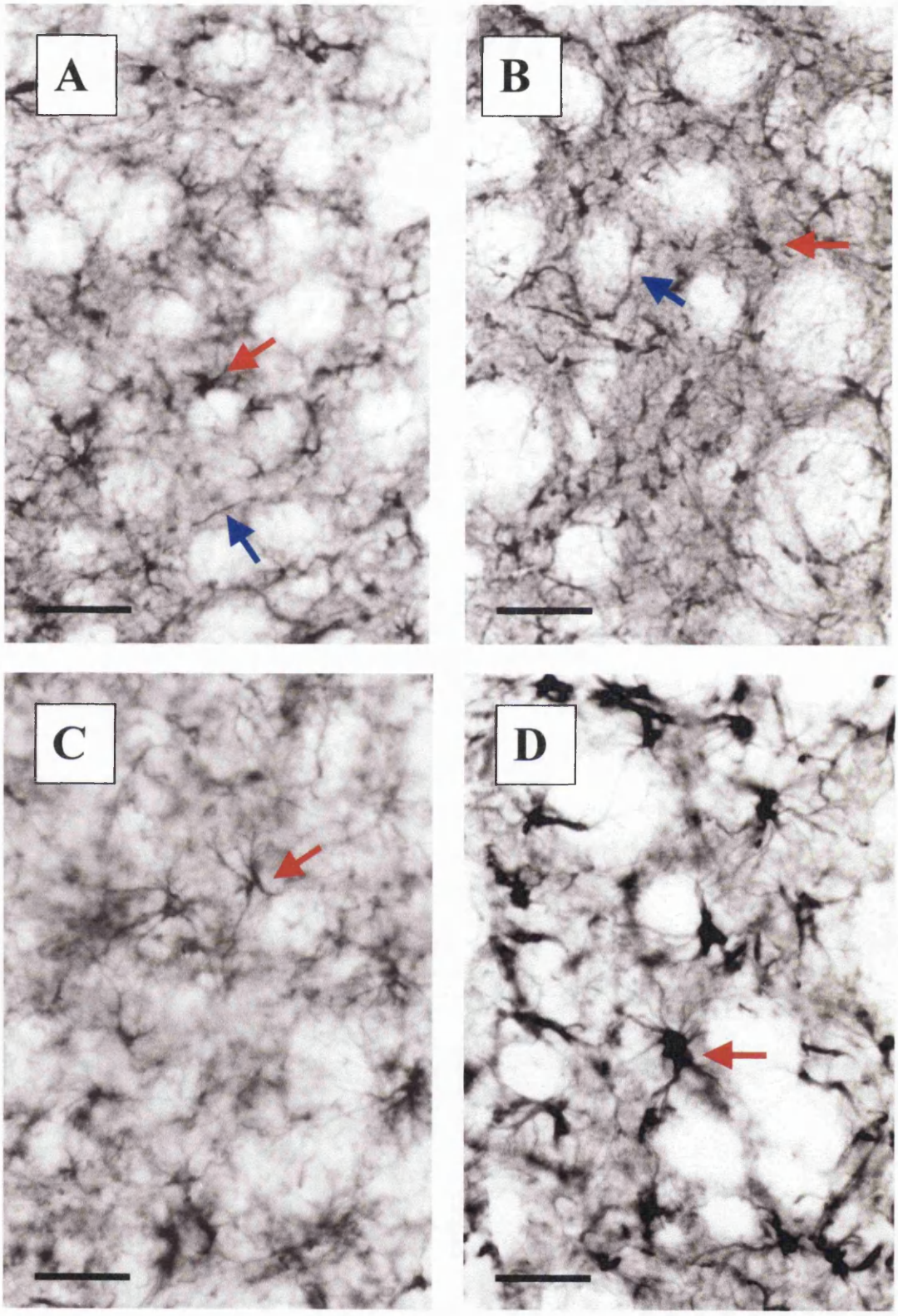
A
B
C
D

Figure. 3.1/6

Cellular expression (immunocytochemistry) of GFAP in rat striatum following QA lesion

(A) Photomicrograph of immunoreactivity for glial fibrillary acidic protein (GFAP) 48 hours following QA lesion in striatum. GFAP reactive cell bodies can be observed. Antibody used Sigma G-A-5 monoclonal at 1:1000. Scale bar = 30 μm.

(B) Photomicrograph of immunoreactivity for glial fibrillary acidic protein (GFAP) in striatum at 120 hours (five days) following QA lesion. GFAP reactive processes radiating from astrocytes are visible (red arrow). Scale bar = 20 μm.

(C) Photomicrograph of GFAP reactive astrocyte in striatum at 120 hours (five days) following QA lesion. Processes of various sizes are clearly visible. Scale bar = 20 μm.

(D) Photomicrograph of immunoreactivity for GFAP in QA lesioned striatum at 168 hours (seven days) post lesion. Dark GFAP reactive astrocytes can clearly be seen in the striatum with radiating filamentous processes (red arrows), but these astrocytes do not appear as hypertrophied as those observed after CNTF treatment. Scale bar = 40 μm.

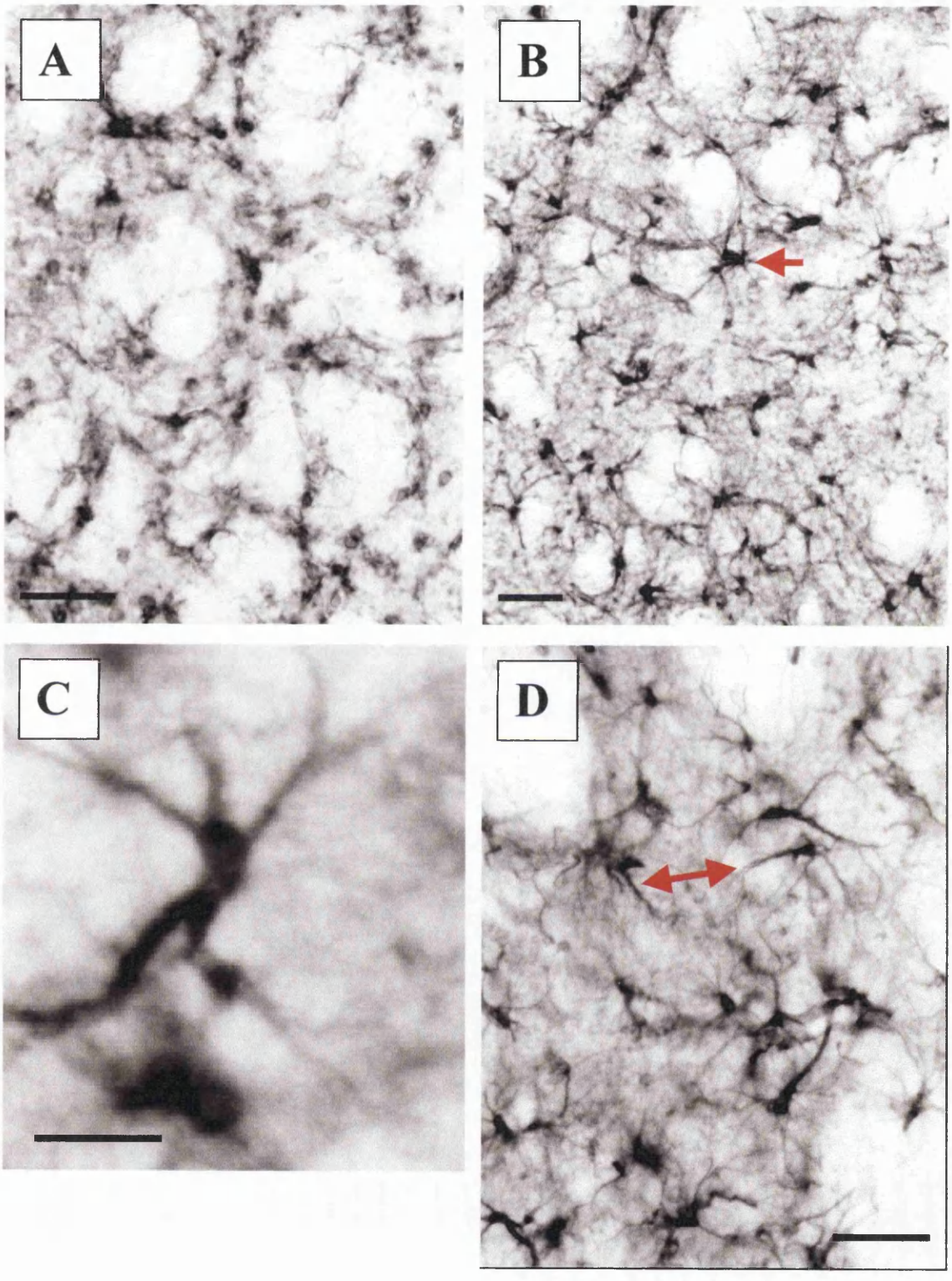
A
B
C
D

Figure. 3.1/7

Cellular expression (immunocytochemistry) of OX-42 in rat striatum following QA lesion and in controls

(A) Photomicrograph of immunoreactivity for OX-42 protein in control striatum. Immunoreactivity of 'resting' microglial processes can be observed. Antibody used MAS 370C monoclonal at 1:1000. Scale bar = 40 μm.

(B) Camera lucida line diagram of a 40 μm coronal half section through anterior rat brain demonstrating distribution of ameboid microglia in the striatum at 168 hours (seven days) post control saline infusion. A small group of ameboid microglia below and adjacent to the needle tract could be observed, but were not found to be widespread (compare to following diagrams post QA and CNTF treatment). This diagram is intended only to indicate distribution and number of cells, dots indicative of cells do not accurately represent cell size. Scale bar = 2 mm.

(C) Photomicrograph of OX-42 immunoreactivity in striatum at 168 hours (seven days) following QA lesion. Ramified microglia can be seen, with processes radiating from the central cell body. These 'activated' microglia are found surrounding areas ameboid microglia and at seven days following 60 nmol QA lesion usually occupy the entire half of the brain which has been lesioned and can not infrequently be observed in the non-lesioned side also. Scale bar = 40 μm.

(D) Two OX-42 reactive, ramified 'activated' microglia observed at higher magnification. The contact observed between the processes of the two cells may indicate the means by which resting microglia form a network and maintain contact throughout the entire CNS, allowing them to react quickly to any insult. When in contacted by appropriate stimuli ramified microglia adopt the macrophagic ameboid morphology (see following plates). Scale bar = 20 μm.

A

B

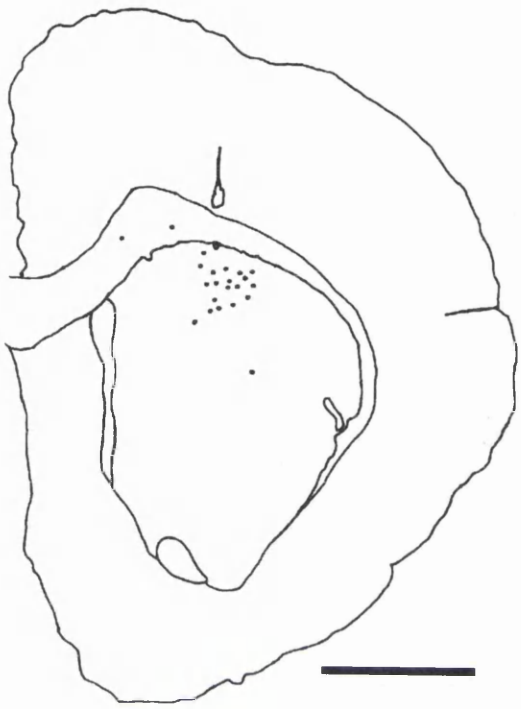

C

D

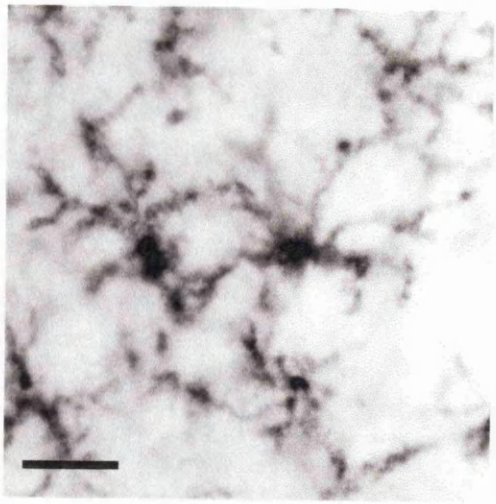

Figure. 3.1/8

Cellular expression (immunocytochemistry) of OX-42 in rat striatum following CNTF treatment

(A) Photomicrograph of immunoreactivity for OX-42 protein in striatum at 72 hours (three days) following CNTF administration. Immunoreactivity of ramified microglial cells can be observed. Antibody used MAS 370C monoclonal at 1:1000. Scale bar = 30 μm.

(B) Photomicrograph of immunoreactivity for OX-42 protein in striatum at 120 hours (five days) following CNTF administration. Immunoreactivity now appears to demonstrate ramified cells 'retracting' their processes and moving towards an ameboid morphology, although at this stage no rounded macrophagic ameboid cells can be observed. Antibody used MAS 370C monoclonal at 1:1000. Scale bar = 30 μm.

(C) Camera lucida line diagram of a 40 μm coronal half section through anterior (+1.6 mm from bregma) rat brain demonstrating distribution of ameboid microglia in the striatum at 168 hours (seven days) following CNTF treatment. Ameboid microglia can be observed in the overlying cortex and corpus callosum as well as spread throughout the striatum. These diagrams are intended only to indicate distribution and number of cells, dots indicative of cells do not accurately represent cell size. Scale bar = 2 mm.

(D) Camera lucida line diagram of a 40 μm coronal half section through a rat brain taken at a slightly less anterior (+1.2 mm) position from bregma demonstrating distribution of ameboid microglia in the striatum at 168 hours (seven days) following CNTF treatment. Ameboid microglia can again be observed in the overlying cortex and corpus callosum as well as spread throughout the striatum. These diagrams are intended only to indicate distribution and number of cells, dots indicative of cells do not accurately represent cell size.

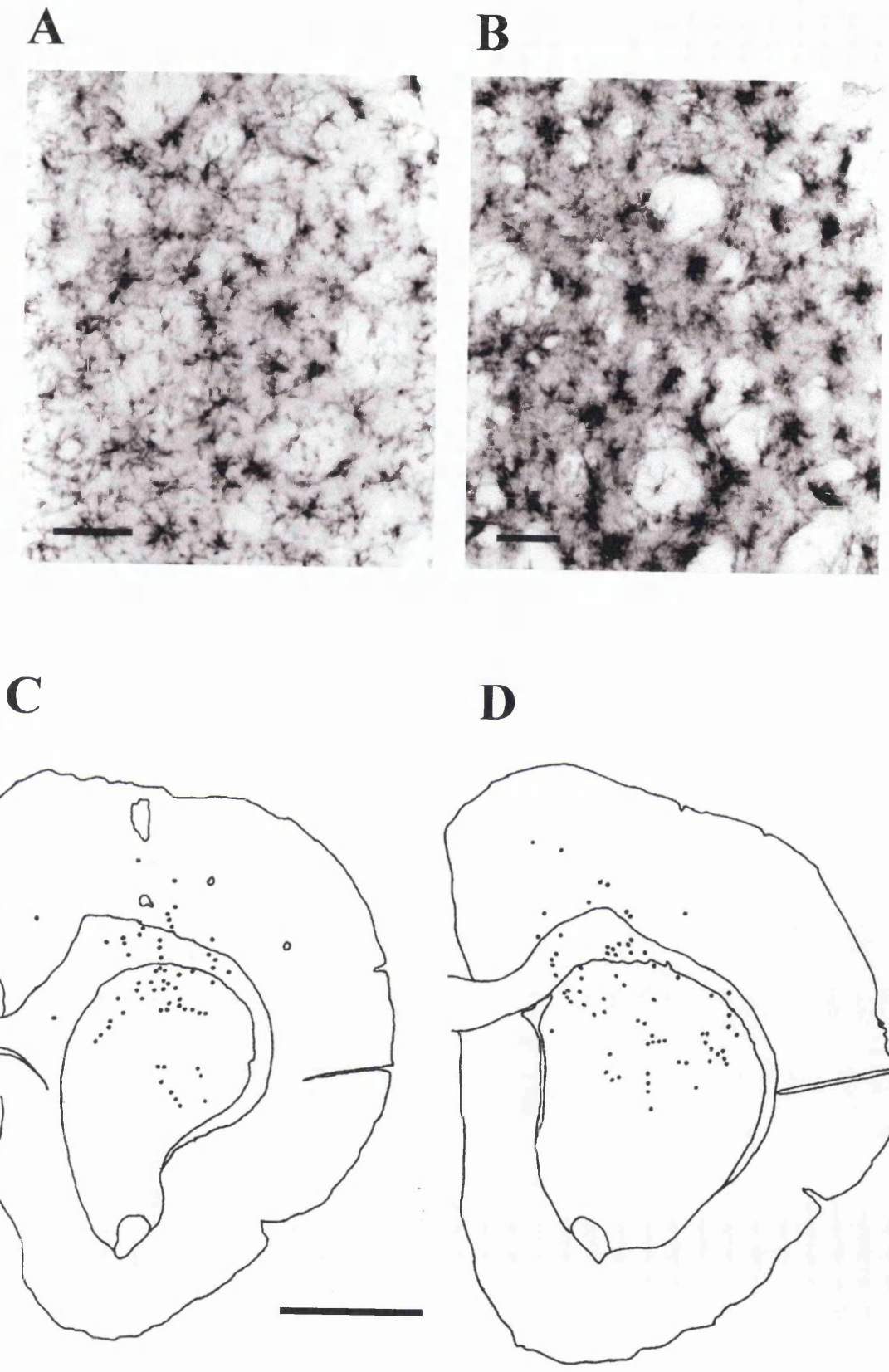
A
B
C
D

Figure. 3.1/9

Cellular expression (immunocytochemistry) of OX-42 in rat striatum following QA lesion

(A) Photomicrograph of immunoreactivity for OX-42 protein in striatum at 120 hours (five days) following QA lesion. Immunoreactivity of ramified ameboid cells can be clearly observed. Antibody used MAS 370C monoclonal at 1:1000. Scale bar = 30 μm. Compare with corresponding diagram B.

(B) Camera lucida line diagram of a 40 μm coronal half section through anterior (+1.6 mm from bregma) rat brain demonstrating distribution of ameboid microglia in the striatum at 120 hours (five days) following QA lesion. Ameboid microglia can be observed in the overlying cortex and corpus callosum as well as spread throughout the striatum, as with CNTF treated brains, although more ameboid cells are visible. These diagrams are intended only to indicate distribution and number of cells, dots indicative of cells do not accurately represent cell size. Scale bar = 2 mm.

(C) Photomicrograph of immunoreactivity for OX-42 protein in striatum at 168 hours (seven days) following QA treatment. Ameboid microglia have increased in number and are the dominant type of microglia observed. Scale bar = 40 μm. Compare with corresponding diagram D.

(D) Camera lucida line diagram of a 40 μm coronal half section through anterior (+1.6 mm from bregma) rat brain demonstrating distribution of ameboid microglia in the striatum at 168 hours (seven days) following QA lesion. Ameboid microglia can be observed in the overlying cortex and corpus callosum as well as spread throughout the striatum, where they have dramatically increased in number and dominate the section.

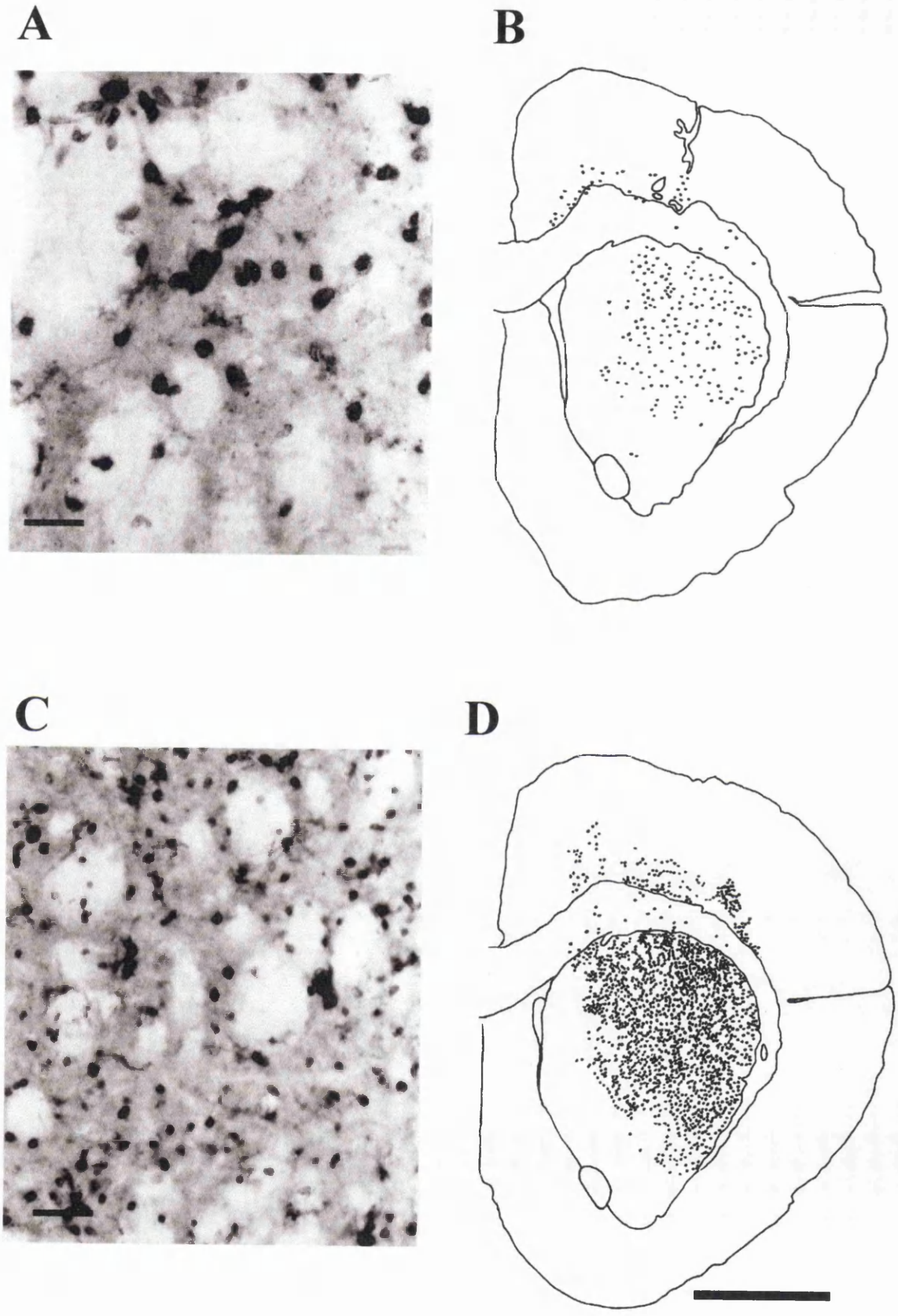
A
B
C
D

3.2 LOCALISATION OF NF-κB PROTEINS AFTER QA OR CNTF STRIATAL TREATMENT

Localisation of p65 in the rat cortex and striatum following QA or CNTF treatment

In control animals or the unlesioned striatum of QA or CNTF treated animals, immunocytochemistry for the p65 subunit of NF-κB using the SC-109 antibody demonstrated widespread immunoreactivity. This was primarily demonstrated in the perikarya of medium sized striatal cells (approximately 15 μm in diameter, Fig.3.2/1A and B) and medium sized perikarya in the cerebral cortex (Fig.11/1B). Some perikarya in the internal capsule and corpus callosum could also be seen to be immunoreactive. No large neuronal perikarya (approximately 20-22 μm in diameter) or small striatal perikarya (>10 μm in diameter) could be seen to be reactive in the striatum. In CNTF treated animals, no difference in immunoreactivity could be detected at any time point following administration.

In QA treated animals, smaller darker nuclei become visible at 48 hours and at 120 hours the outline of glial cells demonstrating an astrocytic morphology could be seen to be immunoreactive with the antibody (Fig.3.2/1C&D).

Localisation of p50 in the rat cortex and striatum following QA or CNTF treatment

Immunocytochemistry of striatal tissue from control animals using the SC-114 p50 antibody demonstrated light immunoreactivity of medium sized neuronal perikarya in the striatum and cortex. Immunoreactivity of small perikarya could be observed in the internal capsule and corpus callosum. In general a very similar if not identical pattern of staining to that seen for p65 was presented, but large neuronal perikarya could sometimes also be seen to be immunoreactive in some regions of the striatum. No significant difference in staining could be discerned after treatment with CNTF or QA at 24 hours or beyond.

Localisation of p52 in the rat cortex and striatum following QA or CNTF treatment

Immunocytochemistry using the K-27 p52 antibody demonstrated a striking immunoreactivity of small bodies within the nucleus of medium sized neurones and that of perikarya of some medium sized neurones throughout the striatum (Fig.3.2/2A&B, Fig.

3.2/3). The cells displaying perikaryal immunoreactivity appear to constitute a specific sub-group of medium sized neurones, which are found mainly in the dorso-lateral aspect of the striatum (Fig. 3.2/3). These cells appear to be quite large for medium sized neurones, but their distribution indicates that they are not giant cholinergic neurones (Fig. 3.2/3 B,C & D). Two to eight nuclear bodies were visible in nuclei of medium sized neurones. As with all NF-κB antibodies, immunoreactivity, in this case of nuclear bodies, could be abolished by pre-incubating the p52 antibody for one hour with the peptide to which it was raised at concentrations recommended by the producer.

At 24 hours following CNTF treatment, dark cells resembling the morphology of microglia, could be seen in the treated striatum and the overlying cortex. At twenty four hours following QA lesion a much greater proliferation of these cells can be seen spreading throughout the lesioned striatum and overlying cortex and even into the contralateral, untreated striatum (Fig.3.2/3/4). These dark ameboid cells eventually spread throughout the lesioned striatum, almost filling it at 120 and 168 hours following lesion (Fig.3.2/2/3/4). At 120 hours and beyond, cells exhibiting an astrocyte-like morphology can be distinguished in the striatum (Fig.3.2/2C). These astrocytes, however, are not as numerous as those immunoreactive for CNTF, p65 or GFAP and appear to present a different morphology.

Figure. 3.2/1

Cellular expression (immunocytochemistry) of NF-κB p65 in controls and following QA lesion at 48 and 120 hours post-lesion.

(A) Photomicrograph of p65 immunoreactivity in control (untreated) striatum. Scale bar =100 μm. Numerous medium sized striatal neurones can be observed. Pale areas indicate white fibres of the internal capsule passing through the striatum. Antibody used Santa Cruz SC-109 rabbit polyclonal recognising amino acids 3-19 of amino terminal,used at 1:2000.

(B) Photomicrograph of p65 immunoreactivity in control (untreated) striatum. Scale bar =30 μm. Numerous medium sized striatal neurones can be observed. In some neurones the nucleus can be seen to be more darkly immunoreactive than that in others.

(C) Photomicrograph of p65 immunoreactivity in QA lesioned striatum at 48 hours following lesion. Scale bar = 40 μm . Loss of the density of medium sisized neurone staining can be observed.

(D) Photomicrograph of p65 immunoreactivity in a region of QA treated striatum at 120 hours following lesion, scale bar =30 μm. The field of medium sized neurones is replaced by one of reactive astrocytes immunoreactive for p65.

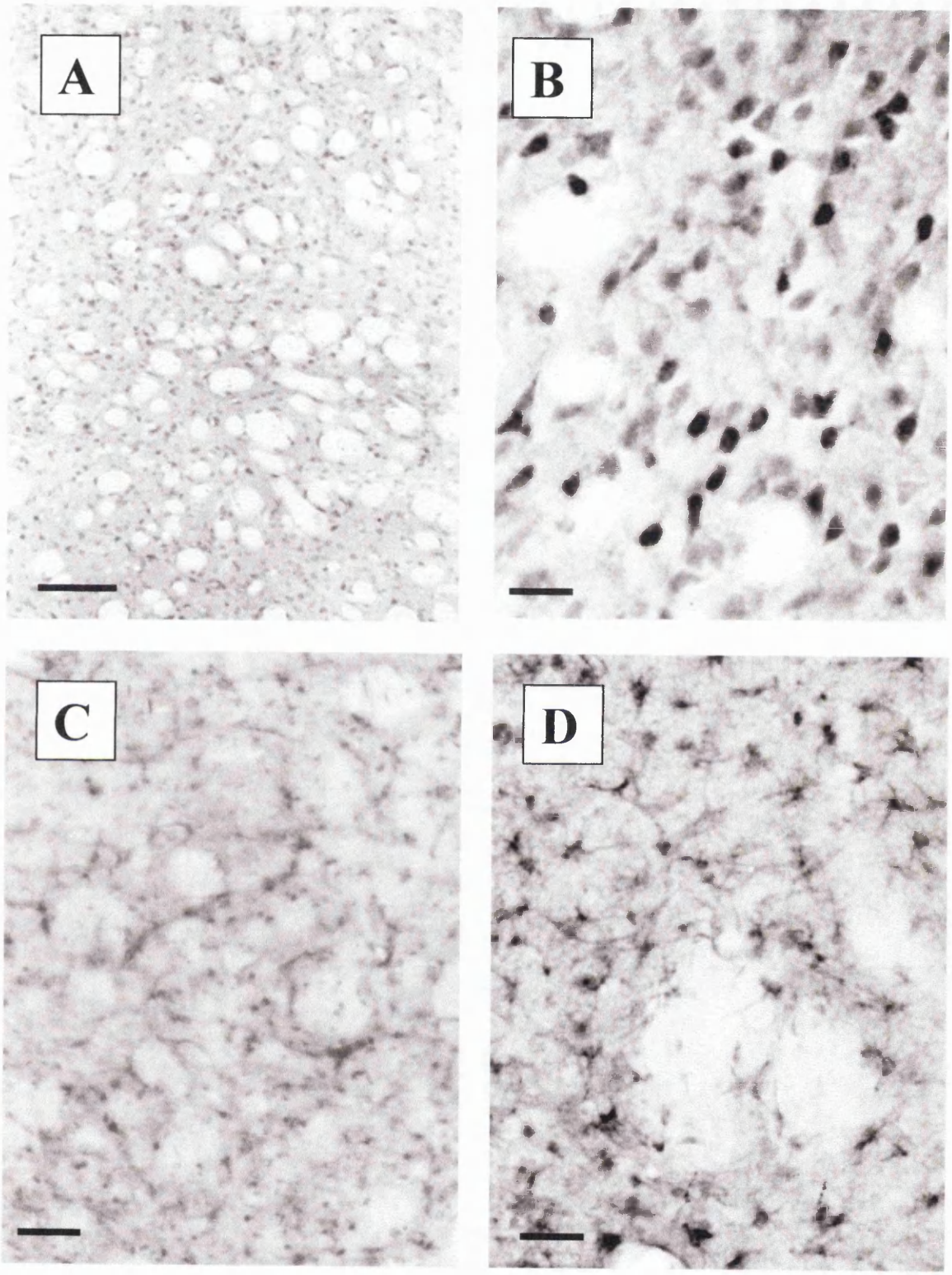
A
B
C
D

Figure. 3.2/2

Cellular expression (immunocytochemistry) of NF-κB p52 in control striatum

(A) Photomicrograph of p52 immunoreactivity in control (untreated) striatum. Scale bar = 15 μm. Immunoreactivity of small bodies can be observed within the nuclei of a cluster of medium sized neurones (black arrow) and the medium sized perikarya and nuclei can be seen to be lightly immunoreactive. Two to eight bodies can be observed in each nucleus. Antibody used was Santa Cruz K-27 rabbit polyclonal used at 1:1000 dilution.

(B) Photomicrograph demonstrating p52 reactive lesion tract 168 hours (seven days) following QA lesion. The red arrow indicates densely packed dark cells with ameboid microglial-like morphology filling the lesion tract. The blue arrow indicates p52 reactive filaments which appear similar to astrocyte processes. It appears that both p52 reactive astrocytes and microglia are present in the tract. Scale bar = 40 μm.

(C) Photomicrograph of p52 immunoreactive perikarya at a lower magnification (scale bar = 60 μm. Widespread immunoreactivity can be observed throughout the striatum. Medium sized neurones are indicated by the arrows.

(D) Photomicrograph of p52 reactive astrocyte adjacent to a myelinated fibre fasicle in the striatum at 120 hours (five days) following QA lesion. The astrocyte processes appear to be in contact with the fasicle (arrow). Scale bar = 20 μm.

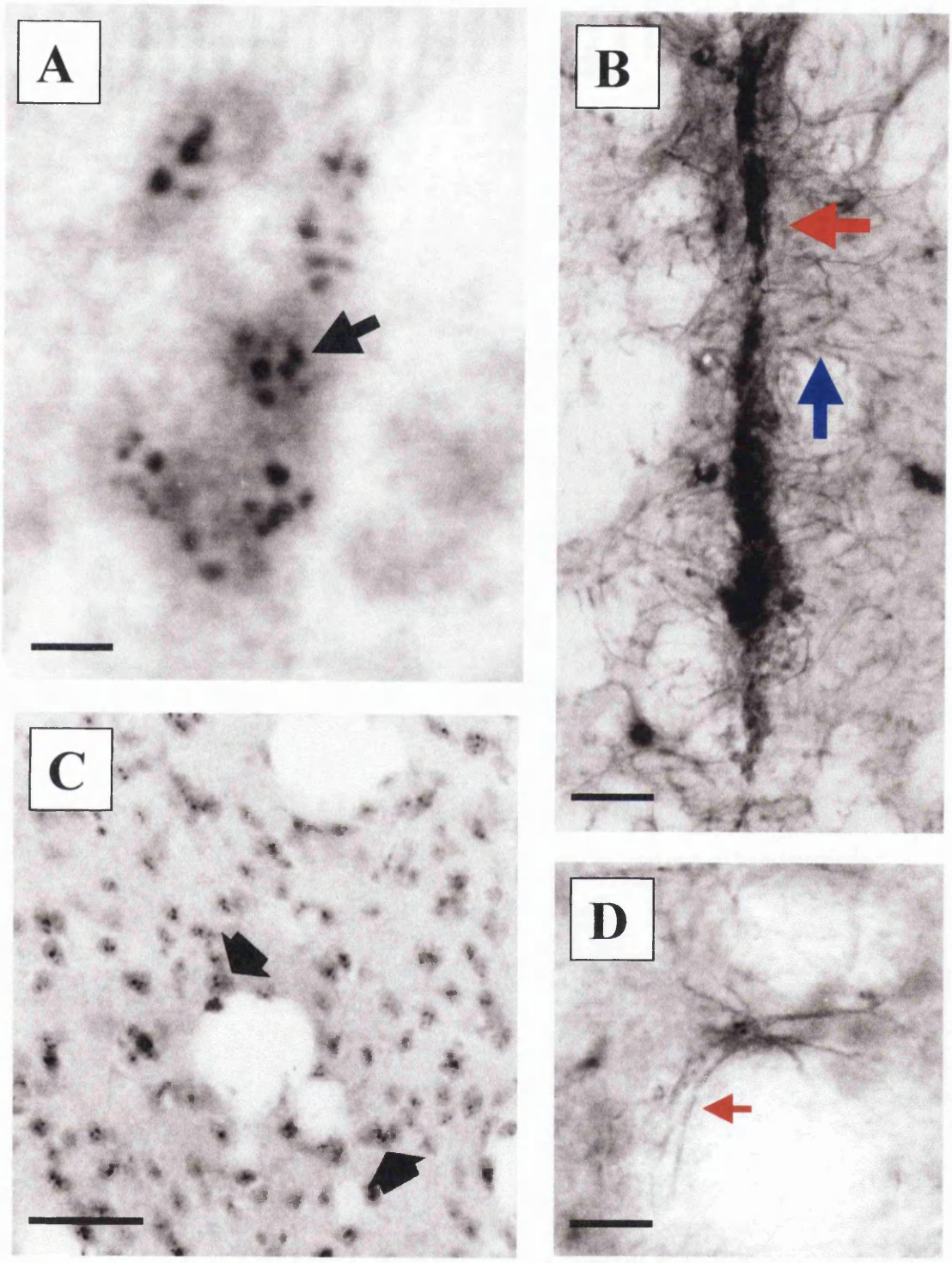
A
B
C
D

Figure. 3.2/3

Cellular expression (immunocytochemistry) of NF-κB p52 in control striatum

(A) Photomicrograph of p52 immunoreactivity in control (untreated) striatum demonstrating complete p52 immunoreactivity of neuronal perikarya (red arrow). These cells appear to represent a distinct sub-population of medium sized cells in the striatum, as opposed to those cells expressing strong immunoreactivity for p52 in nuclear bodies alone (blue arrow). The distribution of these cells is indicated by the following camera lucida drawings. Antibody used was Santa Cruz K-27 rabbit polyclonal used at 1:1000 dilution. Scale bar = 30 μm

(B) Camera lucida line diagram of a 40 μm coronal half section through anterior (+1.7 mm from bregma) rat brain demonstrating distribution of neurones demonstrating perikaryal p52 immunoreactivity. These diagrams are intended only to indicate distribution and number of cells, dots indicative of cells do not accurately represent cell size or morphology. Note the predominant dorso-lateral position of this population of cells. Scale bar relative to all illustrations = 2 mm.

(C) Camera lucida line diagram of 40 μm coronal half section through anterior (+ 1.2 mm from bregma) rat brain demonstrating distribution of neurones demonstrating perikaryal p52 immunoreactivity.

(D) Camera lucida line diagram of 40 μm coronal half section through anterior (+ 0.2 mm from bregma) rat brain demonstrating distribution of neurones demonstrating perikaryal p52 immunoreactivity.

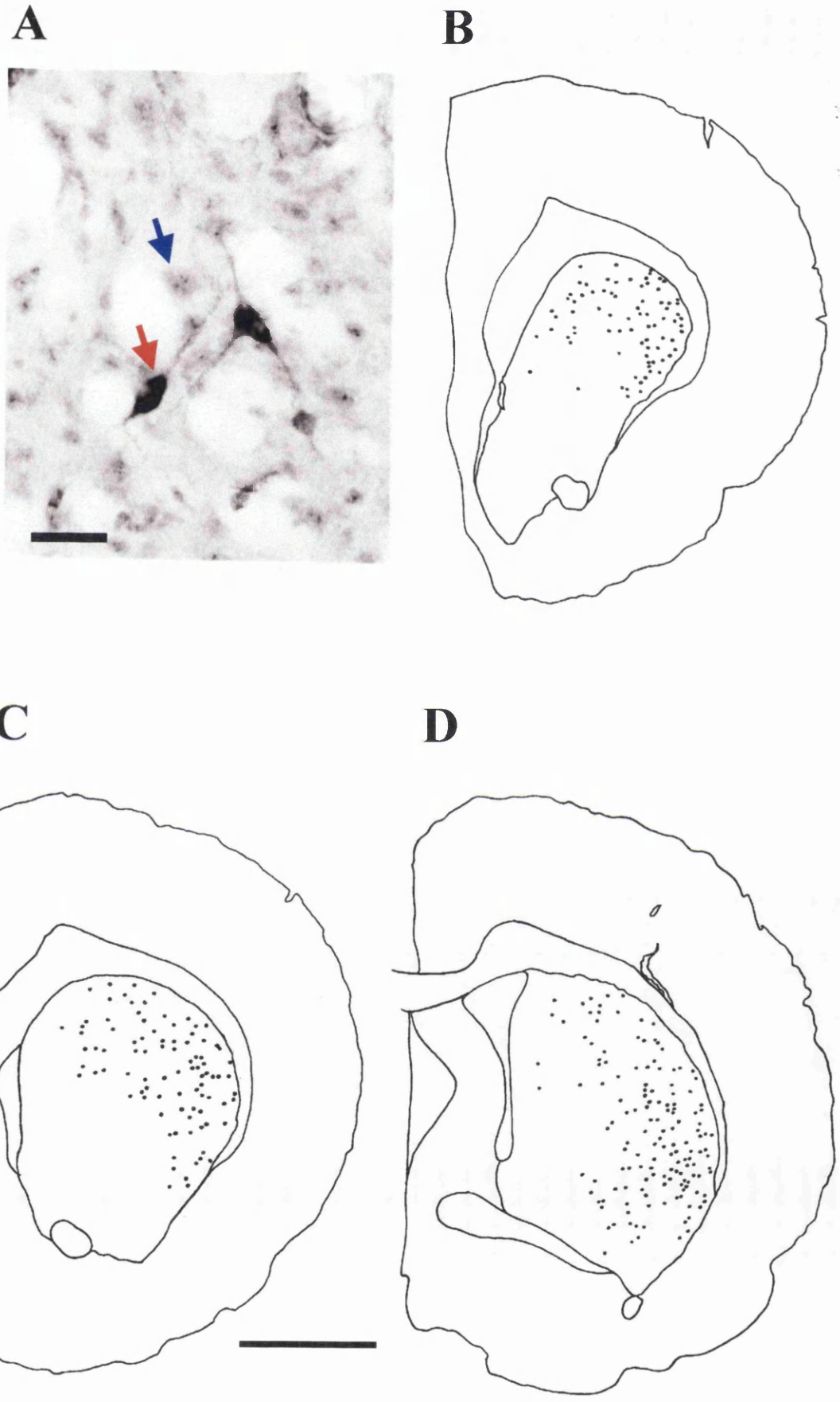
A
B
C
D

Figure. 3.2/4

Cellular expression (immunocytochemistry) of NF-κB p52 in saline and CNTF treated striatum at 168 hours (7 days) post-lesion

(A) Photomicrograph of p52 immunoreactivity in saline treated striatum 168 hours after lesion. Scale bar = 30 μm. Immunoreactivity of a few large dark bodies (putative ameboid microglia, red arrow), can be observed in the striatum. Antibody used was Santa Cruz K-27 rabbit polyclonal used at 1:1000 dilution. Note corresponding diagram (B). Medium sized neurones expressing p52 immunoreactivity of nuclear bodies can still be seen (blue arrow).

(B) Camera lucida line diagram of a 40 μm coronal half section through anterior (+1.2 mm from bregma) rat brain 168 hours following saline injection, demonstrating distribution of p52 reactive dark bodies (putative ameboid microglia). These diagrams are intended only to indicate distribution and number of cells, dots indicative of cells do not accurately represent cell size or morphology. Scale bar = 2 mm.

(C) Photomicrograph of p52 immunoreactivity in CNTF treated striatum 168 hours after treatment. Scale bar = 40 μm. Immunoreactivity of large dark bodies (putative ameboid microglia, red arrow), can be observed in the striatum. Note corresponding diagram (D).

(D) Camera lucida line diagram of a 40 μm coronal half section through anterior (+1.2 mm from bregma) rat brain 168 hours following CNTF treatment, demonstrating distribution of p52 reactive dark bodies (putative ameboid microglia). These diagrams are intended only to indicate distribution and number of cells, dots indicative of cells do not accurately represent cell size or morphology. The dotted line delineates the boundary above which p52 reactive astrocytes may be observed.

A

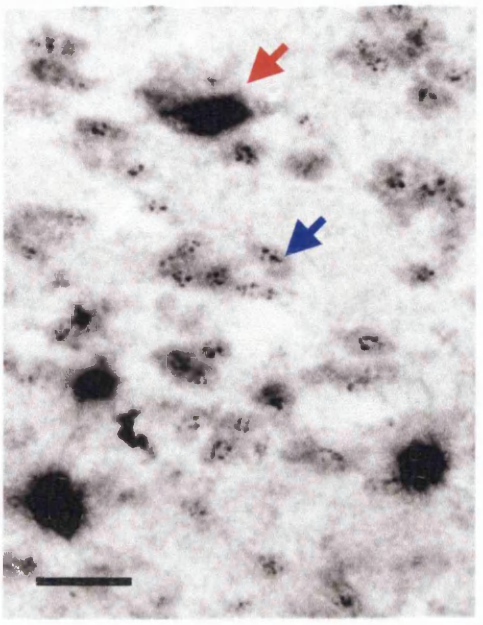

B

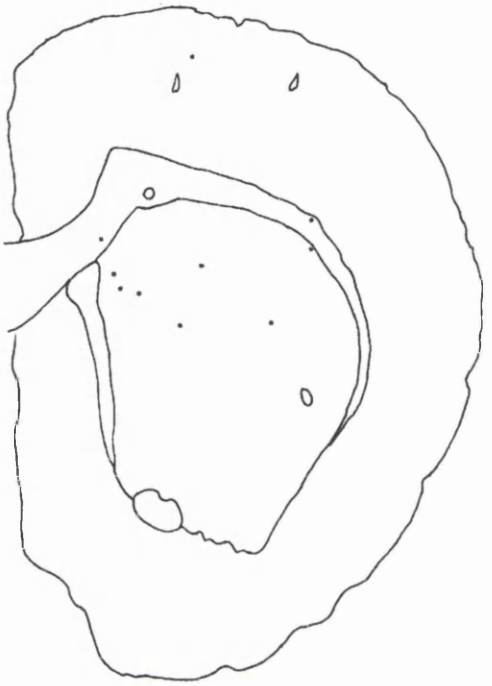

C

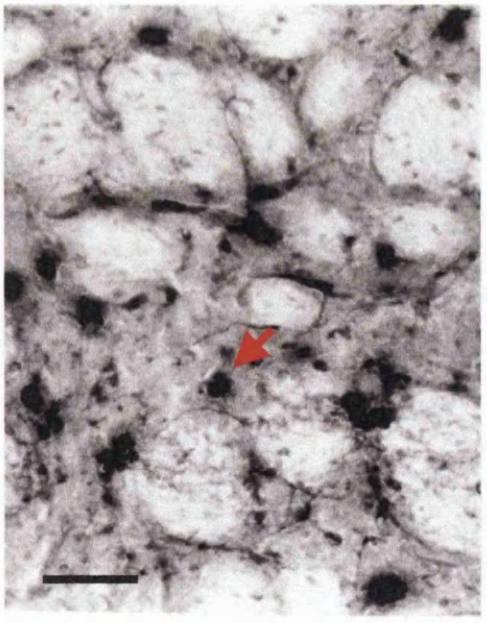

D

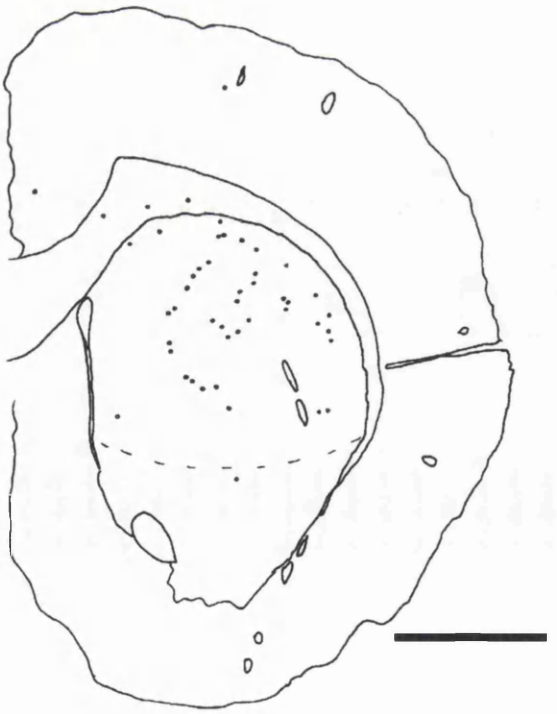

Figure. 3.2/4

Cellular expression (immunocytochemistry) of NF-κB p52 in QA lesioned striatum at 120 hours (5 days) and 168 hours (7 days) post-lesion

(A) Photomicrograph of p52 immunoreactivity in QA lesioned striatum 120 hours (five days) after lesion. Scale bar = 40 μm. Immunoreactivity of large dark bodies (putative ameboid microglia), can be observed close to the lesion tract left by needle insertion. Some of the reactive cells clearly possess an ameboid morphology. Antibody used was Santa Cruz K-27 rabbit polyclonal used at 1:1000 dilution. Note corresponding diagram

(B) Camera lucida line diagram of a 40 μm coronal half section through anterior (+1.2 mm from bregma) rat brain 120 hours following QA lesion, demonstrating distribution of p52 reactive dark bodies (putative ameboid microglia). These diagrams are intended only to indicate distribution and number of cells, dots indicative of cells do not accurately represent cell size or morphology. The number of p52 reactive cells is greater than that seen in CNTF treated brain at seven days.

(C) Photomicrograph of p52 immunoreactivity in QA lesioned striatum 168 hours after injection. Scale bar = 80 μm. Immunoreactivity of large dark bodies (putative ameboid microglia) can be observed spreading throughout the striatum. Note corresponding diagram (D).

(D) Camera lucida line diagram of a 40 μm coronal half section through anterior (+1.4 mm from bregma) rat brain 168 hours (seven days) following QA lesion, demonstrating distribution of p52 reactive dark bodies (putative ameboid microglia). The p52 reactive cells can be observed to be widespread throughout the striatum and spreading deep into the overlying and lateral cortex. The dotted line delineates the boundary above which p52 reactive astrocytes may be observed.

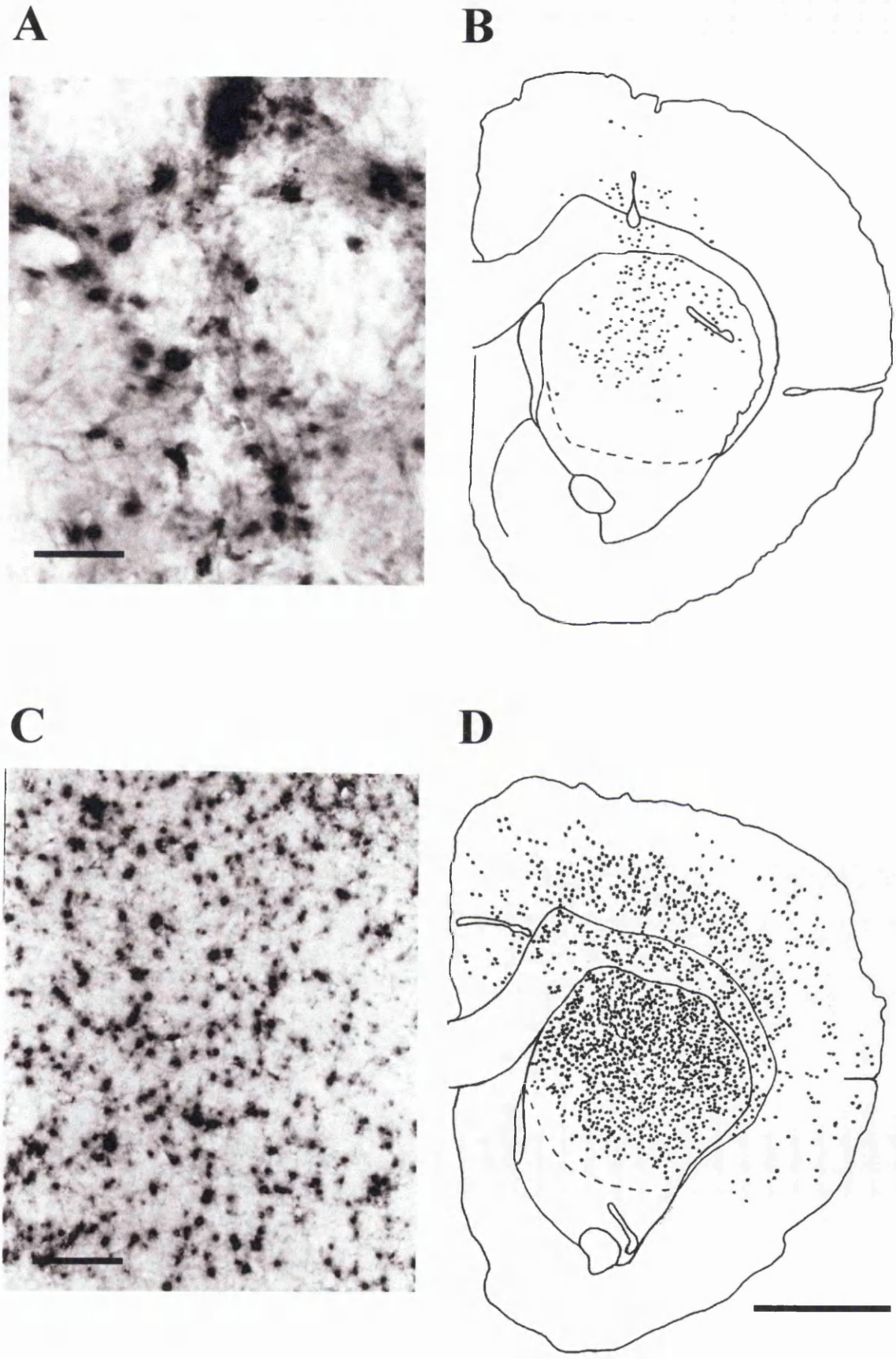
A
B
C
D

3.3 EXPRESSION OF NF-κB PROTEINS AFTER QA OR CNTF STRIATAL TREATMENT

Expression of p65 in the rat striatum following QA or CNTF treatment

The antibody SC-109 p65 recognises a protein of a molecular weight of 50 kD on western blots, in unlesioned control and both QA and CNTF treated animals in nuclear protein preparations (Fig.3.3/1 A&B). No other prominent protein is seen, although sometimes a much weaker band at ~55 kD can be observed after CNTF treatment. The 50 kD protein is readily abolished by pre-incubating the antibody with 10x of the peptide immunogen (Fig.3.3/1B). To determine if this antibody recognised a prominent protein at 50 kD in other cell types and test system integrity, EGF stimulated A431 whole cell lysate was run alongside QA stimulated striatal nuclear preparation. The SC-109 antibody is known to recognise a protein migrating at 65 kD in A431 cell lysates. A prominent protein at 65 kD was visible in direct contrast to the 50 kD protein seen in striatal homogenate. No protein was seen in the A431 sample at 50 kD (Fig.3.3/1A). Confirmation of the molecular weight of the observed protein was confirmed using three different types of molecular weight markers (Fig. 3.3/2). Densitometric analysis of western blots demonstrated no significant difference between control animals and those treated with QA or CNTF (Fig.3.3/G1&G2).

Expression of p50 in the rat striatum following QA or CNTF treatment

The antibody SC-114 p50 NLS recognises several proteins in both control, QA and CNTF treated animals in cytoplasmic and nuclear preparations (Fig. 3.3/3 A,B & C). Two high molecular weight proteins running at ~70 and 100 kD are extremely prominent in cytoplasmic preparations and may sometimes be seen weakly in nuclear preparations. Most strikingly in nuclear preparations are a 50 kD protein and an inducible 35 kD protein in QA and CNTF treated animals (Fig. 3.3/3 A & B, Fig. 3.3/4 A). Immunoreactivity for all proteins could be reduced prominently by pre-incubating the antibody with the peptide immunogen at 10x concentration and totally at 20x concentration (Fig.3.3/4 B&C).

Optical densitometry of western blots indicated no significant increase in protein levels in both QA and CNTF treated animals at any time points after controls, apart from the appearance of the 35 kD protein (Fig. 3.3/G3, 3.3/G4 & 3.3/G5). The level of expression of the 35 kD protein varied greatly, but appeared to be significantly present only in individuals studied at specific time points. These were 24 hours post-lesion (Fig.3.3/3 A) in QA treated animals (also visible at 16 and 20 hours post lesion, (Fig. 3.3/4 A) and at 12 hours post treatment in CNTF treated animals (Fig. 12/3 B). Animals that exhibited a protein at 35 kD in striatum also exhibited a 35 kD protein in nuclear cortical preparations (not shown).

Expression of p52 in the rat striatum following QA and CNTF treatment

The K-27 antibody recognises two main proteins weakly on western blots, one of 40 kD and another of 50 kD (Fig.3.3/5). Higher molecular weight proteins like those observed with the p50 antibody can also occasionally be observed in nuclear preparations and are always present in cytoplasmic preparations. The 50 kD protein is abolished by pre-incubation with 10x of the peptide immunogen (Fig.3.3/5). In striatal nuclear preparations there is no significant increase in optical density at all time points after QA treatment (Fig. 3.3/G6).

Expression of IκB-alpha in the rat striatum following QA and CNTF treatment

The C-21 IκB-alpha antibody reveals the presence of IκB-alpha in the nuclear fraction of homogenised rat striatum, although this is usually detected as a faint immunoreactivity in comparison to the dense 40 kD IκB-alpha protein band detected in cytoplasmic samples. No significant difference could be detected between cytoplasmic IκB-alpha levels in control animals and that in striata 24 and 168 hours following QA administration (Fig.3.3/6).

Figure. 3.3/1

NF-κB p65 protein expression (PAGE) in controls and following quinolinic acid lesion and CNTF treatment at 12, 24, 48, 120 and 168 hours post lesion.

(A)Western blot showing p65 protein expression in control (untreated) (C) and quinolinic acid (QA) treated striatum at various time points post-lesion. Densitometric analysis demonstrates that no significant difference in protein expression can be detected between control tissue and QA treated tissue at any time point following lesion (Fig.3.3/G1&G2). However, of interest is the fact that the protein in rat striatum recognised by the p65 antibody does not migrate at 65 kD on western blot, but at 50 kD (molecular weights are arrowed). No other prominent protein is seen. To determine if this antibody recognised a prominent protein at 50 kD in other cell types and test system integrity, EGF stimulated A431 whole cell lysate was run alongside QA stimulated (Q24) striatal nuclear preparation (A431). The SC-109 antibody is known to recognise a protein migrating at 65 kD in A431 cell lysates. A prominent protein at 65 kD was visible in direct contrast to the 50 kD protein seen in striatal homogenate. No protein was seen in the A431 sample at 50 kD.

(B) Western blot showing p65 protein expression in control (untreated) and ciliary neurotrophic factor (CNTF) treated striatum at various time points post-lesion. Densitometric analysis demonstrates that no significant difference in protein expression can be detected between control tissue and CNTF treated tissue at any time point following administration (Fig.3.3/G1&G2). Incubation of antibody with immunogen peptide (at concentration recommended by producer) prior to blot development abolished the 50 kD protein in 24 and 48 hour QA treated samples (B24 and B48) indicating specifity of antibody for 50 kD protein.

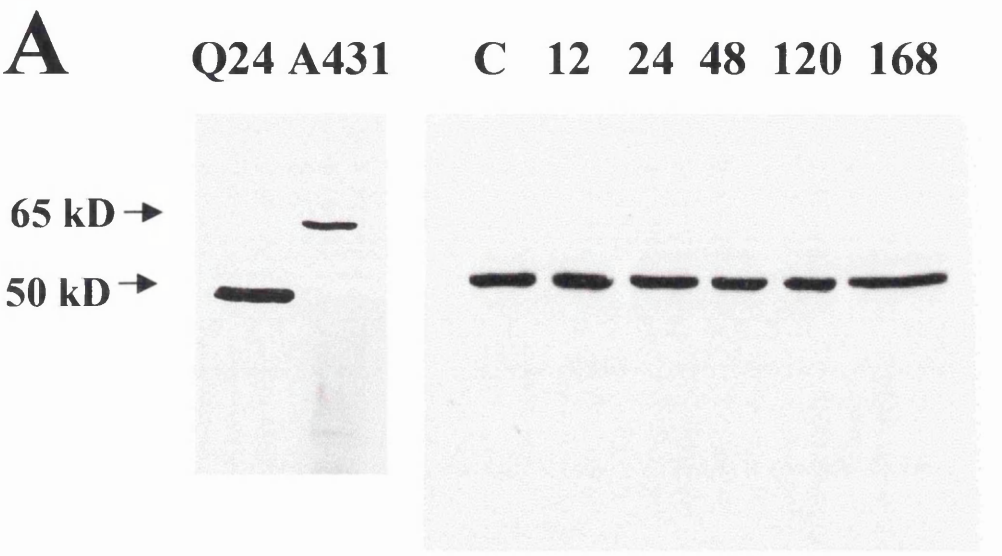
A
Q24 A431
C 12 24 48 120 168
65 kD
50 kD

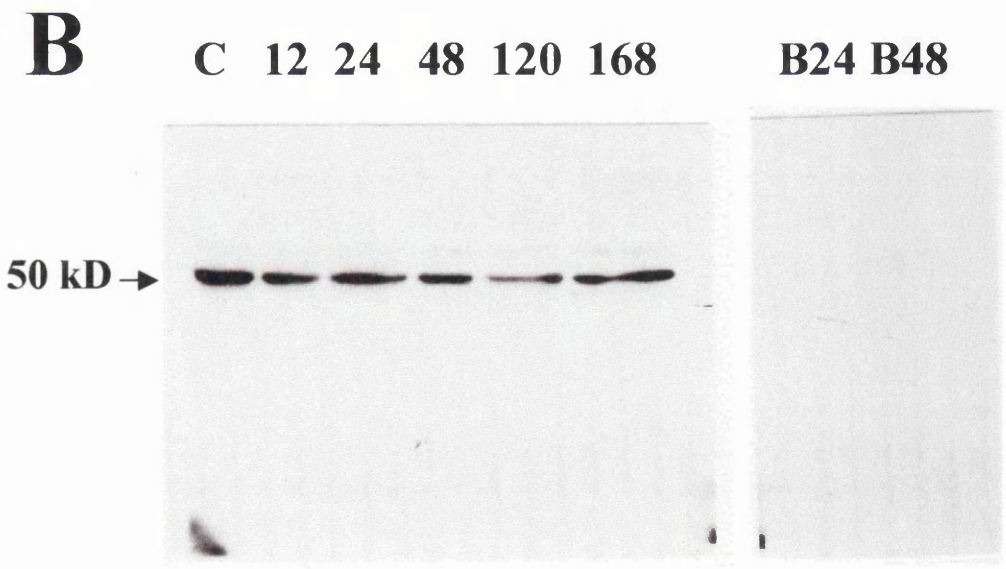
B
C 12 24 48 120 168
B24 B48
50 kD

Figure. 3.3/G1

Densitometric analysis of p65 protein expression (PAGE) in the striatum in controls and following QA lesion at 12, 24, 48. 120 and 168 hours post-lesion.

The graph opposite illustrates the protein expression p65 in mean arbitrary densitometric units (ADU) following QA administration at various time points. Time after lesion is displayed in the key to the right. Bars demonstrate the standard error of each population from which the mean value was obtained. Densitometric analysis and Student's two-tailed t-test revealed no significant difference between control and lesioned brains. Number of brains (N) = 6 per time period, pooled as groups of two (i.e. experiment conducted three times per time period). Total N= 36.

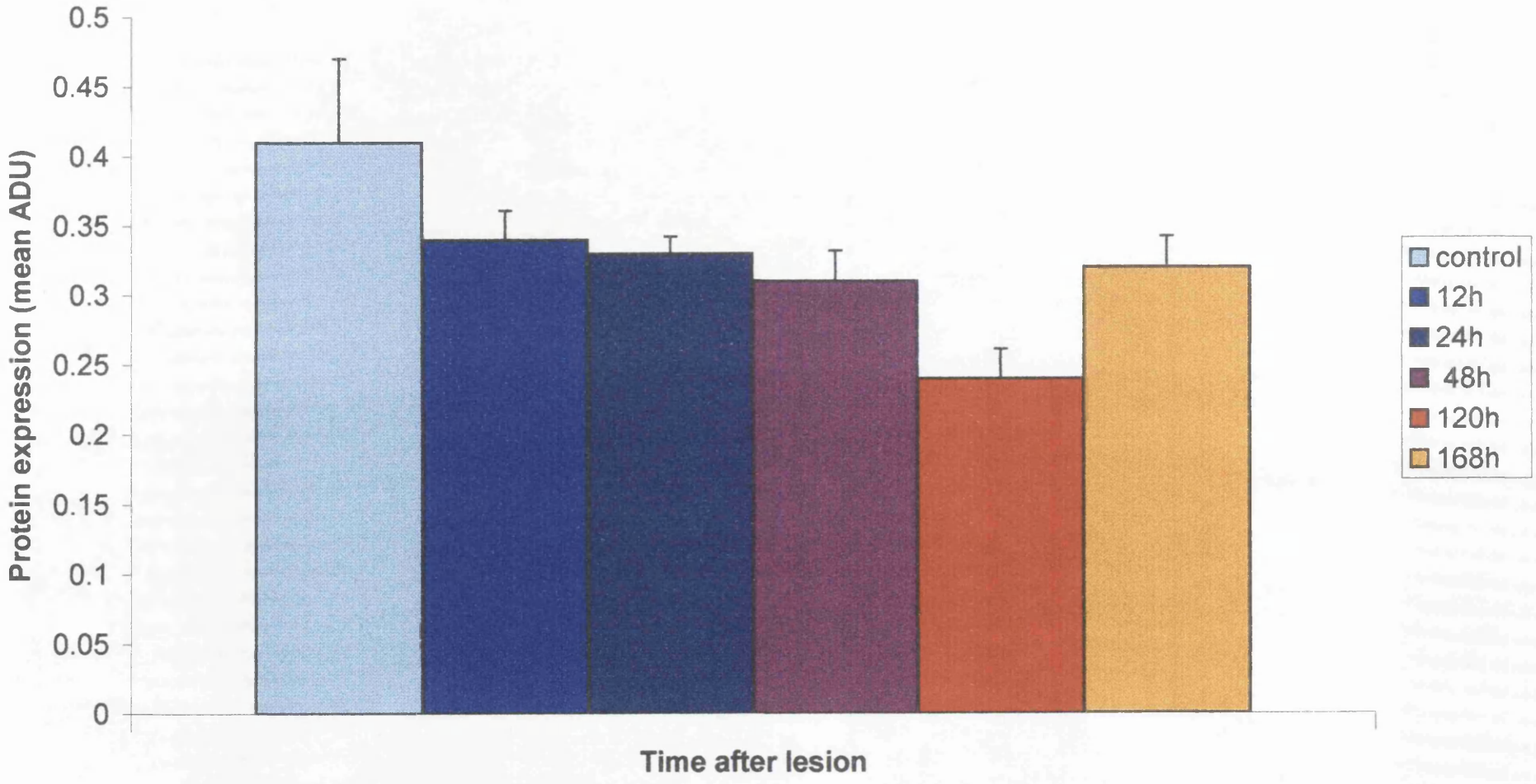
0.5
0.45
0.4
0.35
0.3
0.25
0.2
0.15
0.1
0.05
0
Protein expression (mean ADU)
Time after lesion
control
12h
24h
48h
120h
168h

Figure. 3.3/G2

Densitometric analysis of p65 protein expression (PAGE) in the striatum in controls and following CNTF treatment at 12, 24, 48. 120 and 168 hours post-lesion.

The graph opposite illustrates the protein expression p65 in mean arbitrary densitometric units (ADU) following CNTF administration at various time points. Time after lesion is displayed in the key to the right. Bars demonstrate the standard error of each population from which the mean value was obtained. Densitometric analysis and Student's two-tailed t-test revealed no significant difference between control and lesioned brains. Number of brains (N) = 6 per time period, pooled as groups of two (i.e. experiment conducted three times per time period). Total N= 36.

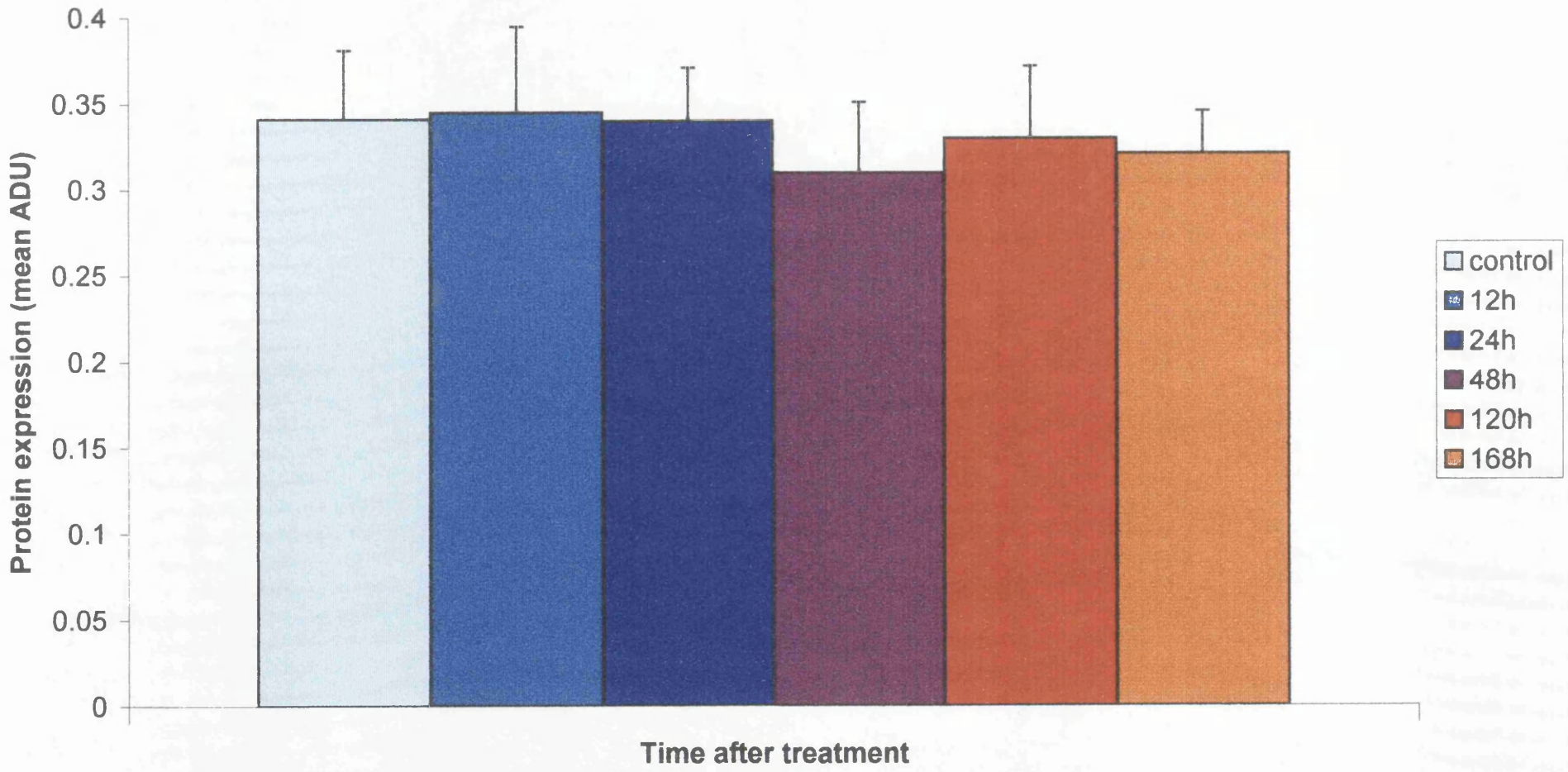
0.4
0.35
0.3
0.25
0.2
0.15
0.1
0.05
0
Protein expression (mean ADU)
Time after treatment
control
12h
24h
48h
120h
168h

Figure. 3.3/2

NF-κB p65 protein expression ;determination of molecular weight using molecular weight markers

To ensure system integrity and accuracy of molecular weight markers used throughout this thesis, three commercial molecular weight markers were used to check that the rat striatal nuclear protein recognised by the p65 antibody does indeed migrate at 50 kD. The figure opposite shows a developed film of a western blot upon which three molecular weight markers and homogenised rat striatum (cytoplasmic fraction) were electrophoresed. The filter was cut in three and exposed to the p52, p50 and p65 antibodies respectively (variation in band density indicates the reduced sensitivity of the p52 antibody). Markers are indicated by the designations M1, M2 and M3. All markers accurately predicted and resembled the molecular weights indicated by each other, however because of distortion of the gel markers do not match exactly upon opposite sides. The cytoplasmic 35 kD band recognised by anti-p50 can also be observed. The coloured arrows represent the following molecular weights respectively:

RED:	120 kD
BLUE:	80 kD
ORANGE (left):	55 kD
GREEN:	60 kD
YELLOW (right):	50 kD
GREY:	40 kD
BLACK:	30 kD

The p65 protein can clearly be seen to migrate at ~50 kD rather than 65 kD in brain tissue.

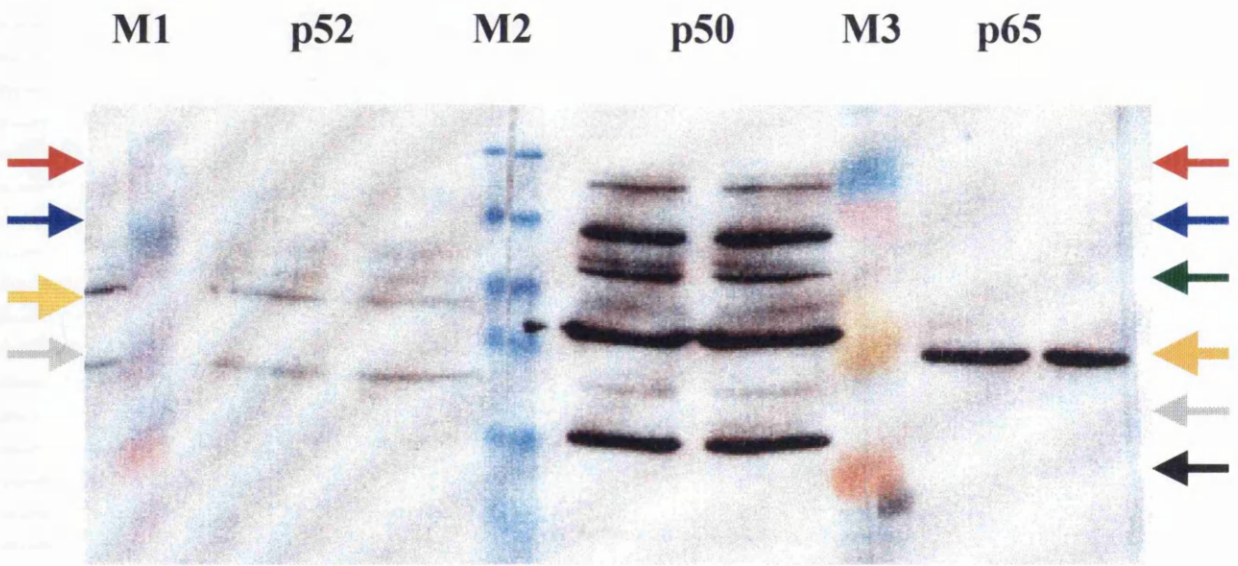
M1
p52
M2
p50
M3
p65

Figure. 3.3/3

NF-κB p50 protein expression (PAGE) in control striatum (nuclear and cytoplasmic) and following quinolinic acid lesion and CNTF treatment at 12, 24, 48, 120 and 168 hours post lesion.

(A)Western blot showing p50 protein expression in control (untreated) and quinolinic acid (QA) treated striatal nuclear samples at various time points post-lesion. Weak upper molecular weight protein bands can be seen and may represent cytoplasmic contamination. The arrow at 50 kD indicates a protein migrating at the correct molecular weight for p50, and densitometric analysis reveals no significant difference between controls and any time point following QA lesion (Fig.3.3/G3). The 35 kD arrow indicates an inducible, unknown protein that is only seen in treated tissue after QA or CNTF application. This is extremely unlikely to be a cytoplasmic contaminant since the nuclear sample demonstrates a stronger protein band than that seen in the cytoplasmic fraction (Fig.3.3/3C). As demonstrated here, it is seen most strongly 24 hours after QA lesion, but can also be detected at earlier time points (Fig.3.3/4A). Antibody used was Santa Cruz SC-114 p50 recognising amino acids 350-363 (NF-κB nuclear localisation sequence, NLS) used at 1:2000 dilution.

(B) Western blot demonstrating p50 protein expression in control (untreated) and ciliary neurotrophic factor (CNTF) treated striatal nuclear samples at a range of time points post-lesion. The arrow at 50 kD indicates a protein migrating at the correct molecular weight for p50, and densitometric analysis reveals no significant difference between controls and any time point following QA lesion (Fig.3.3/G4). The 35 kD arrow indicates an inducible, unknown protein that is only seen in treated tissue after CNTF application. This protein is seen most strongly 12 hours following CNTF treatment, and cannot be detected at the earlier time point of 10 hours, or later point of 14 hours post-treatment. Antibody used was Santa Cruz SC-114 p50 recognising amino acids 350-363 (NF-κB nuclear localisation sequence, NLS) used at 1:2000 dilution.

(C) Western blot showing p50 protein expression in control (untreated) and quinolinic acid (QA) treated striatal cytoplasmic samples at various time points post-lesion. The upper molecular weight bands at approximately at 100+, 100 and 70 kD (without arrow) are likely to be post-translationally modified NF-κB precursor molecules. An intermediate protein can be seen between the 50 and 35 kD bands, as can very low molecular weight proteins. Antibody used was Santa Cruz SC-114 p50 recognising amino acids 350-363 (NF-κB nuclear localisation sequence, NLS) used at 1:2000 dilution.

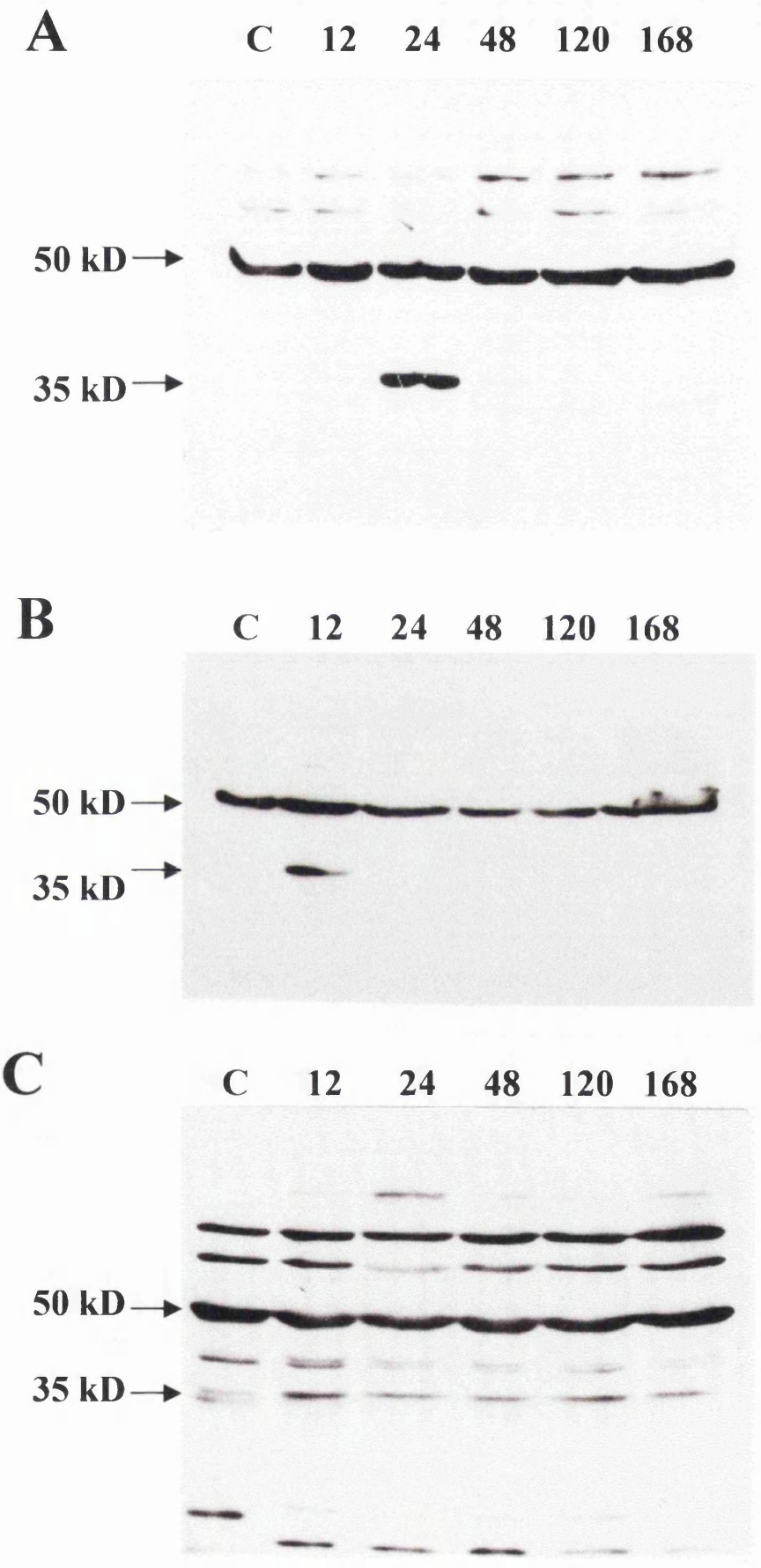
A
C 12 24 48 120 168
50 kD
35 kD
B
C 12 24 48 120 168
50 kD
35 kD
C
C 12 24 48 120 168
50 kD
35 kD

Figure. 3.3/G1

Densitometric analysis of p50 protein expression (PAGE) in the striatum in controls and following QA lesion at 12, 24, 48. 120 and 168 hours post-lesion.

The graph opposite illustrates the protein expression p50 in mean arbitrary densitometric units (ADU) following QA administration at various time points. Time after lesion is displayed in the key to the right. Bars demonstrate the standard error of each population from which the mean value was obtained. Densitometric analysis and Student's two-tailed t-test revealed no significant difference between control and lesioned brains when the 50 kD band was analysed. However at 24 hours following lesion a 35 kD was present which could not be detected in controls or at 12, 48, 120 or 160 hours. The presence of this band was obviously highly significant ($P=.0004$, $P<0.005$). Number of brains (N) = 10 per time period, pooled as groups of two (i.e. experiment conducted five times per time period). Total N= 60.

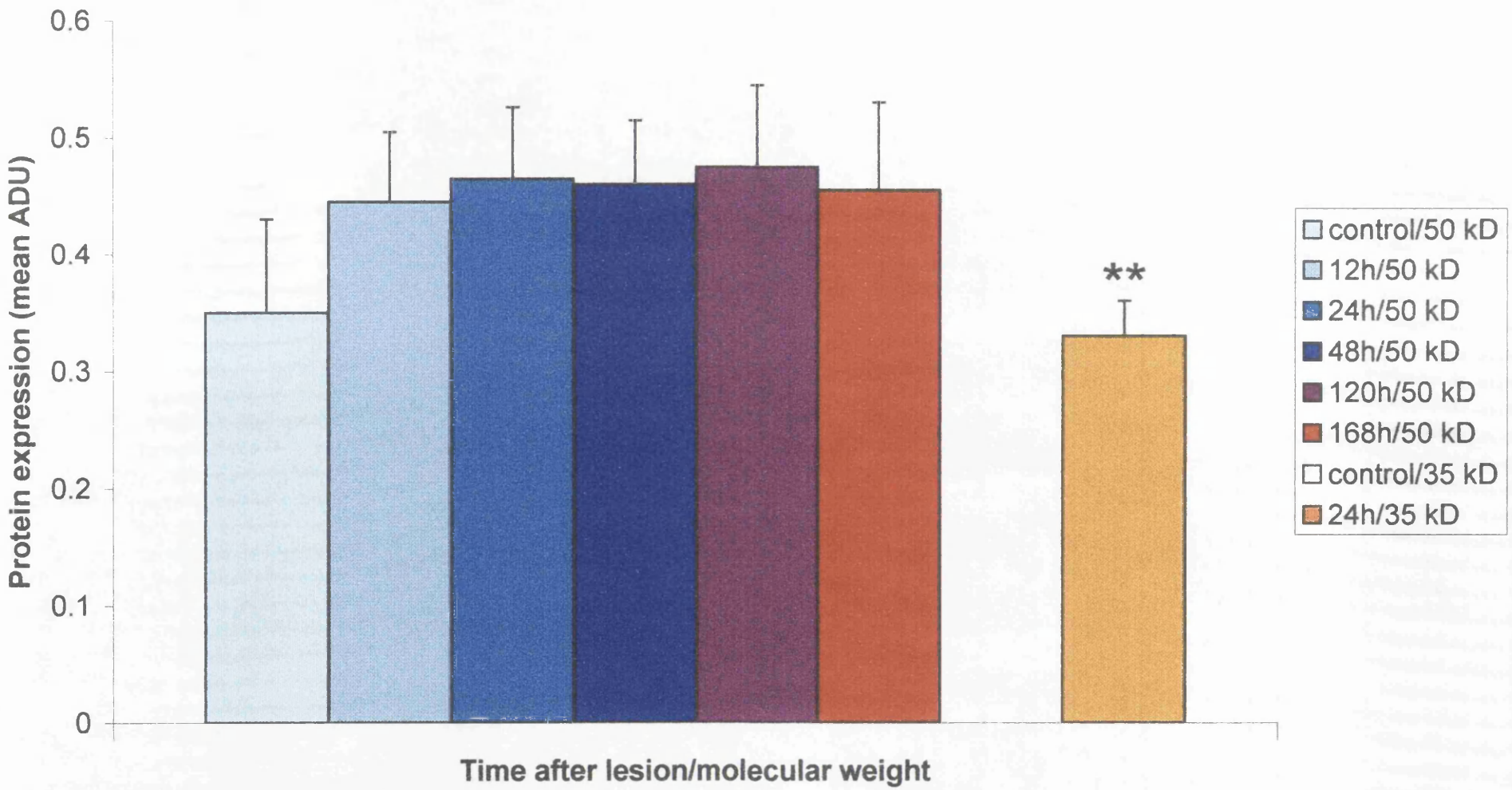
0.6
0.5
0.4
0.3
0.2
0.1
0
Protein expression (mean ADU)
**
Time after lesion/molecular weight
control/50 kD
12h/50 kD
24h/50 kD
48h/50 kD
120h/50 kD
168h/50 kD
control/35 kD
24h/35 kD

Figure 3.3/G2

Densitometric analysis of p50 protein expression (PAGE) in the striatum in controls and following QA lesion at 12, 24, 48. 120 and 168 hours post-lesion (II).

This graph represents a three dimensional representation of the graph G1, illustrating more clearly the expression relationship of the 35 kD protein to that of the 50 kD protein over time after QA treatment.

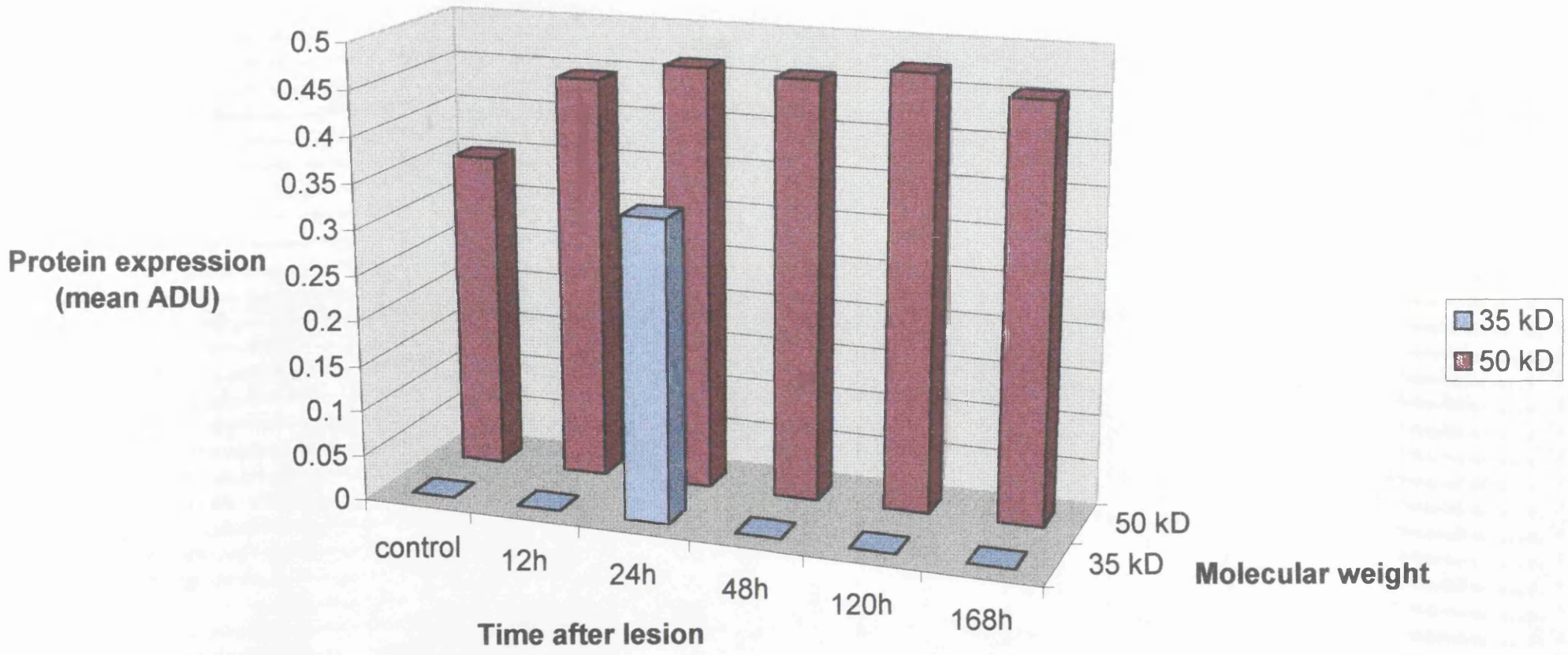
Protein expression
(mean ADU)
0.5
0.45
0.4
0.35
0.3
0.25
0.2
0.15
0.1
0.05
0
control
12h
24h
48h
120h
168h
Time after lesion
50 kD
35 kD
Molecular weight
35 kD
50 kD

Figure. 3.3/G3

Densitometric analysis of p50 protein expression (PAGE) in the striatum in controls and following CNTF treatment at 12, 24, 48. 120 and 168 hours post-lesion.

The graph opposite illustrates the protein expression p50 in mean arbitrary densitometric units (ADU) following QA administration at various time points. Time after lesion is displayed in the key to the right. Bars demonstrate the standard error of each population from which the mean value was obtained. Densitometric analysis and Student's two-tailed t-test revealed no significant difference between control and lesioned brains when the 50 kD band was analysed. However at 12 hours following CNTF treatment a 35 kD protein was present which could not be detected in controls or at 24, 48, 120 or 160 hours. The presence of this band was obviously highly significant ($P=.0007$ $P<0.005$). Number of brains (N) = 6 per time period, pooled as groups of two (i.e. experiment conducted three times per time period). Total N= 36.

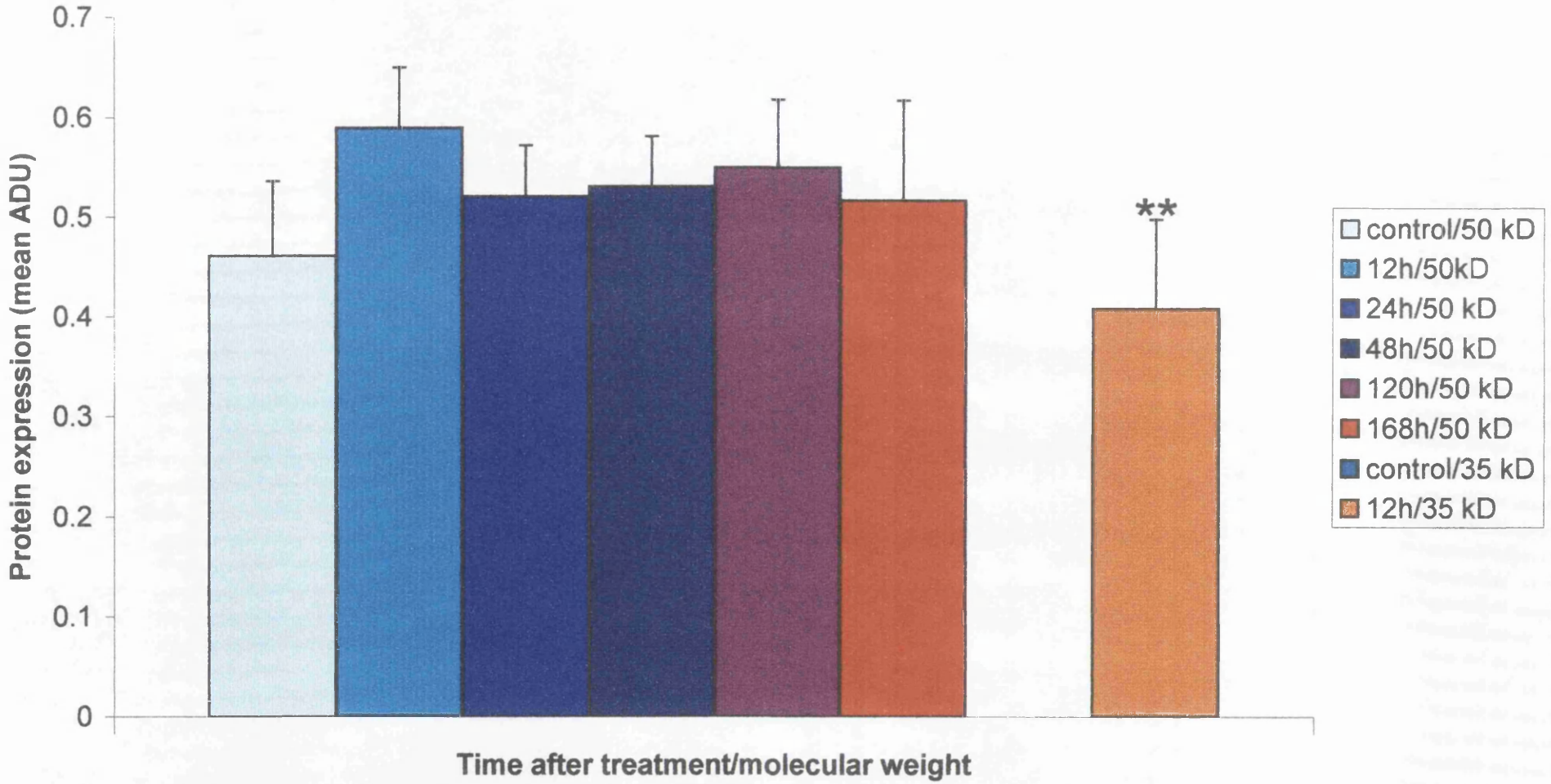
0.7
0.6
0.5
0.4
0.3
0.2
0.1
0
Protein expression (mean ADU)
**
Time after treatment/molecular weight
control/50 kD
12h/50kD
24h/50 kD
48h/50 kD
120h/50 kD
168h/50 kD
control/35 kD
12h/35 kD

Figure 3.3/G4

Densitometric analysis of p50 protein expression (PAGE) in the striatum in controls and following CNTF treatment at 12, 24, 48. 120 and 168 hours post-lesion (II).

This graph represents a three dimensional representation of the graph G3. This illustrates more clearly the expression relationship of the 35 kD protein to that of the 50 kD protein over time after CNTF treatment.

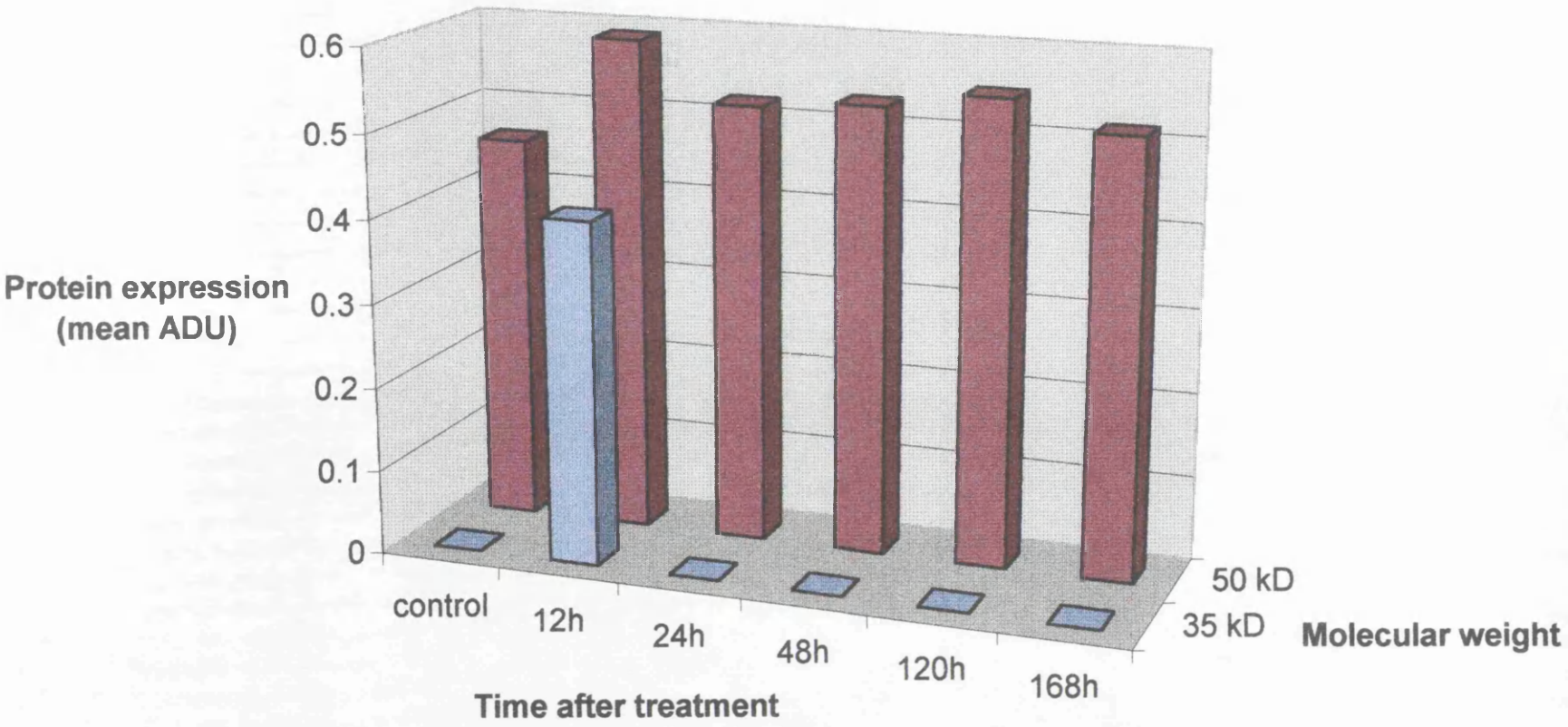
Protein expression
(mean ADU)
0.6
0.5
0.4
0.3
0.2
0.1
0
control
12h
24h
48h
120h
168h
Time after treatment
50 kD
35 kD
Molecular weight
35 kD
50 kD

Figure. 3.3/4

NF-κB p50 protein expression (PAGE) control experiments, left and right striatum (nuclear preparations).

(A) Western blot showing p50 protein expression in lesioned right striatum and unlesioned left striatum from the same quinolinic acid (QA) treated 1= left striatum, 12 hours post-lesion, 2= right striatum, 12 hours post –lesion, 3= left striatum, 16 hours post-lesion, 4= right striatum, 16 hours post-lesion, 5=left striatum, 20 hours post-lesion, 6= right striatum 20 hours post lesion. The 35 kD protein can be seen at both 20 and 22 hours post-lesion in the right striatum. Number of brains (N) = 2 per time period. Total N= 12. Antibody used was Santa Cruz SC-114 p50 recognising amino acids 350-363 (NF-κB nuclear localisation sequence, NLS) used at 1:2000 dilution.

(B) Western blot showing p50 protein expression in QA lesioned right striatum after variation in protein load to examine absence or presence of 35 kD protein (lanes 1-8). Blocking of antibody using peptide to which it was raised was conducted using concentration recommended by the producer as a guide (B 24 and B 48). Lane 1=control (untreated) striatum, 2 = 12 hour post-lesion, 3 =24 hour post-lesion, 4= 24 hour post-lesion at 50 % concentration, 5= 24 hour post-lesion at 25 % concentration. (35 kD band is still visible despite protein concentration being reduced by $^{3}/_{4}$ concentration) 6= 48 hours post lesion, 7= 48 hours post lesion at 200% concentration, 8 =48 hours post lesion at 300% concentration (35 kD protein is not visible despite concentration being raised to 2.5 times). Lane B24 (24 hour post-lesion sample) and B 48 (48 hour post-lesion sample) demonstrate abolition of all bands when antibody is pre-incubated at $^{1}/_{2}$ peptide concentration recommended by the producer prior to exposure to filter.

(C) Western blot showing p50 protein expression in CNTF treated right striatum after variation in protein load to examine absence or presence of 35 kD protein (lanes 1-7). Blocking of antibody using peptide to which it was raised was conducted using concentration recommended by the producer as a guide (B 12 and B 24). Lane 1=control (untreated) striatum, 2 = 12 hour post-lesion, 3 =12 hour post-lesion at 50 % protein concentration, 4= 12 hour post-lesion at 25 % concentration. (35 kD band is still visible despite protein concentration being reduced by $^{3}/_{4}$ concentration) 5= 24 hour post-lesion, 6= 24 hours post lesion at 200% concentration, 7= 24 hours post lesion at 300% concentration, (35 kD protein cannot clearly be seen despite concentration being raised to 2.5 times). Lane B12 (12 hour post-lesion sample) and B 24 (24 hour post-lesion sample) demonstrate partial abolition of all bands when antibody is pre-incubated at $^{1}/_{2}$ peptide concentration recommended by the producer prior to exposure to filter. Bands are totally abolished at producers recommended concentration.

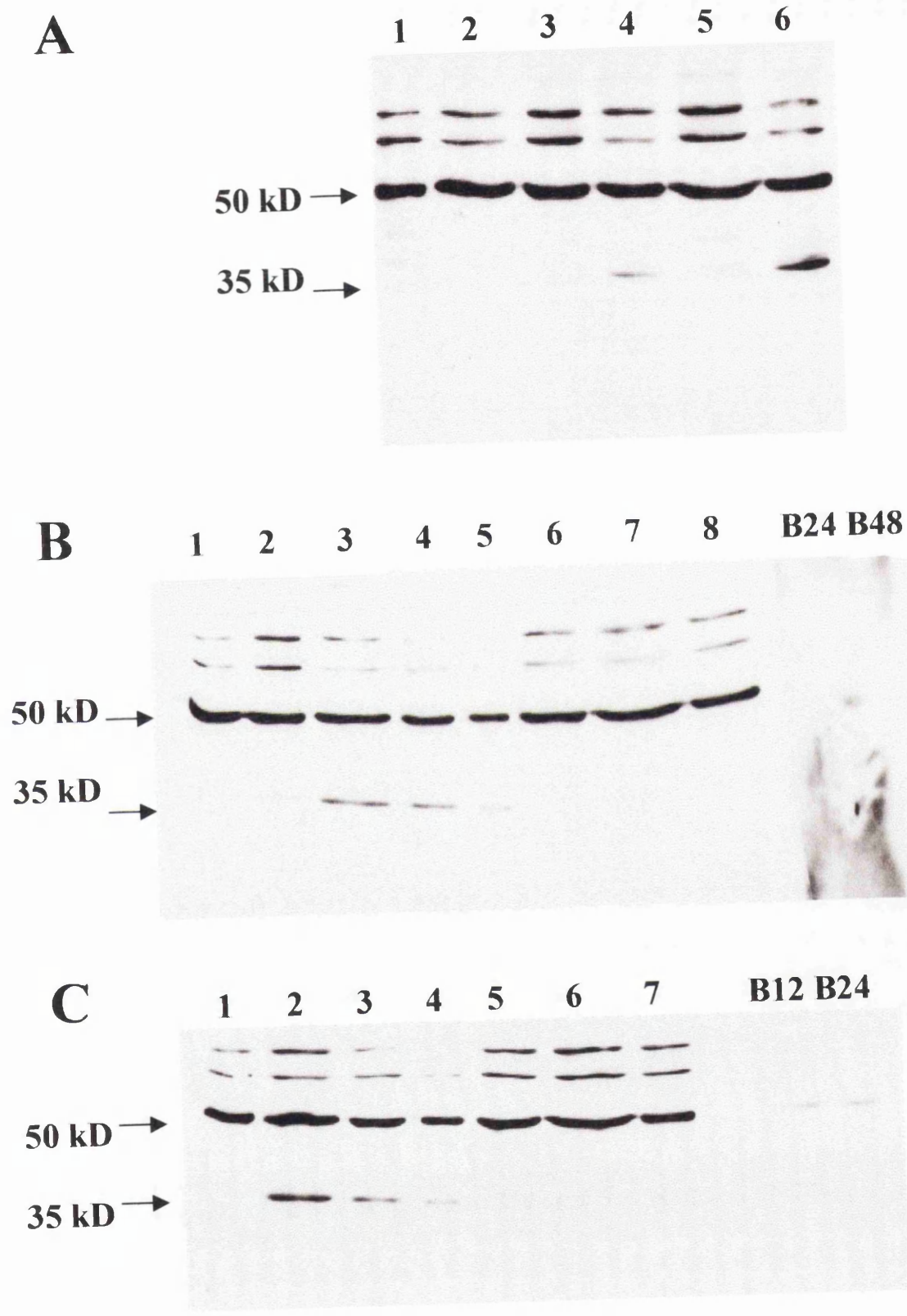
A
1 2 3 4 5 6
50 kD
35 kD
B
1 2 3 4 5 6 7 8 B24 B48
50 kD
35 kD
C
1 2 3 4 5 6 7 B12 B24
50 kD
35 kD

Figure. 3.3/5

NF-κB p52 protein expression (PAGE) in control striatum (nuclear preparations) and following quinolinic acid lesion and CNTF treatment at 12, 24, 48, 120 and 168 hours post lesion.

(A)Western blot showing p52 protein expression in control (untreated) and quinolinic acid (QA) treated and post-CNTF treated (12h) striatal nuclear samples at various time points post-lesion. Weak upper molecular weight protein bands can be seen and may represent cytoplasmic contamination by NF-κB precursors. The arrow at 50 kD indicates a protein migrating at the approximate molecular weight for p52, and densitometric analysis reveals no significant difference between controls and any time point following QA lesion (Fig.3.3/G6). The 40 kD arrow indicates a non-specifc band which cannot be fully blocked by incubation with the peptide to which the antibody was raised (BC 12, 12 hour post CNTF treatment and BQ 24, 24 hour post QA treatment). Antibody used was Santa Cruz K-27 rabbit polyclonal raised to amino acids 298-324 and used at 1:1000 dilution.

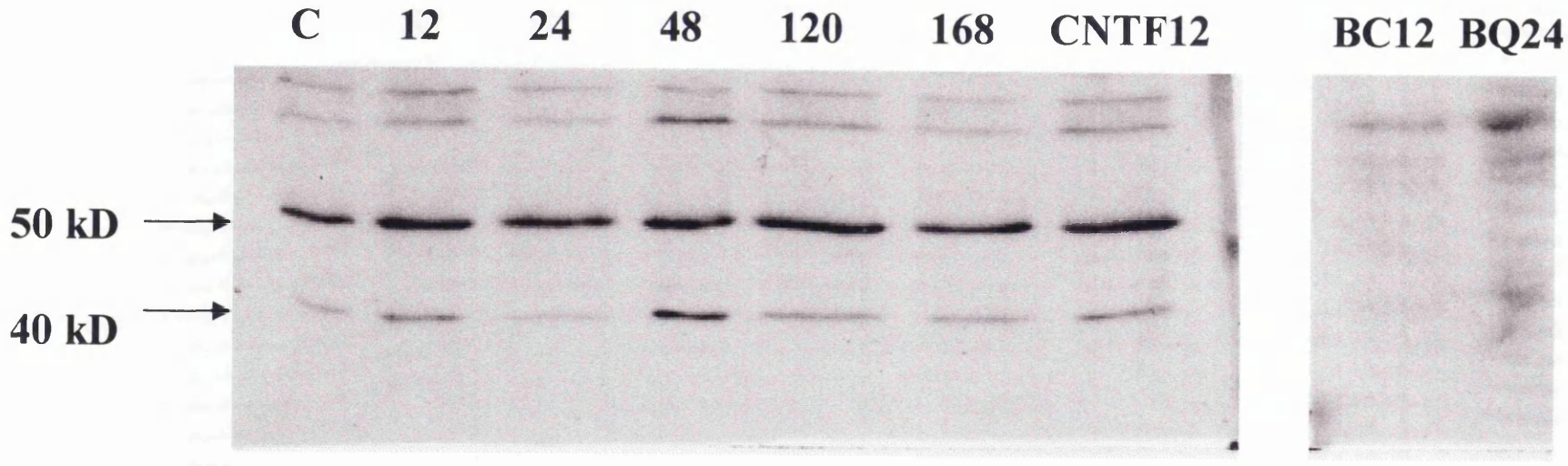
C
12
24
48
120
168
CNTF12
BC12
BQ24
50 kD
40 kD

Figure. 3.3/G6

Densitometric analysis of p52 protein expression (PAGE) in the striatum in controls and following QA and CNTF treatment at 12, 24, 48. 120 and 168 hours post-lesion.

The graph opposite illustrates the protein expression p52 in mean arbitrary densitometric units (ADU) following QA and CNTF administration at various time points. Time after lesion is displayed in the key to the right. Bars demonstrate the standard error of each population from which the mean value was obtained. Densitometric analysis and Student's two-tailed t-test revealed no significant difference between control and lesioned brains when the 50 kD band was analysed. Number of brains (N) = 6 per time period, pooled as groups of two (i.e. experiment conducted three times per time period). Total N=36.

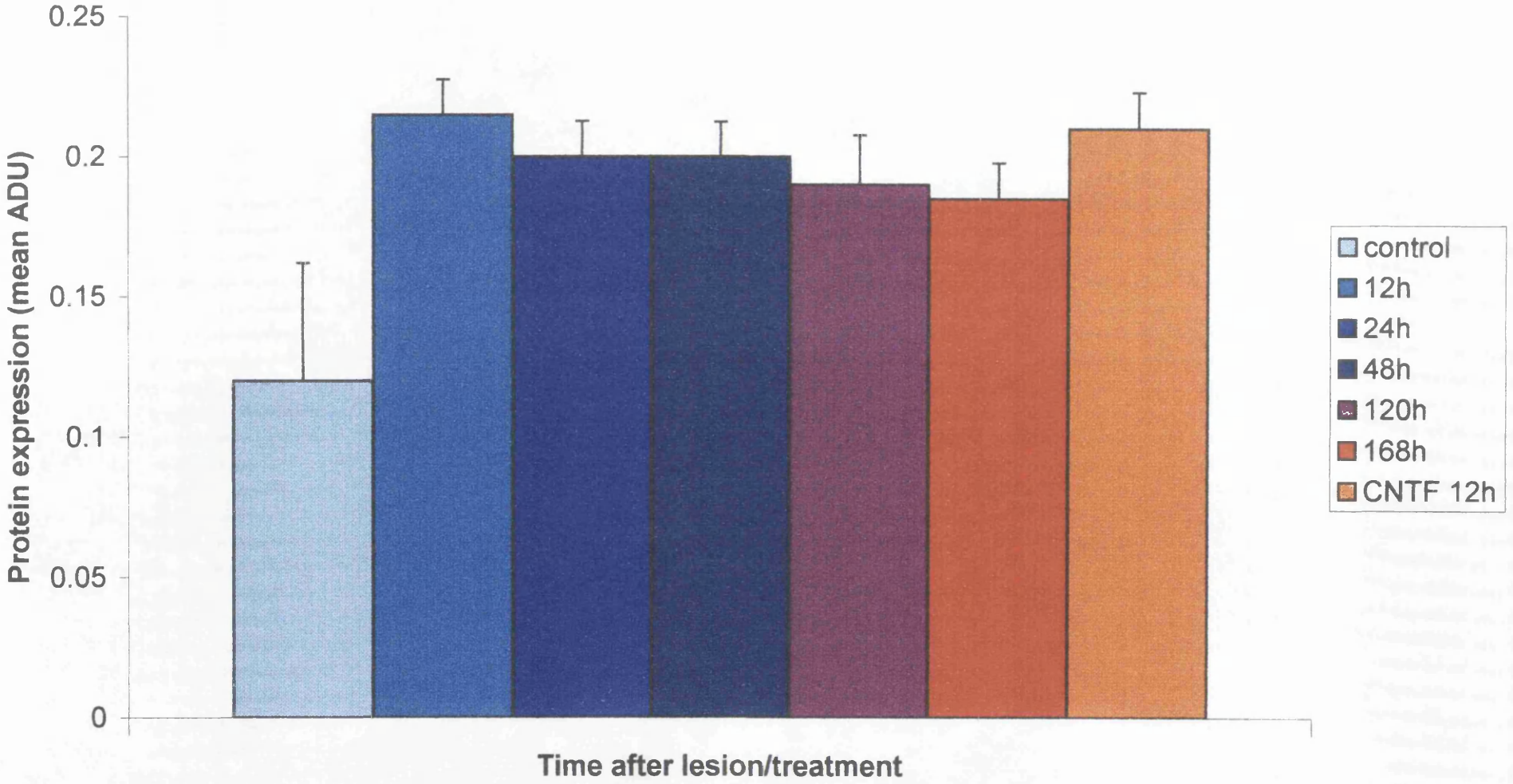
0.25
0.2
0.15
0.1
0.05
0
Protein expression (mean ADU)
Time after lesion/treatment
control
12h
24h
48h
120h
168h
CNTF 12h

Figure. 3.3/6

I-κB-alpha protein expression (PAGE) in control striatum (nuclear and cytoplasmic) and following quinolinic acid lesion and CNTF treatment at 24 and 168 hours post lesion.

(A)Western blot showing I-κB-alpha protein expression in control (untreated) and quinolinic acid (QA) treated and post-CNTF treated (12 and 168 hours/ 7 days) striatal nuclear samples. The arrow at 40 kD indicates a protein migrating at the approximate molecular weight for I-κB-alpha. The greater amount of I-κB-alpha is localised in the cytoplasmic fraction, with a faint protein band indicating the presence of some nuclear I-κB-alpha. Antibody used was Santa Cruz C-21/SC-371 rabbit polyclonal raised to amino acids 297-317 and used at 1:2000 dilution.

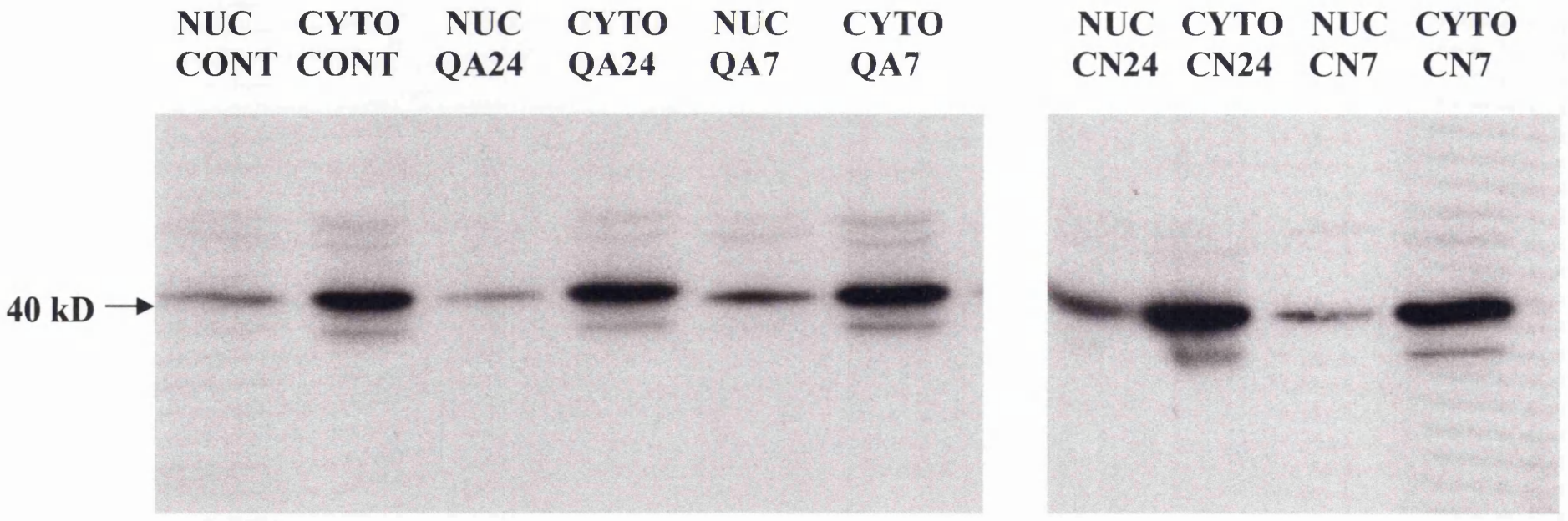
NUC CONT
CYTO CONT
NUC QA24
CYTO QA24
NUC QA7
CYTO QA7
NUC CN24
CYTO CN24
NUC CN7
CYTO CN7
40 kD

3.4 PROTEIN BINDING TO NF-κB CONSENSUS SITE DNA AFTER QA OR CNTF TREATMENT

Electrophoretic mobility shift assay (EMSA) of both QA and CNTF treated striatal nuclear extract demonstrates increased binding of protein to the DNA oligonucleotide of the NF-κB binding sequence (Fig. 3.4/1C and 3.4/2B). This was indicated by increased size of the protein/DNA complex and density on autoradiograph which was confirmed by densitometric analysis (Fig. 3.4 G1 & G2). The specifity of the DNA-binding complex is demonstrated by abolishing the protein binding activity with 10x unlabelled NF-kB oligonucleotide (Fig. 3.4/1 B) and by retention of binding when 10x of a SP-1 consensus site unlabelled oligonucleotide is added (Fig.3.4/1 A). QA treated brains demonstrated a peak of binding at 24 hours whereas CNTF treated brains demonstrated a significant increase in binding at 12 hours following treatment. Protein binding appeared to decrease at time points after this, but again increased significantly above control levels at 168 hours (seven days) in both CNTF and QA treated animals (Fig 3.4 G1 & G2). Although not recommended by the producer (Santa-Cruz Biotechnology) for such, the p50, p52 and p65 antibodies already used in this thesis were employed in an attempt to 'supershift' the NF-κB/DNA binding complex and reveal its protein components (3.4/2C). Addition of the p52 antibody to the undenatured striatal nuclear protein homogenate prior to incubation with the p32 labelled NF-κB oligonucleotide probe resulted in the appearance of a higher molecular weight binding complex above the main binding complex. Addition of the p50 antibody repeatedly resulted in the obliteration of the major binding complex. A faint high molecular weight binding complex could be seen, but not of the same density of the major binding complex. Addition of the p65 antibody repeatedly failed to obtain any obliteration or shifting of the major binding complex (3.4/2C).

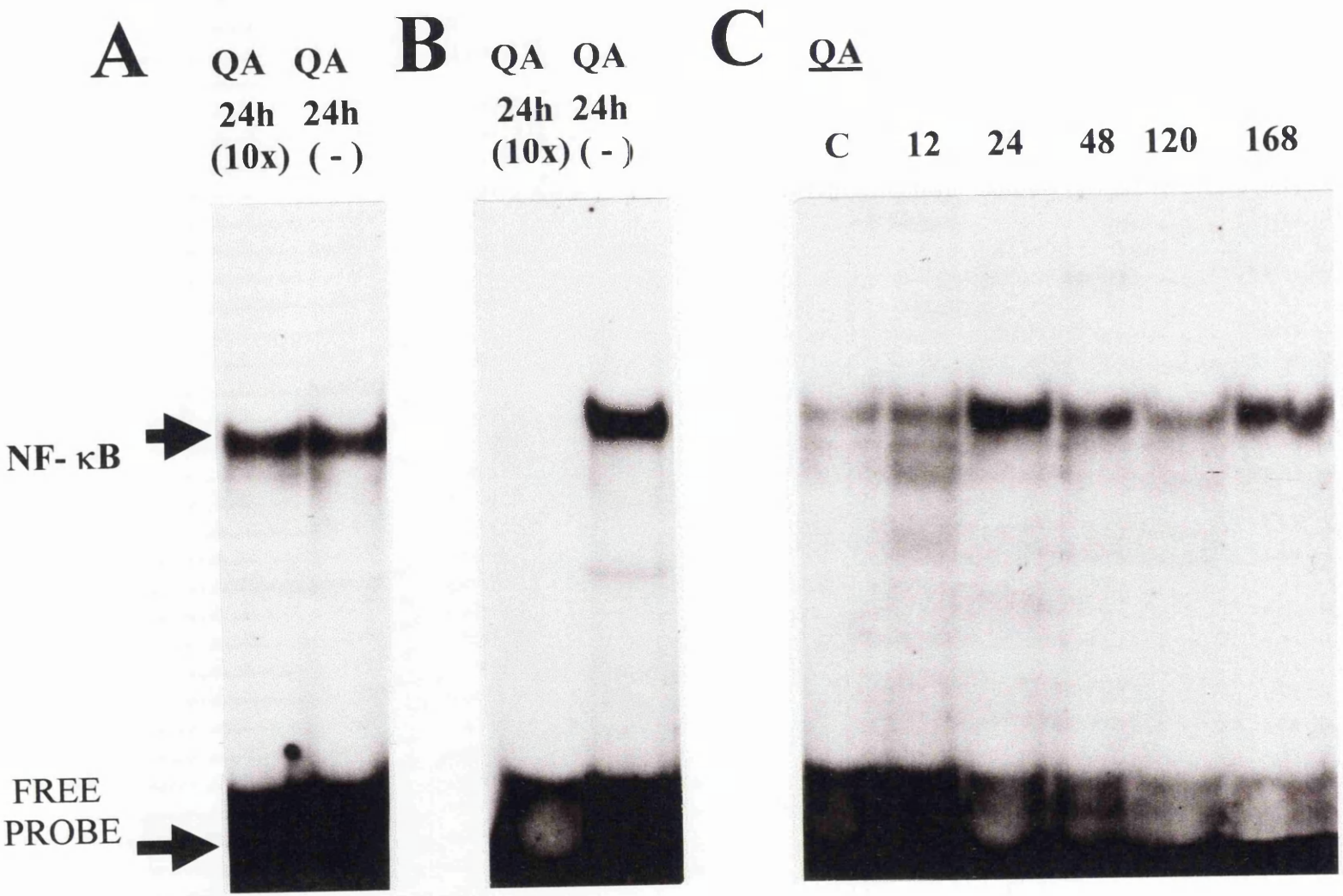
A
QA 24h (10x)
QA 24h (-)
B
QA 24h (10x)
QA 24h (-)
C
QA
C
12
24
48
120
168
NF- κB
FREE PROBE

Figure. 3.4/2

Electrophoretic mobility shift assay (EMSA) of control striatal nuclear preparation and at 12, 24, 48. 120 and 168 hours following CNTF treatment using NF-κB consensus oligonucleotide.

(A&B)(B) EMSA of striatal nuclear preparations at 12, 24, 48, 120 and 168 hours after CNTF treatment. Increase in DNA-protein binding can be observed at 12, 24 and 168 hours after administration of QA. (A) compares increased DNA-protein binding in a control (untreated) striatum and that of a CNTF treated striatum 12 hours after administration.

(C) EMSA of QA treated (24h) striatal nuclear homogenate plus the addition of and pre-incubation with goat serum (GS) as a control, anti-GFAP (CAb-control antibody) as a control, anti-p52 (p52), anti-p50 (p50) and anti-p65 (p65). the p50, p52 and p65 antibodies were employed in an attempt to 'supershift' the NF-κB/DNA binding complex and reveal its protein components. Addition of the p52 antibody results in the appearance of a higher molecular weight binding complex above the main binding complex (Q24 p52). Addition of the p50 antibody repeatedly resulted in obliteration of the major binding complex. A faint high molecular weight binding complex could be seen, but not of the same density of the major binding complex (Q24 p50). Addition of the p65 antibody repeatedly failed to obtain any total obliteration or shifting of the major binding complex (Q24 p65), although some reduction in binding is observed. The goat serum appeared to produce a downwards displacement 'smearing' of the binding complex, but no shifting or obliteration of the major binding complex was observed. The GFAP antibody had no visible action upon the binding complex.

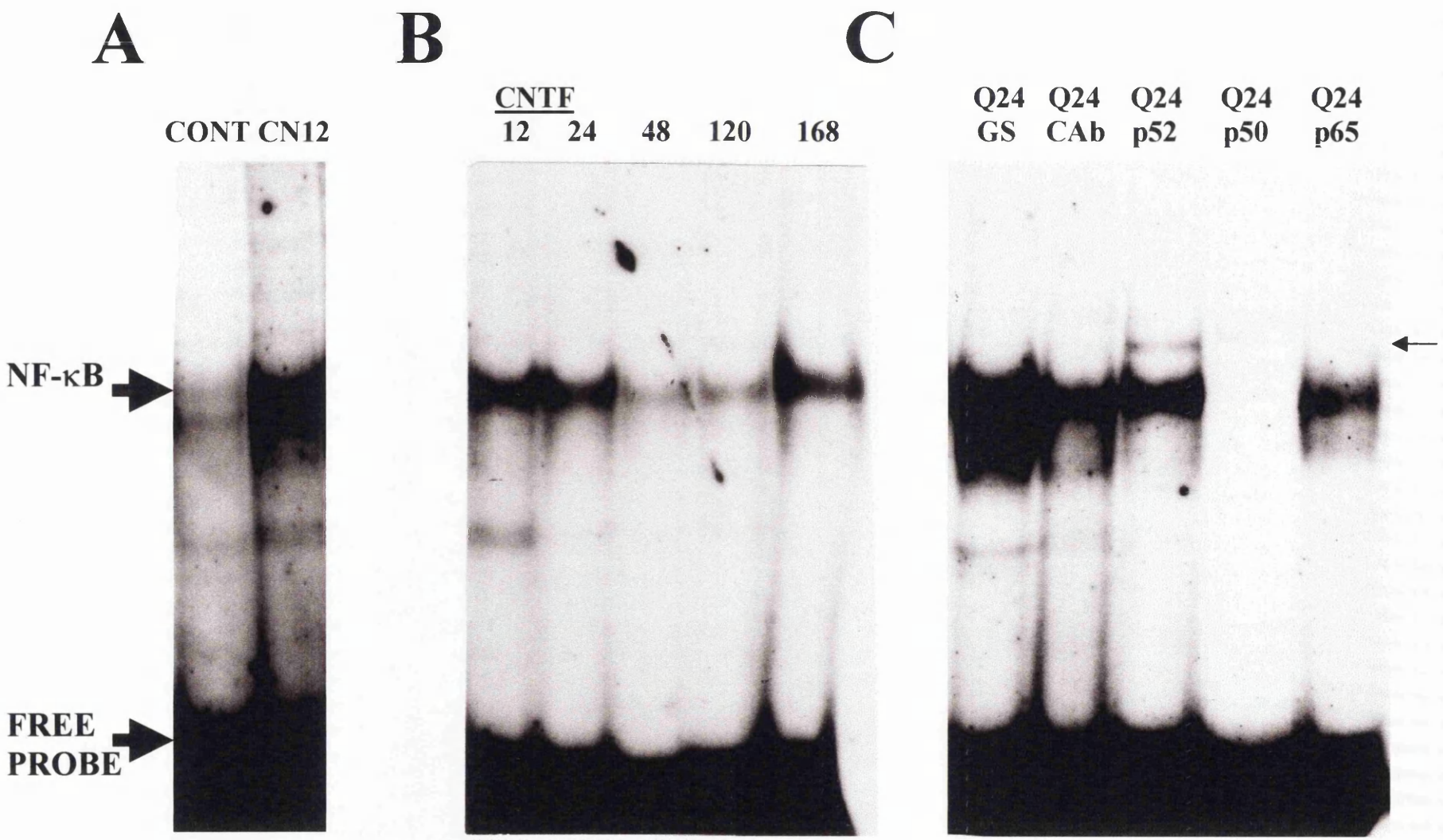
A
B
C
CONT CN12
CNTF
12 24 48 120 168
Q24 GS
Q24 CAb
Q24 p52
Q24 p50
Q24 p65
NF-κB
FREE PROBE

Figure. 3.4/G1

Densitometric analysis of protein binding in the striatum to NF-κB oligonucleotide in controls and after QA treatment at 12, 24, 48, 120 and 168 hours following lesion.

The graph opposite illustrates DNA-protein binding in mean arbitrary densitometric units (ADU) following QA administration at various time points. Time after lesion is displayed in the key to the right. Bars demonstrate the standard error of each population from which the mean value was obtained. Densitometric analysis and Student's two-tailed t-test revealed significant difference in binding between control and lesioned brains at 24 hours: $P=0.02$ ($P<0.05$) and 168 hours (seven days): $P=0.015$ ($P<0.05$) following QA administration. Number of brains (N) = 10 per time period, pooled as groups of two (i.e. experiment conducted five times per time period). Total N= 60.

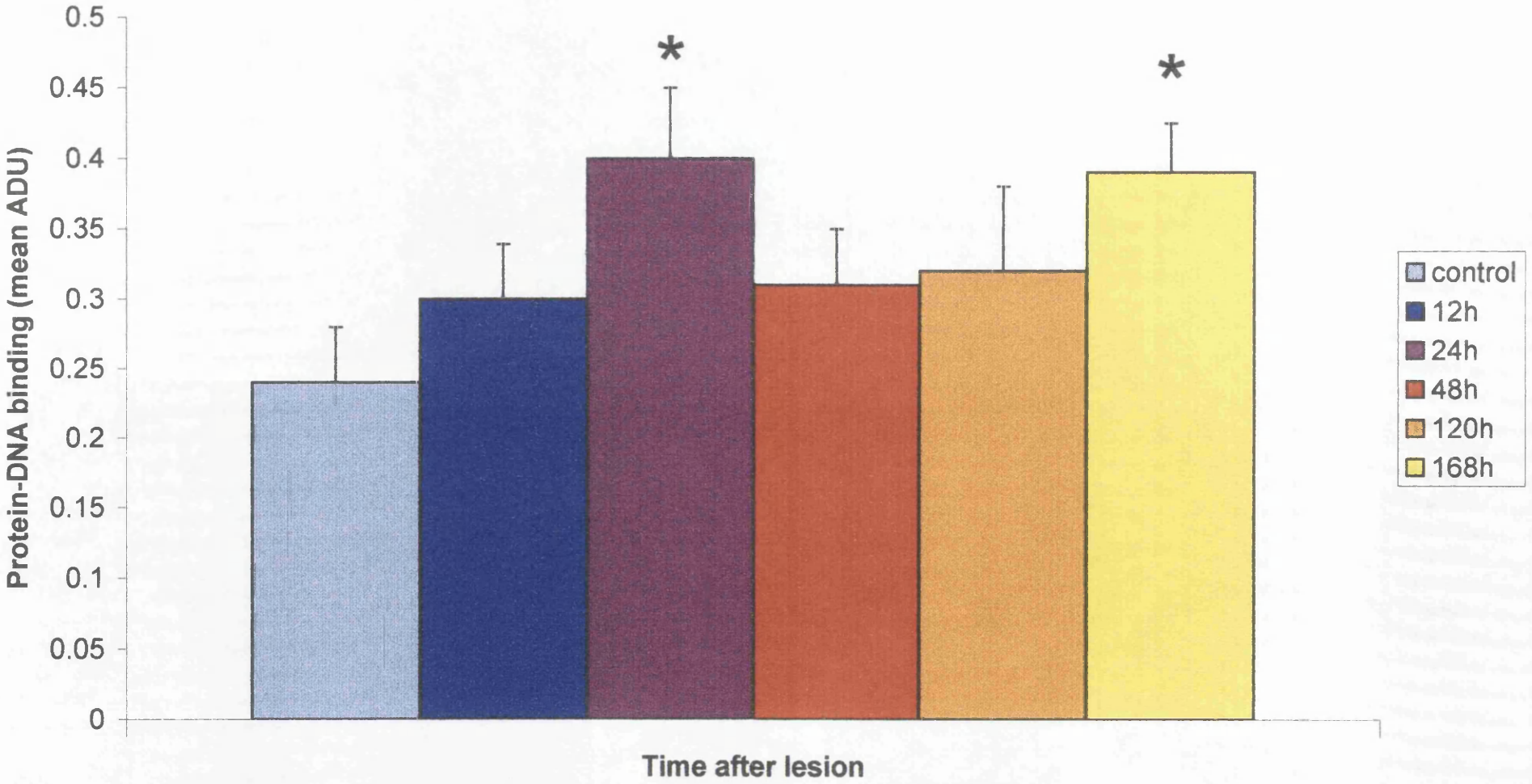
0.5
0.45
0.4
0.35
0.3
0.25
0.2
0.15
0.1
0.05
0
Protein-DNA binding (mean ADU)
*
*
Time after lesion
control
12h
24h
48h
120h
168h

Figure. 3.4/G2

Densitometric analysis of protein binding in the striatum to NF-κB oligonucleotide in controls and after CNTF treatment at 12, 24, 48, 120 and 168 hours following lesion.

The graph opposite illustrates DNA-protein binding in mean arbitrary densitometric units (ADU) following CNTF administration at various time points. Time after lesion is displayed in the key to the right. Bars demonstrate the standard error of each population from which the mean value was obtained. Densitometric analysis and Student's two-tailed t-test revealed significant difference in binding between control and lesioned brains at 12 hours: $P=0.03$ ($P<0.05$), 24 hours: $P=0.048$ ($P<0.05$) and 168 hours (seven days): $P=0.03$ ($P<0.05$) following CNTF administration. Number of brains (N) = 8 per time period, pooled as groups of two (i.e. experiment conducted four times per time period). Total N= 48.

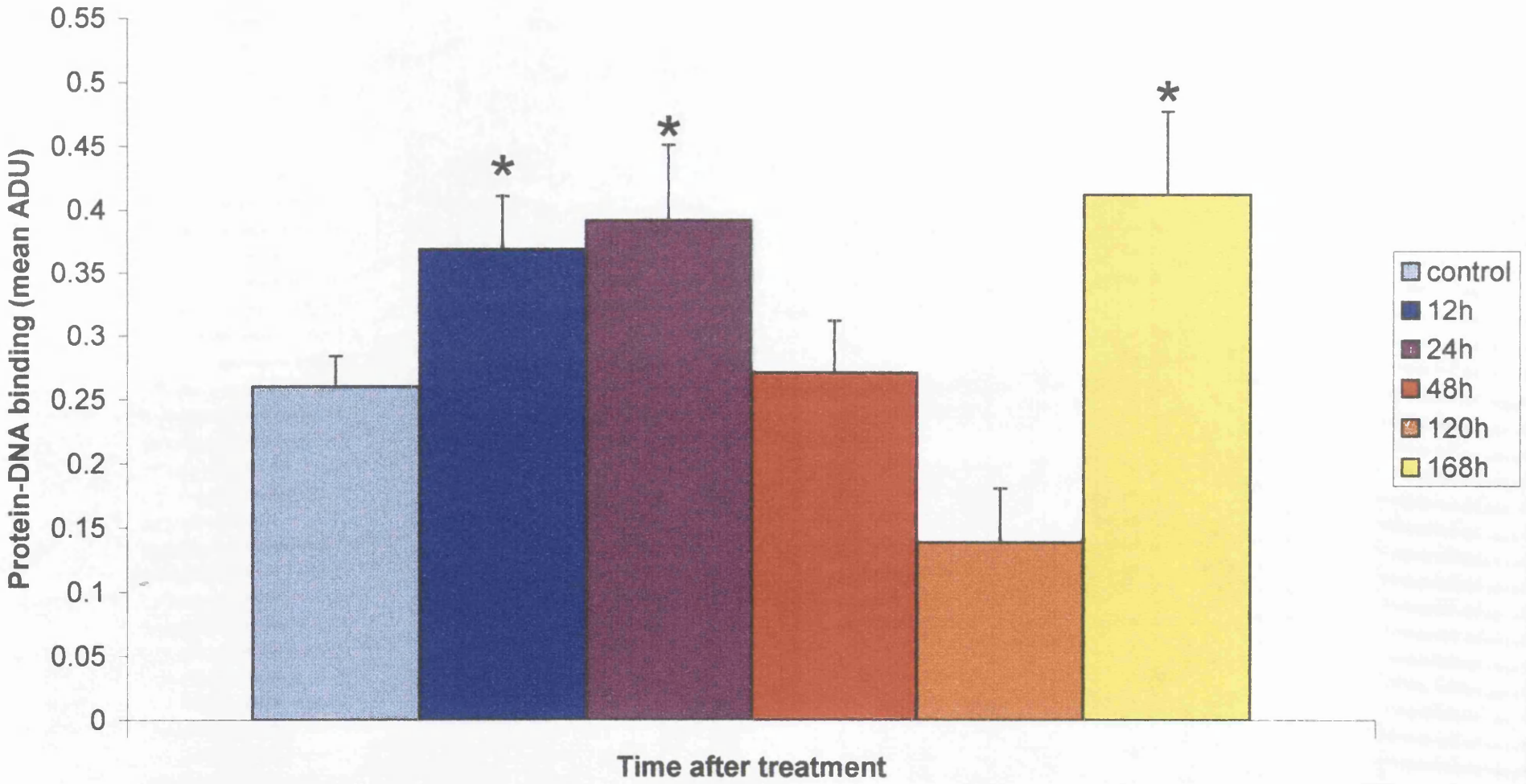
0.55
0.5
0.45
0.4
0.35
0.3
0.25
0.2
0.15
0.1
0.05
0
Protein-DNA binding (mean ADU)
*
*
*
Time after treatment
control
12h
24h
48h
120h
168h

Figure. 3.4/3

Electrophoretic mobility shift assay (EMSA) of saline treated striatal nuclear preparation at 12, 24, 48, 120 and 168 hours following treatment using NF-κB consensus oligonucleotide.

EMSA of striatal nuclear preparations in control (untreated) and at 12, 24, 48, 120 and 168 hours after administration of one microlitre of physiological saline. Saline was administered via Hamilton syringe and stereotaxic apparatus in identical manner to treatment with QA or CNTF.

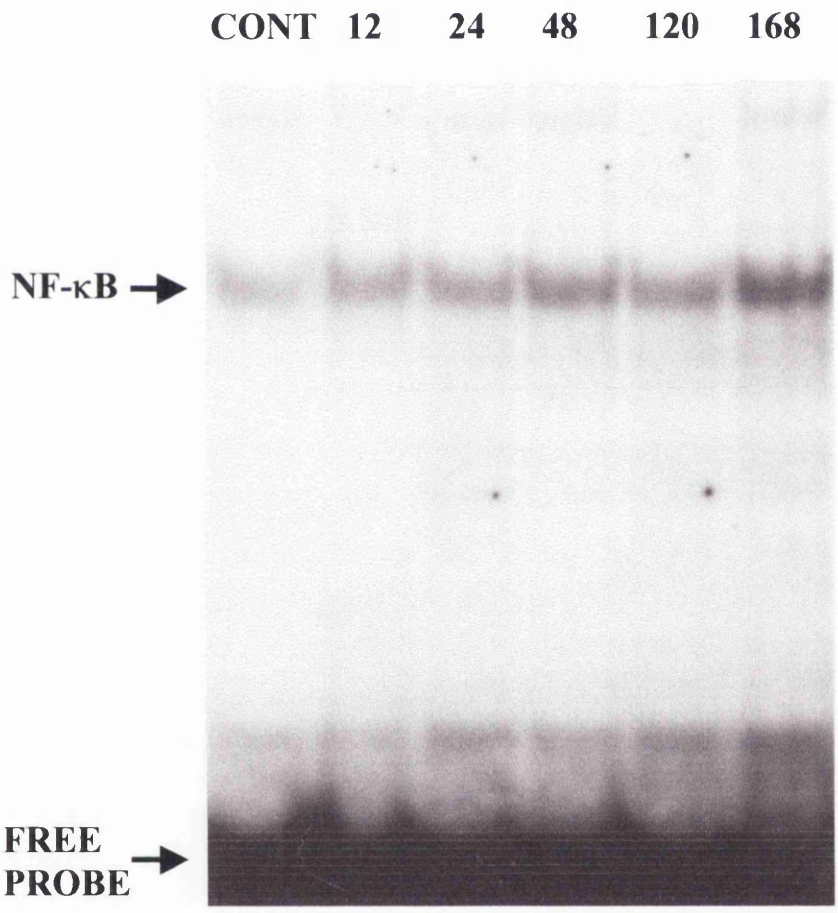
CONT
12
24
48
120
168
NF-κB
FREE
PROBE

3.5 CNS LOCALISATION OF TATA BINDING PROTEIN, BRN-2 AND GLUCORTICOID RECEPTOR IN HUNTINGTON R6/2 TRANSGENIC MICE

Immunocytochemistry using the glucocorticoid receptor antibody (M-20) in both littermate control and R6/2 transgenic mice at 11 weeks of age demonstrated strong nuclear staining throughout the cortex, striatum and in small nuclei, presumably oligodendrocytes, in the corpus callosum. Both large and small nuclei could be distinguished indicating that both neurones and glial cell types were expressing this protein. No apparent morphological differences could be seen when immunoreactivity between littermate controls and transgenic mice, at any time point examined (Fig.3.5/1 A & B) throughout the CNS. No apparent difference in levels of protein could be distinguished by observation using immunocytochemistry. A region of nuclear exclusion (ie. no immunoreactivity) could be observed in the nuclei of both transgenes and control mice in some nuclei, indicative of the nucleolus. No nucleus appeared to contain two regions of exclusion of immunoreactivity.

Immunocytochemistry of cortex and striatum from both littermate controls and transgenic mice at the ages of 11 weeks using either the TBP Santa Cruz antibody or the 2C1, 3G3, 4C2 antibodies (gift of Laszlo Tora) demonstrated a similar pattern of staining. The 3G3 and 4C2 antibodies presented such high background staining, even at extremely low concentrations, that anatomical localisation was very poor. 2C1 provided striking immunoreactivity of nuclei throughout the cortex and striatum, a pattern of staining almost identical to that of the SC-TBP antibody. Nucleolar exclusion could be visualised with both 2C1 and SC-TBP antibodies. No distinction between transgenic nuclear TBP staining and that of littermate controls could be observed, and no difference in the pattern of staining could be discerned between littermate controls and transgenic mice of all ages examined throughout the central nervous system (Fig. 3.5/1, C & D).

Although no difference could be discerned between transgenes and controls using either the SC-/2C1 TBP or GR antibodies for immunocytochemistry, the BRN-2 antibody (C-20) demonstrated some variation in immunoreactivity between littermate controls and R6/2 transgenes. No difference in immunoreactivity could be discerned between the striatum or cortex of littermate controls and transgenes (Fig. 3.5/2E & F), and sectioning

through the brain revealed this to be true of other CNS structures. The BRN-2 antibody provides striking nuclear staining, especially in the upper cortical layers as opposed to the lower layers. Striatal nuclear immunoreactivity is much weaker than that observed in the cortex, and striatal neuropil reactivity is greater than that of the cortex. Staining of glial nuclei in the corpus callosum is again visible. However, initial examination of the paraventricular nucleus of the hypothalamus revealed that this structure contains cell nuclei which are strongly immunoreactive (even more so than the cortical nuclei) to the BRN-2 antibody in litter mate controls (Fig. 3.5/2 A & C). When compared to transgenes at 11 and 13 weeks of age (Fig.3.5/2 A,B,C & D), morphological differences appeared to be seen between the two structures, the transgenic PVN appearing not to be as 'strongly' immunoreactive. It was unclear at this point whether or not this was due to a reduction in cell numbers or due to reduced expression of the protein. Initial observation of immunocytochemical results for all polyglutamine repeat transcription factors had been conducted through mice brains using sections cut at 40μm, taking every third section for a particular antibody or stain. Control and transgenic mice at 11 and 13 weeks of age were taken and sections at 20 μm were cut throughout the PVN. Careful cell counts were conducted throughout the structures stained for Nissl substance (to observe any marked neuronal loss), BRN-2 and another PVN cell marker, vasopressin (antibody 1565) to see if a reduced PVN cell number was present in R6/2 transgenic mice (Fig. 3.5/2 G & H). No significant difference could be found with either BRN-2 or vasopressin counts between littermate controls or transgenes (Fig. 3.5/G1/G2/G3). Immunocytochemistry seems to indicate a decrease in expression of BRN-2 protein in the PVN of transgenic mice when compared to littermate controls. It seems unlikely that this appearance is due to divergent experimental conditions, because control and transgenic sections were processed simultaneously and in a relatively large population of brains used for PVN examination (Control N=5 Transgenic N=7) this difference in staining was consistently seen throughout the PVN. Furthermore, expression as determined by immunocytochemistry in other transgenic structures did not vary when compared to control brains, for example, the cortex (Fig.3.5/2). Of greatest interest, however, is that no clear immunostaining of the neuronal intranuclear inclusion was observed in transgenes.

Figure. 3.5/1

Cellular expression (immunocytochemistry) of GR and TBP in the striatum of littermate controls (LMC) and R6/2 transgenic mice at 13 weeks of age

(A) Photomicrograph of GR immunoreactivity in LMC striatum. Scale bar = 30 μm . Widespread immunoreactivity of neuronal nuclei is visible. Antibody used Santa Cruz M-20 at 1:1000 dilution.

(B) Photomicrograph of GR immunoreactivity in R6/ 2 transgenic striatum. Scale bar = 30 μm. No internal nuclear structures are visible at higher power.

(C) Photomicrograph of TBP immunoreactivity in LMC striatum. Scale bar = 30 μm. Widespread immunoreactivity of neuronal nuclei is visible. Antibody used Santa Cruz N-12 at 1:1000 dilution.

(B) Photomicrograph of TBP immunoreactivity in R6 /2 transgene striatum. Scale bar = 30 μm. No internal nuclear structures are visible at higher power.

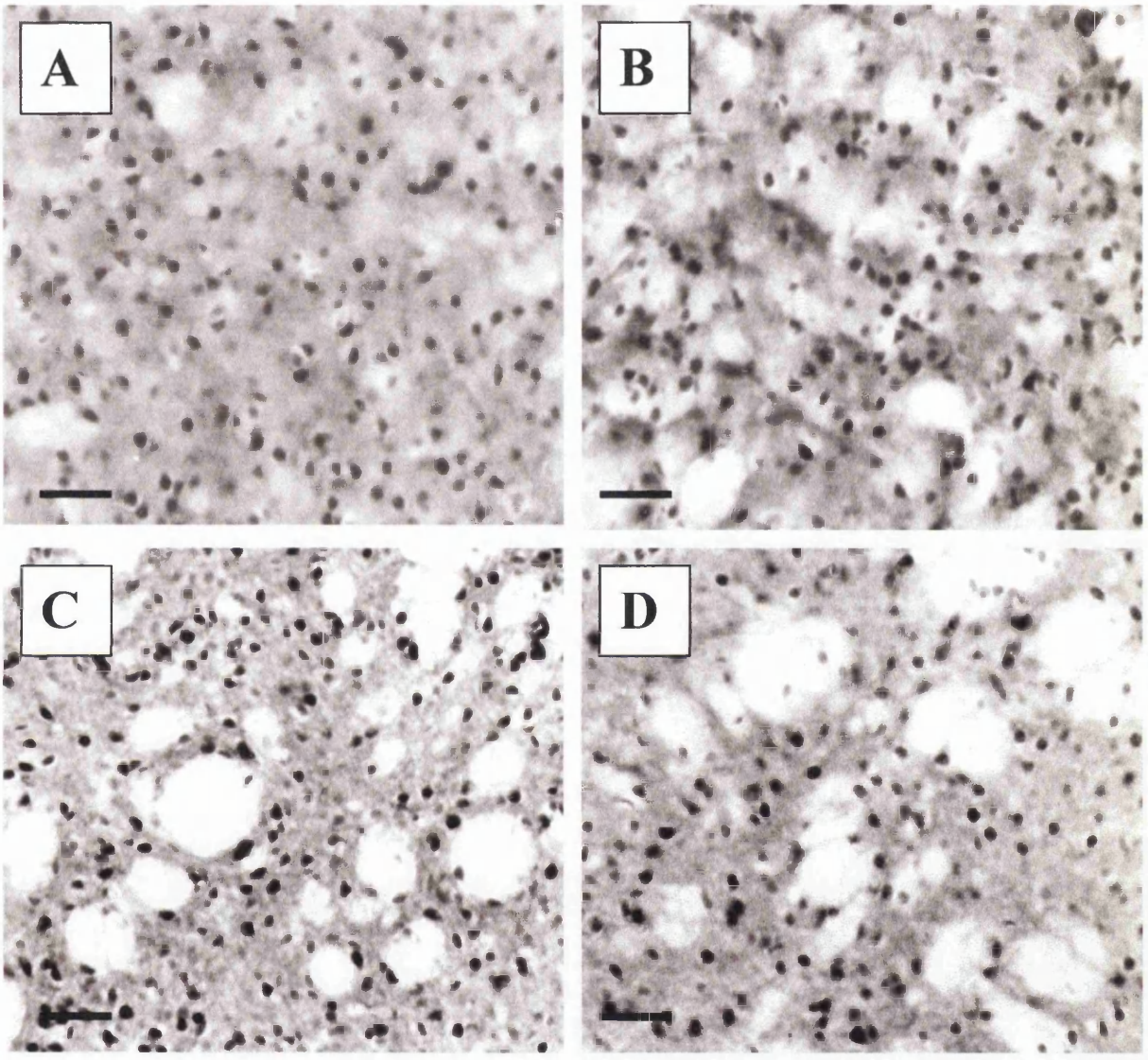
A
B
C
D

Figure. 3.5/2

Cellular expression (immunocytochemistry) of BRN-2 and Vasopressin in the PVN and cortex of littermate controls (LMC) and R6/2 transgenic mice at 11 weeks of age

(A) Photomicrograph of BRN-2 immunoreactivity in LMC PVN. Scale bar = 100 μm. Notice prominently immunoreactive nuclei as found in control cortex. Antibody used Santa Cruz C-20 at 1:1000 dilution.

(B) Photomicrograph of BRN-2 immunoreactivity in R6/2 transgene PVN. A and B are sections through the anterior PVN. Scale bar = 100 μm. Immunoreactivity is much weaker than that observed in LMC PVN and R6/2 cortex (below).

(C) Photomicrograph of BRN-2 immunoreactivity in LMC PVN. Scale bar = 100 μm.

(D) Photomicrograph of BRN-2 immunoreactivity in R6/2 transgene PVN. C and D are sections through the posterior PVN. Scale bar = 100 μm. Immunoreactivity is much weaker than that observed in LMC PVN and R6/2 cortex (below).

(E) Photomicrograph of BRN-2 immunoreactivity in LMC cortex. Scale bar = 40 μm. Antibody used Santa Cruz C-20 at 1:1000 dilution.

(F) Photomicrograph of BRN-2 immunoreactivity in R6/2 transgenic cortex. Scale bar = 40 μm. No internal nuclear structures are visible at higher power. No difference in level of expression or distribution of protein can be visualised between transgenic and control cortex. Nuclear profiles are very distinct.

(G) Photomicrograph of VP immunoreactivity in LMC PVN. Scale bar = 100 μm. Antibody used Chemicon 1565 at 1:1000 dilution.

(H) Photomicrograph of VP immunoreactivity in R6/2 PVN. Scale bar = 100 μm. VP immunoreactive neurones and axons can clearly be seen. Level of expression of VP appears the same when comparing individual neurones in either transgenic or control PVN and cell counts indicate no significant difference in cell number.

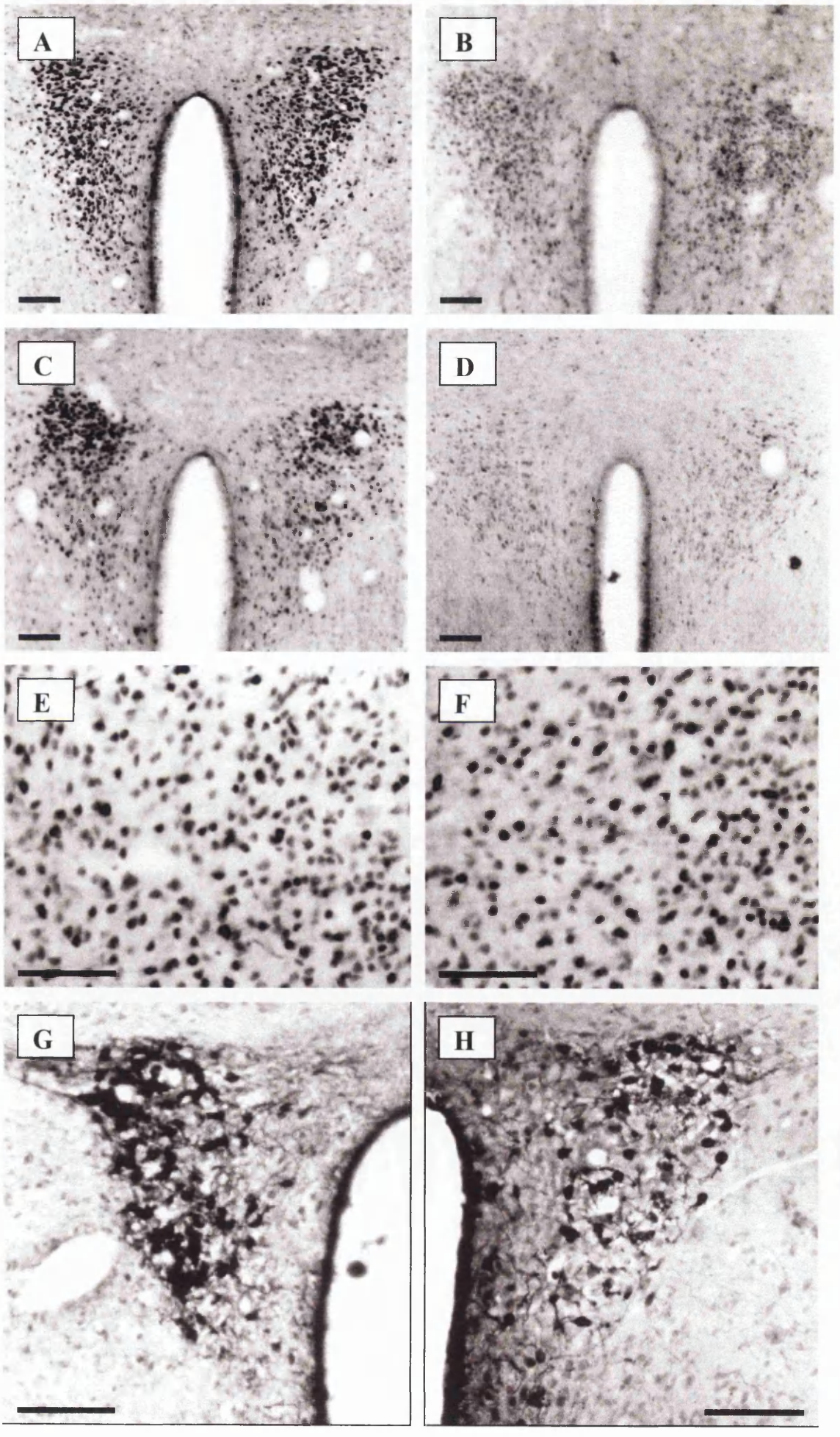
A
B
C
D
E
F
G
H

Figure. 3.5/G1

Total cell number of BRN-2 immunoreactive nuclei of PVN neurones in LMC and R6/2 transgenes at 10 weeks of age from 20 micrometre sections

The graph opposite illustrates the Abercrombie corrected (average perikaryal area = 12 μm). Total numbers of BRN-2 immunoreactive nuclei at 10 weeks of age in R6/2 transgenic mice and littermate controls (LMC). Counts are taken from a one in three series of sections (therefore an approximate figure for the total number of BRN-2 reactive neurones in the PVN can be obtained by multiplying by three). Bars demonstrate the standard error of each population (ie. comparison of the number of cells per section per PVN). No significant difference between transgene and LMC brains was observed, Students t-test providing a value of $P=0.392$ ($P>0.05$). Weaker immunoreactivity of BRN-2 in transgenic PVN appears to be due to reduced expression of the protein as opposed to cell loss. Number of brains (N) = 2.

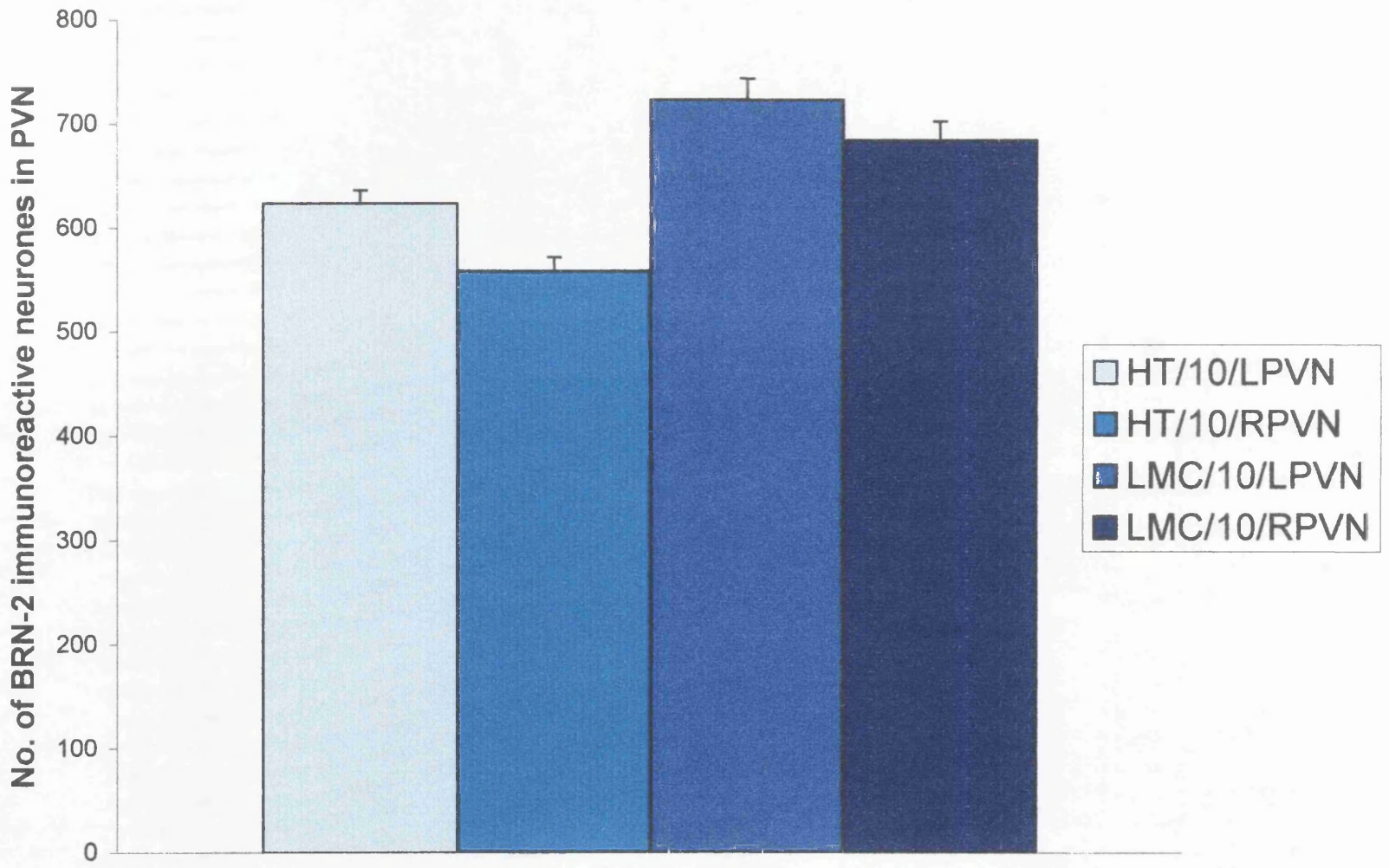
No. of BRN-2 immunoreactive neurones in PVN
800
700
600
500
400
300
200
100
0
HT/10/LPVN
HT/10/RPVN
LMC/10/LPVN
LMC/10/RPVN

Figure. 3.5/G2

Total cell number of Vasopressin (VP) immunoreactive neurones of the PVN in LMC and R6/2 transgenes at 10 weeks of age from 20 micrometre sections

The graph opposite illustrates the Abercrombie corrected total numbers of vasopressin immunoreactive neurones at 10 weeks of age in R6/2 transgenic mice and littermate controls (LMC). Counts are taken from a one in three series of sections (therefore an approximate figure for the total number of vasopressin reactive neurones in the PVN can be obtained by multiplying by three). Bars demonstrate the standard error of each population (ie. comparison of the number of cells per section per PVN). No significant difference between transgene and LMC brains was observed, Students t-test providing a value of $P=0.542$ ($P>0.05$). It is interesting to note that fewer nuclei in the PVN are vasopressin immunoreactive than BRN-2 reactive. Number of brains (N) = 2, number of sections counted per brain = 12.

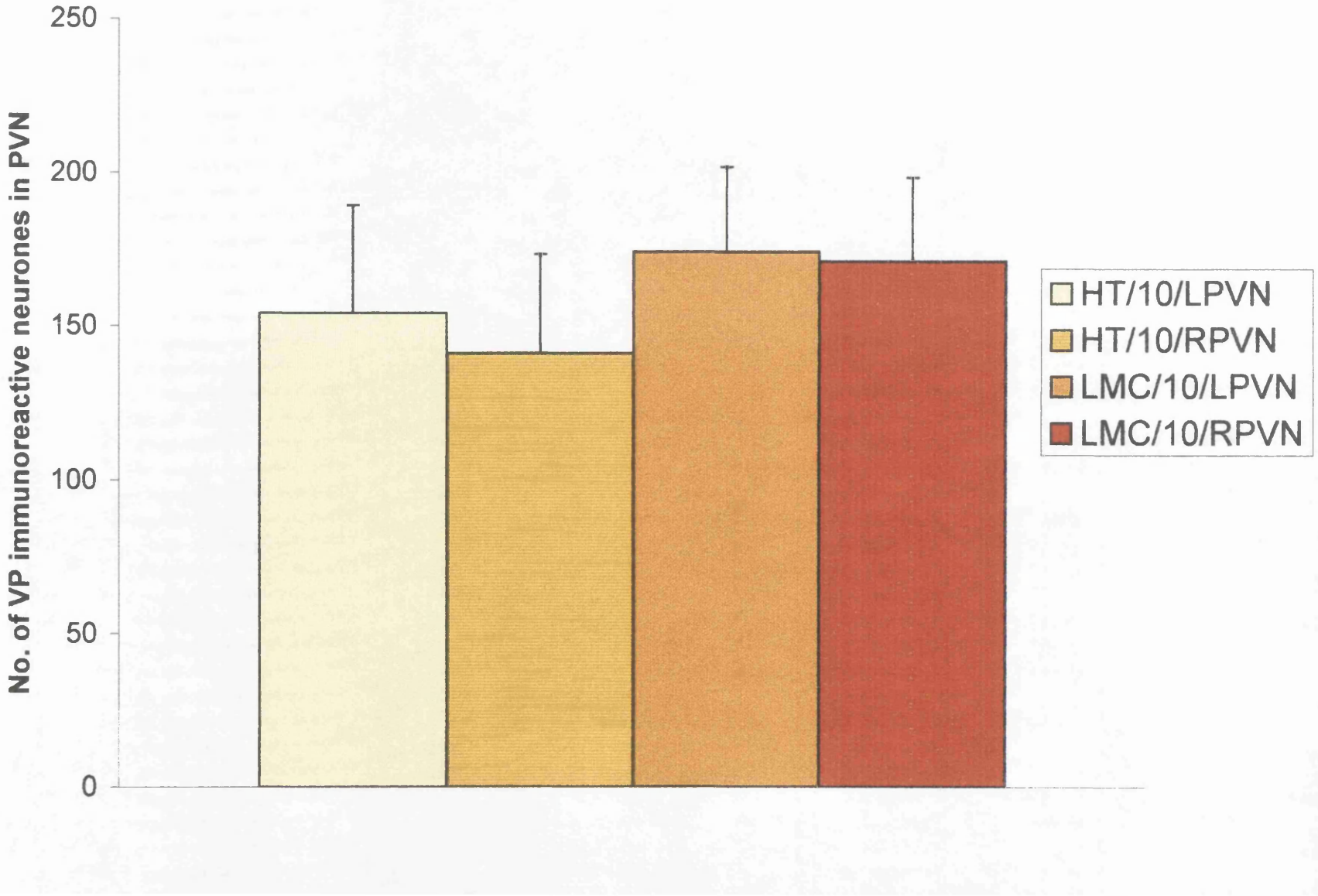
No. of VP immunoreactive neurones in PVN
250
200
150
100
50
0
HT/10/LPVN
HT/10/RPVN
LMC/10/LPVN
LMC/10/RPVN

Figure. 3.5/G3

Mean cell number of BRN-2 immunoreactive nuclei of PVN neurones in LMC and R6/2 transgenes at 12 weeks of age from 40 micrometre sections

The graph opposite illustrates the Abercrombie corrected total numbers of BRN-2 immunoreactive nuclei at 12 weeks of age in R6/2 transgenic mice and littermate controls (LMC). Counts are taken from a one in three series of sections. Bars demonstrate the standard error of each population (ie. comparison of the mean number of cells per PVN per brain). No significant difference between transgene and LMC brains was observed, Students t-test providing a value of $P= 0.0943$ ($P>0.05$). Number of brains (N) =5.

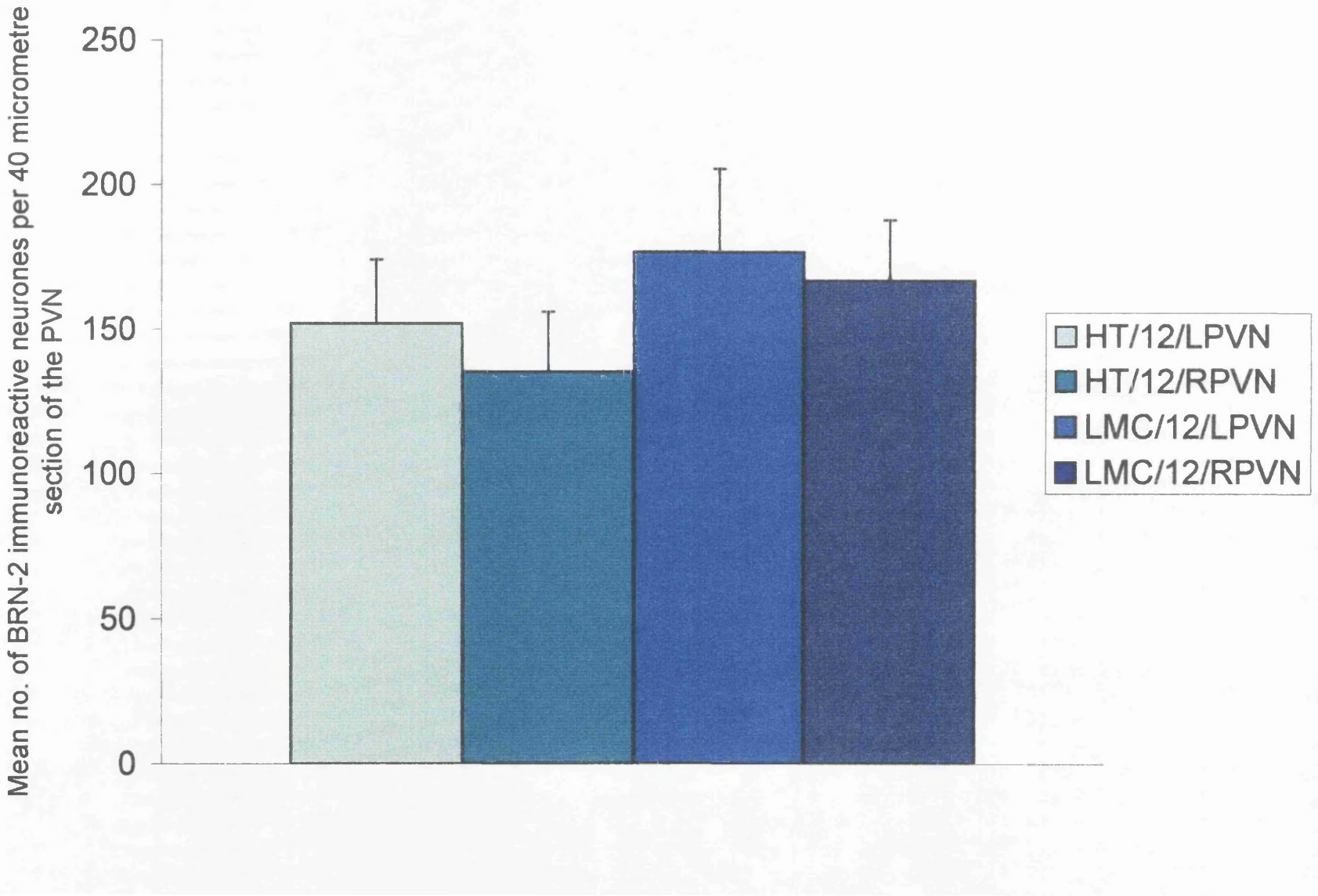
Mean no. of BRN-2 immunoreactive neurones per 40 micrometre section of the PVN
250
200
150
100
50
0
HT/12/LPVN
HT/12/RPVN
LMC/12/LPVN
LMC/12/RPVN

3.6 EXPRESSION OF TATA BINDING PROTEIN, BRN-2 AND GLUCOCORTICOID RECEPTOR IN HUNTINGTON R6/2 TRANSGENIC MICE

The GR antibody (M-20) recognises a protein of ~80 kD upon western blot. This protein band could be abolished by pre-incubating the antibody to the peptide immunogen to which it was raised (Fig.3.6/1A). In comparing littermate control and R6/2 transgenic mouse striatum, cortex and cerebellum from transgenes at the age of 11 or 13 weeks, no significant difference could be observed or detected after densitometric analysis of the protein bands (Fig.3.6/1A, Fig, 3.6/G1). This is consistent with GR immunocytochemistry.

All TBP antibodies (N-12/SC-204, Santa Cruz) and 2C1, 3G3 and 4C2 (Lazlo Tora) demonstrated a protein band at close to 40 kD, the approximate weight of the TBP protein. The antibodies 2C1, 3G3 and 4C2 also recognised multiple bands at various molecular weights making analysis very difficult to interpret. Purified TBP was not available to conduct control experiments. However, pre-incubation of the SC-TBP antibody to the peptide immunogen to which it was raised resulted in abolition of the 40 kD band when incubated with the filter. However, densitometric scanning of the protein band at 40 kD recognised by any antibody, which is close to the identified weight of the TBP protein (37 kD) demonstrated no significant difference between transgenic or control striatum, cortex or cerebellum (Fig.3.6/2, Fig.3.6/G3).

The BRN-2 antibody identified two proteins at very similar molecular weights, both at approximately 80 kD, the molecular weight expected for BRN-2 (Fig.3.6/1B). Both protein bands could be abolished by pre-incubating the antibody to the peptide immunogen to which it was raised. Densitometric analysis of both protein bands demonstrated no difference in protein levels between R6/2 transgene and control striatum, cortex and cerebellum, which is consistent with immunocytochemistry (Fig.3.6/G2). Due to the small size of the structure and the number of brains that would be needed, it was unrealistic to conduct BRN-2 antibody PAGE analysis on PVN tissue.

Figure. 3.6/1

GR and BRN-2 protein expression (PAGE) in littermate controls and huntingtin R6/2 transgenes (11 weeks old)

(A) (Left)Western blot showing GR protein expression in control in littermate control striatum, cerebellum and cortex (CS, CCB, CCX) and R6/2 transgenic mouse striatum, cerebellum and cortex from 11 week old animals (HS, HCB, HCX). One clear protein band correlating to the molecular weight of the glucocorticoid receptor protein can be visualised. Optical densitometry revealed no significant difference between control animals and transgenes, although it is interesting to note an apparent increase of expression in the transgenic striatum. The protein band recognition could be abolished by pre-incubating the antibody to the peptide immunogen to which it was raised (left), BCS = blocked LMC stiatum, BHS = blocked R6/2 striatum. Lower protein bands are presumed to be GR breakdown products since they too are abolished (10x peptide to antibody by weight, Santa Cruz). Antibody used Santa Cruz M-20 1:1000 dilution.

(B) (Right)Western blot showing BRN-2 protein expression in control in littermate control striatum, cerebellum and cortex (CS, CCB, CCX) and huntingtin transgene striatum, cerebellum and cortex from 11 week old animals (HS, HCB, HCX). Two protein bands, both at approximately 80 kD, the expected molecular weight of the BRN-2 protein can be observed. Optical densitometry revealed no significant difference between control animals and transgenes although appearances of single bands upon individual blots varied. Both proteins could be abolished by pre-incubating the antibody with the peptide to which it was raised (left), BCS = blocked LMC stiatum, BHS = blocked R6/2 striatum. Antibody used Santa Cruz C-20 1:1000 dilution.

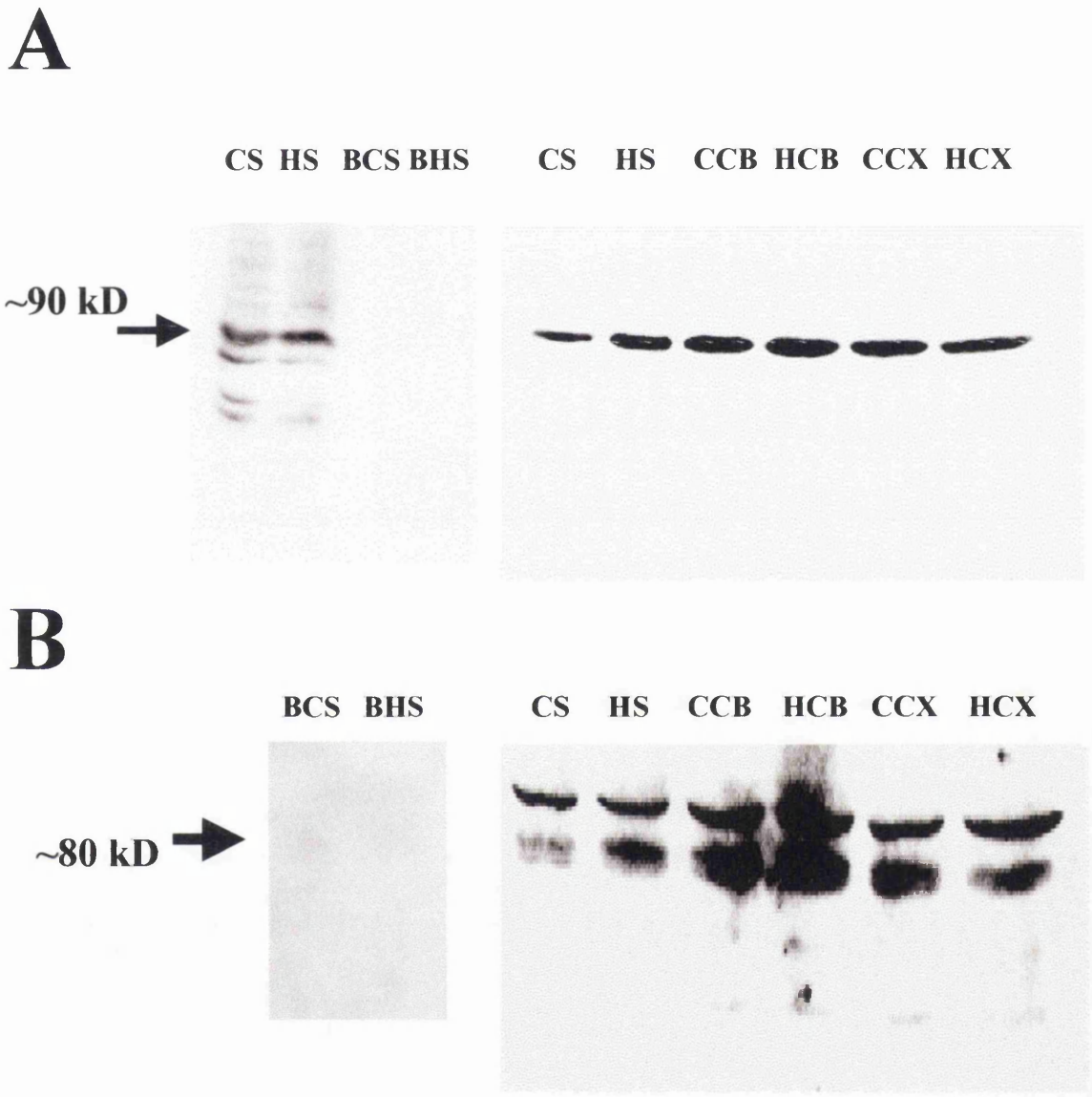
A
CS HS BCS BHS
CS HS CCB HCB CCX HCX
~90 kD
B
BCS BHS
CS HS CCB HCB CCX HCX
~80 kD

Figure. 3.6/G1

Densitometric analysis of GR protein expression (PAGE) in littermate controls and huntingtin R6/2 transgenes (11 weeks old)

The graph opposite illustrates the protein expression GR in mean arbitrary densitometric units (ADU) in 11week old R6/2 transgenes and littermate control mice. No significant difference was observed between controls and transgenic mice in the striatum, cerebellum and cortex using Student's two-tailed t-test. Number of brains (N) = 3 per experiment, pooled as groups of three (experiment conducted three times). Total N= 9.

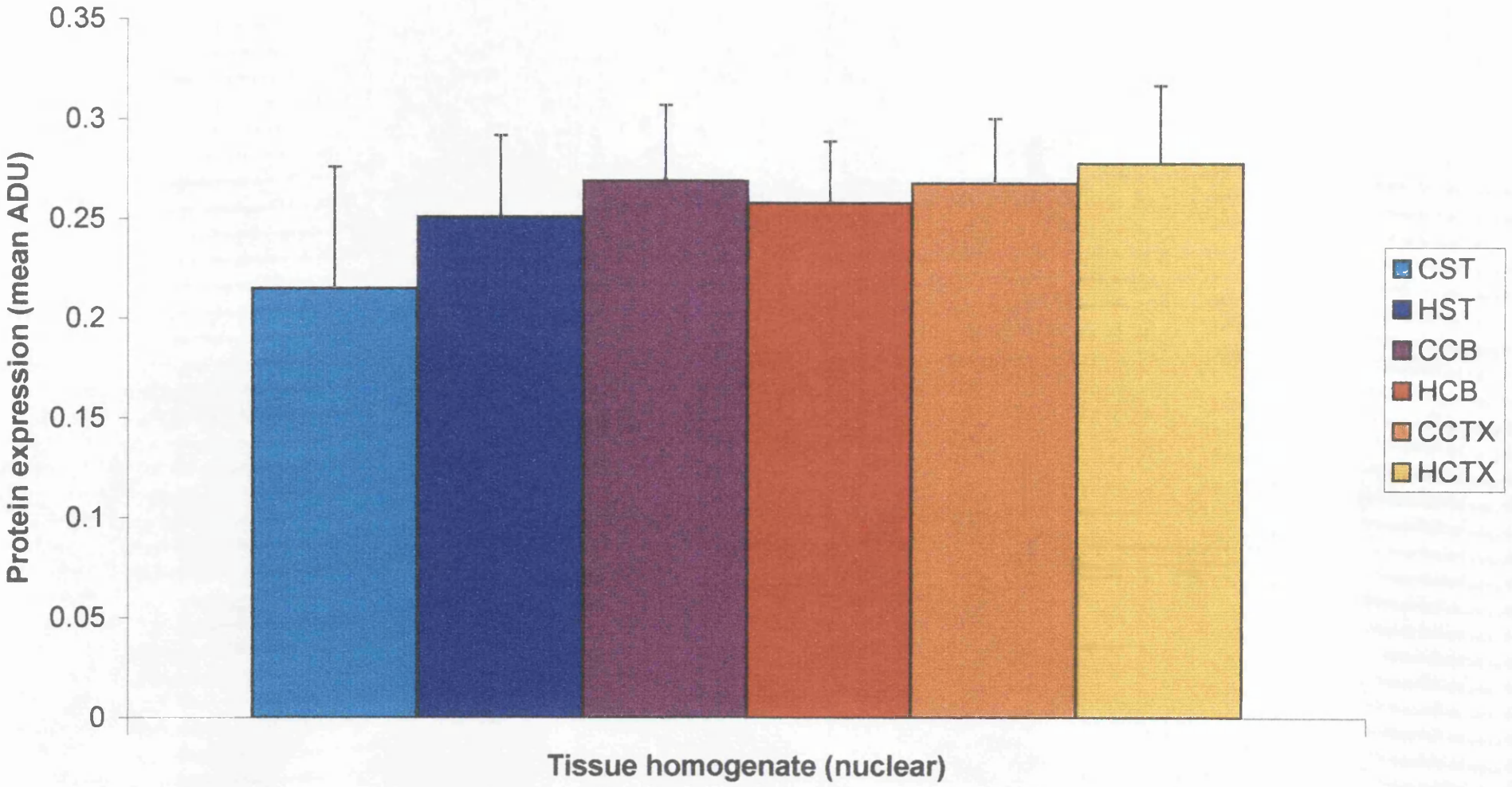
0.35
0.3
0.25
0.2
0.15
0.1
0.05
0
Protein expression (mean ADU)
Tissue homogenate (nuclear)
CST
HST
CCB
HCB
CCTX
HCTX

Figure. 3.6/G2

Densitometric analysis of BRN-2 protein expression (PAGE) in littermate controls and huntingtin R6/2 transgenes (11 weeks old)

The graph opposite illustrates the protein expression of BRN-2 in mean arbitrary densitometric units (ADU) in 11week old huntingtin transgenic mice and littermate control mice. No significant difference was observed between controls and transgenes in the striatum, cerebellum and cortex using Student's two-tailed t-test. Number of brains (N) = 3 per experiment, pooled as groups of three (experiment conducted three times). Total N= 9.

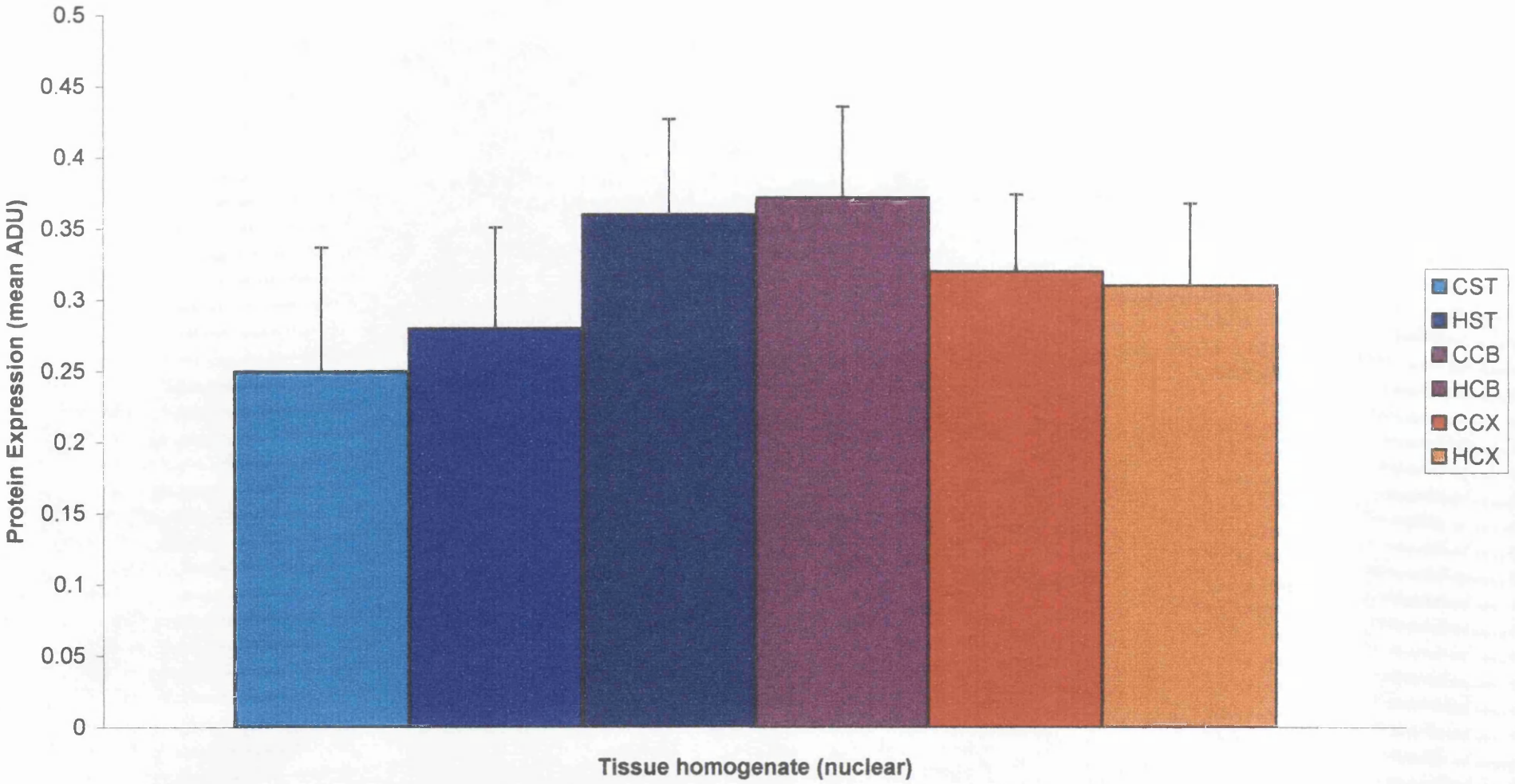
0.5
0.45
0.4
0.35
0.3
0.25
0.2
0.15
0.1
0.05
0
Protein Expression (mean ADU)
Tissue homogenate (nuclear)
CST
HST
CCB
HCB
CCX
HCX

Figure. 3.6/2

TBP protein expression (PAGE) in littermate controls and R6/2 transgenes (11 weeks old)

Western blots showing TBP protein expression in control in littermate control striatum, cerebellum and cortex (CS, CCB, CCX) and R6/2 transgene striatum, cerebellum and cortex from 11 week old animals (HS, HCB, HCX). A range of polyclonal antibodies raised to the TFIID subunit/TBP protein (Santa Cruz N-12 SC-204, or 2C2, 3G3, and 4C2, courtesy of Dr. Laslo Tora) were employed. A 40 kD protein band correlating approximately to the molecular weight of the mammalian TFIID/TBP protein (the polyglutamine containing protein) can be visualised with all antibodies used. Optical densitometry of the protein recognised by the Santa Cruz antibody revealed no significant difference between expression of this suspected TFIID protein in control animals and transgenes. The blocking experiment demonstrates abolition of the 40 kD protein recognised by the SC-204 antibody when exposed to control, (CS) and R6/2, (H) striatal nuclear homogenate after pre-incubation with the peptide to which the antibody was raised. CS1/HS1 demonstrate 20x by weight (peptide to antibody) and CS2/HS2 10x.

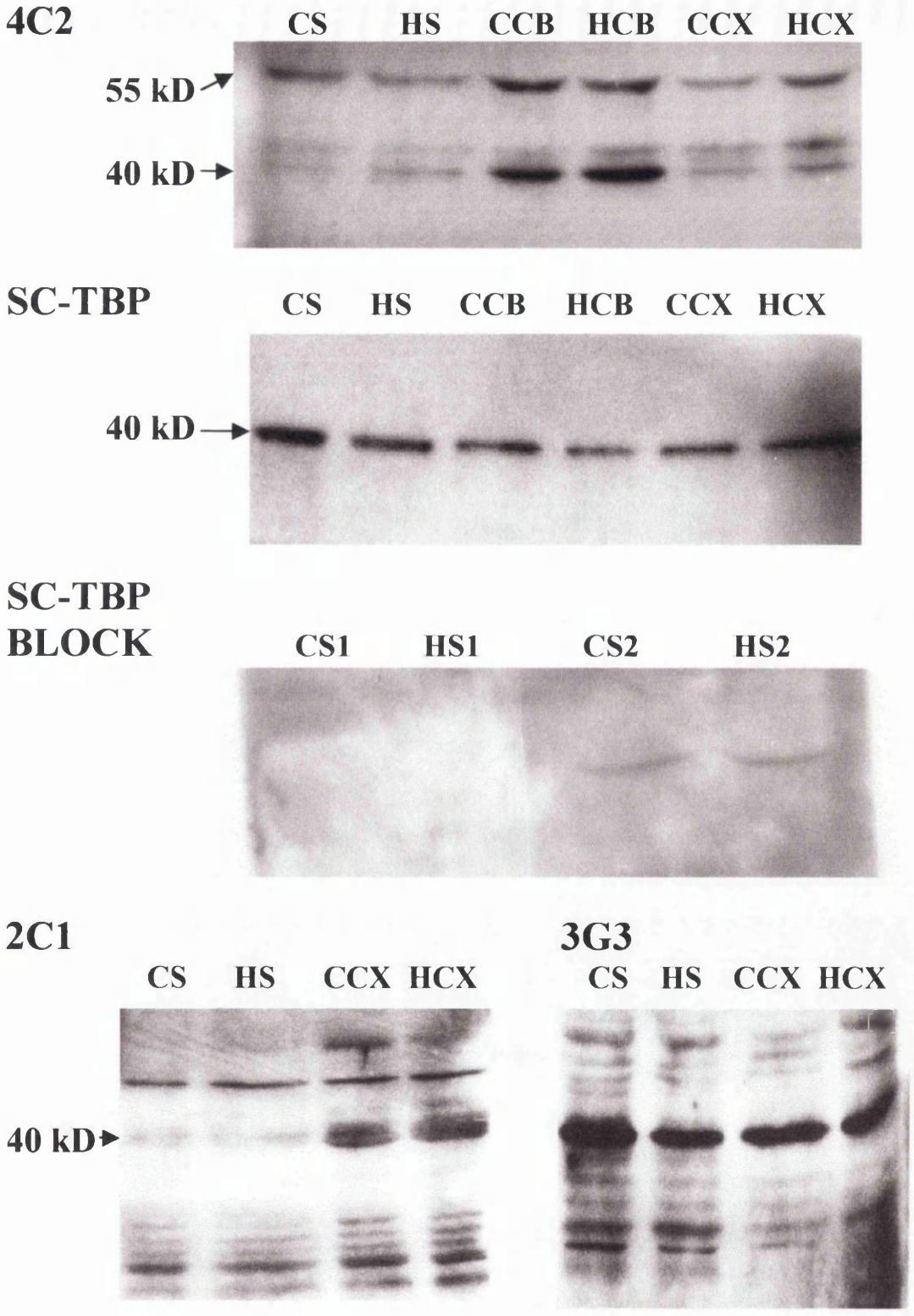
4C2
CS
HS
CCB
HCB
CCX
HCX
55 kD
40 kD
SC-TBP
CS
HS
CCB
HCB
CCX
HCX
40 kD
SC-TBP
BLOCK
CS1
HS1
CS2
HS2
2C1
CS
HS
CCX
HCX
40 kD
3G3
CS
HS
CCX
HCX

Figure. 3.6/G3

Densitometric analysis of TBP protein expression (PAGE) in littermate controls and huntingtin R6/2 transgenes (11 weeks old)

The graph opposite illustrates the protein expression of TBP in mean arbitrary densitometric units (ADU) in 11 week old R6/2 transgenes and littermate control mice. This protein was detected using the Santa Cruz N-12 SC-204 antibody at 1:1000 dilution). No significant difference was observed between controls and transgenes in the striatum, cerebellum and cortex using Student's two-tailed t-test. Number of brains (N) = 3 per experiment, pooled as groups of three (experiment conducted three times). Total N= 9.

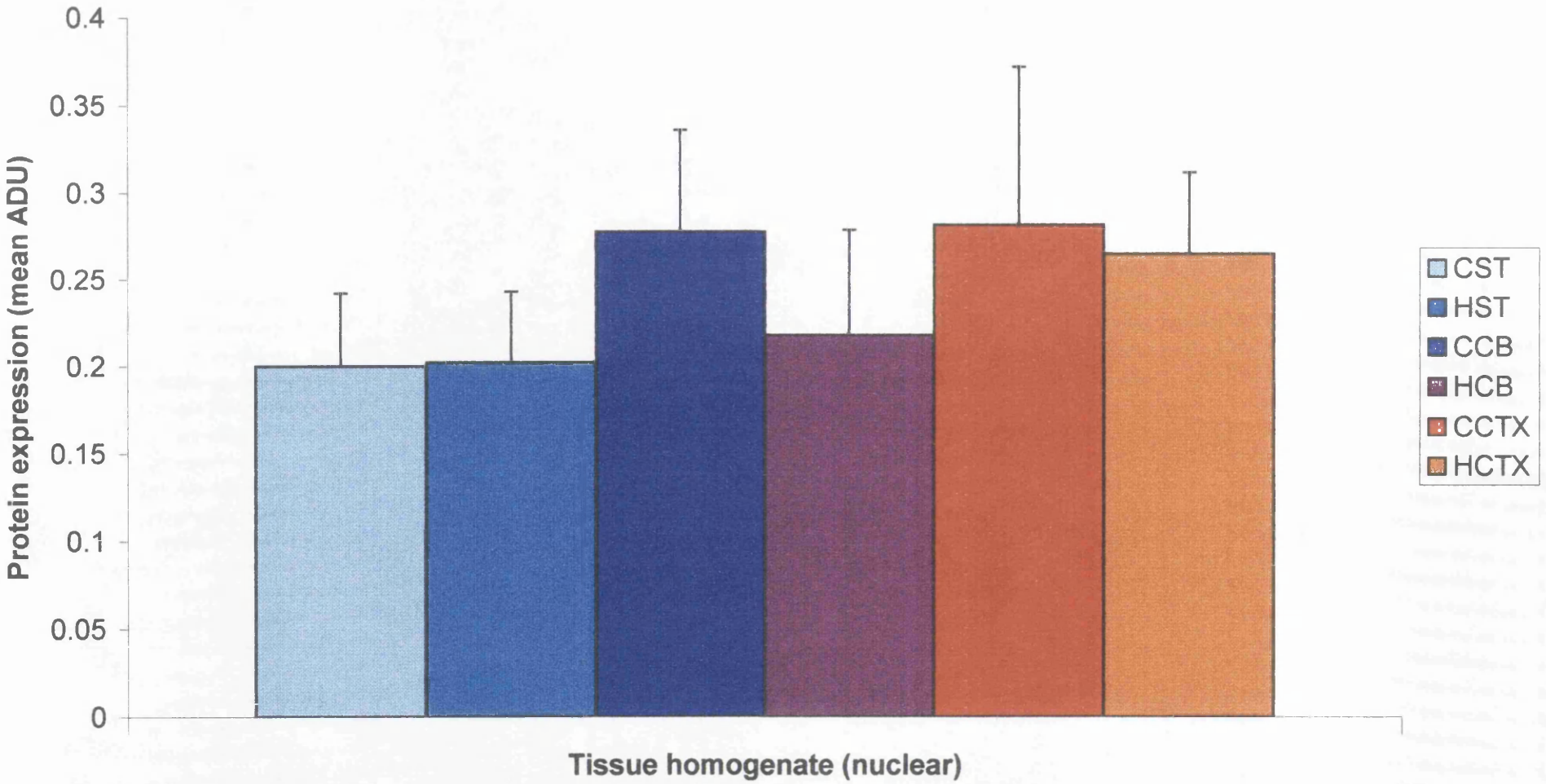
0.4
0.35
0.3
0.25
0.2
0.15
0.1
0.05
0
Protein expression (mean ADU)
Tissue homogenate (nuclear)
CST
HST
CCB
HCB
CCTX
HCTX

3.7 PROTEIN BINDING TO POLYGLUTAMINE TRANSCRIPTION FACTOR CONSENSUS SITE DNA IN R6/2 TRANSGENIC MICE

EMSA of littermate control and R6/2 transgenic mouse striatum, cortex and cerebellum using the glucocorticoid receptor consensus site oligonucleotide (Promega) 5'..GAC CCT AGA GGA TCT GTA CAG GAT GTT CTA GAT.. 3' produced a major binding complex which could be totally abolished when 10x unlabelled oligonucleotide was added (Fig. 3.7/1A). Furthermore, when 10x of an unrelated oligonucleotide was added (SP-1 consensus site, Promega), the binding complex was not disrupted (Fig. 3.7/1B). The binding complex was not clearly defined and was difficult to analyse visually. However, when subjected to densitometric analysis, no significant difference in protein-DNA binding could be detected in the major binding complex (Fig.3.7/G1). Occasionally much weaker bands much heavier and lighter than the main complex could be visualised (Y&Z, Fig.3.7/1A&B), but their variable nature made it difficult to carry out further analysis. Whenever a blocking experiment was conducted with GR oligonucleotide, these bands were also abolished, but as they were very often not present, even with a dark major complex, their nature remains elusive.

EMSA of control and transgenic tissue using the TBP consensus oligonucleotide (Promega) 5'... GCA GAG CAT ATA AGG TGA GGT AGG A...3' produced two, possibly three binding complexes, two which together are usually indistinguishable and form a major binding complex (Band 2 Fig. 3.7/2 A,B & C) and a smaller but much heavier complex, more variable in presence than the major complex (Band 1, Fig3.7/2, A, B & C). The variability of presence of the heavier (1) complex made it difficult to visualise any consistent pattern and only by repetition and densitometric analysis could it be determined that no significant difference in protein-DNA binding could be detected between any transgenic or control tissue (Fig.3.7/G2). Control experiments determined that addition of 20x unlabelled TBP oligonucleotide abolished all binding complexes (Fig. 3.7/2B) and addition of 10x of an unrelated consensus site oligonucleotide (SP-1, Promega) did not alter any of the binding complexes (Fig.3.7/2A).

EMSA using the OCT consensus sequence (Promega) 5'... TGT CGA ATG CAA ATC ACT AGA A ..3' to which BRN-2 is known to bind revealed three binding

complexes (OCT1, OCT 2 and N-OCT 3/BRN-2). This banding pattern has been reported before (See introduction). All three binding complexes could be abolished with addition of 10x unlabelled OCT consensus oligonucleotide (Fig.3.7/3&4), demonstrating specifity.

Visual inspection and denstiometric analysis revealed a striking difference between protein-DNA binding between control and transgenic tissue (Fig.3.7/3&4). Initially, it appeared upon visual inspection that the OCT-3 binding complex displayed increased DNA binding in striatum, cerebellum and cortex of transgenic brain. However, as the data population grew, densitometric analysis revealed that there was no significant difference in protein-DNA binding in striatal and cerebellar tissue samples when control tissue was compared to transgene (Fig.3.7/G3). However, a highly significant difference between control and transgenic protein-DNA binding was observed in cortex. OCT-3 binding complex density was increased in transgenic cortex (Fig3.7/G3). As more cortical samples were obtained, this was further confirmed. Also of interest is the presence of the heavier complexes, OCT 1 and OCT 2. Cortical samples generally revealed a much reduced presence of OCT 1 and OCT 2 complexes (whether control or transgene) when compared to striatal and cerebellar samples (Fig. 3.7/ 3&4, A Fig.3.7/G3).

Figure. 3.7/1

Electrophoretic mobility shift assay (EMSA) of littermate control and R6/2 transgene striatal, cerebellar and cortical nuclear preparation in 11 week old mice using glucocorticoid receptor (GR) consensus oligonucleotide.

(A) (left) Specificity of protein-DNA binding is observed by abolition of the protein-DNA binding complex when a LMC striatum sample is run and diluted along with 10x unlabelled GR oligonucleotide (B10x). The following lanes are LMC and R6/2 transgene striatum (CS/HS), cerebellum (CC/HC) and cortex (CCX/HCX). One major binding complex can be observed and is labelled 'GR' and marked with an arrow (far left). (Right) The specifity of the protein binding to the GR oligonucleotide is demonstrated by the retention of the DNA binding complex when 10x unlabelled SP-1 oligonucleotide is run along with labelled GR oligonucleotide and protein (CST (10x) =SP-1 present, CST (-) = SP-1 absent.

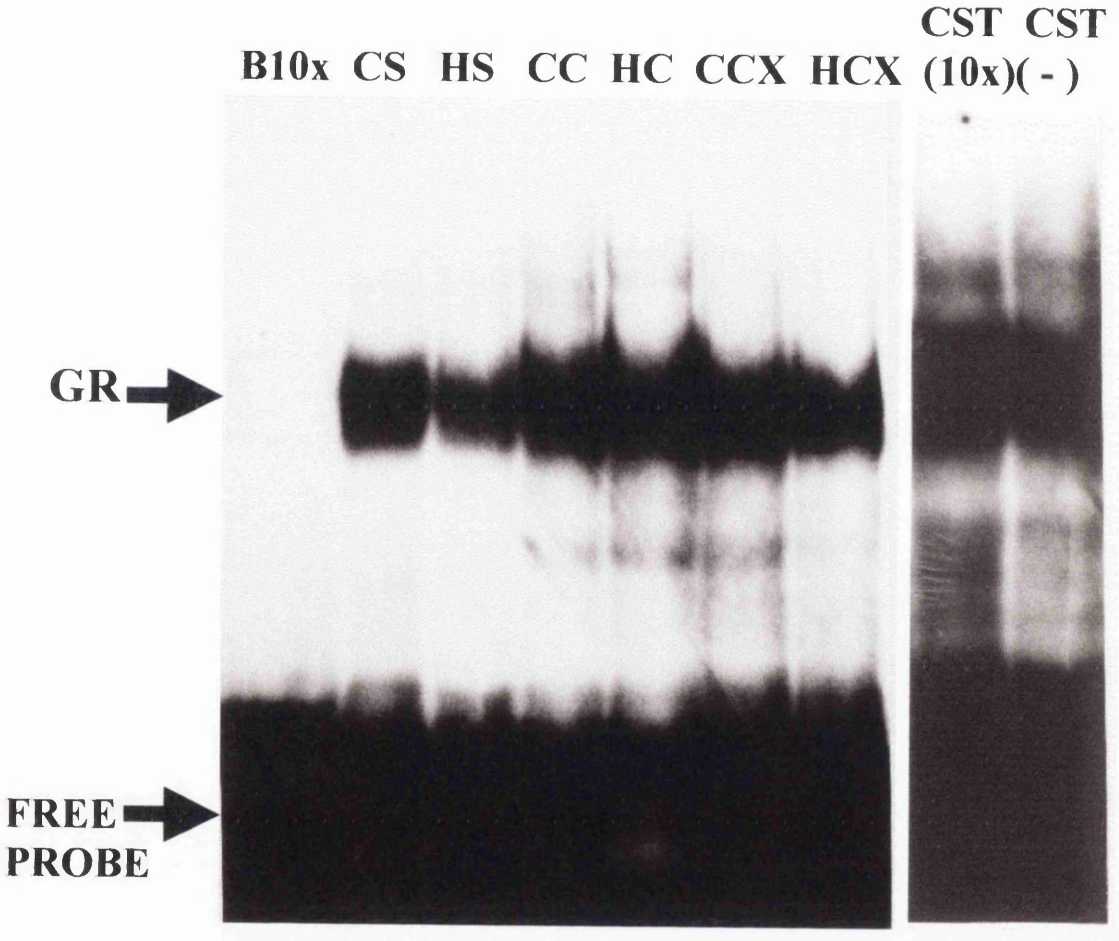
B10x
CS
HS
CC
HC
CCX
HCX
CST (10x)
CST (-)
GR
FREE PROBE

Figure. 3.7/G1

Densitometric analysis of protein binding in the striatum to glucocorticoid receptor oligonucleotide in 11 week old littermate control (LMC) and HD transgenic mouse striatum, cortex and cerebellum.

The graph opposite illustrates DNA-protein binding in mean arbitrary densitometric units (ADU) in LMC and transgene brain. Tissue type is displayed in the key to the right (CST/HST= control/transgene striatum, CCB/HCB = control/ transgene cerebellum, CCTX/HCTX = control/ transgene cortex). Bars demonstrate the standard error of each population from which the mean value was obtained. Densitometric analysis and Student's two-tailed t-test reveal no significant difference in DNA binding between control and HD transgene brains in each brain region. Number of brains (N) = 6 per brain region, pooled as groups of three, EMSA run three times for each group. All binding complexes scanned and mean value taken.

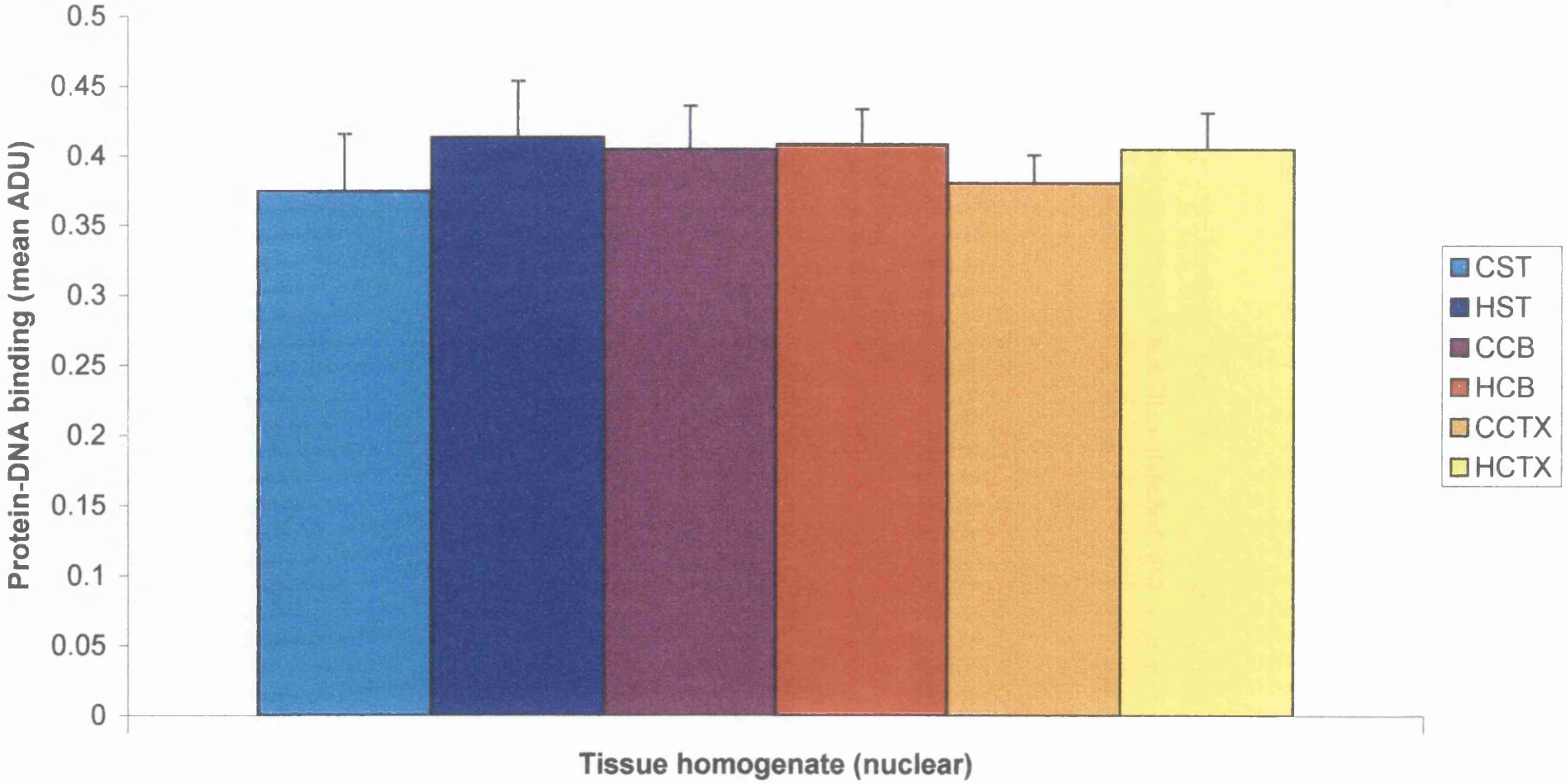
0.5
0.45
0.4
0.35
0.3
0.25
0.2
0.15
0.1
0.05
0
Protein-DNA binding (mean ADU)
Tissue homogenate (nuclear)
CST
HST
CCB
HCB
CCTX
HCTX

Figure. 3.7/2

Electrophoretic mobility shift assay (EMSA) of litter mate control and HD transgene striatal, cerebellar and cortical nuclear preparation in 11 week old mice using TBP consensus oligonucleotide.

(A) The specificityof the protein binding to the TBP oligonucleotide is demonstrated by the retention of the DNA binding complex when 10x unlabelled SP-1 oligonucleotide is run along with labelled TBP oligonucleotide and protein (CST (10x) =SP-1 present, CST (-) = SP-1 absent.

(B) Specificity of protein-DNA binding is observed by abolition of the protein-DNA binding complex when a LMC striatum sample is run and diluted along with 20x unlabelled TBP oligonucleotide [CST(20x)].

(C)The following lanes are LMC and R6/2 transgene striatum (CS/HS), cerebellum (CC/HC) and cortex (CCX/HCX). Two binding complexes can be observed and are labelled 1 (minor high molecular weight complex) and 2 (major low molecular weight complex) marked with an arrows (far left).

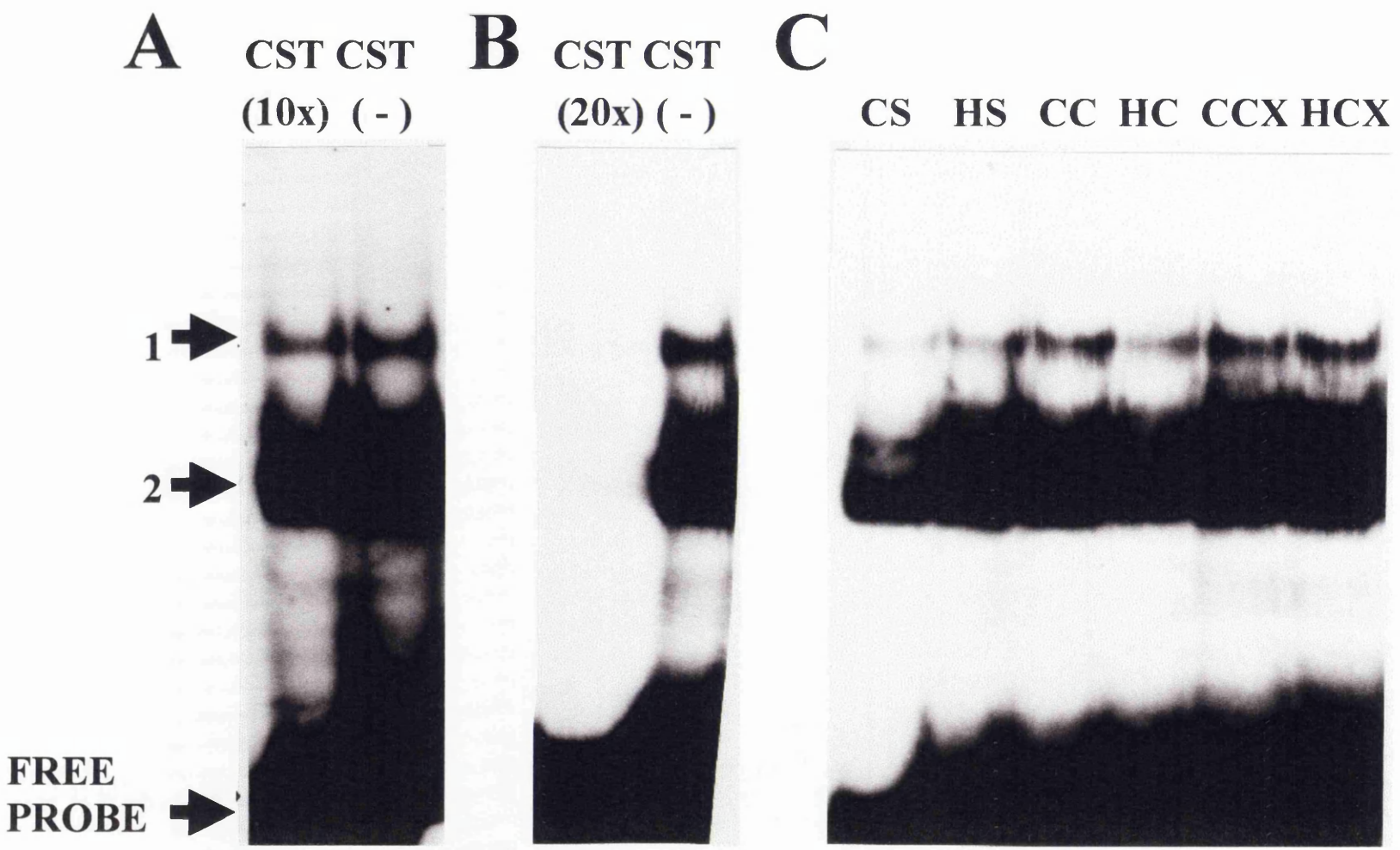
A
CST CST
(10x) (-)
B
CST CST
(20x) (-)
C
CS HS CC HC CCX HCX
1
2
FREE
PROBE

Figure. 3.7/G2A

Densitometric analysis of protein binding in the striatum to TBP oligonucleotide (minor high molecular weight complex) in 11 week old littermate control (LMC) and R6/2 transgenic mouse striatum, cortex and cerebellum.

The graph opposite illustrates DNA-protein binding in mean arbitrary densitometric units (ADU) in LMC and R6/2 transgene brain in the minor high molecular weight complex (band 1) observed with TBP oligonucleotide. Tissue type is displayed in the key to the right (CST/HST= control/transgene striatum, CCB/HCB = control/ transgene cerebellum, CCTX/HCTX = control/ transgene cortex). Bars demonstrate the standard error of each population from which the mean value was obtained. Densitometric analysis and Student's t-test reveal no significant difference in DNA binding between control and HD transgene brains in each brain region. Number of brains (N) = 6 per brain region, pooled as groups of three, EMSA run three times for each group. All binding complexes (6) scanned and mean value taken.

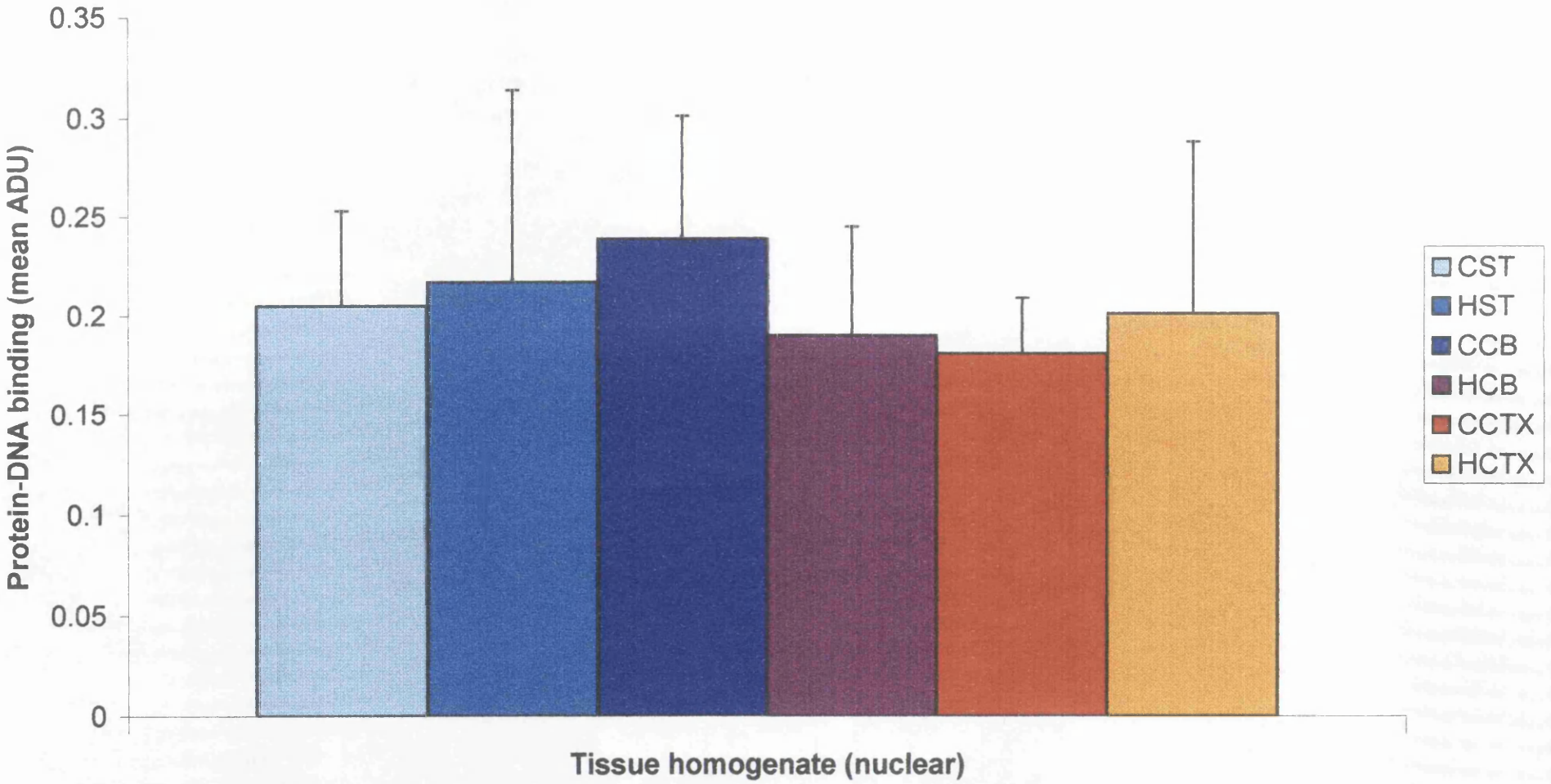
0.35
0.3
0.25
0.2
0.15
0.1
0.05
0
Protein-DNA binding (mean ADU)
Tissue homogenate (nuclear)
CST
HST
CCB
HCB
CCTX
HCTX

Figure. 3.7/G2B

Densitometric analysis of protein binding in the striatum to TATA binding protein (TBP) oligonucleotide (major low molecular weight complex) in 11 week old littermate control (LMC) and R6/2 transgenic mouse striatum, cortex and cerebellum.

The graph opposite illustrates DNA-protein binding in mean arbitrary densitometric units (ADU) in LMC and R6/2 transgenic brain in the major low molecular weight complex (band 2) observed with TBP oligonucleotide. Tissue type is displayed in the key to the right (CST/HST= control/transgene striatum, CCB/HCB = control/ transgene cerebellum, CCTX/HCTX = control/ transgene cortex). Bars demonstrate the standard error of each population from which the mean value was obtained. Densitometric analysis and Student's t-test reveal no significant difference in DNA binding between control and HD transgene brains in each brain region. Number of brains (N) = 6 per brain region, pooled as groups of three, EMSA run three times for each group. All binding complexes (6) scanned and mean value taken.

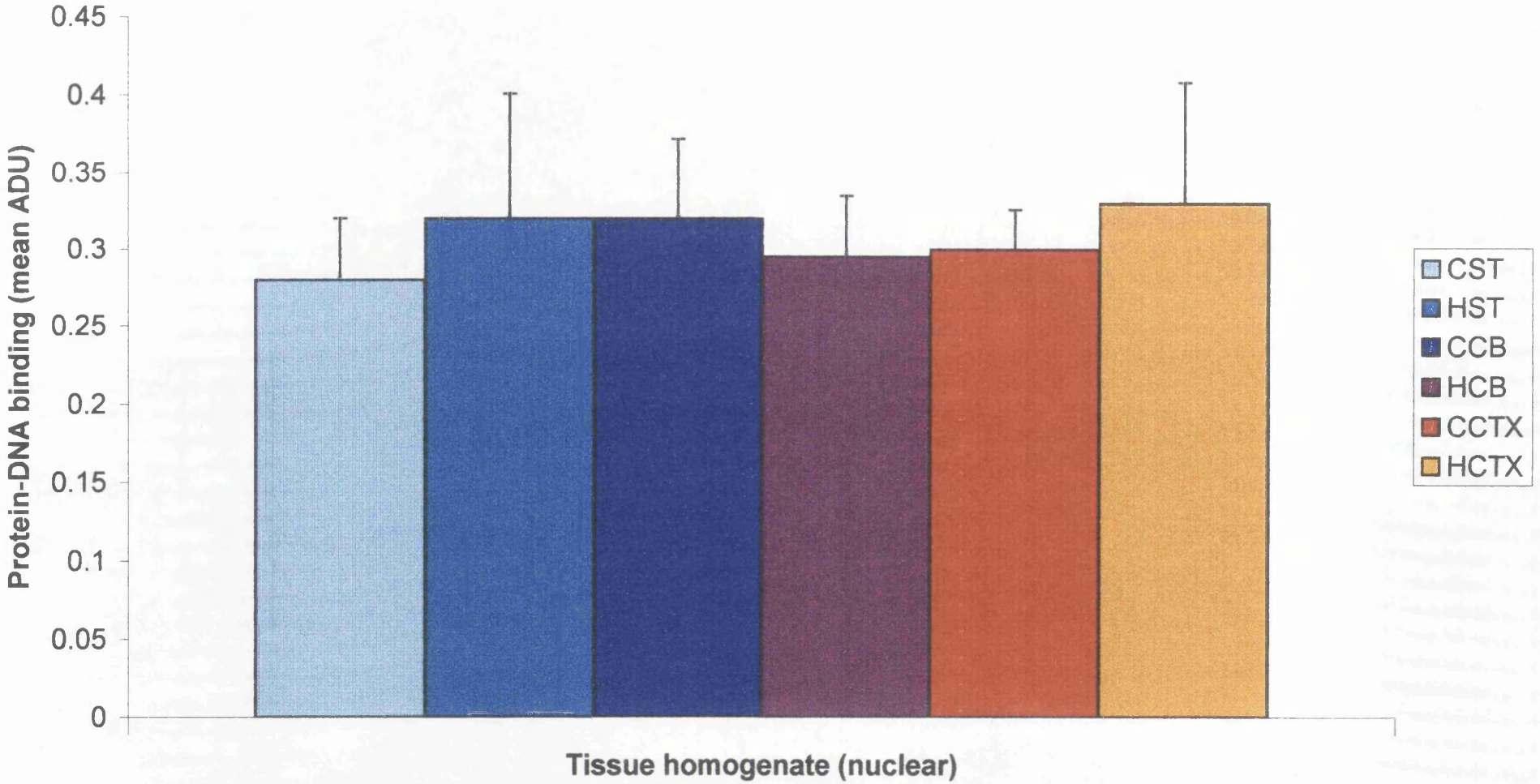
0.45
0.4
0.35
0.3
0.25
0.2
0.15
0.1
0.05
0
Protein-DNA binding (mean ADU)
Tissue homogenate (nuclear)
CST
HST
CCB
HCB
CCTX
HCTX

Figure. 3.7/G2C

Densitometric analysis of protein binding in the striatum to TBP oligonucleotide (low and high molecular weight complex, band 1 and 2) in 11 week old littermate control (LMC) and R6/2 transgenic mouse striatum, cortex and cerebellum.

This graph represents a three dimensional representation of the graphs 3.7/G2A & B, illustrating more clearly the expression relationship of the low and high molecular weight DNA binding complexes observed upon EMSA using the TBP oligonucleotide.

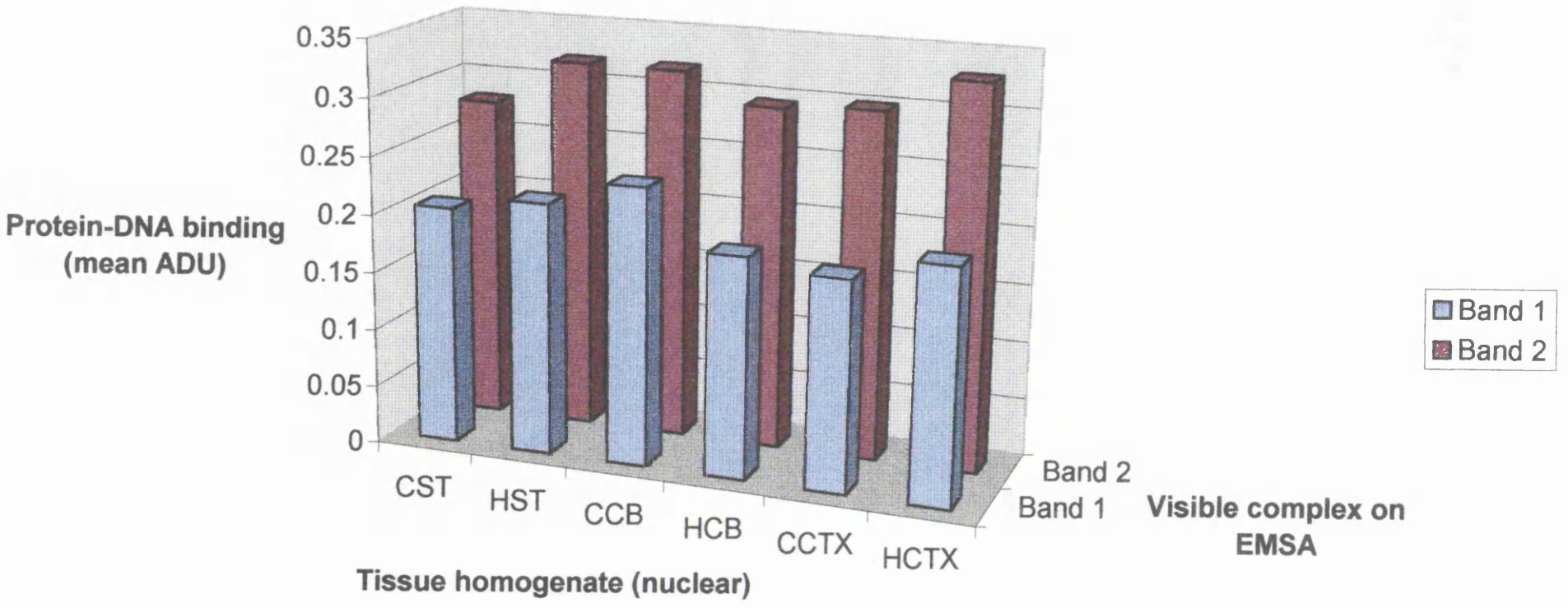
Protein-DNA binding
(mean ADU)
0.35
0.3
0.25
0.2
0.15
0.1
0.05
0
CST
HST
CCB
HCB
CCTX
HCTX
Tissue homogenate (nuclear)
Band 2
Band 1
Visible complex on
EMSA
Band 1
Band 2

Figure. 3.7/3A

Electrophoretic mobility shift assay (EMSA) of litter mate control and R6/2 transgene striatal, cerebellar and cortical nuclear preparations in 11 week old mice using the OCT consensus oligonucleotide.

(A) Specificity of protein-DNA binding is observed by abolition of the protein-DNA binding complex when a LMC striatum sample is run and diluted along with 10x unlabelled OCT oligonucleotide (B10x). The lane titles indicate control and transgenic striatum (CS/HS), cerebellum (CC/HC) and cortex (CX/HX). Two sets of cortical samples are visible upon this EMSA (X1 and X2). Increased band three density can be visualised in the transgenic cortical sample.

(B) Attempted 'supershift' experiment upon 11 week old transgenic mouse nuclear cortical sample using BRN-2 antibody. Abolition of band 3 (SHX2) can be observed when nuclear tissue homogenate is incubated with BRN-2 antibody prior to being exposed to radiolabelled oligonucleotide.


A
B10x
CS
HS
CC
HC
CX1
HX1
CX2
HX2
B
HX2
SHX2
1
2
3
FREE
PROBE

Figure. 3.7/3B

Electrophoretic mobility shift assay (EMSA) of litter mate control and R6/2 transgene striatal, cerebellar and cortical nuclear preparations in 11 week old mice using the OCT consensus oligonucleotide (2).

(A) Specificity of protein-DNA binding is observed by abolition of the protein-DNA binding complex when a LMC striatum sample is run and diluted along with 10x unlabelled OCT oligonucleotide (B10x). The lane titles indicate control and R6/2 transgenic striatum (CS/HS), cerebellum (CC/HC) and cortex (CX/HX). Two sets of cortical samples are visible upon this EMSA (X1 and X2). This EMSA, when compared to the one on the previous page, demonstrates the relative variability of density of the upper OCT bands (1 and 2). However, increased density of band three (BRN-2), can again be visualised in the transgenic cortical sample, this remaining relatively consistent and statistically significant. This EMSA more clearly demonstrates the apparent increase of BRN-2 DNA binding in transgenic striatum and cerebellum, when compared to littermate controls. This relationship does not appear to be significant, however.

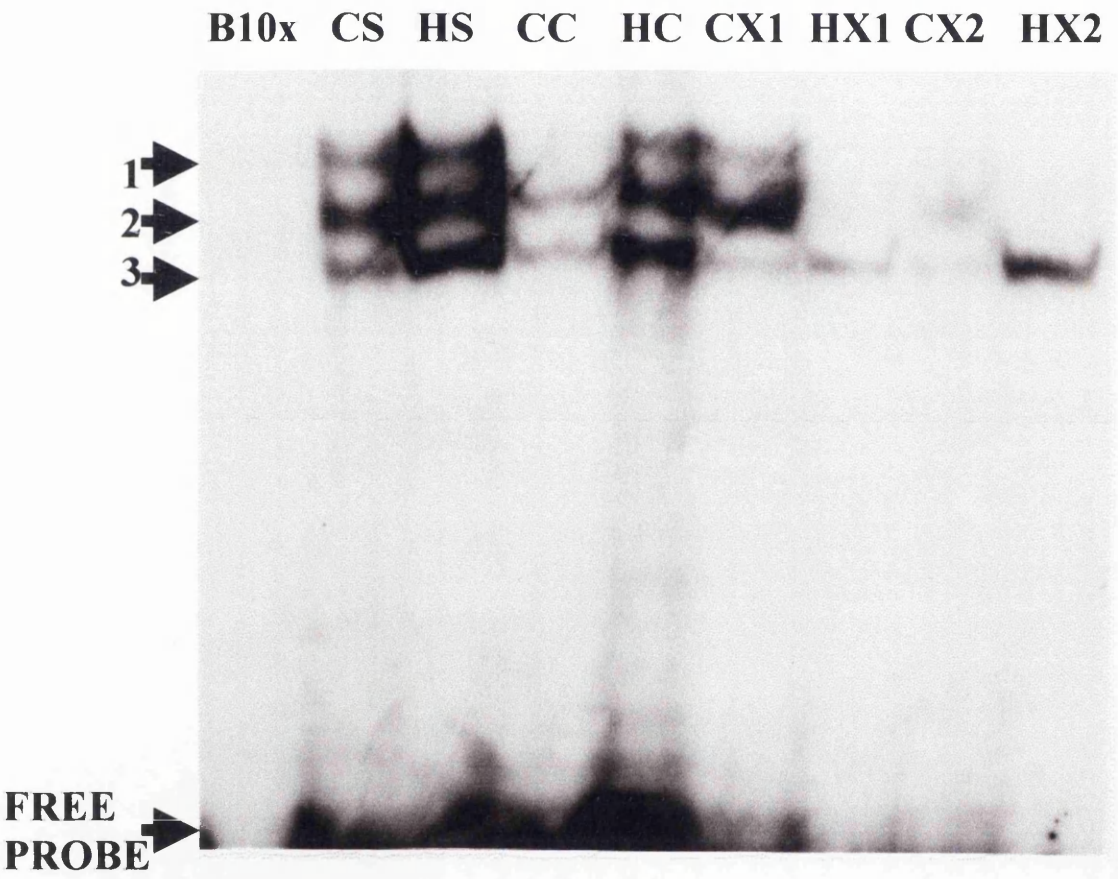
B10x
CS
HS
CC
HC
CX1
HX1
CX2
HX2
1
2
3
FREE
PROBE

Figure. 3.7/G3A

Densitometric analysis of protein binding in the striatum to OCT oligonucleotide (BAND 3) in 11 week old littermate control (LMC) and R6/2 transgenic mouse striatum, cortex and cerebellum.

The graph opposite illustrates DNA-protein binding in mean arbitrary densitometric units (ADU) in LMC and R6/2 transgene brain to the OCT consensus sequence oligonucleotide (Band 3). Tissue type is displayed in the key to the right (CST/HST= control/transgene striatum, CCB/HCB = control/ transgene cerebellum, CCTX/HCTX = control/ transgene cortex). Bars demonstrate the standard error of each population from which the mean value was obtained. Densitometric analysis and Student's t-test reveal a distinct significant difference in DNA binding between control and HD transgene cortex in band 3. P= ($P<0.005$) =highly significant. Number of brains (N) = 6 per brain region, pooled as groups of three, EMSA run three times for each group. All binding complexes (6) scanned and mean value taken.

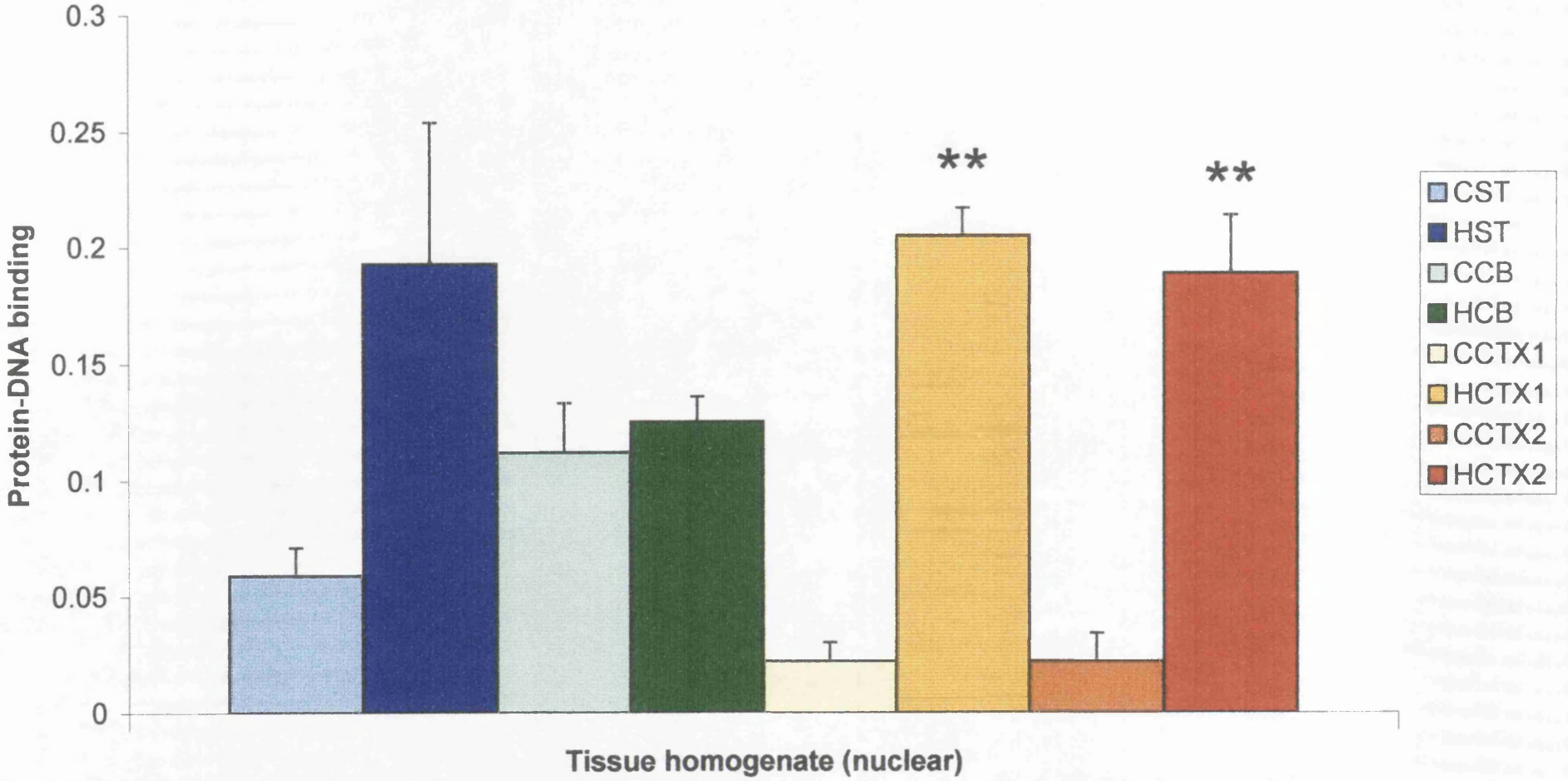
0.3
0.25
0.2
0.15
0.1
0.05
0
Protein-DNA binding
**
**
CST
HST
CCB
HCB
CCTX1
HCTX1
CCTX2
HCTX2
Tissue homogenate (nuclear)

Figure. 3.7/G3B

Densitometric analysis of protein binding in the striatum to OCT oligonucleotide (Bands 1, 2 and 3) in 11 week old littermate control (LMC) and R6/2 transgenic mouse striatum, cortex and cerebellum.

This graph represents a three dimensional representation of the OCT EMSAs (mean values) obtained from the 11 week old LMC and R6/2 mice and the graph of band three above (3.7/G3A), illustrating more clearly the expression relationship of all three DNA binding complexes observed upon EMSA.

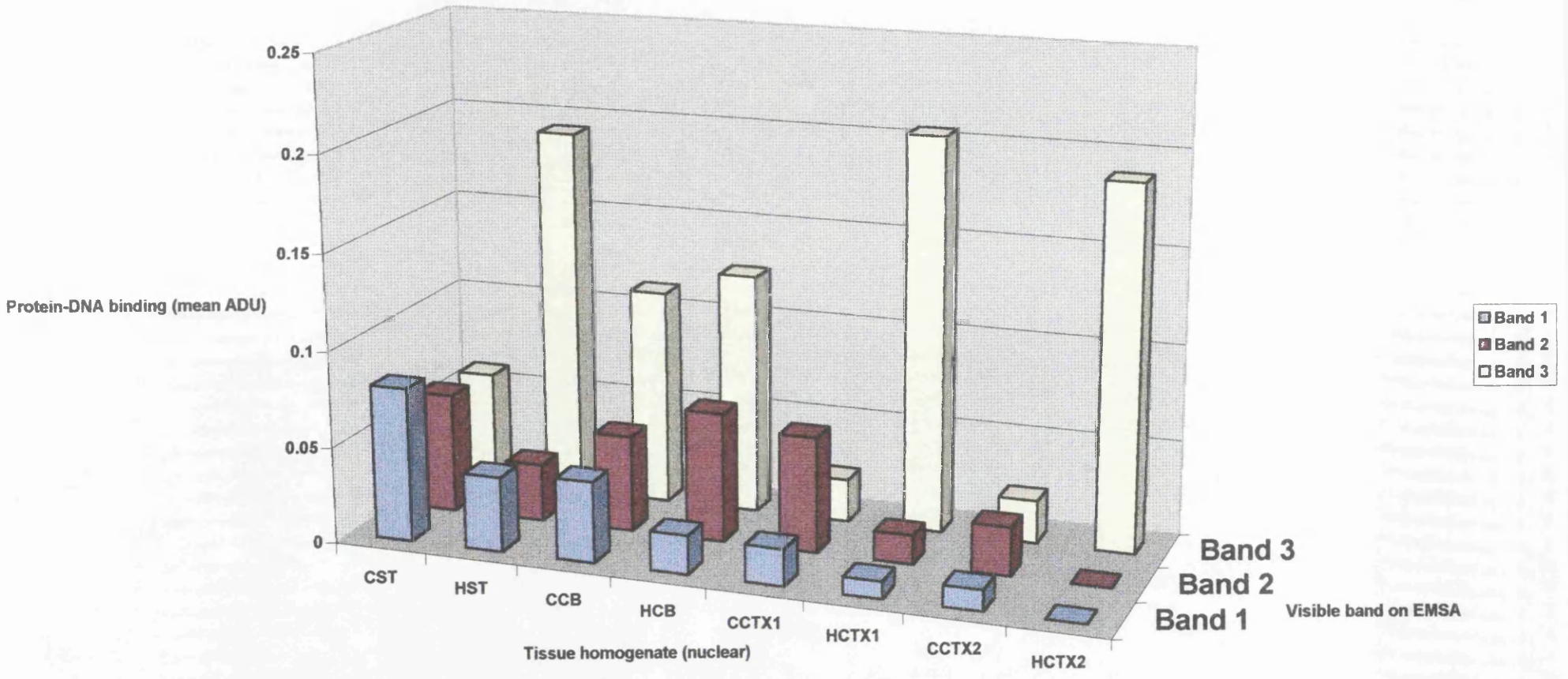
Protein-DNA binding (mean ADU)
0.25
0.2
0.15
0.1
0.05
0
CST
HST
CCB
HCB
CCTX1
HCTX1
CCTX2
HCTX2
Tissue homogenate (nuclear)
Band 3
Band 2
Band 1
Visible band on EMSA
Band 1
Band 2
Band 3

DISCUSSION

Introduction to CNTF and NF-κB studies

No detailed study of the NF-κB protein subunits present in the adult rat striatum (notably p65, p52 and p50) has previously been undertaken. This work has atttempted to determine the localisation and expression of each of these subunits and the overall DNA binding activity of NF-κB in the adult rat striatum (and other CNS regions), in both normal animals and following QA lesion or CNTF treatment. Further to this, a greater understanding of the exogenous activity of CNTF upon striatal neurones exposed to the excitotoxin QA, as well as the endogenous function of CNTF, was sought.

4.1 Ciliary Neurotrophic Factor

4.1A Exogenous action of CNTF in normal and QA lesioned rat striatum.

Although it has been previously been demonstrated that NF-κB can be activated by other, non-CNS specific cytokines such as interleukin-1 (Moynagh et al. 1993, Sparacio et al. 1992) and tumour necrosis factor (TNF) (Wood, 1995), research concerning its activation by CNTF, a nervous system specific cytokine involved in response to neural injury has been neglected. Prompted by the work outlined in the introduction indicating that CNTF may be protective in certain experimental neurodegenerative models (Carnow et al. 1985, Arakawa et al. 1990, Sendtner et al. 1990, Tolosano et al. 1996) and specifically in excitotoxic models of HD (Emerich et al. 1995, Anderson et al, 1996), it was attempted to establish the following. Would CNTF have any action upon the neurones and glia of the striatum following QA lesion? The work described in this thesis was conducted with particular reference to the survival of projection neurones and two defined classes of striatal interneurones, notably the cholinergic and NADPH-diaphorase positive cells. Furthermore this study further undertook to analyse any form of cellular response to the application of CNTF following QA lesion, by measuring the cell area of neuronal cell types, to reveal any change in the somal area of these cells. This would provide some indication of any physiologic action of CNTF upon striatal cells. The concept and rationale for this work was derived from the earlier study of nerve growth factor (NGF) upon striatal cells carried out by Beardsall and Davies (1992). This earlier work specifically studied the action of NGF when co-injected with 60 nmol quinolinic

acid (QA). Cholinergic interneurones are a striatal cell type which appear to be at least partially resistant to QA administration and HD pathology (Ferrante et al.1987, Davies and Roberts, 1988). Beardsall and Davies further demonstrated that co-injected NGF (1μg) protected cholinergic neurones from QA lesion. The numbers of cholinergic cells in a section from a NGF + QA treated striatum demonstrated no significant difference from the number of cholinergic cells in control animals. Animals treated with QA alone demonstrated an approximate loss of one third of cholinergic cells present. No increase in survival rate of NADPH diaphorase cells was observed. Further to this, the morphology of cholinergic cells was significantly altered, on average the cholinergic cells somal cross sectional area increased from ~300 μm^2 to ~450 μm^2. Cholinergic cells were also reported to be more intensely stained, with a prominent (but not enlarged) nucleus and 30% enlarged nucleolus (Davies and Beardsall, 1992). No change in morphology of other striatal interneurones was observed. No such survival of striatal neurones or change in their morphology could be detected if NGF was administered 3-4 days after QA lesion.

The study conducted in this thesis was intended to obtain insight into CNTF action in the QA lesioned striatum. In the NGF study, it was known that cholinergic cells express the NGF receptor (Trk A neurotrophin receptor). However, according to the various studies outlined in the introduction the CNTF-alpha receptor has been localised generally to the striatal region (Ip et al. 1993) and specifically to both glial cells (Clatterbuck et al.1996) and striatal neurones (Kordower et al.1997)[23]. Further to this, work in this thesis clearly demonstrates the presence of CNTF in reactive astrocytes by immunocytochemistry in QA treated rat striatum (see results, section 3.1/4 and next section, 4.2,) and the presence of CNTF protein by PAGE in the normal striatum of the rat (results, 3.1/2). If this is taken into account, the striatum appears to possess a potential for great neuronal and glial response to CNTF action. This indicates that ,potentially, release of CNTF could be mediated by neurones or glia. The manner in which CNTF is released is still unknown (Stockli et al. 1989).

Previous work by Anderson et al. (1996) and Emerich et al. (1995) in which CNTF was introduced to the rat striatum 3/4 to 12 days before QA lesion appeared to

[23] Kordower et al. remark that CNTFR-alpha immunoreactive neurones can be observed in the caudate nucleus and putamen in the monkey (*Cebus apella*), but immunoreactivity is not as strong as that observed in motor nuclei or the entorhinal cortex and cingulate gyrus (Kordower et al, 1996)

produce a significant increase in the survival of medium sized projection neurones. However the action of CNTF when administered at the same time as the excitotoxin was not examined. If CNTF is to be used in clinical trials upon HD patients, pathology and cell death will presumably already be quite extensive. The authors of the above papers did not appear to take into account the potent activation of glia this early administration of CNTF would almost certainly produce or the action long-term reactive gliosis could produce. Other works outlined in the introduction (Kahn et al. 1995, Clatterbuck et al. 1996, Winter et al.1995, Lisovoski et al. 1997) clearly indicate CNTF as invoking dramatic change in glial morphology. It is quite possible that the application of CNTF into the rat striatum in the work of Emerich and Anderson is dramatically altering the activity and possibly the number of glial cells. These cells could, in the short term at least, produce the protective action as observed by increased survival of projection cells. The activated astrocyte could possess an enhanced capacity to protect neurones from QA. To see if glial activation could produce an increased level of protection, I used another, if less potent, glial activator, interleukin-1 applied at a similar concentration to CNTF three days before QA lesion. No increase in interneurone survival was observed, although glial activation was indicated by GFAP immunoreactive reactive astrocytes. It is therefore likely that the CNTF survival effect is specifically due to the action of CNTF upon striatal neuronal CNTF receptors. However, the secondary effect of widespread reactive gliosis that these treatments undoubtedly activate cannot be ignored.

In this thesis, CNTF was applied by injection at a similar dosage as that which produces neuronal survival in the rat striatum when administered 3-4 days prior to QA lesion (1.5μg/ml as compared to 0.78μg/ml at 0.5μl/hour in the Anderson study). At seven days following the joint administration of QA and CNTF 40 μm sections were cut throughout the entire rat striatum and careful counts of sampled projection cells (thionin stain), cholinergic interneurones (ChAT positive) and NADPH diaphorase interneurones were taken. Thionin count revealed an approximately 50% loss of projection cells (Results; 3.1/G1), in both QA lesioned and joint CNTF+QA treated striata. Furthermore, no significant difference could be determined between surviving cholinergic or diaphorase interneurones (Results: 3.1/G2). No significant difference in somal area of surviving diaphorase or cholinergic interneurones was apparent (Results: 3.1/G3 and 3.1/G4).

In conclusion, the work of Emerich and Anderson indicates that CNTF specifically acts upon striatal neurones, invoking an unknown mechanism which permits these cells to become more resistant to the QA excitotoxic lesion when CNTF is administered before any insult. This is proposed by these authors as a basis for CNTF to be used in clinical trials upon HD patients. However, HD patients will undoubtedly have some degree of brain pathology, with cell death or dysfunction occurring throughout the striatum. The study in this thesis demonstrates that when CNTF is administered at the time of insult, it provides no apparent protective action to striatal medium sized projection neurones and cholinergic or NADPH interneurones. Therefore, it would probably be necessary to administer CNTF prior to symptomatic onset in HD, which apart from being highly impractical (not least because no efficient delivery system exists), would induce major reactive gliosis (particularly at the levels required to produce neuronal protection). The long-term action of reactive glia is not understood clearly, although an evolutionary viewpoint indicates that it may not produce a conducive environment for long-term neuronal survival. Ultimately, it must also be considered that even if the striatum could be preserved by CNTF or indeed the application of any molecule, this would only allow the patient to survive long enough for the rest of the CNS, particularly the cortex and cerebellum, to undergo further degeneration. However, this study does provide a useful result for understanding NF-κB function covered later in this discussion, for it clearly demonstrates that CNTF does not increase QA induced neuronal loss. There is some basis to believe that CNTF could have a negative action upon neurone survival, as it is related in three-dimensional structure to IL-6 (and indeed shares IL-6 receptor components-see introduction). IL-6 is a potent inflammatory molecule implicated in rheumatoid arthritis, postmenopausal osteoporosis and multiple myeloma (Arika et al, 1990). For further discussion of CNTF activity in the striatum, see section 4.3E.

4.2 Endogenous action of CNTF in normal and QA lesioned rat striatum.

Western blots using the G1631 anti-CNTF antibody clearly demonstrate the presence of CNTF protein in the normal rat striatum, cortex and cerebellum at very similar concentrations (Results: 3.1/2 A,B &C). The 40 kD protein recognised by the CNTF antibody G1631 is dimeric CNTF, which appears to retain its integrity after denaturation

of the component molecules (McDonald et al. 1991). The 20 kD band corresponds to the correct molecular weight for the CNTF monomer. The purified CNTF used in this thesis was recombinant human CNTF, and when run upon western blot this protein also clearly demonstrated two specific bands migrating at 20 and +40 kD (Results: 3.1/2A). The other immunoreactive bands visible using this antibody could all be abolished with l0x concentration of CNTF to antibody by weight. At 168 hours (seven days) following QA administration, a significant increase in dimeric CNTF could be detected by densitometric analysis of western blots. It is difficult to establish the status of levels of the monomeric CNTF protein since levels are typically low and sometimes the band cannot be observed clearly. Although the monomeric CNTF may sometimes appear to be increased, this observation is erratic and a reliable set of data could not be obtained. Multi-anomalous diffraction (MAD) phasing analysis has indicated that the CNTF monomer is theoretically the only entity capable of binding the CNTF alpha receptor (McDonald et al. 1995), but dimeric CNTF appears to be the major molecular form found within this system. It could be that the dimeric CNTF acts as a reservoir to replace the active monomeric CNTF after receptor binding has been completed and the monomer is broken down. As already stated, western blot also reveals a distinct increase in endogenous levels of CNTF following QA treatment (Results: 3.1/2 A&B). This increase is significantly different from control animals and all preceeding time points at 168 hours (7 days) (Results: 3.1/G5). The western blot increase corresponds with the appearance of CNTF reactive astrocytes using the G1631 antibody for immunocytochemistry (Results: 3.1/4 C). This increase in CNTF and localisation to reactive astrocytes corresponds with reactive gliosis observed in the rat striatum following QA as observed with anti-GFAP. Western blot with the GFAP antibody Z334 indicated a gradual increase in GFAP after QA lesion with maximum levels present at seven days post-lesion, however a dramatic increase in GFAP can be observed as early as 24 hours post-lesion (Results: 3.1/3A). In CNTF treated animals, the increase in endogenous GFAP upon western blots was not as dramatic as that following QA lesion. However, an increase in GFAP could be visualised as early as 12 hours following CNTF administration (Results: 3.1/3B), again providing evidence for a central role of CNTF as a potent activator of glia. The endogenous increase in GFAP on western blot corresponds well with immunocytochemical analysis of astrocytes using the

monoclonal GFAP antibody and the OX 42 antibody, which recognises microglia, following both QA and CNTF treatment (Results: 3.1/5, 3.1/6, 3.1/7, 3.1/8 and 3.1/9). Localisation of endogenous CNTF to astrocytes supports the previously mentioned *in situ* hybridisation data outlined in the introduction (Ip et al. 1993) which localised CNTF to the edge of wound sites in the CNS. These results, when considered with the following NF-κB DNA binding data indicate that the second phase of increased NF-κB DNA binding and the high levels of CNTF seen at the same time point, correspond with the peak of gliosis (activation of both microglia and astrocytes). This CNTF production and the increased DNA binding could possibly reflect the molecular activity of these reactive glia and their response to QA induced or direct action of cytokines. The simultaneous peak of GFAP and CNTF expression at the time period of maximum presence of astrocytes, as determined by this study and that of Asada et al. 1995 (in which reactive astrocytes were observed to be present in greatest number at seven days following striatal biopsy), strongly indicates that the CNTF increase correlates with glial proliferation. Further discussion of CNTF action in the striatum is undertaken at the end of the CNTF/ NF-κB section of the discussion (4.3E).

4.3 NF-κB

As an anatomical study of the localisation of the three NF-κB subunits reported to be present in mammalian brain, (notably p65, p50 and p52 as reported by Bakalkin et al. 1993) has not previously been undertaken in the striatum, this would be the main objective of this section of work. However an insight into the role of NF-κB in the degenerating CNS would also be sought. Prompted by the observation of Perez-Otano et al. (1996) and others that reactive glia were immunoreactive for the p65 subunit of NF-κB, a hypothesis is proposed that NF-κB may play an active role in the brains response to injury, particularly reactive gliosis. I set out to try to investigate several points of inquiry i). Would a known glial activator (CNTF) induce a NF-κB response in a brain away from the site of immediate lesion, thus implicating NF-κB in the glial activation pathway? ii). After both direct glial activation with CNTF and indirect glial activation after lesion (QA) which NF-κB sub-units could be localised to glial cells using immunocytochemistry? iii). Attempt to define the time course of the NF-κB response after these treatments and

develop a hypothesis concerning the activity of CNTF and NF-κB in the QA lesioned striatum iv). Attempt to define a further hypothesis concerning the mechanism by which NF-κB subunits function in the CNS following lesion. More specifically to determine if it is sufficient for extant NF-κB to enter the nucleus and induce transcription, or if protein synthesis/increase in protein load of cellular NF-κB is required.

4.3A p65 expression and localisation in the striatum after CNTF or QA treatment

On western blots, the SC-109 p65 antibody clearly recognises one specific protein species, which is abolished with a 10 fold concentration by weight of peptide immunogen (3.3/1). However, this protein migrates at 50 kD when extracted from striatal nuclear protein extracts , not at 65 kD as observed in other tissues and cell lines, including a recent study on the substantia nigra pars compacta (Hunot et al.1997). When A431 cell lysate is run alongside striatal protein extract, the antibody recognises a 65 kD protein and none at 50 kD (3.3/1A). Extreme care was taken to determine the exact molecular weight of this protein, using three separate types of molecular weight markers (Sigma, Biorad and Biolabs) all of which localise the protein at approximately 48-50 kD (3.3/2). The antibody is raised to amino acids 3- 19 of the amino terminus of the p65 antibody and does not apparently cross react with either p50 or p52 NF-κB proteins. This could indicate that this 50 kD striatal protein is perhaps a splice variant of p65 or is possibly a post-translationally modified form of p65. It is perhaps not impossible that since this antibody is so specific and clearly recognises one protein, that other groups reporting this protein as full length p65 in neural tissue have not measured its molecular weight with due care. However, this protein does not appear to significantly increase in concentration in nuclear samples at any time point following QA or CNTF treatment. This indicates that it may not play a major part in the increased DNA binding, or that if it does, it is somehow regulated in a manner which makes its binding activity not dependent merely upon levels of the protein alone. Possible mechanisms for intra-nuclear regulation of the NF-κB proteins include phosphorylation state and even the action of nuclear I-κB. Although it was initially believed that IκB was restricted to the cytoplasm, it has been proposed that IκB can enter the nucleus and disassociate NF-κB from DNA (Gilmore, 1996, Zabel and Baeuerle,

1990). This work is supported by PAGE in this thesis using anti- IκB which demonstrates nuclear IκB-alpha (Results 3.3/6). Thus, IκB could act as an intra-nuclear regulator of p65 (albeit at much lower concentration than it is found in the cytoplasm) and indeed, the other NF-κB protein subunits. A remaining point to consider is that the NF-κB family are phosphoproteins, requiring phosphorylation by an as yet unknown species to bind DNA. In vitro studies upon c-Rel and v-Rel indicate that protein kinase A (PKA) can phosphorylate a serine residue in a consensus recognition sequence (Arg-Arg-X-Serine) just outside the nuclear localisation sequence of the Rel domain (Mosialos et al. 1991 and Mosialos et al. 1993). It has not been possible to determine what proportion of nuclear p65 (or indeed any of the NF-κB proteins) is phosphorylated and therefore free and able to bind DNA and activate transcription. This could indicate that although nuclear protein levels do not increase on PAGE to correspond with increased DNA-binding, the proportion which is phosphorylated and able to bind DNA does. The only final consideration is that perhaps the NF-κB transcriptional system is so exquisitely sensitive, that only a very low concentration of additional NF-κB protein is required to 'unbalance' the system. This small amount of additional protein could provide the difference between mere constitutive 'housekeeping' functions and the extra concentration required to mobilise the cell machinery for a response to insult. The optical densitometry system, although useful does have its limitations of sensitivity (see Materials and Methods) and it may be beyond its range of detection to report such a minor increase in nuclear protein. Ultimately, the extra p65 (or indeed p50 and p52) protein migrating to the nucleus is masked by the NF-κB subunits already there, activating transcription of CNS genes needed for normal cellular function. There is some evidence to support this hypothesis. Work by Prasad et al. (1994) detects a significant increase in p50 protein levels at 12, 24, 48, 96 and 120 hours following administration of pentylene tetrazole (PTZ) to the rat brain. However a different optical densitometry system to the one employed in this thesis was used. The western blot in question, however is remarkably similar to those of NF-κB subunits contained in this thesis, no visible increase can be seen at any time point. It is worth considering that if it is a tiny increase in a finely tuned transcriptional system we are looking for, the OD system employed in this thesis simply may not be sensitive enough to

detect it. The NF-κB system is quite unusual in the manner by which it is retained in the cytoplasm. It may also have an unusual mode of operation.

Immunocytochemistry with this antibody indicates that the p65 immunoreactive protein is present in both neurones and glia in the striatum in control (normal) animals (Results: 3.2/1). The number of immunoreactive medium sized neurones indicates that this protein is indeed expressed in the striatal medium sized densely spiny projection neurones, but by no means all of them. This can be observed by comparing Nissl staining with p65 imunoreactivity. The distribution of staining indicates that neurones in both patch and matrix compartments express this protein. The absence of large immunoreactive (>22μm diameter) neuronal perikarya indicates that this protein may not be expressed by the large cholinergic interneurones of the striatum. Immunoreactivity of small perikarya in the overlying corpus callosum and fasicles of the internal capsule running through the striatum indicates that oligodendroglia express this protein in normal conditions. As early as 48 h following QA lesion and beyond (but more typically at 120 hours), as is also seen in the hippocampus following kainic acid lesion (Perez-Otano et al. 1996) immunoreactivity of astrocytes in the striatum was found (results: 3.2/1D).

4.3B p50 expression and localisation after CNTF or QA treatment

On western blots, the p50 antibody SC-114 NLS recognises several proteins in both control, QA and CNTF treated animals. The high molecular weight proteins at between 70 kD and 100 kD, which are seen faintly in nuclear preparations and more intensely in cytoplasmic preparations (Results: 3.3/3A-C) have previously been proposed to be post-translationally modified p105 precusor molecules (Blank et al. 1991). This 'post-translational modification' is likely to simply imply that these proteins are partially degraded p105 molecules (Kaltscmidt et al. 1993) which, of course, contain the p50 sequence to which the antibody was raised. The precursors would be expected to be present at greater concentration in the cytoplasmic samples since the ankyrin repeat domains should retain these proteins as primarily cytoplasmic entities. Their weak presence in nuclear protein samples may indicate some cytoplasmic contamination or possibly that prescursor molecules may actually be present in the nucleus. Although the

latter possibility seems unlikely, it has already been proposed by some authorities that the IκB proteins are capable of entering the nucleus (see introduction and above). The prominent 50 kD band is almost certainly the protein p50/ NF-κB 1 as it, and all other proteins present can be abolished by pre-incubating the antibody with the peptide to which it was raised (Results: 3.3/4 B&C).

Densitometric analysis of western blots of this protein (p50) reveal no significant difference following treatment with either QA or CNTF. This is quite suprising since other work has indicated that p50 is indeed a component of the DNA binding complex in neural tissue. This may again indicate that the mechanism of increased binding may not depend upon direct increase of nuclear levels (see above) of the proteins involved, or that the required increase in protein is extremely low and beyond the sensitivity range of the image analysis system used. The 50 kD band is present in both cytoplasmic and nuclear samples, as would be expected if it was being retained cytoplasmically by the IkB family of molecules and active in the nucleus.

Of interest is the 35 kD protein recognised by this antibody (Results: 3.3/3 A-C) which appeared to be constitutively present in cytoplasmic samples, but inducible after both QA and CNTF treatment in nuclear striatal preparations and the corresponding nuclear cortical preparations. 35 kD NF-κB proteins have been observed before in whole cell lysates (from carcinoma cell lines) in immunopreciptation experiments and visualised upon western blots using antibodies to v-Rel (Schmid et al. 1991) and p50 (Blank et al. 1991, raised to the c-terminal of p105). However, little information has been provided about the possible nature of these proteins, in fact the investigators did not remark upon their presence. It is possible that functional lower molecular weight NF-κB proteins do exist. The 35 kD protein observed in this work is present at 24 h after lesion with QA, and can also be found at 16 and 20 hours post lesion (Results: 3.3/4A) and at 12 hour following CNTF administration. Although the density of this band is variable, it has appeared in 100 % of QA 24 h nuclear samples tested. It has also been seen following CNTF administration in 12h nuclear samples with a more variable frequency of about 75%. There are several possibilities concerning the identity and origin of this protein, all unfortunately are speculation at this stage. The 35 kD protein may be a breakdown product of p50, although since there is no significant rise in nuclear p50 it would be hard to

explain how such dramatic production of a breakdown product occurs in the nucleus when there is no corresponding increase in p50. NF-κB p50 level remains the same as other time points where the 35 kD protein does not appear. One hypothesis is that this breakdown is of (possibly irreversibly?) phosphorylated p50 in the nuclear protein pool. It is unlikely to be a non-specific protein band, for addition of the peptide immunogen abolishes the 35 kD protein. It is beyond the scope of this initial study to further investigate the nature of this protein. However even if the protein is merely a breakdown product, its appearance at similar time points to increased DNA binding on EMSA for both QA and CNTF provides an interesting clue to NF-κB processing and activity in the striatum and is extremely intriguing. It could even provide further hypothetical evidence for an increase in nuclear p50, even though this increase cannot be detected. Since the p50 antibody recognises the p50 precursor, p50 itself and a 35 kD protein, immunocytochemistry is somewhat limited in the information it can provide about the anatomical localization of active p50 protein alone. The 35 kD protein can be disregarded as a confounding factor in normal animals and those at time points where it does not appear. However, immunocytochemistry will apparently recognise breakdown products of p50, as well as its precursor. Nonetheless, immunocytochemistry does provide an anatomical understanding of where p50/p105 activity is localised. Immunoreactivity in control animals was very similar, if not identical to that seen with the p65 antibody. No difference was apparent after treatment with CNTF or QA at 24 h or beyond. This indicates that p50 does not appear to play a role in the glial activation following administration of either QA or CNTF since it cannot be localised to reactive glia, as can p65 and as we shall see, p52. This would indicate the relative importance of p52 homodimers and or p65:p52 heterodimers in glial activation, perhaps indicating that there is a compositonal change in the proportion of DNA binding subunits at the 168 hour/7 day period of increased DNA binding seen on EMSA after QA or CNTF.

4.3C p52 expression and localisation after QA and CNTF treatment

The 50 kD protein recognised by the p52 antibody on Western blots is abolished by the peptide immunogen at 10x concentration by weight to antibody and is therefore presumed to be p52 NF-κB2 (Results: 3.3/5). Previous studies indicate that this antibody

recognises a ~40 kD/ lower molecular weight non-specific protein band (Clemens et al. 1997) and this also appears to be the case here. Densitometry indicated no significant increase in p52 levels following either treatment.

Immunocytochemistry using the p52 antibody was particularly striking (3.2/3). Neuronal perikarya, possibly a previously undescribed population of medium sized neurones, were immunoreactive in control animals, as were small bodies in the nucleus of medium-sized neurones. The neurones which presented with complete perikaryal reactivity are not NADPH diaphorase interneurones or even large cholineric interneurones for their distribution is distinct from these cells (results 3.2/3), the perikaryal reactive cells apparently being restricted to the dorso-lateral aspect of the striatum. The specifity of this immunoreactivity is clearly demonstrated by prior incubation of the p52 antibody to the peptide to which it was raised (again, 10x by weight relative to antibody). All nuclear body staining is abolished, leaving a weak background staining which may be the non-specific protein recognised at ~40 kD on the p52 western blot (3.3/5). The number of neurones seen to be immunoreactive (nuclear body staining) indicated that medium sized densely spiny projection neurones express p52. It is unclear what the nuclear bodies are, although each nucleus of the medium sized neurones seems to possess between two to eight bodies. Several structures have been demonstrated in previous studies by electron and immunofluorescence microscopy within the nucleus and termed `nuclear bodies'. The nucleolus derived coiled bodies involved in pre-mRNA processing have been identified by electron and light microscopy using antibodies to the proteins p80 coilin and p34 fibrillarin (Brasch and Ochs, 1992; Roth, 1995). The `Gemini of coiled bodies', nuclear structures closely associated to the coiled bodies, which can be stained using antisera to the survival of motor neurones (SMN) protein which is mutated in spinal muscular atrophy (SMA), have also recently been described (Liu and Dreyfuss, 1996). The nature of the p52 positive nuclear bodies identified in this study deserves an investigation of its own.

Loss of p52 nuclear body immunoreactivity occurs after QA and CNTF treatment in the core of the striatum, where concentrations of QA or CNTF are at their greatest. At 24 h, but most strikingly at 120 and 168 hours, following both CNTF and QA treatment, highly immunoreactive, large, dark bodies displaying a distribution similar to reactive glia

were apparent in the striatum and overlying cortex (Results: 3.2/4 A&B). QA treated striata demonstrated a greater response and the dark glia could also be seen spreading into the contralateral, untreated striatum. The morphology of these cells is particularly unusual and their exact type cannot be distinguished, however, some such cells close to the lesion tract do resemble ameboid microglia as already observed with the activated microglial marker anti-OX-42 (results: 3.1/9[OX-42] and 3.2/2B[p52]). The temporal and spatial distribution of these cells also closely matches that of OX-42 reactive ameboid microglia (3.1/9, A-D and 3.2/4 A-D).

At 120h and beyond, immunoreactivity of reactive astrocytes is clearly visible. These cells present a typical, very different profile, to those immunostained at 24h and beyond following treatment. The density of these cells is much reduced when compared to the p65 reactive astrocytes. Their morphology has been compared to that of O2A precursor/type 2 astrocyte cells observed *in vitro* (B.Fulton, personal communication). Immunocytochemistry therefore clearly demonstrates an important role for p52 in glial activation (of microglia and an astrocyte subclass), along with p65. The role of p52 in nuclear bodies requires further investigation.

4.3D DNA binding of NF-κB proteins in the rat striatum after CNTF or QA treatment

The study of DNA binding of NF-κB proteins in the rat striatum after either treatment by EMSA, provides a useful technique whereby NF-κB translocation to the cell nucleus and binding to the NF-κB promoter sequence can be examined. EMSAs in this thesis demonstrate one major NF-κB binding complex and the specifity of this complex is proved by the 'blocking out' or abolition of protein binding by adding a moderate (10x) quantity of unlabelled NF-κB oligonucleotide, which successfully abolishes the binding complex. This is a control experiment conducted in almost every other NF-κB EMSA conducted upon mammalian brain tissue by other groups (see table below). In addition to this, the presence of 10x concentration of an unrelated oligonucleotide, that of the SP-1 transcription factor, does not diminish the binding of the NF-κB binding complex, further demonstrating binding specifity.

It is worth noting that EMSAs in this thesis demonstrate one major NF-κB DNA binding complex, and this is also observed in other NF-κB EMSAs using neural tissue homogenate. However some groups have observed more than one binding complex. In whole cell lysates from cortex Perez-Otano et al. demonstrate one NF-κB binding complex and the specifity of this complex is indicated by an abolition of binding with 100x unlabelled oligonucleotide (Perez-Otano et al. 1996). A 100x blocking concentration appears to be unnecessarily high and such a concentration could interfere with the binding of other, non-specific proteins. One binding complex from whole (brain) cell lysate and nuclear extract alone is also observed by other workers, using much lower blocking concentrations of unlabelled oligonucleotide, yet other groups recognise two or more binding complexes (see table below). In adult brain, most groups describe a single DNA binding complex using NF-κB oligonucleotides. However, in the developing murine brain, things are different, with three complexes being present, apparently composed of (I) a p50 homodimer, (II) a p50-p65 or c-Rel-p50 heterodimer and (III) a c-Rel and p65 heterodimer (Bakalkin et al. 1993 and also Guerrini et al. 1997). However, in the literature cited below, three papers indicate two or more binding complexes in adult brain. The work by Heese et al. (1998) states that four binding complexes (a,b,c and d) are visible on NF-κB EMSA using lipopolysaccharide (LPS) stimulated microglial cell culture. However no blocking or mutant oligonucleotide control experiment is conducted to demonstrate the specifity of these binding complexes. Further to this, work by Barger and Harmon (1997) also demonstrates a three band binding complex after application of secreted amyloid peptide (sAPP-α) to microglial cell culture, but again no specifity control was employed. Since the specifity of these bands cannot be demonstrated, neither can their identity. In the work of Rong and Baudry (1996), a 100x unlabelled oligonucleotide blocking experiment is again used to demonstrate specifty of both bands. However such a high concentration of oligonucleotide could possibly interfere with all DNA-protein binding. The lower molecular weight complex is suggested to be a p50 homodimer, yet a second binding complex appearing the same as the one upon the NF-κB EMSA in this paper also appears upon an AP-1 EMSA on the same page. Here the complex is disregarded. I find it unlikely that this dual complex is genuine. Finally the work of Kaltschmidt et al. (1993) identifies two binding complexes upon NF-κB EMSA.

The complexes are so closely related that they could easily be considered one complex, but in certain lanes a region of clear film can be discerned apparently seperating two 'bands'. It may well be the case that the one major NF-κB binding complex may comprise two closely associated components, but this is far from clear. Kaltschmidt et al., in line with the work of Bakalkin suggest that these complexes are a p50 homodimer and a p50-p65 heterodimer. For the sake of this thesis, only one NF-κB binding complex will be discussed, but the possibility of it comprising two (or more) NF-κB complexes should always be considered.

Table D1

Comparison of NF-κB EMSA experiments conducted upon neural cell culture or whole brain regions.

Following page: CONT/L = control experiment, SHIFT=supershift, DAMGO=μ opiod receptor agonist, LPS lipopolysaccharide, *=non-specific band reported, ** two bands reported, one not abolished, *** p50 abolished not shifted, $ exceptionally high concentration, ^ control, did not produce shift.

INSULT	GROUP	TISSUE	BAND	CONT/L	SHIFT	TIME
IL-1/TNF	SPARACIO ET AL.1992	RAT ASTROCYTE CULTURE	ONE	100X BLOCK	NO	1-3h
N/A NORMAL (ADULT)	BAKALKIN ET AL. 1993	CEREBRUM (CORTEX)	ONE	BLOCK+ MUTANT OLIGO	P50 & P65 SHIFT ***	N/A
PTZ/SEIZURE	PRASAD ET AL. 1994	RAT CORTEX NUCLEAR EXTRACT	ONE*	12X BLOCK	NO	24h/96h and 120h
GLUTAMATE	GUERRINI ET AL. 1995	GRANULE CELL CULTURE (WHOLE)	ONE*	NO	NO	15-30 mins
KAINIC ACID/ PILOCARPINE /LITHIUM	UNLAP & JOPE, 1995	RAT CORTEX & HPC WHOLE LYSATE	ONE	NO	NO	25 MIN FOL.SE -IZURE
NGF	WOOD,1995	DRG GANGLIA NUCLEAR EXTRACT	ONE**	20X NF-κB 20X OCT^	P52 SHIFT	6-24h?
TRAUMA	YANG ET AL. 1995	RAT CORTEX NUCLEAR EXTRACT	ONE*	20X BLOCK	NO	3 to 10 days
DAMGO	HOU ET AL. 1996	RAT CORTICAL NEURONE CULTURE	ONE*	20X BLOCK	NO	4h to 72h
KAINIC ACID	PEREZ-OTANO ET AL.1996	EN.CORTEX WHOLE CELL LYS.	ONE*	100X[$] BLOCK	NO	24-48h
ISCHEMIA	CLEMENS ET AL. 1997	HIPPO-CAMPUS	ONE	.1μg/ml	NO	24-72h
N/A ADULT	KALTSCH-MIDT ET AL. 1993	CORTEX: CYTO PLASMIC FRACTION	TWO	MUTANT OLIGO-NUCLEO-TIDE	NO	N/A
KAINIC ACID	RONG AND BAUDRY 1996	PIRI.CORTEX HPC &CBM	TWO	100X[$] BLOCK	NO	4h-5days
LPS	HEESE ET AL. 1998	MICROGLIA CELL CULTURE	FOUR[£]	NO	NO	1h

The administration of both QA and CNTF appears to cause an increase in DNA binding of the NF-κB proteins in the striatum. CNTF causes an earlier increase in protein-DNA binding, a significant increase being seen at 12h after CNTF treatment when compared to 24h after QA as determined by optical densitometry. This could indicate that QA treatment causes endogenous levels of CNTF and/or other cytokines to increase or localise extracellularly, thereby activating a glial response. Directly injecting CNTF could immediately bypass the response required by neurones or glia to release or increase CNTF, reducing protein-DNA binding response time and perhaps explaining the earlier binding response seen after CNTF treatment. NF-κB DNA binding has been seen to increase at similar time points in earlier studies. After cortical trauma, binding was found to increase significantly at one day (24h) following trauma, peaking at 3 days (72h) and remaining significantly elevated until 7 days post-trauma (Yang et al. 1995- see above table). In this current study, no time point after 12h for CNTF and 24 h for QA was found to demonstrate a significant increase in protein-DNA binding, until 168 h (seven days) which was significantly increased in both groups. Therefore both QA and CNTF treated striata show two points of increased DNA binding, an early point at 12/24 h and a later one of 168 h. Although the time points are not identical, this `biphasic' occurrence of NF-κB DNA binding is similar to that seen after pentylene-tetrazole induced clonic-tonic seizures in rats. In this work DNA binding is found to peak at 24 h following seizure, decrease at 48 h to constitutive levels and then increase again at 96 h and 120 h (Prasad et al. 1994). The physiological function of this response is not clear. However it is interesting to note that the seven day increase in binding corresponds with the increased level of endogenous CNTF and GFAP in the striatum, indicating that this second binding response may be linked to an increase in glial activity (see also Asada et al. 1991). Since NF-κB sub-units have also been extensively localised in striatal neurones, the initial peak might possibly indicate a neuronal response to NMDA/ CNTF receptor activation in addition to a possible glial response. There appears to be no greater increase in glial activation as determined by immunocytochemistry at this time point (12-24h) than when compared to 7 days. Attempts were made to identify the protein subunit composition of the 24 hour increased NF-κB binding complex, by pre-incubating the undenatured nuclear protein extract with antibodies recognising either the p50, p52 or p65 factors. The

antibody should interefere with protein DNA binding leading to abolition of the binding complex or supershifting of the binding complex band. These antibodies are raised to peptide sequence fragments identical to the sequence of certain sections of the NF-κB proteins. The producer (Santa Cruz Autogen Bioclear) does not recommend these antibodies for supershift studies, but no clear reason for this is given; they instead recommend separate antibodies specifically produced for supershift. It is possible that when an antibody binds to its target protein, the antibody interferes with the ability of the native protein to bind its DNA consensus sequence, thereby demonstrating the presence of that protein in the binding complex by absence of the binding complex altogether from the gel. When the antibody to p50 was used, abolition of the NF-κB binding complex was obtained, although on closer inspection a weak, higher molecular weight band does appear to have been shifted (Results:3.4/2C [arrow]). This strongly indicates that the p50 protein is a major component of the binding complex. This is not greatly suprising, since p50 has been demonstrated in this thesis and other works (see introduction) to be present in the mammalian CNS and since p65 cannot heterodimerise it would be expected to be present. Application of the p52 antibody appeared to cause the appearance of a small, heavier molecular weight binding complex, indicating that some proportion of the NF-κB binding complex may well incorporate p52. When the p65 antibody was applied, no abolition of binding or shifting of the complex could be attained. This would lead one to propose that the NF-κB DNA binding complex most probably consists predominantly of p50 homodimers, due to the abolition with the p50 antibody and the small band shifted with the p52 antibody. It would also be possible to state that there would also be a proportion of p50:p52 heterodimers and possibly a small proportion of p52 homodimers present in the complex, the amounts of each (if both present) undetermined (Results: 3.4/2). However, immunocytochemistry clearly demonstrates strong perikaryal (including nuclear) immunoreactivity for p65, and western blot indicates strong nuclear presence of this protein. The identification of a 65 kD protein in A431 cells rules out the possibility that the p65 antibody is inexplicably recognising p50, thus accounting for the 50 kD weight observed on western blot (see 4.3B) and the strong immunocytochemistry. The p65 immunoreactivity of striatal cells is indeed abolished by pre-incubation with the peptide to which it was raised, ruling out the possibility of non-specific staining. It is

frustrating that these results lack consistency, but the evidence (including the use of the antibody by other groups) supports the p65 antibody for immunocytochemical use (Perez-Otano et al, 1996, Hunot et al, 1997). One is left to conclude that the p65 antibody is not suitable for use in supershift experiments and yet it is difficult to form a hypothesis to explain why. However, these results do show that the NF-κB binding complex does contain p50 and that p50 is most likely the partner molecule to any other NF-κB proteins forming this complex since the binding complex band is totally abolished. As a control, goat serum and other, unassociated antibodies (anti-GFAP is demonstrated in the results) were pre-incubated with the undenatured nuclear striatal protein. The presence of these antibodies/proteins never caused shifting or abolition of the NF-κB DNA binding complex, whereas the p50 antibody repeatedly did so. A curious action of the application of goat serum is the slight 'downward' (lower molecular weight) smearing of the binding complex.

Finally the work presented in this thesis has recently been partially confirmed by Hong Qin et al. (1998). This group reports increase NF-κB DNA binding following administration of QA into the rat striatum. Time points studied were 2, 6, 12 and 24 hours following lesion. Significant increase in binding was observed at 6, 12 and 24 hours following lesion. The earlier increase in binding observed in this work may be due to the greater dose of QA administered (120 nmols as opposed to 60 nmols as used in this thesis). Nonetheless, although the experimental paradigms vary somewhat, an early increase in NF-κB DNA binding following QA administration has been confirmed by both this thesis and Hong Qin et al. Unfortunately this group did not pursue its observations beyond 24 hours post-lesion.

A summary of the NF-κB EMSA results in this thesis is provided in the table below and the following graph (D/G1).

Table D2

Comparison of NF-κB EMSA experiments conducted upon rat striatal nuclear extract following QA lesion.

T/MENT	GROUP	TISSUE	BANDS	S/SHIFT	CONT/L	TIME
QA	THIS THESIS	RAT STRIATUM NUCLEAR EXTRACT	ONE BINDING COMPLEX	P50 ABOLISHED P52 SHIFT?	10X BLOCK	24H AND 168H
CNTF	THIS THESIS	RAT STRIATUM NUCLEAR EXTRACT	ONE BINDING COMPLEX	P50 ABOLISHED P52 SHIFT?	10X BLOCK	12,24 AND 168H
QA	HONG QIN ET AL. 1998	RAT STRIATUM NUCLEAR EXTRACT	ONE BINDING COMPLEX	NOT CONDUCTED	60x BLOCK	12H AND 24 H (168H not examined)

D/G1 Schematic graph illustrating the temporal relationship between QA and CNTF stimulated increase in NF-κB protein DNA binding

Approximate increase in binding is provided along the y axis (units as ADU) and time in hours along the x axis. 'Line of significance' indicates time points at which binding values tested statistically significant above control values. Red line indicates NF-κB protein DNA binding following QA treatment and the blue line following CNTF administration.

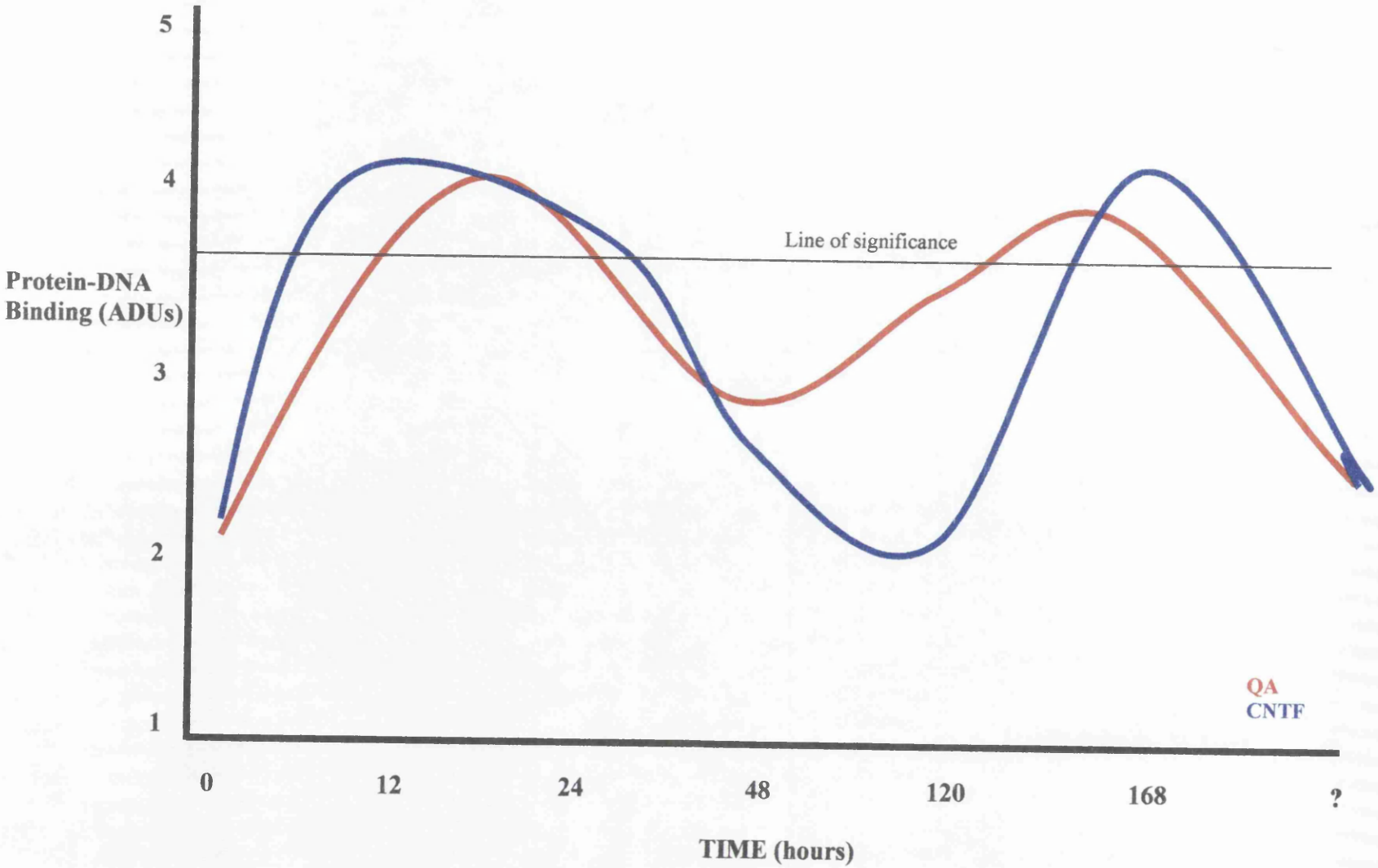
5
4
3
2
1
Protein-DNA Binding (ADUs)
Line of significance
QA
CNTF
0
12
24
48
120
168
?
TIME (hours)

4.3E QA, CNTF, NF-κB, neuronal life, death and reactive gliosis in the rat striatum

The work presented here and complemented by the research of other groups indicates that NF-κB plays an important function as a transcription factor in the central nervous system, fulfilling a potentially great variety of roles. This work indicates that one of these functions appears to be controlling the transcription of genes within glial cells reacting to CNS insult, but also provides some evidence that NF-κB plays an important role in the neuronal reaction to excitotoxic injury and the presence of CNTF. This study has confirmed and expanded upon the previous observations by Kaltschmidt et al. (1994) and others (see introduction) that NF-κB is constitutively present in the CNS (p65) and that in normal rat brain the subunits p65, p50 and p52 can all be localised to medium sized neurones, large neurones (p50) and oligodendrocytes. It has further been demonstrated that NF-κB is constitutively active in the brain as binding to DNA (NF-κB oligonucleotide) can be observed using normal brain nuclear extract. Like the OCT factors, NF-κB appears to help maintain 'housekeeping' gene expression in the CNS.

If QA or CNTF is administered to the striatum, a dramatic increase in NF-κB protein binding to DNA can be observed on EMSA at 12/24 hours. At this time point however, no p50, p65 or p52 immunoreactivity can be detected within astrocytes or microglia. This would suggest that the increase in NF-κB binding is occurring in the predominant p50/p65 immunoreactive cell type, the medium sized neurone of the striatum. What does this increased DNA binding imply? It is proposed that this increased activity of NF-κB reflects a direct response of these neurones to insult. It may be, for example, that the initial DNA binding response reflects NF-κB activity in neurones responding to NMDA receptor activation and the necrotic release of various factors from surrounding dying neurones. QA is a demonstrated excitotoxin causing damage to these cells. CNTF is a potentially lesion-released molecule that undoubtedly activates glia (see introduction and results), but must also have an action upon neurones possessing CNTFR-alpha (eg. striatal neurones).

Recent work has implied that NF-κB may transcribe genes leading to cell survival and cell death, particularly if NF-κB is activated via tumour necrosis factor (TNF) binding to its type one receptor (TNFR1). Activation of TNFR1 can activate the signal

transduction molecules RIP and TRAF2, which are capable of activating both NF-κB and the JNK protein kinase. Activation of NF-κB by transient action of TRAF2 or RIP prevents HeLa cells from undergoing apoptotic death (Liu et al. 1996). The TNFR1 is also capable of inducing apoptosis via activation of the signal transducing molecules TRADD and FADD. Despite both apoptosis and survival (antiapoptosis) being potentially mediated by the same receptor, the addition of the p65 subunit (or c-Rel) of NF-κB can protect HeLa cells against TNF induced apoptosis (Liu et al. 1996). This work explains the potent anti-apoptosis activity of IL-1 (Holtmann and Wallach, 1987), which, as already stated in the introduction, is an activator of NF-κB. The observation that one receptor can induce such potentially divergent actions gives some indication of how biological systems can be finely balanced.

Despite this discovery, NF-κB is also implicated directly in inducing cell death, possibly via the range of inflammatory genes it is able to transcribe (see introduction). The work of Grilli et al. (1996) has already been described, and indicates that NF-κB is capable of activating an apoptotic death pathway if neurones are exposed to excitotoxic levels of glutamate. It has also been demonstrated that reactive oxygen species (ROS) which may be formed by NMDA receptor activation (see introduction) are possibly capable of activating the kinases responsible for I-κB degradation, the resultant nuclear translocation of NF-κB being potentially responsible for apoptotic death (Lipton and Rosenberg, 1994). It is interesting to note that the increased NF-κB DNA binding following QA administration corresponds with QA induced apoptotic cell death in the striatum. DNA fragmentation studies ('DNA laddering') and TUNEL positive nuclei indicate this apoptosis occurs principally at 12 to 24 hours following lesion, 24 hours appearing to be the peak of cell death with 50-65% of striatal nuclei being TUNEL positive (Carolyn Walker, unpublished observations and Hong-Qin et al. 1998).

I would like to propose that the 'early' (12-24h) increased activity of NF-κB may indicate the activation of a 'program' which leads to a 'decision' about whether the cell should undergo apoptotic cell death. This may seem somewhat bizarre, since NF-κB is implicated as central to the inflammatory process and apoptotic cell death. However, even if gliosis is considered as the neuronal correlate of inflammation, the genes activated in glial cells may differ to those regulated in neurones. The primary reason for this is that

CNTF does not appear to have a negative action upon neuronal survival, in fact the opposite appears to be the case. However CNTF appears to have no secretory mechanism apart from release from damaged cells, so neurones would possibly react to increased extracellular CNTF as a signal indicating an impending or instant stressful change to their environment. Exogenous CNTF causes a dramatic increase in NF-κB activity, indicating it is activating a survival program in the absence of a deleterious stimulus. There is no agent present to induce cell death.

Returning to the hypothesis outlined at the beginning of this chapter, NF-κB activity is also undoubtedly involved in activation of glia in response to injury as immunocytochemistry demonstrates p52 immunostaining of astrocytes and what appear to be microglia and p65 immunostaining of astrocytes. It is interesting to note that the p65 immunoreactive astrocytes appear to be of a different morphological type when compared to the p52 immunolabelled astrocytes. The p52 reactive astrocytes are also present in a lower number than the p65 reactive ones. This time period of increased p52/ p65 immunoreactivity coincides with GFAP and endogenous CNTF increase after QA, particularly the dramatic increase in p65 and p52 reactive astrocytes at 120 and 168 hours. This indicates that increased NF-κB DNA binding observed on EMSA at the same time point (168h) is probably also representing predominantly glial activty.

The molecular mechanisms controlling the activation of glia are far from clear, despite the importance of this cellular response in almost all forms of neurodegenerative disease and various forms of trauma to the central nervous system. It is known from work by Bonni et al. (1993) that CNTF induces downstream tyrosine phosphorylation of the transcription factor p91 in SK-N-MC cell cultures. This is via the CNTF-RE sequence and a sequence resembling this is present in the mouse and human GFAP genes, which suggests that p91may play an important role in upregulating GFAP in astrocytes. However the possible involvement of other transcription factors in inducing chemical and morphological change in astrocytes and microglia and transcribing genes which contribute to their secretory profile, particularly the wider actions of CNTF and NF-κB, needs to be further investigated. The one problematic result in this work is the apparent lack of change of NF-κB expression upon PAGE. If p52 is so dramatically increased in glial cells following QA lesion, why is this increase not observed on western blot? One possible

explanation is that as neuronal p52/p65 decreases due to loss or damage of neurones, it is compensated by increasing glial p52/p65. However, this still does not explain the consistency of p50 levels observed on western blot. If p50 is not involved in the glial response as immunocytochemistry would suggest, levels of this protein should decrease as cell death increases, unless of course p50 levels are correspondingly increased in the surviving neuronal population as a response to injury. PAGE results have not been in line with what would have been expected throughout this work. Although I cannot explain this anomaly of apparently static protein expression despite fluctuating levels of NF-κB activity and expression by other cell types, I believe that a greater understanding of the activation of NF-κB by direct phosphorylation may provide the answer.

NF-κB may be activated by a variety of different stimuli and it is here demonstrated that CNTF and QA must also be added to this list (see table, section 4.3A). QA, by stimulating NMDA receptors and ultimately inducing necrotic and apoptotic cell death and CNTF via activation of the CNTF receptor complex induce NF-κB DNA binding. Since CNTF induces gliosis and activated glia are found to express the NF-κB subunits p65 and p52 at approximately both peaks of increased DNA binding (p52 at 24 and 120/168h h following QA lesion and CNTF treatment, and p65 at 120/168 h following QA lesion), it appears that NF-κB may play a role in regulating the glial response to cytokine activation after various forms of brain injury and stimulation. This is further suggested by the slight delay in reaching maximum DNA-binding after QA lesion when compared to CNTF treatment, while endogenous cytokines, including CNTF, become localised extracellularly to activate cytokine receptor complexes and possibly cause downstream activation of NF-κB which may play a role in activating glia. Direct injection of CNTF may bypass this stage of glial response. However, it is unlikely that CNTF works alone in initiating glial activation, since other cytokines have been demonstrated to cause similar changes to glia. These include IL-1 (Giulian, 1988) as well as IL-2, IL-6, TNF-α, γ- IFN and M-CSF (Balasingham et al., 1994) and transgenic mice deficient for IL-6 show a reduced glial response after facial nerve transection (Klein et al. 1997). Other, undefined but related molecules may also bind the CNTFR α, since although mice with a disrupted CNTF gene demonstrate little abnormality (Masu et al. 1993), mice lacking the CNTFRα itself die shortly after birth (De Chiara et al. 1995). The peak of endogenous

CNTF levels seen at seven days may simply reflect the increased levels of activated astrocytes and other glia present at this time. This in turn is a reflection of the sheer number of CNTF synthesizing astrocytes present, the activation of which was induced by the initial release of CNTF from damaged neurones and glia following QA administration. This has been suggested previously by in situ hybridisation studies after aspiration lesion, (Asada et al .1995). It may also be possible that as well as being a marker of activated glia and an activator of glia, the CNTF gene may also be regulated by the NF-κB family of transcription factors.

Furthermore, the affects of glial activation upon surrounding neurones is not clearly understood and it is possible that reactive glia are neurotoxic and detrimental to CNS repair and recovery following trauma, not only by forming a structural barrier to neurone sprouting, but by also secreting a range of cytotoxins (Chao et al, 1995 and McGeer and McGeer, 1995). Although I have proposed above that CNTF is capable of inducing a short term survival program in neurones (although this is admittedly conjectural), this is always followed by glial activation and presumably this glial activation will be maintained as long as CNTF is administered. If CNTF was to be administered directly to the CNS as Emerich et al, and Anderson et al, have proposed, the consequences of long term glial activation must be considered. Is this glial activation beneficial? It is not suprising that one of the side effects of CNTF when administered in clinical trials for ALS was inflammation at site of injection, due to its similarity to the interleukin family and its activation of NF-κB as demonstrated in this thesis. What if glial activation on this scale is detrimental to long term neuronal survival itself? This could replace or even enhance the pathological action of the disease itself. If NF-κB is central to glial activation, there may be the potential therapeutic options available to reduce the extent of gliosis and its possible damaging impact. As already outlined in the introduction, the activated glucocorticoid receptor is able to bind to the p65 subunit of NF-κB, preventing it from binding DNA (Ray and Prefontaine, 1993 and Mukaida et al. 1994) as well as apparently increasing levels of IκB to further prevent NF-κB binding (Scheinman et al, 1995). However, high levels of glucocorticoids may themselves be damaging to the CNS, particularly the hippocampus (Sapolsky, 1992), ruling them out as an agent of NF-κB inhibition. However, another therapeutic option may include the salicylate compounds,

including aspirin and sodium salicylate, which also appear to reduce NF-κB activity in hippocampal slices (Grilli et al. 1996). This is merely conjecture and the side effects of CNTF administration to the CNS are far from clear, as are the benefits and practical application of salicylates. The localisation of all NF-κB subunits in striatal neurons also indicates a particularly important constitutive role for NF-κB in the striatum and indeed, perhaps the whole CNS as well.

The localisation of CNTF receptor complexes upon specific neuronal subtypes in the striatum is not clearly defined at present (Kordower et al. 1997). The possible interaction between NF-κB proteins and other transcription factors also needs to be considered. The p65 subunit can physically interact with Fos and Jun transcription factors, via its Rel domain linking with the bZIP domain of these proteins, and successfully bind to the κB and AP-1 response elements (Stein et al. 1993). Both Fos, Jun and related proteins are activated following QA lesion in the striatum (Hollen et al. 1997 and Purkiss et al. 1993). NF-κB can also interact with the transcription factor ATF-2, which along with Jun can be phosphorylated by the c jun N-terminal kinase (JNK) by agents which increase NF-κB activity, notably UV radiation and IL-1 (Gupta et al. 1995). It is possible that a complex interaction of these various factors is occurring within the lesioned or CNTF treated striatum. Despite this, it is hoped that this study clearly demonstrates the important role of NF-κB in regulating the gliotic response of the striatum to excitotoxic injury and its potential role in activating genes responsible for neuronal survival.

Figure D1: A simplified hypothetical model of NF-κB action as central to neuronal life and death

Both CNTF and QA induce increased NF-κB- DNA binding at 12-24 hours. The pathways by which this activity is mediated are not clear, but it has already been demonstrated that signalling via the TNFR1 can produce anti-apoptotic action via NF-κB activation. However, NF-κB has also been demonstrated to control the transcription of genes which could induce neuronal swelling and is implicated in apoptotic death (which in the QA lesioned striatum occurs at 12-24 hours). The TNFR1 pathway may be involved in the increased NF-κB binding observed. FR/ROS= Free radicals/Reactive oxygen species.

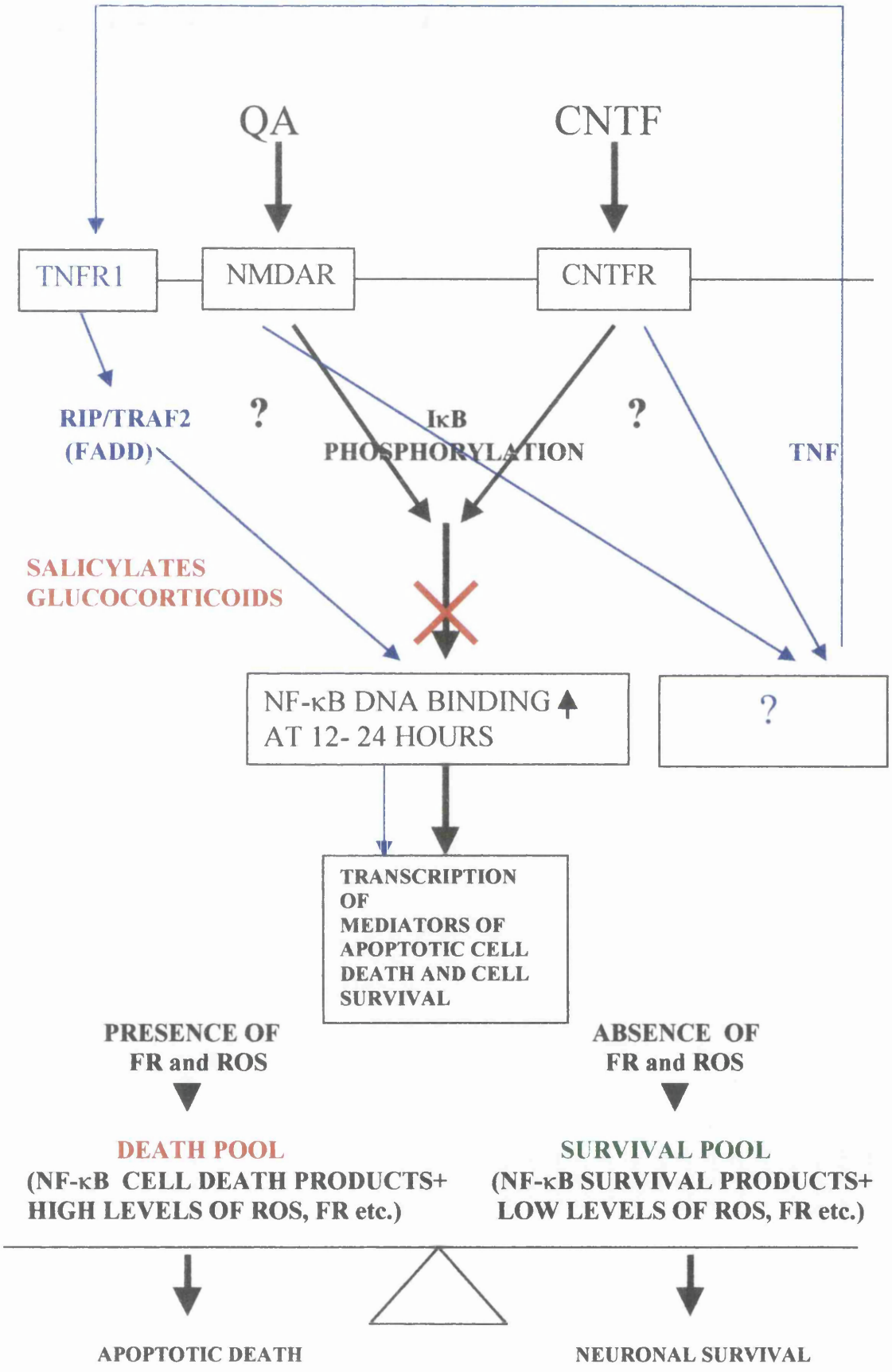
QA
CNTF
TNFR1
NMDAR
CNTFR
RIP/TRAF2
(FADD)
?
IκB
PHOSPHORYLATION
?
TNF
SALICYLATES
GLUCOCORTICOIDS
NF-κB DNA BINDING
AT 12- 24 HOURS
?
TRANSCRIPTION
OF
MEDIATORS OF
APOPTOTIC CELL
DEATH AND CELL
SURVIVAL
PRESENCE OF
FR and ROS
ABSENCE OF
FR and ROS
DEATH POOL
(NF-κB CELL DEATH PRODUCTS+
HIGH LEVELS OF ROS, FR etc.)
SURVIVAL POOL
(NF-κB SURVIVAL PRODUCTS+
LOW LEVELS OF ROS, FR etc.)
APOPTOTIC DEATH
NEURONAL SURVIVAL

D/G2 A Model of NF-κB DNA binding activity

The 12-24 hour increase in DNA binding is classified as a 'Neuronal Early Response' since at this point few or no glial (astrocytes/microglia) cells can be demonstrated to be p65 or p52 immunoreactive. The 'Glial Cumulative Response' is hypothesised to be an incremental increase NF-κB DNA binding in glial cells, which correlates with an increase in glial cell number. This is further supported by the maximum expression of CNTF and GFAP also correlating with the 168 peak of DNA binding/glia cell number. Hypothesised glial NF-κB DNA binding activity is shown by hatched lines.

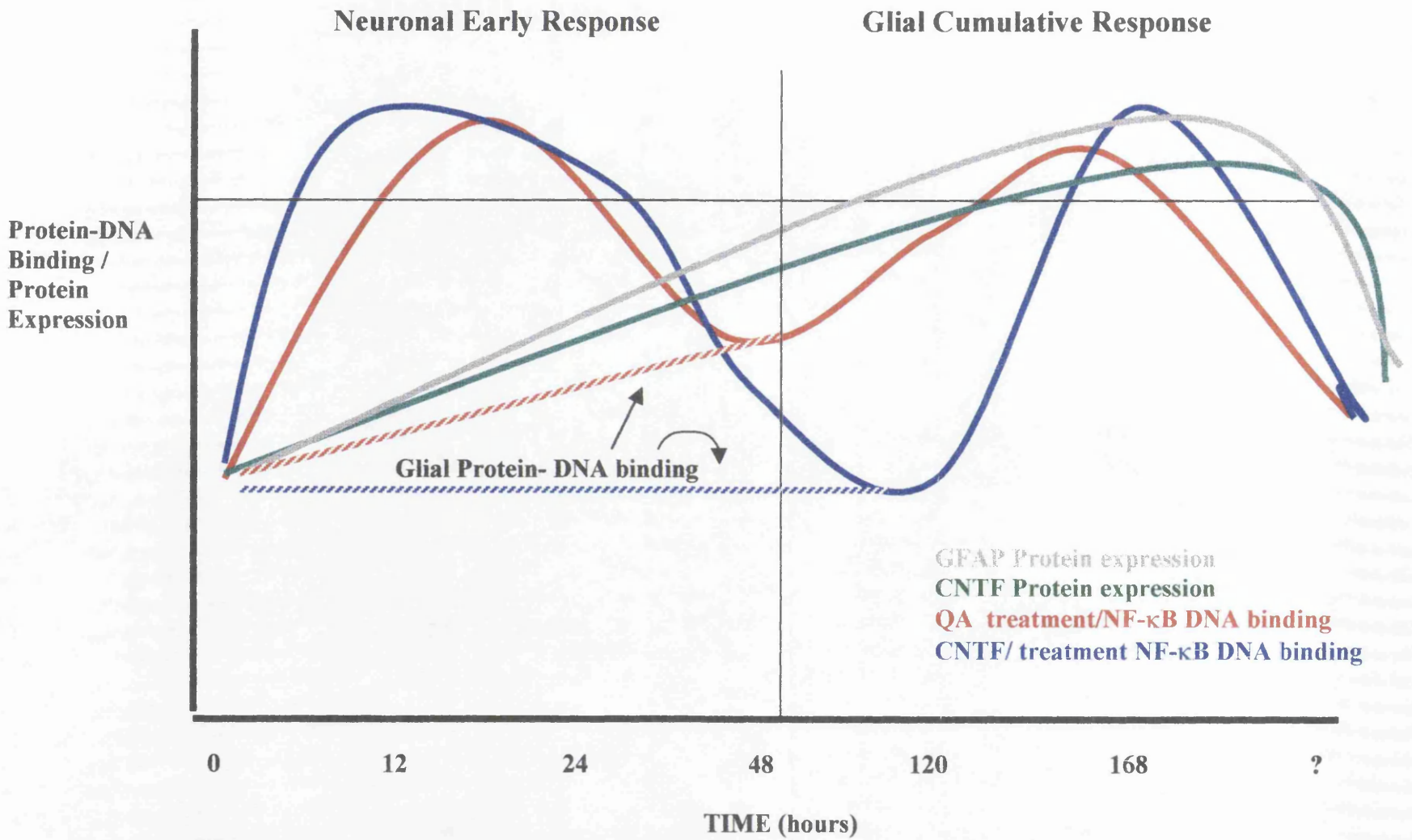
Neuronal Early Response
Glial Cumulative Response
Protein-DNA Binding / Protein Expression
Glial Protein- DNA binding
GFAP Protein expression
CNTF Protein expression
QA treatment/NF-κB DNA binding
CNTF/ treatment NF-κB DNA binding
0
12
24
48
120
168
?
TIME (hours)

4.4 Huntington R6/2 transgenic mice and polyglutamine repeat transcription factors

A possible aspect of pathological accumulation of polyglutamine repeat proteins could involve the binding of polyglutamine repeat transcription factors to large nuclear inclusions of abnormal huntingtin protein. These large nuclear inclusions, initially discovered in the huntingtin transgenic mice by Davies et al. have also been demonstrated in human tissue, the initial observation being made by Roizin et al. (1976), although at this first observation the composition and nature of this inclusion was unknown. Perutz proposes that polyglutamine repeat proteins with repeats of a certain length may form polar zippers and link via hydrogen bonding (see introduction). Many transcription factors possess large stretches of polyglutamine repeats and could possibly be subject to 'interference' from a large, constantly present, mass of huntingtin protein. Part of this thesis work has been to carry out a preliminary study into the function of the three transcription factors with the longest stretches of polyglutamine repeats (TBP, GR and BRN-2/N-OCT-3) in the transgenic mice. Put simply, immunocytochemistry, western blotting and EMSA were employed to establish if any abnormality could be observed in anatomical location, level of expression or ability to bind DNA of these factors in R6/2 transgenic mice, compared to littermate control mice. Immunocytochemistry at light level clearly labels the nuclear inclusions if antibodies to huntingtin protein or ubiquitin are employed (see introduction). The three factors studied are all constitutive in the nervous system, so it was unknown whether or not nuclear inclusion localisation could be easily determined since the rest of the cell nucleus would of course be immunoreactive. I considered it possible, however, that it could still be possible to distinguish transcription factor immunostaining of the neuronal inclusion. Western blotting appeared to be an ideal way to observe expression of the proteins. It was difficult to hypothesise if protein loads would be decreased (due to binding out and partial breakdown of free transcription factors) or increased (as the cell attempts to compensate for the 'imprisonment' of polyglutamine repeat transcription factors within the growing inclusion. A negative result (i.e. a result identical to the control brain) using immunocytochemistry or western blotting would of course not provide absolute empirical evidence that the polyglutamine transcription factor activity was normal in R6/2 transgenes (and indeed I believe this has

been shown to be the case). It has proved very difficult to clearly examine nuclear profiles at light level using antibodies to the polyglutamine transcription factors, and so the absence of these factors in the inclusion cannot be guaranteed. Since nothing is known about the state of any normal cellular proteins bound to the nuclear inclusion, it could be that the denaturation process employed prior to western blotting could free these proteins, allowing protein load to appear normal (and indeed any number of any other possible hypothetical outcomes). However, EMSA appears to be an extremely useful technique in examination of this problem. If transcriptional dysregulation is a crucial factor in producing the symptoms in these transgenic models, then ultimately the binding of these factors to DNA must be the point at which this biological system fails. EMSA allows the observation of this binding. If we follow the hypothesis that the inclusion is interfering with neuronal transcription factor binding, we could predict that there would be reduced binding in R6/2 transgenes. This would appear to support the theory proposed by Max Perutz (1994). As the following results will demonstrate, there is no prominent evidence indicating that inhibition of polyglutamine transcription factor-DNA binding is retarded by the presence of a large nuclear inclusion of huntingtin protein. However, I still regard this study as a preliminary work.

4.4A Glucocorticoid receptor localisation, expression and DNA binding in R6/2 transgenes and litter-mate controls

The M-20 anti-GR antibody clearly immunoreacts with neuronal and glial nuclei in both the R6/2 cortex and striatum and as with the localisation of TBP, no difference in nuclear morphology, level of expression or number of reactive nuclei could be discerned. As with TBP, only nucleolar exclusion could be observed in neuronal nuclei. Western blot for GR demonstrated one protein recognised by the M-20 antibody migrating at 80 kD, the correct weight for the GR receptor. Longer exposure times of ECL labelled blots to X-ray film reveal weaker immunoreactivity with proteins of a lower molecular weight, but these proteins can be abolished by pre-incubating the antibody to the peptide to which it was raised indicating that these are likely to be cellular GR degradation products. Densitometric analysis of protein expression upon western blots from cortex, striatum and

cerebellum revealed no significant difference between 11 week old R6/2 and littermate control mice.

EMSA analysis of GR protein DNA binding in nuclear extract from mouse striatum, cortex and cerebellum demonstrated one major binding complex. The specifity of this complex is determined by abolition with 10x unlabelled GR oligonucleotide. Densitometric analysis revealed no significant difference between GR DNA binding in littermate controls or R6/2 transgenes at 11 weeks of age.

4.4B TBP localisation, expression and DNA binding in R6/2 transgenes and littermate controls

The results of the studies into both TBP (TFIID) and GR indicate no apparent difference between littermate controls and R6/2 transgenes of 11 and 13 weeks of age. All TBP antibodies used for immunocytochemistry revealed no visible difference in anatomical localisation or level of expression of TBP. The 3G3 and 4C2 antibodies appear to be unsuitable for use for immunocytochemistry due to high background immunoreactivity. Immunostaining of striatal and cortical neurones in both the R6/2 transgenes and littermate controls using the 2C1 and SC-TBP (SC-204) antibodies demonstrated no difference in nuclear morphology, level of expression or apparent number of reactive neurones. Immunostaining of the neuronal intranuclear inclusions (NII) could be discerned in the R6/2 tissue. However the possibility that TBP is a component of the NII cannot be beyond consideration entirely, since although the exclusion of the nucleolus could be observed in the nucleus of some neurones, NII exclusion (as would be evidenced by two regions of immunoreactive exclusion) was not visible.

All TBP antibodies recognised a protein migrating on western blot at approximately 40 kD, the correct molecular weight for TBP protein TFIID subunit. Antibody 2C1 recognised multiple proteins upon western blot, although a particularly strong level of immunoreactivity was observed at 40 kD in both R6/2 and littermate control cortices, but oddly this level of immunoreactivity was reduced in striatal nuclear tissue samples. Both 2C1 and 4C2 recognise a protein at 55 kD, but 4C2 recognises two proteins migrating at or close to 40 kD, presumably again TBP, being expressed most

strongly in cerebellum. The antibody 3G3 recognises a 40 kD protein extremely strongly in striatum, cerebellum and cortex, other proteins are weakly recognised, mainly at lower molecular weights and possibly breakdown products. These results are somewhat bizarre, for although 3G3 most strongly recognises TBP upon western blot, it demonstratesthe highest level of background immunoreactivity when immunocytochemistry is conducted. This PAGE data also reduces the viabilty of 2C1 immunocytochemistry, for this antibody also clearly recognises other protein species as strongly as TBP. Despite this apparently confusing set of results, 3G3 is the most suitable TBP antibody for analysing TBP expression upon western blot. Unfortunately purified TBP was not available to conduct blocking experiments to determine the specifity of any of the protein bands observed with 2C1, 3G3 or 4C2. However, no difference in level of expression of the ~40 kD protein recognised by these antibodies could be detected between R6/2 mice and littermate controls if densitometrically scanned. The SC-TBP antibody most strongly recognised a 40 kD protein in all nuclear brain tissue samples, and recognition of this 40 kD protein could be abolished by pre-incubation of the antibody with the peptide to which it was raised. This antibody also weakly recognises several other protein bands at both higher and lower molecular weights at longer exposure times. These proteins cannot be abolished by pre-incubation with TBP peptide and are therefore non-specific recognition products. This antibody is taken as the most reliable protein for recognising TBP used in this thesis. No difference in expression of TBP upon western blot, as determined by densitometric scanning, could be determined between R6/2 and littermate control mice.

EMSA analysis of TBP DNA binding in both R6/2 and control nuclear samples extracted from cortex, striatum and cerebellum demonstrates two binding complexes. This has been observed before, for example upon the EMSA conducted by Bellorini and colleagues presented in the introduction. In this case the two complexes are presumably TFIID (lower molecular weight, lower complex) and TFIIA (higher molecular weight, upper complex) since these are the only two protein complexes present able to bind the TATA sequence in this particular experiment (Bellorini et al. 1995). However, when the *in vivo* environment is considered, the two complexes could possibly indicate the two predominant DNA binding states which TBP is hypothesised to exist, the higher molecular weight complex could indicate the larger, closed pre-initiation complex (PIC),

ie. TBP/TFIID plus all other associated TF complexes while the larger DNA binding complex could represent the initial DNA binding complex of TFIID plus TFIIA (or indeed the residual DNA binding complex of the same composition: TBP+TAFs+TFIIA). Occasionally the major binding complex can be visualised as two complexes rather than one. This could indicate a further stage in the assembly or breakdown of the core basal transcription machinery. However, this is all hypothetical, but the TBP EMSA does appear to present two (or more) specific binding complexes since the presence of both can be abolished by blocking the binding of protein to the labelled oligonucleotide by a twenty-fold excess of unlabelled TATA oligonucleotide. The upper complex indicated the greatest variation in density, but no significant difference in TBP-DNA binding could be consistently observed between R6/2 transgenes and their littermate controls in striatum, cortex or cerebellum. When the vital role of TBP is taken into consideration, it would perhaps be expected that some abnormality would be observed in R6/2 mice if transcriptional dysregulation was the major cause of neuronal dysfunction in these animals. However no difference can be observed in the expression, localisation or DNA binding between 11 week old R6/2 transgenes and controls. This is not to rule out some interaction between TBP and htt, (indeed if polyglutamines do indeed possesses such high binding affinities as proposed, some interaction may be inevitable). However disrupted TBP-DNA binding does not appear to be a major factor in the aetiology of R6/2 transgene symptomatic onset and probably HD.

The results concerning both TBP and GR expression and DNA binding provide no evidence to suggest that there is any abnormality in polyglutamine transcription factor function between littermate controls and R6/2 transgenic mice. Although these results do not totally rule out transcriptional dysregulation due to polyglutamine repeat interaction between the transcription factors studied and the abnormal huntingtin protein, they do suggest that such dysregulation is not the major factor which leads to the neuronal dysfunction observed in huntingtin transgenic mice.

4.4C BRN-2 localisation, expression and DNA binding in R6/2 transgenes and littermate controls

The study of the BRN-2 transcription factor revealed the most interesting (and indeed unexpected) set of results. Immunocytochemistry using the anti-BRN-2 antibody demonstrated clear nuclear staining throughout the mouse CNS, demonstrating the constitutive action of this transcription factor. Most studies have emphasised its importance in development of the mammalian CNS (see introduction and below), but it undoubtedly is of great importance in maintenance of the CNS. No difference could be discerned in anatomical localisation or intensity of staining of BRN-2 in the striatum and cortex when comparing littermate controls to R6/2 transgenes. Careful analysis of nuclei at high power, disappointingly, revealed little in the way of internal structure and the nuclear inclusion could not be discerned. However, as examination proceeded throughout the CNS, the paraventricular nucleus of the hypothalamus appeared to demonstrate reduced staining and possibly reduced cell number. Counting of BRN-2 positive cells (and also Nissl stained nuclei as well as vasopressin immunoreactive cells) indicated there was no significant difference in cell number in the PVN between R6/2 transgenes and littermate controls. However, the intensity of immunostaining for BRN-2 in the PVN was markedly and repeatedly reduced in R6/2 transgenes. To ensure this was not due to experimental factors, the staining of other structures in the transgenes, notably the transgenic cortex and striatum was compared to the transgenic PVN. The level of immunoreactivity here was stronger and comparable to the staining observed in control brains. These results strongly indicate that BRN-2 expression is reduced in both 11, 13 and 16 week old transgenic mice in the PVN. Mice of both sexes were examined in equal number, and reduced expression was observed in both male and female transgenes repeatedly, ruling out heterogeny due to sexual dimorphism of this nucleus. Frustratingly, this hypothalamic nuclear structure is too small to allow substantial amounts to be harvested from tissue available for analysis upon western blot. These results are intriguing. Reduced expression of BRN-2 in the PVN could support the transcriptional dysregulation hypothesis, but this does not adequately explain why expression should appear to be normal throughout the rest of the mouse CNS. One important point of consideration is that the PVN could be the first CNS structure to be profoundly altered by

the presence of the neuronal inclusions. This does seem unlikely however, for in 16 week old mice reduced expression could not be visualised elsewhere in the CNS, and this is at an age where anterior cingulate cortex degeneration is extensive (S.W.Davies and M.Turmaine, personal communication) and death of the mice at 13 weeks of age is not uncommon.

Regardless of this, however, reduced BRN-2 expression does indicate an abnormality in the function of the PVN in transgenic mice. The genes controlled by BRN-2 are not yet fully established, so it may be fruitless to attempt to hypothesise how PVN function is being deleteriously altered. This finding does provide a potential clue to some of the symptoms observed in trangenic mice. The PVN is rich in neuropeptides, which it secretes to regulate hormonal release from the pituitary gland and control the autonomic nervous system (ANS). Oxytocin is secreted by a large body of cells found centrally in the nucleus and vasopressin is expressed by a population of cells around the lateral edge of the structure. These are collectively known as magnocellular neurones A variety of peptides, including corticotrophin releasing hormone/factor (CRH/F) cholecystokinin (CCK), angiotensin 2 (A2), enkephalin (ENK), neurotensin (NT), somatostatin (SOM), thyrotrophin releasing hormone (TRH), vasoactive intestinal polypeptide (VIP) and vasopressin (VP) are expressed centro-medially. The most medial aspect of the nucleus contains a population of cells, which secrete somatostatin (SOM) (Kiss et al. 1988 and Swanson and Sawchenko, 1983). Projections from the PVN reach the posterior pituitary (mainly vasopressin and oxytocin), the autonomic nervous system (mainly oxytocin) and the median eminence of the hypothalamus, which receives the other peptides listed above. This is obviously an extremely complex structure, controlling a variety of neuroendocrine function and the PVN is essential for controlling lactation and uterine contraction via oxytocin release (Lincoln and Wakerley, 1974) as well as controlling water re-absorption in within the kidneys via vasopressin secretion (Sundsten and Sawyer, 1961). Disruption of the function of the nucleus could possibly explain some of the symptoms observed in the huntingtin transgenic mouse and, indeed, HD patients, particularly the high intake of food coupled with cachexia (see introduction). The PVN appears to have an essential role in controlling feeding behaviour as well as the functions outlined above. Work by Leibowitz and Stanley demonstrates that stimulation of the PVN by applying

noradrenaline greatly stimulates feeding behaviour, presumably by producing firing of PVN neurones which then secrete any of the range of neuropeptides the PVN contains, triggering a downstream pituitary response. Furthermore, stimulation of the PVN does not just simply increase feeding behaviour, but also causes the animal to select particular food types. Noradrenaline, for example, leads to the ingestion of carbohydrate rich foods at the expense of declining fat and protein. This aspect of nutritional selectivity may not be of relevance to the transgenic mice, but is worthy of consideration in HD patients (Leibowitz and Stanley, 1986). If the PVN is abnormal in the transgenes, this could possibly explain the chronic weight loss and feeding disturbances observed in these animals. This observation requires further investigation, however work conducted by some investigators does indicate the importance of BRN-2 in regulating oxytocin and vasopressin expression (see below).

Brn-2 is essential for the normal development of the paraventricular nucleus and possibly the entire CNS. Targeted disruption of the brn-2 gene in mice (Brn-$2^{\Delta C}$) does not lead to embryonic lethality in Brn-$2^{\Delta C}$ heterozygotes but Brn-$2^{\Delta C}$ homozygotes carrying two disrupted copies of the gene die shortly after birth (Nakai et al. 1995). Most of these Brn-$2^{\Delta C}$ homozygotes die two days following birth and at this stage do not appear grossly different from littermate controls, however those that survive beyond two days demonstrate dramatically reduced growth, their body weights being half that of littermate controls at post-natal day 4. All Brn-$2^{\Delta C}$ homozygotes die by ten days following birth. Interestingly no abnormalities are visible in any major body systems, but the homozygotes appear to die of severe malnutrition, since they possess no body fat, subcutaneous adipose tissue being totally absent and 'brown fat' was depleted of adipose deposition. More detailed examination of the CNS revealed that the posterior lobe of the pituitary gland (neurohypophysis) was hypoplastic. The oxytocin and vasopressin secreting magnocellular neurones of the paraventricular nucleus and the supraoptic nucleus were absent in these animals and CRF and TRH secreting parvocellular neurones were reduced in number. Brn-$2^{\Delta C}$ heterozygous mutants demonstrated no histological abnormality, but levels of oxytocin and vasopressin in these animals was reduced by half (Nakai et al. 1995). The somatostatin producing neurones of the medial periventricular region (described by Swanson and Sawchenko, see above) are also absent in homozygotes. This

absence of certain populations of hypothalamic neurones appears to be caused by the death of neuronal precursors of these cells (particularly magnocellular neurones) at around E12.5. This was determined by conducting immunocytochemistry to a developmental marker for these cells, a calbindin family member named spot 35 (Nakai et al. 1995). This reinforces the work by Hagino-Yamagishi et al. (1997, see introduction) which indicates the importance of BRN-2 in CNS development, possibly via the regulation of NCAM-H. Magnocellular neurone precursors arise from neuroepithelial cells at around E10.5 and finally form the PVN or supraoptic nuclei region at around E14.5 to E16.5. Neuropeptides normally begin to be secreted while the cells are still migrating at E14.5. The work of Nakai et al. is supported by a similar study conducted by Schonemann et al. (1995) in which another transgenic mouse with a disrupted brn-2 locus also failed to develop fully functional PVN and supraoptic nuclei. Brn-2(-/-) mice again demonstrated severe (~50%) weight difference when compared to controls at post-natal day ¾ and did not survive beyond postnatal day 9/10. Since Nakai et al. could find no major histological abnormality in the PVN of Brn-$2^{\Delta C}$ heterozygotes, this strongly indicates that BRN-2 is both responsible for development of the PVN magnocellular and parvocellular neurones and regulation of vasopressin and/or oxytocin expression in normal adult mice.

Western blotting using the BRN-2 antibody demonstrated one major protein migrating at 80 kD, the estimated weight of BRN-2. However, when film exposure time to ECL was reduced, or a lower dilution of antibody used, this one complex was revealed to consist of two closely associated proteins. Both proteins could be abolished in a 'blocking' experiment whereby the antibody was incubated with the peptide to which it was raised prior to exposure to the filter. Since therefore both proteins indicated a form of BRN-2, perhaps BRN-2 and a degradation product (which would indicate a dramatically rapid turnover of the protein) or a post-translationally modified form, the protein bands were optically scanned together. Visually, there occasionally appeared to be a reduced density of the lower molecular weight protein in the control striatum when compared to the transgenic striatum, although the higher molecular weight protein never displayed this. The often observed merging of these protein bands made defining their boundaries difficult and separate scanning almost impossible. Overall, no significant difference could be found between expression of BRN-2 protein in littermate controls or transgenes. With

the exception of reduced immunoreactivity in the PVN, no abnormality could be observed in BRN-2 expression in transgenic mice.

EMSA using nuclear extract from 11 week old control and transgenic mice demonstrated significantly increased BRN-2 binding to DNA oligonucleotide of the OCT consensus sequence in cortical samples of transgenic mice. No significant increase in DNA binding could be detected in striatal or cerebellar samples. Three DNA binding complexes could be identified upon OCT EMSAs of neural tissue and these appear to correspond to the DNA binding complexes of OCT 1 (band 1), N-OCT-2 (band 2) and N-OCT-3 (BRN-2) identified previously by Schreiber et al. (1990). The lower molecular weight (faster migrating) binding complex 3 not only corresponded to the N-OCT-3 complex, but attempts to supershift this complex using the SC-BRN-2 antibody repeatedly resulted in abolition of this binding complex. No supershifted complex was seen, but this could be due to the antibody interfering with the ability of the native transcription factor to bind to the oligonucleotide and retard its own migration through the gel. This particular antibody is not recommended for supershift by the producers, presumably precisely because of this reason, but abolition of this binding complex does appear to confirm that the BRN-2 antibody does disrupt binding, indicating that this binding factor is indeed N-OCT-3/BRN-2. Attempts to analyse the upper complexes of OCT-1 and N-OCT-2 did not reveal any significant recurring pattern of binding, although basic observation did appear to indicate a reduced presence of OCT-1 and OCT-2 binding in the transgenic striatum and cortex. Despite this confusing variation in OCT-1 and 2 binding, BRN-2 binding was consistently increased in cortex. This observation seems to be directly opposed to any hypothesis proposing reduced capability of polyglutamine transcription factors to bind DNA due to the presence of inclusions of abnormal huntingtin protein. It does, however, leave the question of why there is increased BRN-2 binding in the cortex of transgenic animals. BRN-2 has been previously demonstrated to be of prime importance in the development of both the cortex and the PVN (introduction and work of Nakai et al/Schonemann et al., above) and differences in expression of this transcription factor have been observed in both of these structures in transgenes. As yet, it is impossible to accurately speculate why such abnormalities are present, but such dramatic increase in cortical binding could indicate reinitiation of a developmental process under conditions of

cellular stress. Significant degeneration of cortical neurones, especially in the anterior cingulate cortex has been reported in these transgenic mice (Davies and Turmaine, personal communication) and previous studies have indicated the potential role of BRN-2 in controlling expression of neural cell adhesion molecules during cortical development (Hagino-Yamagishi et al. 1997). Perhaps this increased cortical DNA binding reflects a reactivation of developmental processes as an attempt to retain cortical integrity while cell death occurs. Likewise, this degeneration of other CNS structures could result in reduced stimulus of the pathways responsible for activating BRN-2 expression in PVN cells, which in turn could alter PVN function. It is curious though, that although BRN-2 expression appears to be reduced in the PVN of R6/2 transgenes, vasopressin expression (which appears to be regulated by BRN-2) appears normal. Further research is needed to answer these questions and clarify these proposals.

4.4D Huntington's disease, neuronal intra-nuclear inclusions and polyglutamines: A brief overview

The importance of polyglutamines in trinucleotide repeat disorder pathogenesis is indisputable. The formation of NII in these disorders also appears to be a distinct pathological feature common to all trinucleotide repeat disorders. Ubiquitin and ataxin-3 positive NII can be observed in the nuclei of patients with SCA 3/MJD (Paulson et al 1997). Ubiquitin positive NII are also present in post-mortem material from DRPLA patients (Becher et al.1998). Conversely, in the neurological disorder neuronal intranuclear inclusion disease (NINID), it has been demonstrated that the eosinophilic and ubiquitin positive inclusions do indeed contain polyglutamine (Liebermann et al. 1998). The toxicity of polyglutamines is further indicated by the transgenic mouse models of these disorders. Furthermore, two of these models do provide an extremely strong correlation between NII formation in neuronal nuclei and symptomatic onset, a scenario which is difficult to determine using human post-mortem material. Although this alone does not conclusively prove that that NII are responsible for neuronal dysfunction, these observations do provide compelling evidence that this may indeed be the case. The neurological phenotype of R6/2 mice becomes particularly prominent at approximately nine weeks of age, usually two weeks after NII become visible by EM in the neuronal

nucleus (Davies et al. 1997). Simultaneous with these neurological symptoms is the pronounced nuclear indentation, which follows the appearance of NII. However, it is still worth noting that a significant reduction in R6/2 brain weight occurs before NII are widespread and that this correlates with, or occurs just after the appearance of huntingtin protein in the nucleus (4.5-5 weeks). This could indicate a pathogenic capacity for huntingtin protein without it aggregating and forming an inclusion, or it may simply be that the initial stages of NII formation are not easily observed. The correlation between NII formation and symptomatic onset is further supported by the creation of SCA 1 transgenic mice in which a mutant ataxin-1 protein containing 82 polyglutamine repeats is expressed in Purkinje cells (Skinner et al. 1997). A similar pattern to that observed in R6/2 mice is seen. SCA 1 mice demonstrate neurological symptoms (primarily ataxia) at eighteen weeks of age. This follows on from earlier abnormal distribution of ataxin 1 in the nucleus, 25-90% of Purkinje cells demonstrating ataxin-1 reactive NII of 2 microns in diameter at 12 weeks of age. It is worth noting here that Skinner et al. observe wild type ataxin-1 in the Purkinje cell nuclei of control mice, suggesting that the normal role of ataxin-1 is involved with nuclear matrix function. In normal mouse Purkinje nuclei, ataxin-1 is present in several 0.5 micrometre nuclear bodies. This however does not necessarily indicate that abnormal polyglutamine proteins entering the nucleus must cause neuronal dysfunction by disrupting the nuclear matrix. The known function of two trinucleotide repeat disorder proteins, the androgen receptor in SBMA and the SCA 6 calcium ion channel, indicates they do not necessarily relate to nuclear matrix function. It is also worth noting that huntingtin, for example, is normally localised in the cytoplasm of neurones. The HPRT mutant mice (Ordway, et al 1997) further reinforce the importance of polyglutamines as a pathogenic agent. By inserting 146 CAG repeats into the mouse hypoxanthine phosphoribosyltransferase gene (a protein which is not implicated in any neurodegenerative disorder) Ordway et al. demonstrated that a ' classic repeat disorder' gene does not need to be mutated to produce a neurological condition. HPRT JO1 mice demonstrate seizures in response to being handled (as indeed do R6/2 mice, but this is the major phenotype of the JO1). Seizures usually begin to occur in mice older than 18 weeks. Unfortunately mice were only examined for nuclear pathology in significant numbers long after symptomatic onset (30-46 weeks), so a parallel between NII formation

and symptomatic onset cannot be drawn. It is interesting to note that the description of inclusions observed in both R6/2 mice and HPRT JO1 mice using EM indicates similar morphology. Both are described as a mixture of filamentous material and granular matrix (Davies et al. 1997, Ordway et al. 1997). It is clear from this work that polyglutamines are neurotoxic, at least to the extent that they induce neuronal dysfunction, if not actually death of the cell. Despite the specifity of the pathological action of polyglutamines it is still not totally clear if NII are the neurotoxic agents themselves, or how they form. It is likely that large proteins such as huntingtin are cleaved, the polyglutamines forming sub-50 kD fragments that can diffuse through nuclear pores. It has been proposed that proteins such as huntingtin and ataxin-1 aggregate in the nucleus via interaction with specific nuclear proteins for which they have a high binding affinity (Ross, 1997). Work by Scherzinger et al. (1997) has indicated that polyglutamine proteins may form 'amyloid-like' beta pleated sheet aggregates, indicating a parallel process between pathogenesis in CAG repeat disorders and non-repeat disorders, particularly Alzheimers disease.

Polyglutamine repeats appear to be a major factor in the formation of nuclear inclusions, which in turn are temporally associated with the onset of neurological symptoms in both transgenic mice and humans. The potential for polyglutamines to be generally capable of forming inclusions is particularly indicated by the work of Ordway et al. (1997). However, it is still not entirely clear what the cellular process which leads to NII formation is and indeed if polyglutamines are essential for NII formation. This in turn is indicated by other disorders, particularly viral infections, in which NII are pathological features, yet polyglutamines are not indicated in aetiology. It is possible that these seemingly unrelated disorders could teach us something about NII formation. For example, both canine distemper virus (CDV) (Oglesbee, 1992 and Oglesbee and Krakowa, 1993) and human cytomegalovirus (Perlman and Arglye, 1992) are capable of inducing neurological symptoms, and both disorders can feature NII. Canine distemper virus provides an intriguing insight into non-polyglutamine repeat nuclear inclusion formation. Canine distemper virus is a paramyxovirus which contains RNA, not DNA and as such does not need to enter the nucleus of the cell in order to reproduce. However, viral coat protein accumulates in the nucleus of CDV infected astrocytes forming 'granulofilamentous matrix' described by the author as an intranuclear inclusion body

(INB)(Oglesbee, 1992). The mechanism regulating for this process is not clear, and it could indeed constitute some attempt by the virus to interfere with host cell mRNA processing by disrupting the nuclear matrix as proposed by the author. It could also constitute a generalised cellular response to an abnormal or foreign protein presence. Further work by the same author has demonstrated that the cellular stress response plays an important role in the formation of these astrocytic INB. The INB was found to consist of the major CDV nucleocapsid protein (N-protein) and that INB would only form if elevated levels of cytoplasmic heat shock protein 72 (HSP 72) were also present, and if HSP 72 could be localised to the nucleus. HSP 72 appears to be responsible for the nuclear translocation of the N-protein (Oglesbee and Krakowa, 1993). The authors state that INB formation is a unique viral 'cytopathic effect', providing some evidence that NII may indeed be pathogenic agents. HSP 72 seems specifically to be a protein associated with stress induction in the nervous system, increased expression being observed in neurons and glia following percussive brain injury and experimental cerebral ishaemia (McIntosh and Raghupathi, 1995). HSP 72 appears to be normally associated with the nuclear matrix (indeed the only known HSP specifically associated with nuclear structures), being localised in the nucleus and nucleolus, but its exact function is unknown (Marcuccilli and Miller, 1994). Of course, this may not relate at all to NII formation in polyglutamine disorders, but it is worthy of consideration. Polyglutamines obviously play an essential role in the natural history of many neurological disorders. This appears to be beyond question. The role of NII is somewhat less clear, if these bodies are indeed active pathogenic agents the manner by which they dysregulate cell function is yet to be determined. It may also be useful to consider that that there may be other cellular processes capable of forming NII, even where polyglutamines are not implicated. This process hints that there are two totally unrelated cellular processes capable of forming NII in diseased tissue, or that polyglutamines are not directly essential for NII formation, but are most certainly an agent capable of inducing NII formation and pathogenesis.

4.5 Some brief ideas for future work

A. NF-κB in the striatum

NF-κB -p52 localisation to neuronal nuclear bodies

The localisation of the p52 protein to undetermined nuclear bodies has been largely ignored in this thesis. However, this information could prove useful to further dissection of the nuclear matrix. An interesting study would be to conduct dual labelling (eg. immunogold/DAB-DAB nickel) EM in an attempt to discover the nature of these bodies. Immunocytochemical analysis at EM would allow accurate measurement of the p52 reactive bodies, and if available antibodies to the SMN protein (Liu and Dreyfuss, 1996) or p80 coilin (Brash and Ochs, 1992) would determine if these structures were coiled bodies or their gemini. Little is known about nuclear organisation and such a study would hopefully provide valuable information about the function of discrete nuclear structures.

NF-κB p65 /p50-35 analysis in rat brain

NF-κB p65 does not migrate at 65kD when examined by western blotting. This could indicate a variation of processing of this protein in the brain. Ultimately determination of the amino acid sequence of the 50 kD protein observed and comparison to the p65 sequence, would answer this question and indicate conclusively whether or not this protein is a fragment of p65. A similar study would also reveal if the 35 kD protein detected by p50 antisera is merely a breakdown product or a novel protein.

NF-κB p65/p52 role in glial activation

This work hopefully indicates the importance of p65/p52 in the glial response to neural insult. However there is obviously some uncertainty when conducting DNA binding studies *in vivo* to confirm the cell type in which increased DNA binding is occurring. Cell culture studies of astrocytes and microglia could provide more information about expression of p65/p52 in these cells and could confirm almost absolutely, for example, that microglia expressing OX-42 are indeed the same cells that express p52 following QA lesion *in vivo*. The capacity of salicylate compounds to prevent NF-κB DNA binding could be further examined studying microglia and astrocytes *in vitro*.

NF-κB DNA binding following QA and CNTF

NF-κB DNA binding after the administration of both CNTF and QA could be examined at a greater range of time points, particularly between 12 and 24 hours, to provide more detailed information about the peak of DNA binding. Examination of NF-κB DNA binding after 168 hours would also indicate how rapidly NF-kB DNA binding returns to constitutive levels of activity.

B.R6/2 transgenes

BRN-2 function in R6/2 transgenes

This work seems to indicate that there is some abnormality in BRN-2 function in the R6/2 mouse brain. The increased DNA binding observed in the cortex could be the pathologically induced re-activation of a developmental process or a response to cellular stress that has been previously undescribed. Decreased expression of BRN-2 in the PVN could be a result of dysfunctional cortical input into the PVN and may be responsible for some of the symptoms observed in the R6/2 mice. These observations appear to demand further investigation of the role of BRN-2 in Huntington's disease and a deeper study of hypothalamic function in the transgenes.

Could polyglutamines disrupt nuclear transport?

The entry into the nucleus of normally non-nuclear proteins such as fragments of expanded huntingtin could possibly interfere with the nuclear transport mechanism. Any cellular attempt to remove nuclear aggregates could lead to interference with nuclear pore function. There is no direct evidence to suggest this, but the indentation of the nuclear membrane observed in R6/2 transgenes at 9 plus weeks could constitute a cellular attempt to increase nuclear surface area. This could indicate a problem with nuclear transport. Previous work by Mark Turmaine (unpublished observations) and more recently by Hayden, Ross et al. (unpublished observations) has indicated possible intra-nuclear huntingtin aggregation at nuclear pores. A careful EM survey of nuclear pore numbers and morphology, comparing R6/2 transgenic neurones with those of controls, could provide some indication of nuclear transport viability. Similar EM work upon nuclear pores has been conducted before (Daneholt, 1997, see Ullman et al. 1997).

Is the HSP72 response universal in II/NII formation?

The cellular localisation and expression of the heat shock protein 72 in R6/2 transgenes compared to littermate controls would constitute an interesting experiment. The work of Oglesbee and Krakowa (1993) presents a potential role for HSP72 in nuclear inclusion formation in canine distemper virus encephalomyelitus. If polyglutamine toxicity induces a general rather than a specific cellular response, HSP72 may be implicated in polyglutamine NII formation. This work would complement the current interest in the study of chaperonin proteins in CAG repeat disorder pathogenesis.

4.6 In conclusion

This work confirms that:

-The neurocytokine CNTF is a potent glial activator and when administered into the striatum is capable of activating both astrocytes and microglia, as determined by GFAP and OX-42 immunocytochemistry.

-The NF-κB subunits p65, p50 and p52 are expressed in the neurones of the normal rat striatum and that NF-κB is active (ie. bound to DNA) in the normal cortex.

-The NMDA receptor agonist QA induces NF-κB DNA binding following lesion.

This work demonstrates that:

-CNTF, when administered with the excitotoxin QA into the rat striatum, does not alter the rate of survival of medium-sized neurones or cholinergic or NADPH-d positive interneurones. Nor does CNTF induce any significant morphological alteration upon these cell types. However, CNTF is a potent glial activator.

-The p52 NF-kB subunit is expressed 1) in unidentified nuclear bodies within the majority of striatal and cortical neurones and 2) is expressed in the perikarya and processes of a class of medium sized striatal neurones which have a mainly dorso-lateral distribution throughout the striatum.

-The NMDA receptor agonist and excitotoxin QA, and the neurocytokine CNTF, induce increased NF-κB binding to DNA in a biphasic manner. It is hypothesised that the initial period of binding (12-24 hours) is a predominantly neuronal response, while the later (168 hours) response is representative of the increased number of glial cells (astrocyte and microglial-like) expressing NF-κB.

-The NF-κB protein p65 is expressed in astrocyte-like cells and the protein p52 is expressed in microglial-like cells and a sub-class of astrocyte-like cells following QA lesion and to a lesser extent following CNTF administration.

-Localisation, expression and DNA binding capability of the polyglutamine transcription factors TBP and glucocorticoid receptor are not significantly altered in R6/2 transgenic mice models of Huntington's disease. However, there appears to be increased DNA binding activity of the polyglutamine repeat factor BRN-2 in transgenic cortex and decreased expression of BRN-2 in the transgenic paraventricular nucleus.

Appendix 1:Camera lucida drawings of interneurone distribution in the rat striatum

Opposite are two camera lucida diagrams of rat half brains in the coronal plane. These sections are approximately AP+ 0.3 cm from bregma. These diagrams illustrate the fairly homogeneous distribution of (1) cholinergic interneurons as determined by acetylcholinesterase staining (see methods) and (2) NADPH diaphorase interneurons as determined by NADPH staining. They may be used to compare the distribution of these cell types to that of the p52 reactive striatal neurones outlined in this thesis (results: Fig. 3.2/3). Scale bar = 2 mm.

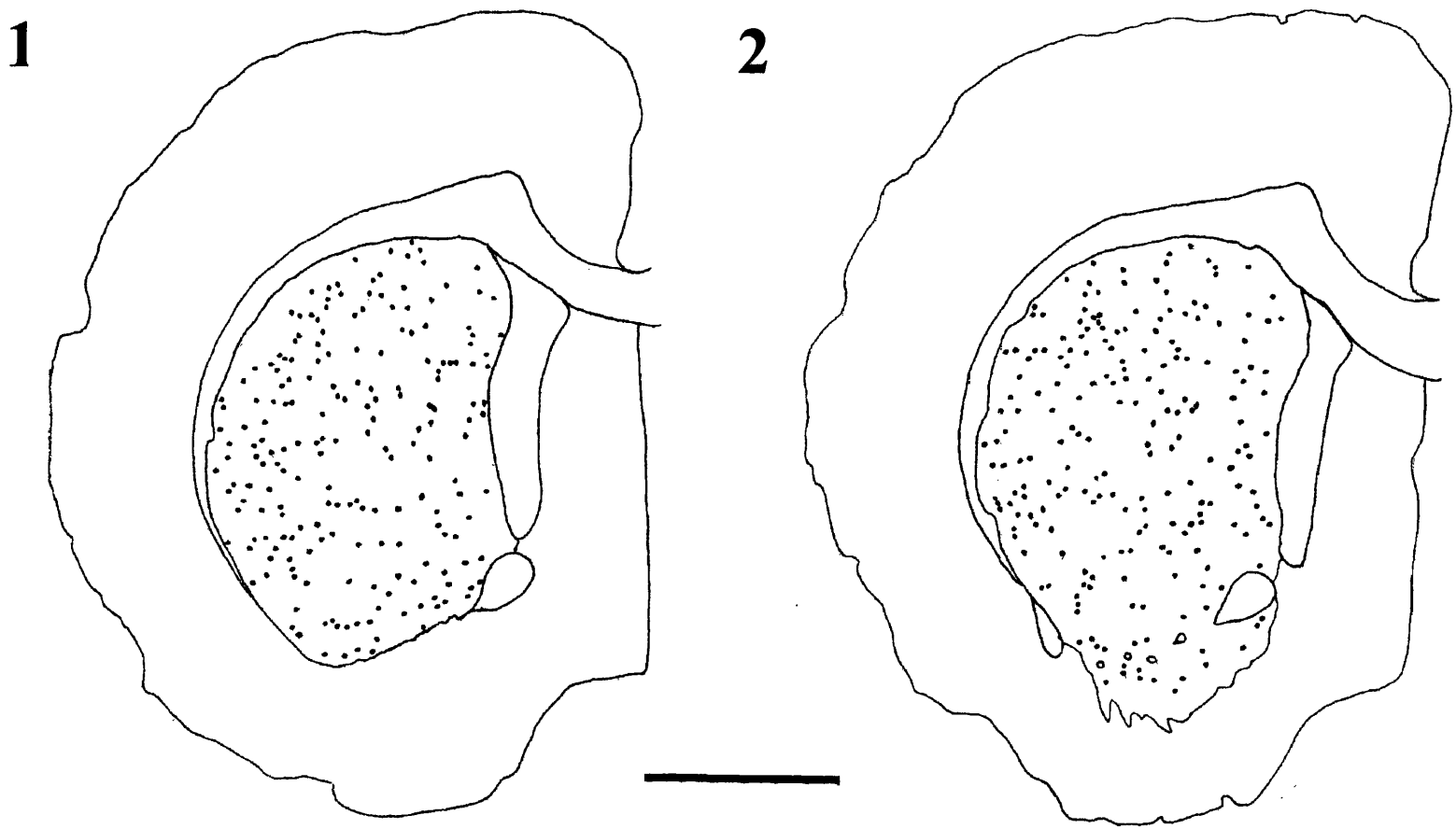
1
2

REFERENCES

Adler, R., Landa, K.B., Manthorpe, M. and Varon, S. Cholinergic, neuroneotrophic factors: intraocular distribution of trophic activity for ciliary neurones. *Science*, 204, (1979), 1434-1436.

Ahima, R. and Harlan, R.E. Charting of type II glucocorticoid receptor like immunoreactivity in the rat central nervous system. *Neuroscience*, 39, (1990), 579-604.

Ahima. R., Krozowski, Z. and Harlan, R. Type I corticosteroid like receptor immunoreactivity in the rat CNS: distribution and regulation by corticosteroids. *J. Comp. Neurol.* 313, (1991), 522-538.

Albin, R.L., Qin, Y., Young, A.B., Penney, J.B. and Chesselet, M-F. Preproenkephalin mRNA containing neurons in striatum of patients with symptomatic and presymptomatic Huntington's disease: An in situ hybridization study. *Ann. Neurol.*, 30, (1991), 542-549.

Alexander, G.E. and Crutcher, M.D. Functional architecture of basal ganglia cicuits, *TINS*, 13, (1990), 266-271.

ALS CNTF treatment study group. A double blind placebo-controlled clinical trial of subcutaeneous recombinant human ciliary neurotrophic factor (rhCNTF) in amyotrophic lateral sclerosis. *Neurology*, 46, (1996), 1244-1249.

Anderson, K.D., Panayotatos, N., Corcoran, T.L., Lindsay, R.M. and Wiegand, S.J., ciliary neurotrophic factor protects striatal output neurons in an animal model of Huntington's disease. *PNAS*, 93, (1996), 7346-7351.

Andrews, N.C. and Faller, D.V. A rapid micropreparation technique for extraction of DNA binding proteins from limiting numbers of mammalian cells, *Nucleic Acids Res.*, 19 (1991) 2499.

Arakawa, Y., Sendtner, M. and Thoenen, H. Survival effect of ciliary neurotrophic factor (CNTF) on chick embryonic motoneurons in culture: comparison with other neurotrophic factors and cytokines. *J. Neurosci.* 10, (1990), 3507-2515.

Arika, S., Isshiki, H., Sugita, T., Tanabe, O., Kinoshita, S., Nishio, Y., Nakajima, T., Hirano, T. and Kishimoto, T. A nuclear factor for IL-6 expression (NF-IL6) is a member of a C/EBP family. *EMBO J.* 9, (1990), 1897-1906.

Aronin, N., Cooper, P.E., Lorenz, L.J., Bird, E.D., Sagar, S.M. Leeman, S.E. and Martin, J.B. Somatostatin is increased in the basal ganglia in Huntington's disease. *Ann. Neurol.*, 13, (1983), 519-526.

Arriza, J.L., Weinberger, C., Cerilli, G., Glaser, T.M., Handelin, B.L., Housman, D.E. and Evans, R.M. Cloning of human mineralocorticoid receptor complementary DNA : structural and functional kinship with the glucocorticoid receptor. *Science*, 237, (1987), 268-275.

Asada, H., Ip, N.Y., Pan, L., Razack. N., Parfitt, M.M. and Plunkett, R.J. Time course of ciliary neurotrophic factor mRNA expression is coincident with the presence of protoplasmic astrocytes in traumatized rat striatum, J. *Neurosci.Res.*, 40 (1995) 22-30.

Auphan, N., DiDonato, J.A., Rosette, C., Helmberg, A. and Karin, M. Immunosuppression by glucocorticoids: Inhibition of NF-kB activity through induction of IkB synthesis. *Science*, 270, (1995), 286-290.

Baeuerle, P.A.,[1] and Baltimore, D. IκB: a specific inhibitor of the NF-kB transcription factor, *Science*, 242 (1988) 540-546.

Baeuerle, P.A.,[2] and Baltimore, D., NF-κB: Ten years after, *Cell*, 87 (1996) 13-20.

Baeuerle, P.A. and Henkel, T. Function and activation of NF-kB in the immune system. *Ann. Rev. Immunol.*, 12, (1994), 141.

Bakalkin, G.Y., Yakovleva, T., and Terenius, L., NF-kB like factors in the murine brain, developmentally regulated and tissue specific expression, *Mol. Brain. Res.*, 20 (1993) 137-146.

Balasingham, V., Tejada-Berges, T., Wright, E., Bouckova, R., and Yong, V.W. Reactive astrogliosis in the neonatal mouse brain and its modulation by cytokines, *J.Neuroscience*, 14 (1994) 846-856.

Baltimore, D. and Beg, A.A. A butterfly flutters by. *Nature*, 373, (1995), 311.

Barbin, G., Manthorpe, M., and Varon, S., Purification of the chick eye ciliary neuronotrophic factor, *J. Neurochemistry*, 43 (1984) 1468-78.

Barger, S.W. and Harmon, A.D. Microglial activation by Alzheimer amyloid precursor protein and modulation by apolipoprotein E. *Nature*, 388, (1997), 878-881.

Barger, S.W., Horster, D., Furukawa, K., Goodman, Y., Kreiglstein, J. and Mattson, M.P. Tumour necrosis factors alpha and beta protect neurons against amyloid beta-peptide toxicity: Evidence for involvement of a kB-binding factor and attenuation of peroxide and calcium accumulation. *PNAS*, 92, (1995), 9328-9332.

Bazan, J.F., Neuropoietic cytokines in the hematpoietic fold, *Neuron*, 7 (1991) 197-208.

Beal, M.F., Kowall, N.W., Ellison, D.W., Mazurek, M.F., Swartz, K.J. and Martin, J.B. Replication of the neurochemical chracteristics of Huntington's disease by quinolinic acid. *Nature*, 321, (1986), 168-171.

Beal, M.F., Ferrante, R.J., Swartz, K.J. and Kowall, N.W., Chronic quinolinic acid lesions in rats closely resemble Huntington's disease. *J. Neurosci.*, 11, (1991), 1649-1659.

Beaumont, K. and Fanestil, D.D. Characterisation of rat brain aldosterone receptors reveals high affinity for corticosterone. *Endocrinology*, 113, (1983), 2043-2051.

Becher, M.W., Kotzuk, J., Sharp, A.H., Davies, S.W., Bates, G.P., Price, D.L, and Ross, C.A, Intranuclear neuronal inclusions in Huntington's disease and dentatorubral and pallidoluysian atrophy: correlation between density of inclusions and IT15 CAG triplet repeat length, *Neurobiology of Disease*, 4, (1998), 387-397.

Beg, A.A., Sha, W.C., Bronson, R.T., Ghosh, S. and Baltimore, D. Embryonic lethality and liver degeneration in mice lacking the Rel A component of NF-kB. *Nature*, 376, (1995), 167-170.

Behl, C., Davis, J.B., Lesley, R. and Schuhert, D. Hydrogen peroxide mediates amyloid beta protein toxicity. *Cell*, 77, (1994), 817-827.

Bellorini, M., Moncollin, V., D'Incalci, M., Mongelli, N. and Mantovani, R. Distamycin A and tallimustine inhibit TBP binding and basal in vitro transcription. *Nuc. Acids Res.*, 23, (1995), 1657-1663.

Bird, E.D. and Iversen, L.L. Huntington's chorea-post-mortem measurement of glutamic acid decarboxylase, choline acetyltransferase and dopamine in basal ganglia. *Brain*, 97 (1974), 457-72.

Bird, E.D. Chemical pathology of Huntington's disease, *Ann. Rev. Pharmacol. Toxicol.*, 20, (1980), 533-551.

Blank, V., Kourilsky, P., and Israel, A., Cytoplasmic retention, DNA binding and processing of the NF-kB p50 precursor are controlled by a small region in its C-terminus, *EMBO J.* 10 (1991) 4159-4167.

Boegman, R.J. and Parent, A. Differential sensitivity of neuropeptide Y, somatostatin and NADPH diaphorase containing neurons in rat cortex and striatum to quinolininc acid. *Brain Res.*, 445, (1988), 358-362.

Boegman, R.J., Smith, Y., and Parent, A., Quinolinic acid does not spare striatal neuropeptide Y-immunoreactive neurons, *Brain Res.*, 415 (1987) 178-182.

Bolam. J.P., Somogyi, P., Takagi, H., Fodor, I. And Smith, A.D. Localisation of substance-P like immunoreactivity in neurons and nerve terminals in the neostriatum of the rat: a corrleated light and electron microscopic study. *J. Neurocytol.*, 12, (1983), 325-344.

Bolam, J.P., Wainer, B.H. and Smith, A.D. Characterisation of rat cholinergic neurones in the neostriatum. A combination of choline acetyltransferase immunohistochemistry, Golgi impregnation and electron microscopy. *Neuroscience*, 12, (1984), 711-718.

Bonni, A., Frank, D.A., Schindler, C. Greenberg, M.E. Characterization of a pathway for CNTF signalling to the nucleus, *Science*, 262 (1993) 1575-79.

Bonni, A., Sun, Y., Nadal-Vicens, M., Bhatt, A., Frank, D.A., Rozovsky, I., Stahl, N., Yancopoulos, G.D. and Greenberg, M.E. Regulation of gliogenesis in the central nervous system by the JAK-STAT signalling pathway. *Science*, 278, (1997), 477-483.

Bouyer, J.J., Park, D.H., Joh, T.H. and Pickel, V.M. Chemical and structural analysis of the relationship between cortical inputs and tyrosine hydroxylase containing terminals in rat neostriatum. *Brain Res.*, 302, (1984), 267-275.

Brasch, K., and Ochs, R.L., Nuclear bodies (Nbs): A newly "rediscovered" organelle, *Exp. Cell. Res.*, 202 (1992) 211-223.

Buratowski, S. The basics of basal transcription by RNA polymerase II. *Cell*, 77, (1994), 1.

Burright, E.N., Clark, H.B., Seravadio, A., Matilla, T., Fedderson, R.M., Yunis, W.S., Duvick, L.A., Zoghbi, H.Y, and Orr H.T. SCA1 transgenic mice: A model for neurodegeneration caused by an expanded CAG trinucleotide repeat, *Cell*, 82, (1995), 937-948.

* **Caldenhoven**, E., Liden, J., Wissink, S., Van de Stolpe, A., Raajimakers, J., Koenderman, L., Okret, S., Gustafsson, JA. and Van der Saag. Negative cross-talk between Rel A and the glucocorticoid receptor: A possible mechanism for the antiinflammatory action of glucocorticoids. *Mol. Endocrinology*, 9, (1995), 401-412.

Carnow, T.B., Manthorpe, M., Davis, G.E. and Varon, S. Localised survival of ciliary ganglionic identifies neuronotrophic bands factor bands on nitrocellulose blots. *J. Neurosci.* 5, (1985), 1965-1971.

Chao, C.C., Hu, S., and Peterson, P.K., Glia, cytokines and neurotoxicity, *Crit. Rev. Neurobiol.*, 9 (1995) 189-205.

Chen, Q. and Reiner, A. Cellular distribution of the NMDAR NR2A/2B subunits in the rat striatum. *Brain Res.* 743, (1996), 346-352.

Chen, Z.J., Parent, L. and Maniatis, T. Site specific phosphorylation of IkB-alpha by a novel ubiquitination dependant protein kinase activity. *Cell*, 84, (1996), 853-862.

Cheeselet. M-F. and Delfs, J.M. Basal ganglia and movement disorders: an update. *TINS*, 19, (1996), 417-421.

Choi, D.W. Nitric oxide: friend or foe to the injured brain? *PNAS*, 90. (1993), 9808-9812.

* **Buzy**, J.M., Lindstrom, L.M., Zink, M.C. and Clemens, J.E. HIV-1 in the developing CNS: developmental differences in gene expression. *Virology*, 210 (1995), 361-371

Clark, S., Stasheff, S., Lewis, D.V., Martin, D. and Wilson, W.A. NMDA receptors, neuronal development and neurodegeneration. In : *The NMDA receptor*, Collingridge,G.L., Watkins, J.C., Oxford University Press (2nd Ed.) 395-427, 1994.

Clatterbuck, R.E., Price, D.L., Koliatsos, V.E., CNTF stimulates the expression of GFAP by brain astrocytes in vivo, *J.Comp. Neurol.*, 369 (1996) 543-551.

Clemens, J.A, Stephenson, D.T., Dixon, E,P., Smalstig, B., Mincy, R.E., Rash, K.S. and Little, S.P. global cerebral ischemia activates nuclear factor-kB prior to evidence of DNA fragmentation. *Mol. Brain Res.*, 48, (1997), 187-196.

Connelly, M.A. and Marcu, K.B. CHUK, a new member of the helix-loop-helix and leucine zipper families of interacing proteins, contains a serine-threonine kinase catalytic domain. *Cell. Mol. Biol. Res.*, 15, (1995), 537, 549.

Cowan, R.L., Wilson, C.J., Emson, P.C. and Heizman, C.W. Parvalbumin-containing GABAergic neurons in the rat striatum. *J. Comp. Neurol.*, 302, (1990), 197-205.

Coyle, J.T. and Schwarcz, R. Lesion of striatal neurones with kainic acid provides a model for Huntington's chorea. *Nature*, 263, (1976), 244-246.

David, G., Abbas, N., Stevain, G., Durr, A., Yvert, G., Cancel, G., Weber, C., Imbert, G., Saudou, F., Antoniou., et al. Cloning of the SCA7 gene reveals a highly unstable CAG repeat expansion. *Nature Genetics*, 17, (1997), 65-70.

Davies S.W. and Beardsall, K. Nerve growth factor selectively prevents excitotoxin induced degeneration of striatal cholinergic neurons. *Neurosci. Letts.*, 140, (1992), 161-164.

Davies, S.W., Beardsall, K., Turmaine, M., DiFiglia, M., Aronin, N. and Bates, G.P., Are intranuclear inclusions the common neuropathology of triplet-repeat disorders with plyglutamine-repeat expansions? *The Lancet*, 351, (1998), 131-133.

Davies, S.W. and Roberts, P.J. No evidence for a selective preservation of striatal neurons by quinolinic acid. *Nature*, 327, (1987), 326-329.

Davies, S.W., and Roberts, P.J., Sparing of cholinergic neurons following quinolinic acid lesions of the rat striatum, *Neuroscience*, 26 (1988) 387-393.

Davies, S.W., Turmaine, M., Cozens, B., Difiglia, M., Sharp, A.H., Ross, C.A., Scherzinger, E., Wanker, E.E, Mangiarini, L. and Bates, G.P. Formation of neuronal nuclear inclusions underlies the neuronal dysfunction in mice transgenic for the HD mutation. *Cell*, 90, (1997) 537-548.

Davis, S., Aldrich, T.H., Valenzuela, D.M., Wong, V., Firth, V., Squinto, M.E. and Yancopoulos, G.D. The receptor for ciliary neurotrophic factor. *Science*, 253, (1993), 59-63.

Dawson, V.L., Dawson, T.M., Bartley, D.A., Uhl, G.R. and Snyder, S.H. Mechanisms of nitric oxide mediated neurotoxicity in primary brain cultures. *J. Neurosci.*, 13, (1993), 2651-2661.

DeChiara, T.M., Vejsada, R., Poueymirou, W.T., Acheson, A., Suri, C., Conover, J.C., Fried man, B., McClain, J., Pan, L., Stahl, N., Ip, N.Y., Kato, A, and Yancopoulos, D., Mice lacking the CNTF receptor, unlike mice lacking CNTF, exhibit profound motor neuron deficits at birth, *Cell*, 83 (1995) 313-322.

DeKloet, E.R. and Reul, J.M.H.M. Feedback action and tonic influence of corticosteroids on brain function: a concept arising from heterogeneity of brain receptor systems. *Psychoneuroendocrinology*, 12, (1987), 83-105.

DeKloet, E.R., Wallach, G. and McEwen, B.S. Differences in corticosterone and dexamethasone binding to rat brain and pitiutary. *Endocrinology*, 96, (1975),598-609.

De la Monte, S.M., Vonsattel, J-P. and Richardson, E.P, Morphometric demonstration of atrophic changes in the cerebral cortex, white matter and neostriatum in Huntington's disease, *J. Neuropath. Exp. Neurol.*, 47, (1988) 516-525.

DeLong, M.R. Primate models of movement disorders of basal ganglia origin, *TINS*, 13, (1990), 281-285.

de Martin, R., Vanhove, B., Cheng, Q., Hofer, E., Csizmada, V., Winkler, H. and Bech, F.H. Cytokine inducible expression in endothelial cells of an IkB alpha-like gene is regulated by NF-kB. *EMBO J*, 12, (1993), 2773.

DiDonato, J.A,. Hayakaya, M., Rothwarf, D.M., Zandi, E. and Karin, M. A cytokine-reponsive IkB kinase that activates the transcription factor NF-kB. *Nature*, 388, (1997), 548-554.

DiFiglia, M. and Aronin, N. Ultrastructural features of immunoreactive somatostatin neurons in the rat caudate nucleus. *J. Neurosci.*, 2, (1982), 1267-1274.

DiFiglia, M., Sapp, E., Chase, K., Schwarz, C., Meloni, A., Young, C., Martin, E., Vonsattel, J-P., Carraway, R., Reeves, S.A., Boyce, F.M. and Aronin, N., Huntingtin is a cytoplasmic protein associated with vesicles in human brain and rat brain neurons. *Neuron*, 14, (1995), 1075, 1061.

Divac, I., Fonnum, F. and Storm-Mathiesen, J. High affinity uptake of glutamate in terminals of corticostriatal axons, *Nature*, 266 (1977), 377-378.

Dugan, L.L. and Choi, D.W. Exctiotoxocity, free radicals and cell membrane changes. *Ann. Neurol.*, 35 Supp. (1994), S17-21.

Dumuis, A., Backaert, J., Sebben, M., Haynes, L. and Pin, J.P. NMDA receptors activate the arachadonic acid cascade system in striatal neurones. *Nature*, 336, (1988), 68-70.

Durr, A., et al. Spinocerebellar ataxia 3 and Machado-Joseph disease: clinical, molecular and neuropathological features. *Ann. Neurol.*, 39, (1996), 490-499.

Duyao, M.P., Auerbach, A.B., Ryan, A., Persichetti, F., Barnes, G.T., McNeill, S.M., Ge, P., Vonsattel, J-P., Gusella, J.F., Joyner, A.L. and MacDonald, M.E. Inactivation of the mouse Huntington's disease gene homolog Hdh. *Science*, 269, (1995), 407-410.

Eddleston, M. and Mucke, L. Molecular profile of reactive astrocytes-implications for their role in neurologic disease. *Neuroscience*, 54, (1993), 15-36.

Emerich, D.F., Lindner, M.D., Winn, S.R., Chen, E-Y., Frydel, B.R. and Kordower, J.H. Implants of encapsulated human CNTF producing fibroblasts prevent behaviuoral deficits and striatal degeneration in a rodent model of Huntington's disease. *J. Neurosci.*,16, (1996), 5168-5181.

Ernsberger, U., Sendtner, M. and Rohrer, H., Proliferation and differentiation of embryonic chick sympathetic neurons: Effects of ciliary neurotrophic factor. *Neuron*, 2, (1989), 1275-1284.

Evans, R.B., Gottlieb, P.D. and Bose, H.R. Identification of a Rel-related protein in the nucleus during S phase of the cell cycle. *Mol.Cell. Biol.*, 13, (1993), 6147.

Evans, R.M. and Hollenberg, S.M. Zinc fingers: gilt by association. *Cell*, 52, (1988), 1-3.

Fagg, G.E. and Foster, A.C. Amino acid neurotransmitters and their pathways in the mammalian central nervous system. *Neuroscience*, 9, (1983), 275-298.

Fan, C.M and Maniatis, T. A DNA binding protein containing two widely seperated zinc finger motifs that recognise the same DNA sequence. *Genes Dev.*, (1990), 29.

Ferrante, R.J., Beal, M.F., Kowall, N.W., Richardson, E.P. and Martin, J.B. Sparing of acetylcholinesterase-containing striatal neurons in Huntington's disease. *Brain Res.*, 411, (1987), 162-166.

Ferrante, R.J., Kowall, N.W., Beal, M.F., Richardson, E.P., Bird, E.D. and Martin, J.B. selective sparing of a class of striatal neurons in Huntington's disease. *Science*, 230, (1985), 561-563.

Ferrer, I., Martin, F., Serrano, T., Reiriz, J., Perz-Navarro, E., Alberch, J., Macaya, A., and Planas, A.M., Both apoptosis and necrosis occur following intrastriatal administration of excitotoxins, *Acta Neuropath (Berlin)*., 90 (1995) 504-510.

Fletcher, C., Heintz, N. and Roeder, R.G. Purification and characterisation of OTF-1, a transcription factor regulating cell cycle expression of a human histone H2b gene. *Cell*, 51, (1987), 773.

Fonnum, F., Storm-Mathiesen, J. and Divac, I. Biochemical evidence for glutamate as a neurotransmitter in corticostriatal and corticothalamic fibres in rat brain, *Neuroscience*, 6, (1981), 863-873.

Forloni, G.L., Angeretti, N., Rizzi, M. and Vezzani, A. Chronic infusion of quinolinic acid in the rat striatum: effects on discrete neuronal populations, *J. Neurol. Sci.*, 108, (1992), 129-136.

Friedman, B., Scherer, S., Rudge, J.S., Helgren, M., Morrisey, D., McClain, J., Wang, D., Wiegand, S.L., furth, M.E., Lindsay, R.M. and Ip, N.Y. Regulation of ciliary neurotrophic factor expression in myelin related Schwann cells in vivo. *Neuron*, 9, (1992), 295-305.

Freund, T.F., Powell, J.F. and Smith, A.D. Tyrosine hydroxylase immunoreactive boutons in synaptic conduct with identified striatonigral neurons, with particular reference to dendritic spines. *Neuroscience*, 13 (1984), 1189-1215.

Fujii, H. and Hamada, H. A CNS specific POU transcription factor, Brn-2, is required for establishing mammalian neural cell lineages. *Neuron*, 11, (1993), 1197-1206.

Gallin, W.J. and Greenberg, M.E. Calcium regulation of gene expression: the mode of entry matters. *Curr. Op. Neurobiol.*, 5, (1995), 367-374.

Gray, H. and Carter, H.V. *Gray's Anatomy*, John.W Parker, London, 1858.

Green, S., and Chambon, P. Nuclear receptors enhance our understanding of transcriptional regulation. *TIGS*, 4, (1988), 309-314.

Gerber, H-P., Seipel, K., Georgiev, O., Hofferer, M., Hug, M., Rusconi, S. and Schaffner, W. Transcriptional activation modulated by homopolymeric and glutamine and proline stretches. *Science*, 263, (1994), 808-811.

Gerfen, C.R. The neostriatal mosaic: compartmentalisation of corticostriatal input and striatonigral output systems. *Nature*, 311, (1984), 461-463.

Gerfen, C.R., The neostriatal mosaic: multiple levels of compartmental organization. *TINS*, 15, (1992), 133-139.

Gerfen, C., Engber, T., Mahan. L., susel, Z., Chase, T., Monsma, F., and Sibley, D. D1 and D2 dopamine receptor regulated gene expression of striatonigral and striatopallidal neurons. *Science*, 250, (1990), 1429-1432.

Gerfen, C. and Young, W.S. Distribution of striatonigral and striatopallidal peptidergic neurons in both patch and matrix compartments: an in situ hybridisation histochemistry and fluorescent retrograde tracing study. *Brain Res.*, 460, (1988), 161-167.

Ghosh. S.,[1] and Baltimore, D., Activation in vitro of NF-kB by phosphorylation of its inhibitor IkB, *Nature*, 344 (1990) 678-682.

Ghosh, S.,[2] Gifford, A.M. Riviere, L.R., Tempst, P., Nolan, G.P., and Baltimore, D., Cloning of the p50 DNA binding subunit of NF-kB: Homology to rel and dorsal, *Cell*, 62 (1990) 1019-1029.

Gilmore, T.D., Regulation of Rel transcription complexes, in: Goodbourn, S., *Eukaryotic transcriptional regulation*, IRL Press/Oxford, New York, (1996), 292 pp.

Giulian, D., IL-1 injected into mammalian brain stimulates astrogliosis and neurovascularization. *J.Neurosci.*, 8 (1988) 2485-90.

Grilli, M., Pizzi, M., Memo, M., and Spano, P., Neuroprotection by aspirin and sodium salicylate through blockade of NF-kB activation, *Science*, 274 (1996) 1383-1385.

Groenewegen, H.J. and Berendse, H.W. Connections of the subthalamic nucleus with the ventral striatopallidal pathway of the basal ganglia in rat. *J. Comp. Neurol.*, 294, (1990), 607-622.

Guerrini, L., Blasi, F. and Denis-Donini, S. Synaptic activation of NF-kB by glutamate in cerebellar granule neurons in vitro. *PNAS*, 92, (1995), 9077-9081.

Guerrini, L., Molteni, A., wirth, T., Kistler, B. and Blasi, F. Glutamate-dependant activation of NF-kB during mouse cerebellum development. *J.Neurosci.*, 17, (1997), 6057-6063.

Gupta, S., Campbell, D., Derijard,B., and Davis, R.J., Transcription factor ATF-2 regulation by the JNK signal transduction pathway, *Science*, 267 (1995) 389-93.

Gusella, J.F., Wexler, N.S., Conneally, P.M., Naylor, S.L., Anderson, M.A., Tanzi, R.E.,Watkins, P.C.,Ottina, K., Wallace, M.R., Sakaguchi, A.Y., Young, A,B., Shoulson, I., Bonilla, E. and Martin, J.B., A polymorphic DNA marker genetically linked to Huntington's disease. *Nature*, 306, (1983), 234-238.

Hagino-Yamagishi, K., Saijoh, Y., Ikeda, M., Ichikawa, M., Minamikawa-Tachino, R. and Hamada, H. Predominant expression of Brn-2 in the post-mitotic neurons of the developing mouse neocortex. *Brain Res.*, 752, (1997), 261-268.

Hantraye, P., Richie, D., Maziere, M. and Isacson, O. A primate model of Huntington's disease:behavioural and anatomical studies of unilateral excitotoxic lesions of the caudate-putamen in the baboon. *Exp. Neurol.*, 108, (1990), 91-104.

Hara, Y., Rovescalli, A.C., Kim, Y. and Nirenberg, M., Structure and evolution of four POU domain genes expressed in mouse brain. *PNAS*, 89, (1992), 3280-3284.

Harper, P.S. Huntington's Disease. WB Saunders Company, London, 1991, 437pp.

He, X., Treacy, M.N., Simmons, D,M., Ingraham, H.A., Swanson, L.W. and Rosenfeld, M.G. Expression of a large family of POU-domain regulatory genes in mammalian brain development. *Nature*, 340, (1989), 35-42.

Heese, K., Fiebich, B.L., Bauer, J. and Otten, U. NF-kB modulates lipopolysaccharide-induced microglial nerve growth factor expression. *Glia*, 22, (1998), 401-407.

Henkel.T., Zabel, U., van Zee. K., Muller, J.M., Fanning, E., and Baeuerle, A., Intramolecular masking of the nuclear location signal and dimerization domain in the precursor for the p50 NF-kB subunit, *Cell*, 68 (1992) 1121-1133.

Hedreen, J.C. and Folstein, S.E, Early loss of neostriatal neurones in Huntington's disease, *J. Neuropath. Exp. Neurol.*, 54, (1995) 105-120.

Helfland, S.L., Smith, G.A. and Wessells, N.K., survival and development in culture of dissociated parasympathetic neurones from ciliary ganglia. *Dev. Biol.*, 50, (1976), 541-547.

Hikosaka, O. and Wurtz, R.M., Visual and oculomotor functions of monkey substantia nigra pars reticulata I. Relation of visual and auditory responses to saccades. J. *Neurophysiology*, 49, (1983), 1230-1253.

Hollen, K.M., Nakabeppu,Y., and Davies, S.W., Changes in expression of ΔFosB and the Fos family proteins following NMDA receptor activation in the rat striatum, *Mol .Brain. Res.*, 47 (1997) 31-43.

Hollman, M. and Heinemann, F. Cloned glutamate receptors. *Ann. Rev. Neuroscience*, 17, (1994), 31-108.

Holtmann, H. and Wallach, D. Down regulation of the receptors for TNF by IL-1 and 4-beta-phorbol-12-myristate-13-acetate. *J.Immunol.*, 139, (1987), 1161-1167.

Hoogeveen, A.T., Willemsen, R., Meyer, N., de Rooij, K.E., Roos, R.A.C., van Ommen, JG.B. and Galjaard, H. Characterization and localization of the Huntington disease gene product. *Human Mol. Gen.*, 2, (1993), 2069-2073.

Hong-Qin, Z., Wang, Y., Nakai, M. and Chase, T.N. Nuclear Factor-kB contributes to excitotoxin-induced apoptosis in rat striatum, *Molecular Pharmacology*, 53 (1998) 33-42.

Hou, Y.N., Vlaskovska, M., Cebers, G., Kasakov, L., Liljequist, S., and Terenius,L., A mu-receptor opioid agonist induces AP-1 and NF-kB transcription factor activity in primary cultures of rat cortical neurons, *Neurosci. Lett*s., 212 (1996) 159-62.

Hughes, S.M., Lillien, L.E., Raff, M. C., Rohrer, H. and Sendtner, M., ciliary neurotrophic factor induces type-2 astrocyte differentiation in culture. *Nature*, 355, (1988), 70-73.

Hunot, S., Brugg.B., Ricard.D., Michel.P.P., Muriel, MP.,Ruberg, M. Faucheux,B.A., Agid, Y. and Hirsch, E.C. Nuclear translocation of NF-kB is increased in dopaminergic neurons of patients with Parkinson disease, *PNAS.*, 94 (1997) 7531-7526.

Huntington, G. On Chorea, *Medical and Surgical Reporter*, 26, (1872), 320-321.[24]

Huntington's Disease Collaborative Research Group, A novel gene containing a trinucleotide repeat that is unstable on Huntington's disease chromosomes, *Cell*, 72, (1993) 971-983.

Ikeda, H., Yamaguchi, M., Sugai, S., Aze, Y., Narumiya, S. and Kakizuka, A. Expanded polyglutamine in the Machado-Joseph disease protein induces cell death in vitro and in vivo. *Nature Genetics*, 13, (1996), 196-202.

Inoue, J. , Kerr, L.D., Kazizuka, A. and Verma, I.M., IkB gamma, a 70 kD protein identical to the c-terminal half of p110 NF-kB: A new member of the IkB family. *Cell*, 68, (1992), 1109-1120.

Ip, N.Y., McClain, j., Barrezuta, N.X., Aldrich, T.H., Pan, L., Li, Y., Wiegand, S.J., Friedman, B., Davis, D. and Yancopolous, G.D. The alpha component of the CNTF receptor is required for signaling and defines potential CNTF targets in the adult and during development. *Neuron.*,10, (1993), 89-102.

Ip ,NY.[2], Wiegand,SJ., Morse,J. and Rudge,JS., Injury induced regulation of CNTF mRNA in the adult rat brain, *Euro. J. Neurosci.*, 5 (1993) 25-33.

Jenkins, J.B. and Conneally, P.M. The paradgim of Huntington's disease. *Am. J. Hum. Genet.*, 45, (1989), 169-175.

Jorgensen, M.B., Finsen, B.R., Jensen, M.B., Castellano, B., Diemer, N.H. and Zimmer, J. Microglial and astroglial reactions to ischemic and kainic acid induced lesions of the adult rat hippocampus. *Exp. Neurology*, 120, (1993), 70-88.

Kahn, M.A., Ellison, G.J., Speight, JdV., CNTF Regulation of astrogliosis and activation of microglia in the developing rat CNS, *Brain Res.*, 685 (1995) 55-67.

Kaltschmidt, C., Kaltschmidt, B. and Bauerle, P.A., Brain synapses contain inducible forms of the transcription factor NF-kB. *Mech. Dev.*, 43, (1993), 135-147.

Kaltschmidt. C., Kaltschmidt, B., Neumann, H., Wekerle, H., and Baeuerle, PA., Constitutive NF-kB activity in neurons, *Mol. Cell. Bio.*, 14 (1994) 3981-92.

[24] Reproduced in Harper, 1991.

Kaltschmidt, C., Kaltschmidt, B., and Baeuerle, PA., Stimulation of ionotropic glutamate receptors activates transcription factor NF-kB in primary neurons, *PNAS*. 92 (1995) 9618-22.

Kaltschmidt,B., Uherek, M., Volk, B., Baeuerle, P.A. and Kaltschmidt, C., Transcription factor NF-kB is activated in primary neurons by B peptides and in neurons surrounding early plaques from patients with Alzheimer disease. *PNAS*, 94 (1997) 2642-2647.

Karnovsky, M.J. and Roots, L. A direct colouring thiocholine method for cholinesterases. *J.Histochem.Cytochem.*, 12 (1964), 219-221.

Kawaguchi, Y., Okamoto, T., Taniwaki, M., Aizawa, M., Inoue, M., Katayama, S., Kawakami, H., Nakamura, S., Nishimura, M., Akiguchi, I., Kimura, J., Narumiya, S. and Kakizuka, A. CAG expansions in a novel gene for Machado-Joseph disease at chromosome 14q32.1. *Nature Genetics*, 8, (1994), 221-228.

Kawaguchi, Y., Wilson, C., Augood, S.J. and Emson, P.C. Striatal interneurons: chemical, physiological and morphological characterization, *TINS*, 18, (1995), 527-535.

Kemp, J.M. and Powell, T.P.S. The structure of the caudate nucleus of the cat: Light and electron microscopy, *Phil. Trans. R. Soc. Lond.*, 262 (1971), 383-401.

Kerr, L.D., Ransome, L.J., Wamsley, P., Scmitt, M.J., Boyer, T.G., Zhou, Q., Berk, A. and Verma, I.M. Association between proto-oncoprotein Rel and TATA-binding protein mediates activation by NF-kB. *Nature*, 365, (1993), 412.

Kieran,M., Blank,V., Logeat, F., Vandekerckhove, J., Lottspeich,F., Le Bail, O., Urban, M.B., Kourilsky, P., Baeuerle, P.A. and Israel, A. The DNA subunit of NF-kB is identical to factor KBF-1 and homologous to the rel oncogene product, *Cell*, 62 (1990) 1007-1018.

Kiss, J.Z. Dynamism of chemoarchitecture in the hypothalamic paraventricular nucleus. *Brain Res. Bull.*, 20, (1988), 699-708.

Kita, H., Kosaka, T. and Heizman, C.W. Parvalbumin immunoreactive neurons in the rat neostriatum: a light and electron microscopic study. *Brain Res.*, 536, (1990).

Klein, M.A., Moller, J.C., Jones, L.L., Bluethmann, H., Kreutzberg, G.W. and Raivich, G. Impaired neuroglial activation in interleukin-6 deficient mice, *Glia*, 19 (1997) 227-233.

Kohler, C. and Schwarcz, R. Comparison of ibotentate and kainate neurotoxicity in rat brain: a histological study. *Neuroscience*, 8, (1983), 819-835.

Koide, R. et al. Unstable expansion of CAG repeat in hereditary dentato-rubral-pallidoluysian atrophy (DRPLA). *Nature Genetics*, 6,(1994), 9-13.

Kontgen, F., Grumont, R.J., Strasser, A., Metcalf, D., Li, R., Tarlington, D. and Gerondakis, S. Mice lacking the c-rel proto-oncogene exhibit defects in lymphocyte proliferation, humoral immunity and interleukin-2 expression. *Genes Dev.*, 9, (1995), 1965-1977.

Kordower, J.H., Chu, Y,. and Maclennan, J., Ciliary neurotrophic factor receptor alpha immunoreactivity in the monkey central nervous system, *J. Comp. Neurol.*, 377, (1997), 365-380.

Kostura, M.J., Tocci, G., Limjuco, J., Chin, P., Cameron, A.G., Hillman, N.A., Chartrain, N. and Scmidt, A. Identification of a monocyte specific pre-interleukin 1B convertase activity. *PNAS*, 86, (1989), 5227-5231.

Kowall, N.W.[1], Ferrante, R.J., Beal, M.F., Richardson, E,P., Sofroniew, M.V., Cuello, A.C. and Martin, J.B. Neuropeptide Y, somatostatin, and reduced nicotinamide adenine dinucleotide phosphate diaphorase in the human striatum: a combined immunocytochemical and enzyme histochemical study. *Neuroscience*, 20 (1987), 817-828.

Kowall, N.W., Ferrante, R.J. and Martin, J.B. Patterns of cell loss in Huntington's disease. *TINS*, 10, (1987), 24-29.

Kubota, Y. and Kawaguchi, Y. Spatial distributions of chemically identified intrinsic neurons in relation to patch and matrix compartments of rat neostriatum. *J. Comp. Neurol.*, 332, (1993), 499-513.

Kumar, U., Asotra, K., Patel, S.C. and Patel, Y.C. Expression of NMDA receptor 1 (NR1) and huntingtin in striatal neurones which co-localize somatostatin, neuropeptide Y and NADPH diaphorase: a double label histochemical and immunohistochemical study. *Exp. Neurol.* 145, (1997), 412-424.

La Spada[1], A.R., Wilson, E.M., Lubahn, D.B., Harding, A.E. and Fischbeck, K.H. Androgen receptor gene mutations in X-linked spinal and bulbar muscular atrophy. *Nature*, 352, (1991), 77-79.

La Spada[2], A.R., Paulson, H.L. and Fischbeck, K.H. Trinucleotide repeat expansion in neurological disease. *Ann. Neurol.*, 36, (1994), 814-822.

Landwehrmeyer, G.B. et al, Huntington's disease gene: regional and cellular expression in brain of normal and affected individuals. *Ann. Neurol.*, 37, (1995), 218-230.

Latchman, D., *Gene regulation*, Chapman and Hall, Oxford, (1995), 271 pp.

Lee, M.Y., Deller, T., Kirsch, M., Frotscher, M. and Hofman, H.D. Differential regulation of ciliary neurotrophic factor (CNTF) and CNTF receptor a expression in astrocytes and neurons of the fascia dentata after entorhinal cortex lesion, *J. Neurosci.*, 17 (1997) 1137-1146.

Lee, D.K., Horikoshi, M., and Roeder, R.G., Interaction of TFIID in the minor groove of the TATA element. *Cell*, 67, (1991), 1241.

Leibowitz, S.F. and Stanley, B.G. Brain peptides and the control of eating behaviour. In: Moody, T.W. *Neural and endocrine peptides and receptors*. New York: Plenum Press. 333-352.

Levison, S.W., Ducceschi, M.H., Young, S.M. and Wood, T.L. Acute exposure to CNTF in vivo induces multiple components of reactive gliosis, *Exp. Neurol.*, 141 (1996) 256-68.

Libermann T.A. and Baltimore, D., Activation of Interleukin-6 gene expression through the NF-kB transcription factor, *Mol. and Cell. Biology*, 10 (1990) 2327-2334.

Lieberman, A.P., Robitaille, Y., Trojanowski, J.Q., Dickson, D.W. and Fischbeck, K.H, Polyglutamine-containing aggregates in neuronal nuclear inclusion disease, *The Lancet*, 351, (1998) 884.

Li, C.C., Dai, R.M., Chen, E. and Longo, D.L., Phosphorylation of NF-kB/p50 is involved in NF-kB activation and stable DNA binding. *J. Biol. Chem.*, 269, (1994), 30089.

Lincoln, D.W. and Wakerley, J.B. Electrophysiological evidence for the activation of supraoptic neurones during the release of oxytocin. *J. Physiol. (Lond).*, 242., (1974), 533-554.

Liu, Q, and Dreyfuss, G., A novel nuclear structure containing the survival of motor neurons protein, *EMBO J*, 15 (1996) 3555-3565.

Liu, Z-G., Hsu, H., Goeddel, D.V. and Karin, M. Dissection of TNF receptor 1 effector functions: JNK activation is not linked to apoptosis while NF-kB activation prevents cell death, *Cell*, 87, (1996) 565-576.

Lisovoski, F., Akli, S., Peltekian, E., Vigne, E., Haase, G., Perricaudet, M., Dreyfus, P.A., Kahn, A. and Peschanski, M. Phenitypic alteration of astrocytes induced by ciliary neurotrophic factor in the intact adult brain, as revealed by adenovirus-mediated gene transfer. *J. Neurosci.*, 17, (1997), 7228-7236.

Lodge, D and Johnson, K.M. Noncompetitive excitatory amino acid receptor antagonists. *TIPS*, 11, (1990), 181-186.

Lucas, D.R. and Newhouse, J.P. The toxic effect of sodium L-glutamate on the inner layers of the retina. *Arch. Opthal.*, 58, (1957), 193-201.

Ludolph,, A.C. and Spencer, P.S. Toxic models of upper motor neurone disease. *J. Neurol. Sci.*, 139, (1996), S3-9.

Mangiarini, L., Sathasivam, K., Seller, M., Cozens, B., Harper, A., Hetherington, C., Lawton, M., Trottier, Y., Lerach, H., Davies, S.W. and Bates, G.P., Exon 1 of the HD gene with an expanded CAG repeat is sufficient to cause a progressive neurological phenotype in transgenic mice, *Cell*, 87, (1996) 493-506.

Marcucilli, C.J. and Miller, R.J. CNS stress response: too hot to handle? *TINS*, 17, (1994), 135-137.

Masu, Y., Wolf, E., Holtmann, B., Sendtner, M., Brem, G.and Thoenen, H., Disruption of the CNTF gene results in motor neuron degeneration, *Nature*, 365 (1993) 27-32.

Mayer, M.L. and Westbrook, G.L. Micromolar concentrations of Zn^{2+} antagonise NMDA and GABA responses of hippocampal neurons. *Nature*, 87, (1987), 640-643.

McDonald, J.R., Ko, C., Mismer, D., Smith, D.J. and Collins, F. Expression and characterization of of recombinant human ciliary neurotrophic factor from Escherichia coli, *Biochimica et Biophysica Acta*, 1090 (1991) 70-80.

McDonald, N.Q., Panayotatos, N. and Hendrickson, W.A. Crystal structure of dimeric human ciliary neurotrophic factor determined by MAD phasing, *EMBO J*, 14 (1995) 2689-2699.

McGeer, P.L., McGeer, E.G., Singh, V.K. and Chase, W.H. Choline acetyltransferase localisation in the central nervous system by immunohistochemistry. *Brain Res.*, 81, (1974), 373-379.

McGeer, P.L. and McGeer, E.G. The inflammatory response system of the brain: implications for therapy of Alzheimer and other neurodegenerative diseases. *Brain Res.Rev.*, 21 (1995) 195-218.

McIntosh, T.K. and Raghupathi, R. Cell stress genes and acute CNS injury. *Neuropathology and Applied Neurobiology*, 21, (1995), 477-479.

Meberg, P.J., Kinney, W.R., Valcourt, E.G., and Routtenberg, A., Gene expression of the transcription factor NF-kB in hippocampus: regulation by synaptic activity, *Mol. Brain. Res.*, 38 (1996) 179-90.

Medina, L. and Reiner, A, Neurotransmitter organization and connectivity of the basal ganglia in vertebrates: implications for the evolution of basal ganglia, *Brain Behav. Evol.*, 46 (1995) 235-258.

Meyer, R., Hatada, E.N., Hohmann HP., Haiker, M., Bartsch, C., Rothlisberger, U., Lahm, HW., Schlaeger, E.J., van Loon. A.P.G.M. and Scheidereit, C. Cloning of the DNA-binding subunit of human nuclear factor kB: The level of its mRNA is strongly regulated by phorbol ester or tumour necrosis factor alpha, *PNAS.*, 88 (1991) 966-970.

Michaely, P. and Bennet, V., The ANK repeat: a ubiquitous motif involved in macromolecular recognition. *Trends Cell. Biol.*, 2, (1992), 127.

Miyamoto, S. and Verma, IM., Rel/NF-kappa B/I kappa B story, *Adv. Cancer. Res.*, 66 (1995) 255-92.

Moriyoshi, K. Masu, M, Ishii, T., Shigemoto, R., Mizuno, N. and Nakanishi, S. Molecular cloning and characterisation of the rat NMDA receptor. *Nature*, 354, (1991), 31-37.

Monaghan, D.T., Bridges, R.J. and Cotman, C.W. The excitatory amino acid receptors: their classes, pharmacology, and distinct properties in the function of the central nervous system. *Ann. Rev. Pharmacol. Toxicol.*, 29, (1989) 365-402.

Monyer, H., Bernashev, N., Laurie, D.J., Sakmann, B. and Seeburg, P.H. Developmental and regional expression in the rat brain and functional properties of four NMDA receptors. *Neuron*, 12, (1994), 529-540.

Monyer, H., Sprengel, R., Schoepfer, R., Herb, A., Higuchi, M., Lomeli, H., Burnashev, N., Sakmann, B. and Seeburg, P.H. Heteromeric NMDA receptors: molecular and functional distinction of subtypes. *Science*, 256, (1992) 1217-1221.

Mosialos, G. and Gilmore, T.D. v-Rel and c-Rel are differentially affected by mutations at a consensus protein kinase recognition sequence. *Oncogene*, 8, (1993), 721.

Mosialos, G., Hamer, P., Capobianco, A.J., Laursen, R.A., and Gilmore, T.D. A protein kinase A recognition sequence is structurally linked to transformation by p59 v-rel and cytoplasmic retention of p68 c-rel. *Mol. Cell. Biol.*, 11, (1991), 5877.

Morton, A.J., Nicholson, L.F.B. and Faull, R.L.M. Compartmental loss of NADPH diaphorase in the neuropil of the human striatum in Huntington's disease. *Neuroscience*. 53, (1993), 159-168.

Moriyoshi, K., Masu, M., Ishii, T., Shigemoto, R., Mizuno, N. and Nakanishi, S. Molecular cloning and characterisation of the rat NMDA receptor. *Nature*, 354, (1991) 31-37.

Moynagh, P.N., Williams,C., and O'Neill, L.A.J. II.-1 Activates transcription factor NF-kB in glial cells, *Biochem. J.*, 294 (1993) 343-7.

Mukaida, N., Morita, M., Ishikawa, Y., Rice, N., Okamoto, S., Kasahara, T. and Matsushima, K. Novel mechanism of glucocorticoid mediated gene repression, *J.Bio.Chem.*, 269 (1994) 13289-13295.

Nakai, S., Kawano, H., Yudate, T., Nishi, M., Kuno, J., Nagata, A., Jishage, K., Hamada, H., Fujii, H., Kawamura, K., Shiba, K. and Noda, T. The POU domain transcription factor Brn-2 is required for the determination of specifc neuronal lineages in the hypothalamus of the mouse. *Genes and Dev.*, 9, (1995), 3109-3121.

Nolan, G.P., Ghosh, S., Liou, HC., Tempst, P. and Baltimore, D. DNA binding and IkB inhibition of the cloned p65 subunit of NF-kB a rel-related polypeptide, *Cell*, 64 (1991) 961-969.

Norenberg, M.D., Astrocyte responses to CNS injury, *J. Neuropath. Exp. Neurol.*, 53, (1994), 213-220.

Oglesbee, M. Intranuclear inclusions in paramyxovirus-induced encephalitus: evidence for altered nuclear body differentiation. *Acta Neuropathol. Berl.*, 84, (1992), 407-415.

Oglesbee, M. and Krakowa, S. Cellular stress response induces selective intranuclear trafficking and accumulation of morbillivirus core protein. *Laboratory Investigation*, 68, (1993), 109-116.

Olanow, C.W., A radical hypothesis for neurodegeneration. *TINS*, 16, (1993), 439-443.

Olney, J.W., Ho, O.I. and Rhee, V. Cytotoxic effects of acidic and sulphur containing aino acids on the infant mouse central nervous system. *Exp. Brain Res.*, 14, (1971), 61-76.

Ordway, J.M., Tallaksen-Greene, S., Gutekunst, C-A., Bernstein, E.M., Cearley, J.A., wiener, H.W., Dure, L.S., Lindsey, R., Hersch, S.M., Jope, R.S., Albin, R.L. and Detloff. P.J. Ectopically expressed CAG repeats cause intranuclear inclusions and a progressive late onset neurological phenotype in the mouse. *Cell*, 91, (1997), 753-763.

Orr, H.T., Chung, M., Banfi, S., Kwiatkowski, T.J., Servadio, A., Beaudet, A.L., McCall, A.E., Duvick, L.A., Ranum, L.P.W. and Zoghbi, H.Y., Expansion of an unstable trinucleotide CAG repeat in spinocerebellar ataxia type 1. *Nature Genetics*, 4, (1993), 221-226.

O, Neill, L.A.J and Kaltschmidt, C., NF-kB: a crucial transcription factor for glial and neuronal cell function. *TINS*, 20, (1997), 252-258.

Parent, A. and Hazrati, L-N. Functional anatomy of the basal ganglia. 1. The cortico-basal ganglia-thalamo-cortical loop, *Brain Res. Rev.*, 20 (1995), 91-127.

Paulson, H.L., Perez, M.K., Trottier, Y., Trojanowski, J.Q., Subramony, S.H., Das, S.S., Vig, P., Mandel, J-L., Fischbeck, K.H. and Pittman, R.N, Intranuclear inclusions of expanded polyglutamine protein in spinocerebellar ataxia type 3, *Neuron*, 19, (1997), 333-344.

Paxinos, G. and Watson, C. *The Rat Brain in Stereotaxic Coordinates*, Academic Press, Sydney, Australia, 1986.

Pearce, D. and Yamamoto, K.R. Mineralocorticoid and glucocorticoid receptor activities distinguished by non-receptor factors at a composite response element, *Science*, 259, (1993), 1161-1165.

Penny, J.B. and Young, A.B. Striatal inhomogeneities and basal ganglia function. *Movement Disorders*, 1, (1986), 3-15.

Perez-Navarro, E., Alberch, J., Arenas, E., Calvo, N. and Marshall, J. Nerve growth factor and basic fibroblast growth factor protect cholinergic neurons against quinolinic acid excitotoxicity in rat neostriatum. *Eur, J. Neurosci.*, 6, (1994), 706-711.

Perez-Otano, I., McMillian, M.K., Chen, J., Bing, G., Hong.J.S., and Pennypacker,K.R., Induction of NF-kB-like transcription factors in brain areas susceptible to kainate toxicity, *Glia*, 16 (1996) 306-15.

Perlman, J.M. and Argyle, C. Lethal cytomegalovirus infection in preterm infants: Clinical, radilogical and neuropathological findings. *Ann. Neurol.*, 31, (1992), 64-68.

Pert, C., Kuhar, M. and Snyder, S. Opiate receptors: autoradiographic location in rat brain. *PNAS*, 73, (1976), 3729-3733.

Perkins, N.D., Edwards, N.L., Duckett, C.S., Agranoff, A.B., Schmid, R.M. and Nabel, G.J. A co-operative interaction between NF-kB and Sp1 is required for HIV-1 enhancer interaction. *EMBO J*, 12, (1993), 3551.

Perutz, M.F., Johnson, T., Suzuki, M. and Finch, J.T., Glutamine repeats as polar zippers: Their possible role in inherited neurodegenerative diseases, *PNAS.*, 91 (1994), 5355-5358.

Peters, M.J., Adcock, I.M., Brown, C.R. and Barnes, P.J. Beta adrenoceptor agonists interfere with glucocorticoid receptor binding in rat lung. *Eur. J. Pharm.*, 289, (1995), 275-281.

Phelps, P.E., Houser, C.R. and Vaughn, J.E. Immunocytochemical localisation of choline acetyltransferase within the rat neostriatum: A correlated light and electron microscopic study of cholinergic neurons and synapses. *J. Comp. Neurol.*, 238, (1985), 286-307.

Pickel, V.M., Sumal, K.K., Beckley, S.C., Miller, R.J. and Reis, D.J. Immunocytochemical localisation of enkephalin in the neostriatum of rat brain: a light and electron microscopic study, *J. Comp. Neurol.*, 189, (1980), 721-740.

Popoli, P., Pezzola, A., Domenici, M.R., Sagratella, S., Diana, G., Caporali, M.G., Bronzetti, E., Vega, J. and Scotti de Carolis, A. Behavioural and electrophysiological correlates of the quinolininc acid rat model of Huntington's disease in rats. *Brain Res. Bull.*, 4, (1994), 329-335.

Prasad, AV., Pilcher,WH., and Joseph, SA., NF-kB in rat brain: Enhanced DNA binding activity following convulsant induced seizures, *Neurosci. Lett*s., 170 (1994) 145-8.

Purkiss, R.J. *Neurotrophins, immediate early genes and neuronal cell death.* Ph.D thesis, University of London, (1993), 198pp.

Purkiss, R.J., Legg, M.D., Hunt, S.P. and Davies, S.W. Immediate early gene expression in the rat forebrain following striatal infusion of quinolinic acid, *Eur. J. Neuro.*, 5(1993) 1653-1652.

Ray, A. and Prefontaine, K.E. Physical association and functional antagonism between the p65 subunit of transcription factor NF-kB and the glucocorticoid receptor, *PNAS.*, 91 (1993) 752-756.

Rattner, A., Korner, M., Walker, M.D. and Citri, Y. NF-kB activates the HIV promoter in neurons. *EMBO J*, 12, (1993), 4261-4267.

Ribak, C.E., Vaughn, J.E. and Roberts, E. The GABA neurons and their axon terminals in the rat corpus striatum as determined by GAD immunocytochemistry. *J. Comp. Neurol.*, 187, (1979), 261-284.

Rice, N.R. and Ernst, M.K. in vivo control of NF-kB activation by IkB-alpha. *EMBO J*, 12, (1993), 2773.

Riviere, Y., Blank, V., Kourilsky, P, and Israel, A. Processing of the precursor of NF-kB by the HIV-1 protease during acute infection. *Nature*, 350, (1991), 625.

Roeder, R.G. The role of general initiation factors in transcription by RNA polymerase II. *TIBS*, 21, (1996), 327-335.

Rong, Y. and Baudry, M. Seizure activity results in a rapid induction of nuclear factor-kB in adult but not juvenile rat limbic structures. *J. Neurochem.*, 67, (1996), 662-668.

Roos, R.A.C. and Bots, G.T.A.M., Nuclear membrane indentations in Huntington's disease. *J. Neurosci.*, 61, (1983), 37-47.

Ross, C., McInnis, M.G., Margolis, R.L. and Li, S-H. Genes with triplet repeats: candidate mediators of neuropsychiatric disorders. *TINS*, 16, (1993), 254-260.

Ross, C.A, Intranuclear neuronal inclusions: A common pathogenic mechanism for glutamine-repeat neurodegenerative diseases? *Neuron*, 19, (1997), 1147-1150.

Roth, M., Spheres, coiled bodies and nuclear bodies, *Curr. Op. Cell. Bio.*, 7 (1995) 325-328.

Rudge, J.S., Eaton, M.J., Mather, P., Lindsay, R.M. and Whittemore, S.R. CNTF induces raphe neuronal precursors to switch from a serotonergic to a cholinergic phenotype in vitro. *Mol. Cell. Neuroscience*, 7, (1996), 204-211.

Rudge, J.S[2]., Li, Y., Pasnikowski, E.M., Mattsson, K., Pan, L., Yancopoulos, G.D., Wiegand, S.J., Lindsay, R.M., and Ip, N.Y. Neurotrophic factor receptors and their signal transduction capabilities in rat astrocytes, *Euro. J. Neurosci.*, 6 (1994) 693-705.

Rudge, J.S[1]., Morrissey. D., Lindsay, R.M. and Pasnikowski, E.M. Regulation of ciliary neurotrophic factor in cultured rat hippocampal astrocytes, *Euro. J. Neurosci.*, 6 (1994) 218-229.

Ryseck, R.P., Bull, P., Takamiya, M., Bours, V., Siebenlist, U., Dobrzanski, P. and Bravo, R. Rel B, a new Rel family transcription activator that can interact with p50-NF-kB, *Mol. and Cell. Biology*, 12 (1992) 674-684.

Saadat, S., Sendtner, M. and Rohrer, H. Ciliary neurotrophic factor induces cholinergic differentiation of rat sympatheric neurons in culture. *J. Cell. Biol.*, 108. (1989), 1807-1616.

Sapolsky, R.M., *Stress, the aging brain, and the mechanisms of neuron death.* MIT Press, Cambridge, Mass.,1992, 429pp.

Sapp, E., Ge, P., Aizawa, H., Bird, E., Penney, J., Young, A,B., Vonsattel, J-P. and Difiglia, M., Evidence for a preferential loss of enkephalin immunoreactivity in the external globus pallidus in low grade Huntington's disease using high resolution image analysis. *Neuroscience*, 64, (1995), 397-404.

Satoh, K., Staines, W.A., Atmadja, S. and Fibiger, H.C. Ultrastructural observations of the cholinergic neuron in the rat striatum as identified by acetylcholinesterase pharmacohistochemistry. *Neuroscience*, 10, (1983), 1121-1136.

Schaffner, W. How do different transcription factors binding the same DNA sequence sort out their jobs? *TIGS*, 5, (1989), 37-39.

Schmidt-Ullrich, R., Memet, S., Lillienbaum, A., Feulliard, J., Raphael, M., and Israel, A. NF-kB activity in transgenic mice: developmental regulation and tissue specificity. *Development*, 122 (1996), 2117-2128.

Shaw, J.A., Perry, V.H. and Mellanby, J. Tetanus toxin induced seizures cause microglial activation in rat hippocampus. *Neurosci. Letts.*, 120, (1990), 166-169.

Scherzinger, E., Lurz, R., Turmaine, M., Mangiarini, L., Hollenbach, B., Hasenbach, R., Bates, G.P., Davies, S.W., Lehrach, H. and Wanker, E.W. Huntingtin-encoded polyglutamine expansions form amyloid-like protein aggregates in vitro and in vivo. *Cell*, 90, (1997), 549-558.

Schoenemann, M.D., Ryan, A.K., McEvilly, R.J., O'Connell, S.M., Arias, C.A., Kalla, K.A., Li, P., Sawchenko, P.E. and Rosenfeld, M.G. Development and survival of the endocrine hypothalamus and posterior pituitary gland requires the neuronal POU domain factor Brn-2. *Genes and Dev.*, 9, (1995), 3122-3135.

Schreiber, E., Harshman, K., Kemler, I., Malipiero, U., Schaffner, W. and Fontana, A. Astrocytes and glioblastoma cells express novel octomer-DNA binding proteins distinct from the ubiquitous Oct-1 and B cell type Oct-2 proteins. *Nuc. Acids Res.*, 18, (1990), 5495-5503.

Schreiber, E., Tobler, A., Malipiero, U., Schaffner, W. and Fontana, A. cDNA cloning of human N-Oct 3, a nervous system specific POU domain transcription factor binding to the octamer DNA motif. *Nuc. Acids Res.*, 12, (1993), 253-258.

Scheinman, R.I., Cogswell, P.C., Lofquist, A.K. and Baldwin, A.S. Role of transcriptional activation of IkBa in mediation of immunosuppression by glucocorticoids, *Science*, 270, (1995), 283-290.

Scheinman, R.I., Gualberto, A., Jewell, C.M., Cidlowski, J.A., and Baldwin, A.S. Characterization of mechanisms involved in transrepression of NF-kB by activated glucocorticoid receptors. *Mol. Cell. Biol.*, 15, (1995), 943-953.

Scherer-Singler, U., Vincent, S.R., Kimura, H. and McGeer, E.G. Demonstration of a unique population of neurons with NADPH-diaphorase histochemistry. *J. Neuroscience Methods*, 9. (1983), 229-234.

Scherzinger, E., Lurz, R., Turmaine, M., Mangiarini, L., Hollenbach, B., Hasenbank, R., Bates, G.P., Davies, S.W., Lehrach, H. and Wanker, E.E. Huntington-encoded polyglutamine expansions form amyloid-like protein aggregates in vitro and in vivo, *Cell*, 90, (1997), 549-558.

Schmid, R.M., Perkins, N.D., Duckett, C.S., Andrews, P.C. and Nabel, G.J. Cloning of an NF-kB subunit which stimulates HIV transcription in synergy with p65, *Nature*, 352 (1991) 733-736.

Schwarcz, R., Whetsell, W.O. and Mangano, R.M. Quinolininc acid: an endogenous metabolite that produces axon-sparing lesions in rat brain. *Science*, 219, (1983), 316-318.

Selkoe, D.J., Salazar, F.J., Abraham, C. and Kosik, K.S. Huntington's disease: changes in striatal proteins reflect astrocytic gliosis. *Brain Res.*, 245, (1982), 117-125.

Sendtner, M., Dittrich, F., Hughes, H. and Thoenen, H. Actions of CNTF and neurotrophins on degenerating motoneurons: preclinical studies and clinical implications. *J. Neurol. Sci.*, 124, (1994), 77-83.

Sendtner, M, Kreutzberg, G.W. and Thoenen, H. Ciliary neurotrophic factor prevents the degeneration of motor neurons after axotomy. *Nature*, 345, (1990), 440-441.

Sendtner, M., Schmalbruch, H., Stockli, K.A., Carroll, P., Kreutzberg, G.W. and Thoenen, H. Ciliary neurotrophic factor prevents degeneration of motor neurons in mouse mutant progressive motor neuropathy. *Nature*, 358, (1992), 502-504.

Sen, R. and Baltimore, D. Multiple nuclear factors interact with the immunoglobulin enhancer sequences, *Cell*, 46 (1986) 921-928.

Sha, W., Liou, H.C., Tuomanen, E.I. and Baltimore, D., Targeted disruption of the p50 subunit of NF-kB leads to multifocal defects in immune responses. *Cell*, 80, (1995), 321.

Sharp, A.H., Love, S.J., Schilling, G., Li, S.H., Jiang Li, X., Bao, J., Wagster, M.V., Kotzuk, J.A., Steiner, J.P., Lo, A., Hedreen, J., Sisodia, S., Snyder, S.H., Dawson, T.M., Ryugo, D.K. and Ross, C., Widespread expression of Huntington's disease gene (IT15) protein product. *Neuron*, 14 (1995), 1065-1074.

Simon, R.P., Swan, J.H., Griffiths, T. and Meldrum, B.S., Blockage of N-methyl-D-aspartate may protect against ischaemic damage in the brain. *Science*, 226, (1984), 2091-2100.

Skinner, P.J., Koshy, B.T., Cummings, C.J., Klement, I.A., Helin, K., Servadio, A., Zoghbi, H. and Orr, H.T, Ataxin-1 with an expanded glutamine tract alters nuclear matrix-associated structures, *Nature*, 389, (1997), 971-974.

Smith, A.D. and Bolam, J.P. The neural network of the basal ganglia as revealed by the study of synaptic connectiobs of identified neurones, TINS, 13, (1990), 259-165.

Sparacio, S.M., Zhang,Y., Vilcek, J., and Benveniste, E.N. Cytokine regulation of IL-6 gene expression in astrocytes involves activation of an NF-kB-like nuclear protein, *J. Neuroimmunology*, 39 (1992) 231-242.

Spencer, P.S., Nunn, P.B., Hugan, J., Ludolph, A.G., Ross, S.M., Roy, D.N. and Robertson, R.C. Guam amyotrophic lateral sclerosis-parkinsonian-dementia linked to a plant excitant neurotoxin. *Science*, 237, (1987), 517-522.

St. Johnston, D. and Nusslein-Volhard, C., The origin of pattern and polarity in the Drosophila embryo. *Cell*, 68, (1992), 209-219.

Stahl, N. and Yancopoulos, D., The tripartite CNTF receptor complex: activation and signalling involves components shared with other cytokines, *J. Neurobiol*,. 25 (1994) 1454-1466.

Stahl, N., Boulton, T.G., Farruggella, T., Ip, N.Y., Davis, S., Witthun, B.A., Quelle, F.W., Silvennoinnen, O., Barbieri, G., Pelligrini, S., Ihle, J.N. and Yancopoulos, G.D. Association and activation of Jak-Tyk kinases by CNTF-LIF-OSM-IL-6 beta receptor components. *Science*, 263, (1994), 92-95.

Stankovski, I. and Baltimore, D., NF-kB activation: The IkB kinase revealed? *Cell*, 91, (1997), 299-302.

Stein, B., Baldwin, A.S., Ballard, D.W., Greene, W.C., Angel, P. and Herrlich, P. Cross-coupling of the NF-kB p65 and Fos/Jun transcription factors produces potentiated biological function, *EMBO J.*, 12 (1993) 3879-3891.

Stockli, K.A.,[1] Lillien, L.E., Naher-Noe, M., Breitfield, G., Hughes, RA., Raff, M.C., Thoenen, H. and Sendtner, M.,. Regional distribution, developmental changes and cellular localization of CNTF-mRNA and Protein in the Rat Brain,. *J.Cell Biology*, 115 (1991) 447-459.

Stockli, K.A.[2], Lottspeich, F., Sendtner, M., Masiakowski, P., Carroll, P., Gotz, R., Lindholm, D. and Thoenen, H., Molecular cloning, expression and regional distribution of rat CNTF, *Nature*, 342 (1989) 920-3.

Strahle, U., Klock, G., and Schutz, G. A DNA sequence of 15 base pairs is sufficient to mediate both glucocorticoid receptor and progesterone induction of gene expression. *PNAS*, 84, (1987), 7871-7875.

Stott, K., Blackburn, J.M.,Butler, P.J.G. and Perutz, M, Incorporation of glutamine repeats makes protein oligomerize:Implications for neurodegenerative diseases, *PNAS*, 92, (1995), 6509-6513.

Strong, T.V., Tagle, D.A., Valdes, J.M., Elmer, L.W., Boehm, K., Swaroop, M., Kaatz, K.W., Collins, F.S. and Albin, R.L. Widespread expression of the human and rat Huntington's disease gene in brain and non-neural tissues. *Nature Genetics*, 5, (1993), 259-265.

Stylianou, E., O'Neill, L.A., Rawlinson, L., Edbrooke, M.R., Woo, P. and Saklatvala, J. IL-1 induces NF-kB through its type 1 but not its type 2 receptor in lymphocytes. *J. Biol. Chem.* 267, (1992), 15836-15841.

Sumiyama, K., Watanabe, K.W. Saitou, N., Hayakawa, T. and Ueda, S. Class III POU genes: Generation of homopolymeric amino acid repeats under GC pressure in mammals. *J. Mol. Evol.*, 43, (1996), 170-178.

Sundsten, J.W. and Sawyer, C.H. Osmotic activation of neurohypophysial hormone release in rabbits with hypothalamic islands. *Exp. Neurol.*, 4 (1961), 548-561.

Swanson, L.W. and Sawchenko, P.E. Hypothalamic integration: organisation of the paraventricular and supraoptic nuclei. *Annu. Rev. Neurosci.*, 6, (1983), 269-324.

Takahashi, H., Ohama, E., Naito, H., Takeda, S., Nakashima, S., Makifuchi, T. and Ikuta, F. Hereditary dentatorubral-pallidoluysian atrophy: clinical and pathological variants in a family. *Neurology*, 38, (1988), 1065-1070.

Teitelbaum, J.S., Zatorre, R.J., Carpenter, S., Gendron, D., Evans, A.C., Gjedde, A. and Cashman, N.R. Neurologic sequelae of domoic acid intoxication due to the ingestion of contaminated mussels. *N.Eng. J. Med.*, 322, (1990), 1781-1787.

Tellez-Nagel, I., Johnson, B. and Terry, R.D. Studies on brain biopsies of patients with Huntington's chorea. *J.Neurocytol.*, 3, (1974), 308-332.

Thanos, D. and Maniatis, T. NF-kB: A lesson in family values, *Cell*, 80 (1995) 529-532.

Thomas, E. and Pearse, A.G.E. The solitary active cells. Histochemical demonstration of damage resistant nerve cells with a TPN-diaphorase reaction. *Acta. Neuropathol. (Berlin).*, 3, (1964), 238-249.

Thompson, J.E., Phillips, R.J., Erdjument-Bromage, H., Tempst, P. and Ghosh, S., IkB-beta regulates the persistent response in a biphasic activation of NF-kB. *Cell*, 80. (1995), 573-582.

Tolosano, E., Cutufia, M.A., Hirsch, E., Stefanuto, G., Voyron, S., Fasolo, A., Silengo, L. and Altruda, F. Ciliary neurotrophic factor constitutively expressed in the nervous system of transgenic mice protects embryoninc dorsal root ganglion neurons from apoptosis. *Eu. J. Neurosci.*, 8. (1996), 521-529.

Tong, L. and Perez-Polo, J.R. Effect of nerve growth factor on AP-1, NF-kB and Oct DNA binding activity in apoptotic PC12 cells: Extrinsic and Intrinsic elements. J. *Neurosci. Res.*, 45, (1996), 1-12.

Truss, M., and Beato, M. Steroid hormone receptors: interaction with deoxyribonucleic acid and transcription factors. *Endocrine Review*, 14, (1993), 459-479.

Turski, L., Bressler, K., Rettig, K.J., Loschmann, P.A. and Wachtel, L. Protection of substantia nigra from MPP+ neurotoxicity by NMDA antagonists. *Nature*, 349, (1991), 414-418.

Ullman, S.U. and Powers, M.A. Nuclear export receptors: from importin to exportin. *Cell*, 90, (1997), 967-970.

Unlap, T. and Jope, R.S., Inhibition of NF-kB DNA binding activity by glucocorticoids in rat brain. *Neurosci. Letts.*, 198. (1995), 41-44.

Van Antwerp, D.J., Martin, S.J., Kafri, T., Green, D.R. and Verma, I.M. Suppression of TNF-alpha induced apoptosis by NF-kB. *Science*, 274, (1996), 787-789.

Verrijzer, C.P., Yokomori, K., Chen, J-L. and Tijan, R. Drosopila TAF150: Similarity to yeast gene TSM-1 and specific binding to core promoter DNA. *Science*, 264, (1994), 933.

Vezzani, A., Forloni, G.L., Serafini, R., Rizzi, M. and Samanin, R. Neurodegenerative effects induced by chronic infusion of quinolininc acid in rat striatum and hippocampus. *Eur. J. Neurosci.*, 3, (1990), 40 –46.

Vincent, S., Hokfelt, T., Christensson, L. and Terenius, L. Immunohistochemical evidence for a dynorphin immunoreactive striato-nigral pathway. *Eur. J. Pharmacol.*, 85, (1982), 251-252.

Vincent, S.R. and Reiner, P.B. A population of very small striatal neurons in the cat displays vasoactive intestinal polypeptide immunoreactivity. *Neurosci. Letts.*, 89, (1988), 277-282.

Vonsattel, J-P., Myers, R.H., Stevens, T.J., Ferrante, R.J., Bird, E.D. and Richardson, E.P. Neuropathological classification of Huntington's disease, *J. Neuropath, Exp. Neurol.*, 44, (1985) 559-577.

Wakai, M., Takahashi, A. and Hashizume, Y. A histometrical study on the globus pallidus in Huntington's disease. *J. Neurol. Sci.*, 119, (1993), 18-27.

Weih, F., Carrasaco, Durham, S.K., Barton, D.S., Rizzo, C.A., Ryseck, RP., Lira, S.A. and Bravo, R. Multiorgan inflammation and hematopoietic abnormalities in mice with a targeted disruption of Rel B, a member of the NF-kB/Rel family. *Cell*, 80, (1995), 331-340.

Wegener, M., Drolet, D.W. and Rosenfeld, M.G. POU domain proteins: structure and function of developmental regulators. *Curr. Opinion Cell. Biol.*, 5, (1993), 488-489.

Whetsell, W.O. Current concepts of excitotoxicity. *J. Neuropath. Exp. Neurol.*, 55, (1996), 1 –13.

Wilhelmsen, K.C and Temin, H.M. Structure and dimorphism of c-rel (turkey), the cellular homolog to the oncogene of reticuloendotheliosis virus strain, T. *J. Virol.*, 49 (1984) 521-529.

Wilson,C.J. Basal Ganglia, in Shepard, G.M. *The Synaptic Organisation of the Brain*, Oxford, New York, (1990), 559pp.

Winter, C.G., Saotome,Y., Levisom, S.W. and Hirsh.D., A role for CNTF as an inducer of reactive gliosis, the glial response to CNS injury, *PNAS.*, 92 (1995) 5865-69.

Wood, J.N., Regulation of NF-kB in Rat dorsal root ganglia and PC12 cells by tumour necrosis factor and nerve growth factor, *Neurosci. Letts.* 192 (1995) 41-44.

Xu, ,X., Proprock, C., Ishikawa, H., Maldonaldo, E., Ito, Y. and Gelinas, C. Functional interaction of the v-rel and c-rel oncoproteins with the TATA-binding protein mediates activation by NF-kB. *Nature*, 365, (1993), 412.

Yan, S.D., Chen, X., Fu, J., Zhu, H., Roher, A., Slattery, T., Zhao, L., Nagashima, M., Morser, J., Migheli, A., Nawroth, P., Stern, D. and Schmidt, AM. RAGE and amyloid beta peptide neurotoxicity in Alzheimers disease. *Nature*, 382, (1996), 685-691.

Yang, K., Mu, X.S. and Hayes, R.L. Increased cortical nuclear factor-kB (NF-kB) DNA binding activity after traumatic brain injury in rats, *Neurosci. Letts.*, 197 (1995) 101-104.

Young, A.B. and Fagg, G.E. Excitatory amino acid receptors in the brain: membrane binding and receptor autoradiographic approaches. *TIPS*, 11, (1990), 126-133.

Zabel, U. and Baeurle, P.A., Purified human IkB can rapidly dissociate the complex of the NF-kB transcription factor with its cognate DNA. *Cell*, 61, (1990), 255-261.

Zabel, U., Henkel, T., Silva, MdS . and Baeuerle, P.A., Nuclear uptake control of NF-kB by MAD-3, an IkB protein present in the nucleus. *EMBO*, 12, (1993), 201-207.

Zandi, E., Rothwarf, D.M., Delhase, M., Hayakawa, M. and Karin, M. The IkB kinase complex (IKK) contains two kinase subunits, IKK-alpha and IKK-beta, necessary for IkB phosphorylation and NF-kB activation. *Cell*, 91, (1997), 243-252.

Zenzie-Gregory, B., Khachi, A., Garraway, I.P. and Smale, S.T. Mechanism of initiator mediated transcription: Evidence for a functional interaction between the TATA binding protein and DNA in the absence of a specific recognition sequence. *Mol. Cell. Bio.*, 13. (1993), 3841.